

Copyright Notices

Notice 1

Under the Copyright Act 1968, this thesis must be used only under the normal conditions of scholarly fair dealing. In particular no results or conclusions should be extracted from it, nor should it be copied or closely paraphrased in whole or in part without the written consent of the author. Proper written acknowledgement should be made for any assistance obtained from this thesis.

Notice 2

I certify that I have made all reasonable efforts to secure copyright permissions for third-party content included in this thesis and have not knowingly added copyright content to my work without the owner's permission.

ERRATA

Spine embossing: "optimization" for "optimixation"

Page VIII, reference 1, "doi: 10.1016.bip.2143, 2010" for "2010,DOI: 10.1016.bip.2143"

Page VIII, Manuscript in preparation, reference 1, "*J.Mol.Biol*" for "*Journal of Molecular Biology*"

Page VIII, Manuscript in preparation, reference 2, "*J.Biol.Chem*" for "*Journal of Biological Chemistry*"

Page 20, Section header "1.4.11" for "1.8.11"

Page 43, Figure 2.1: "RRMKWKKK" for "RRWKMKKK"

Page 89 line 8, "Vermont" for "Vermot"

Page 94 text line 7 "derivatives" for ""drivatives"

Page 95, Figure 4.3: "RRMKWKKK" for "RRWKMKKK"

Page118-P139, chapter header, "antagonists" for "antagoists"

Page 176, line 3, "processes" for "process"

Page 176, line 7, "resolution" for "resolutions"

Page 179, line 5, "beam line." for "beam line as described in."

Page188, 4th text line, "Table 9.1" for "Table 11.1"

Page192, Heading at top, "Grb7" for "Gb7"

Page192, 10th last text line, "Table 9.11" for "Table 11.11"

Page192, 6th last text line, "phosphotyrosine" for "phosphotyrrone"

Page196, Table 9.4 Title, "comparison" for "compassion"

Page 202, line 1, "especially" for "especial"

Page 202, line 5, "as well as the overall" for "as well as he overall"

Page 212, first line, "series" for "serious"

ADDENDUM

Page 27, Figure 1.7: add the following at the end of the figure caption:

“The structure was solved in our laboratory and has been deposited in the pdb database pdb id: 3PQZ.”

Page 43, Figure 2.1: add the following at the end of the figure caption:

“Peptides G7-18NATE-alaser-Biotin and Penetratin-Biotin are the control peptides. G7-18NATE-alaser-Biotin is synthesized to test the impact of the “penetratin” tail on the binding of the G7-18NATE peptide on Grb7 SH2 domain in an SPR experiment. The Penetratin-Biotin is similarly synthesized to check its possible effect on Grb7 expressing cells in cell based assays.

Page 44, Table 2.1: add in table footnote “The amino acids are obtained from Nova-Biochem of Merck Chemicals Ltd”

Page 49, text line 7: add after synthesizer

“(AI, Scientific; 1 Rivett Rd, 2113 North Ryde, NSW)”

Page 143, paragraph 2, the statement “there has not been a single peptide that is progressed into a useful therapeutic agent”, should read as “there has not been a single Grb7 inhibitor peptide that is progressed into a useful therapeutic agent”

Page 167: Comment: The whiskers are not from a live cat but as supplied by manufacturers.

Page 178, text line 11: Delete “and”

Page 187: add at the end of the heading: “Grb7 SH2 domain.”

Page 186, Figure 9.5: add the following after the figure caption

“The electron density is contoured at sigma level of 1.0 in the content map. The additional electron density observed (after using the Grb7-SH2 domain alone as a search model) was interpreted as malonic acid since 1) it possessed exactly the expected shape of malonic acid, 2) was known to be present in the crystallisation buffer and 3) was positioned to form electrostatic interactions with arginine residues in agreement with it being an dicarboxylic acid”

Page 189, Figure 9.7B: add the additional figure and figure caption.

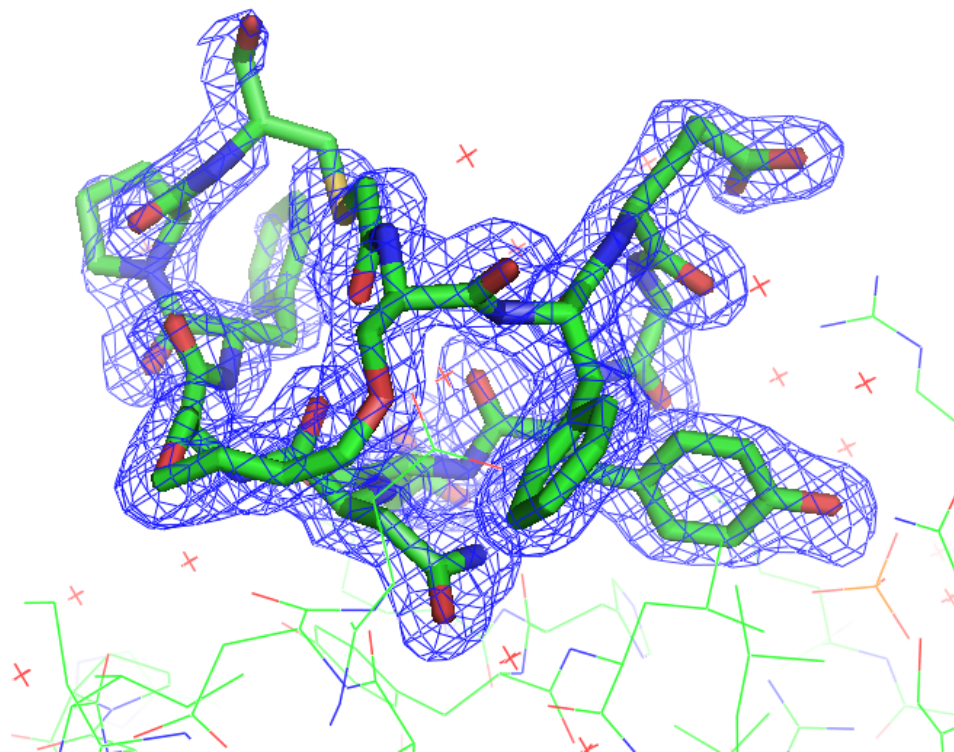
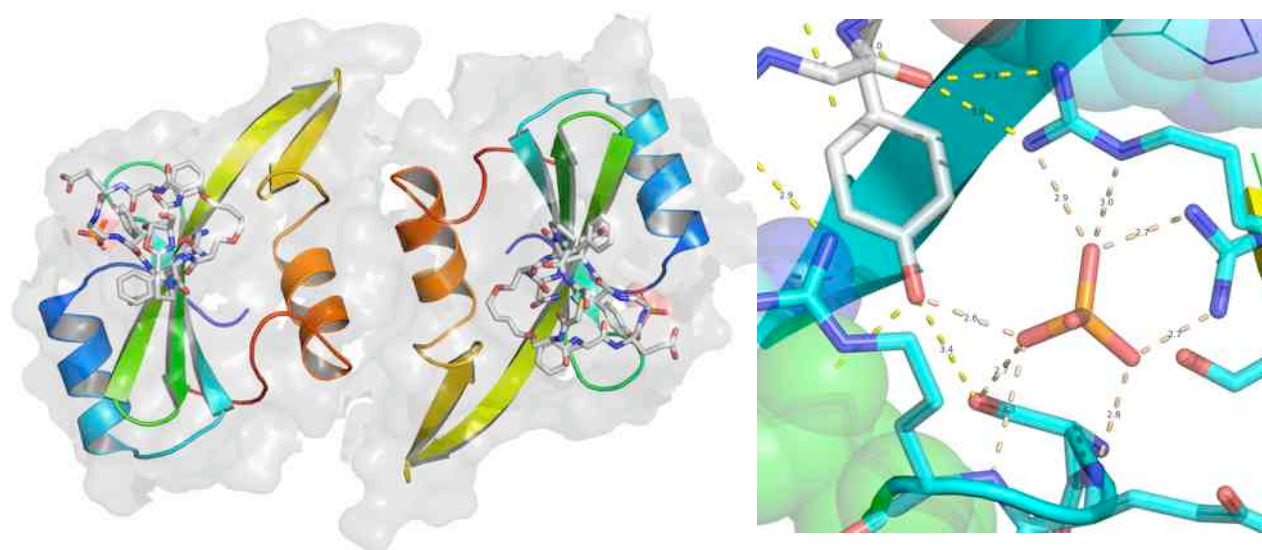


Figure 9.7 B. – The electron density map of the bicyclic G7-18NATE as observed in the binding site of Grb7 SH2 domain. The electron density is shown in blue mesh surrounding the peptide atoms. Protein residues are indicated in lines (Carbon atoms in green; Oxygen atoms in red; Nitrogen atoms in blue). Water molecules are indicated by the red crosses while the phosphate ion is indicated in yellow and red lines adjacent to the phenolic moiety of the peptide's Tyrosine residue. The map clearly shows the localization of peptide in the Grb7 SH2 domain binding site.

P 196, Figure caption 9.13: delete “conservation” and replace it with “identity”

Discovery and Optimization of Grb7 Antagonists as Potential Antitumor Therapeutics



PhD Thesis

Nigus Dessalew Ambaye, M.S.(Pharm.)

December 2010

Discovery and Optimization of Grb7 Antagonists as Potential Antitumor Therapeutics

PhD Thesis

Nigus Dessalew Ambaye, M.S.(Pharm.)

**Department of Biochemistry and Molecular Biology, School of Biomedical
Sciences, Faculty of Medicine, Nursing and Health Sciences
Monash University
Wellington Road, Melbourne, Victoria 3800
Australia**

December 2010

Table of Contents

		Page
i	Table of contents	I
ii	Declaration	VI
iii	Acknowledgment	VII
iv	Publications	VIII
v	List of abbreviations	X
vi	Thesis Abstract	XII
Chapter One	Grb7: An emerging therapeutic target	1
1.1	Signal transduction	2
1.2	The Grb7 gene and protein: biology and chemistry	3
1.2.1	The Grb7 gene structure	3
1.2.2	Homologues of Grb7 gene	4
1.2.3	Expression and Regulation	5
1.2.4	Grb7 as a mediator of signaling pathways	6
1.3	The Molecular architecture of Grb7 protein	8
1.3.1.	The N-terminus domain	9
1.3.2.	The Central GM domain	9
1.3.3.	The C-terminal domain	11
1.3.4.	The 3D-structure of the SH2 domain	12
1.4.	The Potential of Grb7 as a Drug Target	13
1.4.1	Grb7 and Breast Cancer	13
1.4.2	Grb7 and Gastrointestinal Cancer	15
1.4.3	Grb7 and Pancreatic Cancer	16
1.4.4	Grb7 and Oesophageal Cancer	16
1.4.5	Grb7 and Hepatic Cancer	17
1.4.6	Grb7 and Ovarian Cancer	17
1.4.7	Grb7 and Testicular cancer	18
1.4.8	Grb7 and Blood Cancer	19
1.4.9	Grb7 and Rheumatoid Arthritis	19
1.4.10.	Grb7 and Atopic Dermatitis	20

1.4.11	Grb7 and Immune system	20
1.4.12.	Grb7 and Arrhythmia	20
1.4.13.	Grb7 and Translation	21
1.4.14	Grb7 and Analgesia	21
1.5	The Development of Grb7 antagonists	22
1.6	Conclusion and Future outlook	27
1.7	References	28
1.8	Objectives	40
Chapter Two: Sample Preparation and Crystallographic methods		41
2.1.	Solid Phase Peptide Synthesis	42
2.1.1	Background	42
2.1.2	Synthesis of G7-18NATE derivatives and its analogues	43
2.1.3	Resin Treatment	44
2.1.4	Kaiser Test	45
2.1.5	First residue coupling to the resin	46
2.1.6	The biotinylation reaction	48
2.1.7	Synthesis on automated peptide synthesizer	49
2.1.8	Chloracetylation reaction	49
2.1.9	Ring closing metastasis	50
2.1.10	Cleavage, Precipitation and Dissolution of Peptides	52
2.1.11	Removal of CO ₂ adduct	52
2.1.12	Thioether formation	53
2.1.13	Peptide Purification	54
2.1.14	Mass spectrometry analysis	55
2.1.15	Results and Discussion	55
2.2.	Grb7 Expression and Purification	57
2.2.1	Transformation of Grb7-SH2 domain	57
2.2.2	Overexpression of Grb7 SH2 domain	58
2.2.3	Cell Lysis	59
2.2.4	Affinity chromatography separation	60
2.2.5	SDS-PAGE Gel Electrophoresis	61
2.2.6	Dialysis	62

2.2.7	Cation Exchange Chromatography	63
2.2.8	Size Exclusion Chromatography	65
2.2.9	Protein concentration Determination	65
2.2.10	Results of Grb7 SH2 domain preparation	66
2.3.	Crystallography methods	67
2.3.1	Crystallization	67
2.3.2	Crystal Optimization	67
2.3.3	Data Collection	67
2.3.4	Data Reduction	68
2.3.5	Phasing	68
2.3.6	Refinement	69
2.3.7	Model Building	69
2.3.8	References	70

Chapter Three: Uptake of a cell permeable G7-18NATE construct

into cells and binding with the Grb7-SH2 domain	74
Abstract	75
Introduction	75
Experimental Procedures	77
Results	78
Discussion	80
References	82

Chapter Four: Synthesis and Thermodynamic characterization of Second Generation G7-18NATE analogues

Abstract	84
Introduction	85
Material and Methods	86
Results	89
Discussion	102
References	104

Chapter Five: Benzopyrazine derivatives: a novel class of Growth	107
Factor receptor bound protein 7 antagonists	
Abstract	108
Introduction	108
Results	109
Discussion	113
Experimental Section	114
References	115
 Chapter Six: The discovery of Phenylbenzamide derivatives as a	 117
novel class of Grb7 based anti-tumour agents	
Abstract	118
Introduction	119
Results	120
Discussion	130
Materials and Methods	132
References	136
 Chapter Seven: Identification of Phenylpropanone Derivatives as a	 140
novel class of Grb7 antagonists	
Abstract	141
Introduction	142
Material and Methods	143
Results	148
Discussion	156
References	159
 Chapter Eight: Crystallization and Preliminary Characterization of	 163
the Grb7 SH2 domain apo and in complex with a bicyclic polypeptide	
Synopsis	164
Introduction	165
Material and Methods	166
Results and Discussion	169
References	173

Chapter Nine: Crystal structure of Grb7 SH2 domain apo and in complex with bicyclic polypeptide antagonist: A structural basis for binding selectivity	175
Abstract	176
Introduction	177
Materials and methods	178
Results and Discussion	181
References	202
Chapter Ten: General Summary and Discussion	206

Declaration

In accordance with Monash University Doctorate Regulation 17/ Doctor of Philosophy and Master of Philosophy (MPhil) regulations the following declarations are made:

I hereby declare that this thesis contains no material which has been accepted for the award of any other degree or diploma at any university or equivalent institution and that, to the best of my knowledge and belief, this thesis contains no material previously published or written by another person, except where due reference is made in the text of the thesis.

This thesis includes 2 original papers published in peer reviewed journals and 6 unpublished publications. The core theme of the thesis is design of potential antitumor agents. The ideas, development and writing up of all the papers in the thesis were the principal responsibility of myself, the candidate, working within the Department of Biochemistry and Molecular Biology under the supervision of Dr. Jackie Wilce and A/Prof. Matthew Wilce.

Signed: Nigus Dessalew

Date: 15-12-2010

Acknowledgement

First, I would like to thank my supervisors Dr. Jackie Wilce and A/Prof. Matthew Wilce for giving for me the opportunity to undertake this project. Their constant support and encouragement over the last two and half years made the realization of my project possible.

I would like to thank Prof. Mibel Aguilar and Prof. Patick Perlmutter for allowing and guiding me in their peptide synthesis laboratory. I also Thank Prof. Steve Bottomlay and Ms. We wan for their support in the isothermal titration calorimetry experiments. Thanks to Dr. Mike Kuiper of the Victorian Partnership for Advanced Computing for the support got in the computational part of my study.

Many thanks to the current and past members of the Wilce Structural Biology laboratory: Yano Yoga, Dr. Daouda Traore, Dr. Menachem Gunzburg, Dr. Reece Lim, Minyin Yap, Dr. Nicole Pardini, Dr. Simone Beckham, Dr. Andrew Sivakumaran, Dr. Henry Kim, Anna Roth, Jason Brouwer, Chris Szeto. I thank Dr. Daniel Clayton and Dr. Mark Del Borgo for their assistance and mentorship in peptide synthesis.

Finally, to my beloved families, thank you very much for your love, encouragement and understanding.

I whole-heartedly acknowledge the support I got from Monash Graduate Scholarship and Endeavor International Postgraduate Scholarship.

Publications

1. **Ambaye ND**, Lim RC, Clayton DJ, Gunzburg MJ, Price JT, Pero SC, Krag DN, Wilce MC, Aguilar MI, Perlmutter P, Wilce JA. Uptake of a cell permeable G7-18NATE construct into cells and binding with the Grb7-SH2 domain. *Biopolymers (Peptide Science)*. 2010, DOI: 10.1002/bip.21403.
2. **Nigus D Ambaye**, Menachem J Gunzburg, Reece C.C. Lim, John T. Price, Matthew C Wilce, Jacqueline Anne Wilce. Benzopyrazine derivatives: a novel class of Growth factor receptor bound protein 7 antagonists. *Bioorg. Med. Chem.*, doi:10.1016/j.bmc.2010.10.030 .
3. Menachem J. Gunzburg, **Nigus D. Ambaye**, Jack T. Hertzog, Mark P. Del Borgo, Stephanie C. Pero, David N. Krag, Matthew C. J. Wilce, Marie-Isabel Aguilar, Patrick Perlmutter and Jacqueline A. Wilce. Use of SPR to Study the Interaction of G7-18NATE Peptide with the Grb7-SH2 Domain. *Int. J. Pept. Res. Therapeut.*, 177-184,2010.
4. **Ambaye, Nigus**; Gunzburg, Menachem; Lim, Reece; Price, John; Wilce, Matthew; Wilce, Jacqueline. The discovery of Phenylbenzamide derivatives as a novel class of Grb7 based anti-tumour agents. *J. Med. Chem.* (submitted).
5. **Ambaye, Nigus**; Gunzburg, Menachem; Lim, Reece; Price, John; Wilce, Matthew; Wilce, Jacqueline. Identification of Phenylpropanones as a novel class of Grb7 antagonists. *Eur. J. Med. Chem.* (submitted)

Manuscript in preparation

1. **Nigus Ambaye**, Matthew Wilce, Menachem Gunzburg, MinYin Yap, Daniel Clayton, Mark DelBorgo, Patrick Perlmutter, Marie-Isabel Aguilar, David Krag, Stephanie Pero and Jacqueline Wilce. Structural basis of binding by cyclic non-phosphorylated peptide antagonists of Grb7 implicated in breast cancer progression. *Journal of Molecular biology*.
2. **Ambaye, Nigus**; Gunzburg, Menachem; Lim, Reece; Price, John; Wilce, Matthew; Wilce, Jacqueline. Crystal structure of Grb7 SH2 domain in complex with bicyclic polypeptide antagonist: A structural basis for binding selectivity. *Journal of Biological Chemistry*

3. **Nigus Ambaye**, Matthew Wilce, Menachem Gunzburg, MinYin Yap, Daniel Clayton, Mark DelBorgo, Patrick Perlmutter, Marie-Isabel Aguilar, David Krag, Stephanie Pero and Jacqueline Wilce. Crystallization and Preliminary characterization of the Grb7-SH2 domain apo and in complex with a bicyclic polypeptide antagonist. *Acta Crystallographica Section F: Structural Biology and Crystallization Communications*
4. **Ambaye, Nigus**; Gunzburg, Menachem; Lim, Reece; Price, John; Wilce, Matthew; Wilce, Jacqueline. Grb7: An emerging cancer drug target. Current drug targets

Conference Presentations

1. **N. Ambaye**, R. Lim, M. Gunzberg, M. Yap, M. Wilce, D. Clayton, M. Aguilar, P. Perlmutter, S. Pero, D. Krag, J. Wilce. Inhibiting Grb7 in breast cancer cells with cell permeable peptides. 35th Lorne conference on Protein Structure and Function, poster 261, Lorne, Australia, 2010.
2. **Nigus Ambaye**, Daniel Clayton, Menachem Gunzberg, MinYin Yap, Mark DelBorgo, Reece Lim, John Price, Mibel Aguilar, Patrick Perlmutter, Stephanie Pero, David Krag, Matthew Wilce and Jackie Wilce. Identification Of Benzopyrazine Derivatives As A Novel Class Of Grb7 Antagonists. Molecules of life: from discovery to biotechnology, OzBio2010, 26 September to 1 October 2010, Poster 352, Melbourne, Australia

List of Abbreviations

ACN = acetonitrile	GSH = glutathione
AD = Atopic dermatitis	GST = Glutathione S-transferase
AKT = alpha serine/threonine protein kinase	
APS = Ammoniumpersulphate	HATU = (2-(7-Aza-1H-benzotriazole-1-yl)-1,1,3,3-tetramethyluronium hexafluorophosphate)
BOC = tert-butyloxycarbonyl	Hax-1 = Hematopoietic cell-specific 1-associated protein X-1
BPS = between PH and SH2	HBTU = <i>O</i> -benzotriazol-1-yl- <i>N,N,N',N'</i> -tetramethyluronium hexafluorophosphate
CLL = Chronic lymphocytic leukemia	HCC = Hepatocellular cancer
CORT = cloning of receptor targets	hERG = human Ether-à-go-go Related Gene
DCM = Dichloromethane	HER2 = human epidermal growth factor receptor 2
DIPEA = Di-isopropyl ethylamine	
DMF = Dimethylformamide	HEPES = 4-(2-hydroxyethyl)-1-piperazine ethane sulfonic acid
DMSO = dimethylsulphoxide	HoBt = Hydroxybenzotriazole
DRG = Dorsal root ganglion	HPLC = high performance liquid chromatography
DTT = dithiethanol	HuR = ELAV-like protein 1
EDTA = Ethylenediamine tetraacetic acid	IGF-1 = Insulin-like growth factor 1
EGFR2/EGFR3/EGFR4 = Epidermal growth factor receptors 2/3/4	IgG-FITC
EphB1 = Ephrin type-B receptor 1	IPTG = β -D-1-thiogalactopyranoside
ERK1 = extracellular signal-regulated kinase 1	IR = insulin receptor
EDT = Ethanedithiethanol	JNK = c-Jun N-terminal kinases
ErbB2/ErbB3 = Human Epidermal growth factor Receptor 2/3	Kir1.1, Kir1.5, Kir2.2, kir2.4 =
FAK = Focal Adhesion kinase	c-Kit/SCFR = cytokine stem cell factor receptor
FHL2 = four and half lim domains isoform 2	KOR = kappa opioid receptor
FGF = fibroblast growth factor	Kv1.5, Kv4.3 = Potassium voltage gated channel, shaker related subfamily, member 1.5/4.3
Fmoc = 9-fluorenylmethoxycarbonyl	LB = Lysogeny broth
FPLC = fast protein liquid chromatography	
GM = Grb and migratory 10	
Grb 7/10/14 = Growth factor receptor bound proteins 7/10/14	
Mes = 2-(N-morpholino)ethanesulfonic acid	
MWCO = molecular weight cut-off	
Nedd4 = neural precursor cell expressed, developmentally down-regulated 4	

NMP = N-methylpyrrolidone
PAGE = polyacrylamide gel electrophoresis
PDGFR = Platelets derived growth factor
Pro = proline rich domain
PH = pleckstrin homology
PBS = phosphate buffer saline
RA = Rheumatoid arthritis
RA domain = Ras associating domain
RAS = RAt Sarcoma
Ret = rearranged during transfection
Rnd1 = Rho family GTPase 1
ROMK = Renal Outer Medullary Potassium channel
SDS= sodium dodecyl sulphate
Shc = Src homology 2 domain
containing transforming protein 1
SH2 = Src homology 2
SHPTP2
SPOS = solid phase organic synthesis
SPPS = Solid phase peptide synthesis
TEMED = Tetraethylmethylenediamine
Tek/Tie2 = Tyrosine kinase
with immunoglobulin-like
and EGF-like domains 1
TGCT = Testicular germ cell tumors
TIPS = Tri-isopropyl Silan
Trifluoro acetic acid(TFA)
Tris= tris(hydroxymethyl)aminomethane

Thesis Abstract

The growth factor receptor bound protein 7 (Grb7) is a non-catalytic adaptor protein that was originally identified as a binding partner of the growth factor receptor (ErbB-2). Amplification and overexpression of Grb7 is frequently implicated in the development of aggressive, recalcitrant and advanced tumor phenotypes making it a promising target in human cancers. Apart from several peptide-based experimental antagonists, to date there exist no potent drug that is developed or known to act against Grb7. Thus, the overall objective of the research conducted in this thesis was to design novel, potent, selective and cell permeable Grb7 antagonists that may have potential as antitumor therapeutics. The first part of the thesis deals with optimization studies around a known lead polypeptide designed to bind to the Grb7 SH2 domain. A total of 11 polypeptides were synthesized with a yield varying from 2 to 17%. The peptide antagonists were found to have moderate binding affinity ranging from 0.6 – 60 μ M as determined by isothermal titration calorimetry. Moreover, a short 7 residue cell permeablising sequence was incorporated into the inhibitor peptide construct and its ability to translocate peptides across membranes tested in *in vitro* and cell based assays. The second part of the thesis focused on small molecule antagonist discovery and optimization. Starting from known peptide leads and an experimental structure of the Grb7 SH2 domain, a series of ligand design techniques comprising shape based similarity searches, molecular docking and 2D-similarity searching was effected to identify non-peptide antagonists. In total, three structurally distinct classes of small molecular antagonists with moderate *in vitro* affinity and *in vivo* activity were identified from the study. The last part of the project reports the crystal structure determination of two Grb7 SH2 domain constructs. High-resolution crystal structures of the apo- and peptide-bound forms of the Grb7 SH2 domain were determined. All together, extensive biophysical, computational and structural analyses were conducted on the Grb7 SH2 domain and ligands that will form the foundation for future Grb7 inhibitor development.

Chapter 1

Growth Factor Receptor Bound Protein 7: A Novel drug Target

This chapter presents a comprehensive review of the relevance of Grb7 as a potential antitumor therapeutic target. Starting from the basic chemistry and biology of the Grb7 protein, our understanding of the Grb7 protein structure and function is discussed. Other disease state where Grb7 is implicated as well as its regulatory role in wide-ranging biological processes is presented. The last section of this review deals with advances made in the developments of Grb7 antagonists.

1.1. Signal transduction

Signal transduction pathways represent a cascade of biochemical transformation reactions that involve a variety of biomolecules as reactants, catalysts and final products.^{1,2} These pathways impact many aspect of cellular life ranging from protein and nucleic acid synthesis, growth, differentiation and division of cells to migration and ultimate death of cells. As a result, the precise and coordinated execution of every signal transduction pathway is critical for the proper functioning of every organism.³ To effect this, cells have developed a network of communication channels to perceive, process and respond synchronously to any physical, chemical or biological signals.^{4,5} Errors in signal transduction pathways result in a break in cellular regulation that may be commonly manifested in the form of a disorder at the organism level.⁶ In cancer, for example, there frequently is up regulation of signaling events which ultimately give rise to uncontrolled and unwanted cell formation, proliferation and migration.^{7,8} Owing to the importance of controlling signaling events to organismal life and the growing understanding of the molecular mechanisms in signaling pathways, signal transduction inhibitors are increasingly sought as therapeutic agents in human maladies such as cancers⁹⁻¹¹ and inflammatory disorders.^{12,13}

The sequencing of the human genome and the accompanying advances in genomic and proteomic sciences have contributed to the discovery of a myriad of biomolecules as potential drug targets. This is especially evident in diseases such as cancers where there is a huge unmet medical need. Among the many promising novel targets that are being investigated in cancer are intracellular components of growth factor dependent and other oncogenic signal transduction pathways. This review zeroes in on Grb7-a cytoplasmic protein important in a number of signaling pathways-that is rapidly emerging as a relevant antitumor target. Following a description of the fundamental biology and chemistry of Grb7, the main body of this chapter revolves around the relevance of Grb7 as a therapeutic target. The last section will then elaborate on the current state and progress made in the development of Grb7 antagonists. A brief outlook on the future and potential of Grb7 based anticancer drug discovery will conclude this chapter.

1.2. The Grb7 Gene and Protein: Biology and Chemistry

Growth factor receptor bound (Grb) proteins belong to the adaptor protein superfamily of biomolecules.¹⁴ Adaptor proteins are non-catalytic molecules that function as mediators of signal transduction pathways.¹⁵ As the name implies, Grb proteins were originally identified because of their ability to associate with growth factor receptors.¹⁶ Characteristically, Grb proteins form supramolecular complexes with growth factor receptors that are essential for growth factor mediated signal transduction,^{17,18} though interactions with non-growth factor receptors is also well documented, and perhaps equally important.^{16,18} Currently there exist about 14 Grb proteins, where most are being implicated in the genesis and development of human cancers.¹⁶

Grb7 belongs to a subfamily of Grb proteins comprising Grb7, growth factor receptor bound protein 10 (Grb10)^{19,20} and growth factor receptor bound protein 14 (Grb14).^{21,22} This Grb7 family of adaptor proteins is known to have high sequence and functional homology.^{17,22} This class was discovered using a technique dubbed CORT (cloning of receptor targets), an expression/cloning system that uses a tyrosine phosphorylated receptor as a probe to screen protein libraries.²³ Specifically, Grb7 was identified using CORT screening of a mouse cDNA expression library with tyrosine phosphorylated C-terminus of the epidermal growth factor receptor.^{24,25} In common with other adaptor proteins, Grb7 facilitates the coupling of multiple trans membrane and cytoplasmic receptors to downstream effector molecules.^{16, 26}

1.2.1. The Grb7 Gene Structure

The human Grb7 gene is located on the positive strand of chromosome 17. Cytogenetic analysis shows that the gene is mapped to the 17q12-q21 loci, as documented by the National Centre for Biotechnology Information (NCBI) (<http://www.ncbi.nlm.nih.gov/mapview/>). The human Grb7 gene is 9,352 nucleotides in length and known to encode a major primary Grb7 RNA transcript of 4,596 nucleotides in size. The final mature Grb7 mRNA is composed of 14 exons of 1,599 nucleotides in length. The chromosomal location of Grb7 is interesting as it is within the erbB2 amplicon,^{27,28} a region known to comprise genes frequently over

amplified in cancers.²⁹ As will be described later, the localization of Grb7 on the erbB2 amplicon is what appears to be at the heart of most of the human malignancies mediated by Grb7. Fig. 1.1 shows the overall organization of Grb7 gene and its products.

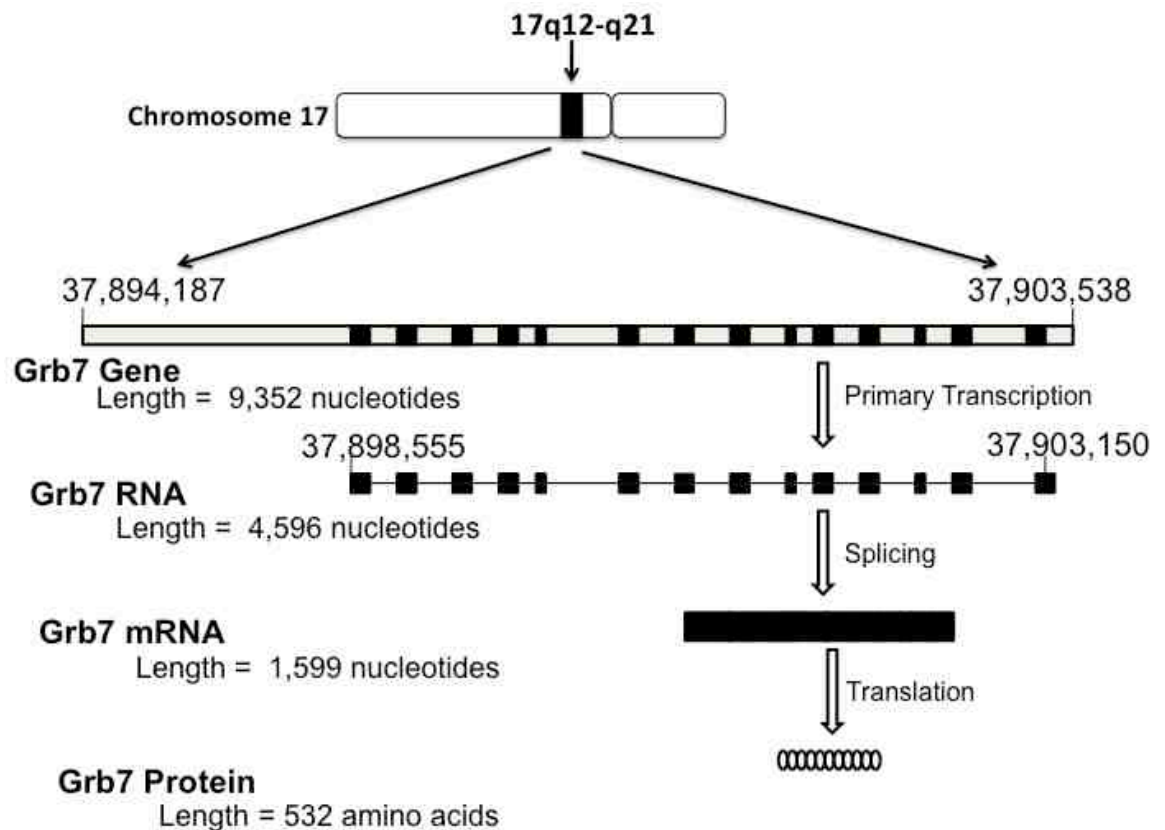


Figure 1.1: The overall organization of Grb7 and its products. Grb7 is localized on the long arm of chromosome 17, at 17q12-q21. It is comprised of 14 exons which are indicated in filled boxes shown in their approximate location. The introns are shown as lines bridging the exons. In Grb7 mRNA all the exons are merged and represented by single full filled rectangle. The numbers on top of each depiction represent the start and end of a given nucleotide sequence. Grb7 protein is represented by a string of ellipses.

1.2.2. Homologues of the Grb7 gene

Model organisms are valuable for the study of the pathophysiological function of a human gene and its product in drug development projects.³⁰ The finding of a homologous gene in a suitable experimental organism and its comparative functional characterization is thus an important undertaking. Analysis of homologous genes Grb7 suggest that it is evolutionarily conserved across mammals as the gene and its protein product are found in a number of mammalian species.

Table 1.1 shows the different animals where orthologues of Grb7 are noted, according to the HomoloGene database of the NCBI interface (www.ncbi.org). Interestingly, the sequence homology found between the Grb7 genes is appreciably high (85-99%) which is also reflected in the Grb7 protein similarity (88-99%). Given the fact that sequence similarity dictates functional similarity, at least in most of the cases, the high sequence homology seen may be usefully exploited in the investigation of potential Grb7 antagonist development, for example, in Grb7 knocked out experiments.

Table 1.1: Sequence similarities of Grb7 homologues to human Grb7

Organism	Chromosomal location	Gene similarity	Protein length	Protein similarity
Human	17	100	532	100
Chimpanzee	17	99.5	532	99.8
Dog	9	88.8	542	93.8
Cattle	19	87.0	532	88.7
Mouse	10	86.2	535	91.0
Rat	11	85.9	535	91.1

1.2.3. Expression and Regulation

The Grb7 protein reportedly displays a distinct expression profiles across species, tissues and organs.²³ It is found to be expressed in number of human tissues including placenta, intestine, brain, lung, kidney, esophagus, mouth, prostate, mammary gland, uterus, ovary, cervix, liver, pancreas, testis, embryonic tissue, lymph node, trachea, larynx, bladder, thymus, skin, eye, ascites, stomach, pharynx and connective tissue [Unigene, www.ncbi.org]. However, it is the overexpression of Grb7 that is associated with a number oncogenic pathways and human maladies (discussed below). As to its cellular localization, Grb7 is an intracellular protein primarily found in the cytosol though it is indicated that it can be found on the focal contacts, mitochondria and cell membrane under certain circumstances.³¹ In addition, Grb7 is found to be localized as an integral component of stress granules. Apart from the main Grb7 protein, a splice variant of Grb7 termed Grb7v is also noted to be expressed in certain tissues.³²

Grb7 has multiple phosphorylation sites that are reported to control its overall signaling function. For example, the phosphorylation of Grb7 on a number of serine and threonine residues is reported. However, the biological significance of such phosphorylation is yet to be fully elucidated.³³⁻³⁵ By far, the most important phosphorylation reaction that is well studied and known to regulate Grb7 function is that of tyrosine phosphorylation. Specifically, the role of the cytoplasmic focal adhesion kinase³⁶ in phosphorylating Grb7 and the impact thereof is widely investigated.³⁷ In a recent report, Chu et al employed a mutagenesis study to investigate the role of Grb7 phosphorylation by FAK on cancer cell migration and proliferation. Their findings showed phosphorylation of Grb7 by FAK at its Y188 and Y338 residues and that by mutating these two residues to F188 and F338, impairment of Grb7 mediated cell migration and proliferation was noted. This might indicate the relevance of Grb7 phosphorylation in tumorigenesis.³⁸ Related studies that establish the role of Grb7 phosphorylation on Grb7 function is that conducted on the interaction of Grb7 with four and half lim domains isoform 2 (FHL2), a transcription regulator important in oncogenesis.³⁹ The report showed the importance of Grb7 phosphorylation for interaction with FHL2 and that mutation of Grb7 Tyr residues to Phe resulted in mutant Grb7 with insignificant affinity to FHL2.³⁹ Furthermore, among the latest roles of Grb7 to be discovered is its ability to act as a translational repressor through binding to RNA for which the phosphorylation status of Grb7 was found to be critical. It was shown that Grb7 phosphorylation on its Y483 and Y495 residues was found to be detrimental for Grb7 binding mRNA.⁴⁰ These examples illustrate the role of Grb7 phosphorylation in the control of the adaptor function of Grb7. Extensive investigation of the impact of Grb7 phosphorylation on its diverse functions is yet to be conducted. Apart from tyrosine phosphorylation, other mechanisms that are suggested to regulate Grb7 function are dimerization⁴¹ and localization.^{42,43}

1.2.3. Grb7 as a mediator of multiple signaling pathways

Though Grb7 was initially identified as a binding partner of growth factor receptors,^{23,35} it has been shown in numerous studies to interact with a diverse spectrum of biomolecules since then. These include the growth factor receptors (EGFR, EGER2/HER2/Neu/ErbB2, EGFR3/erbB3, PDGFR, FGF, IGF-1), trans

membrane receptor tyrosine kinases (IR, Ret, Tek/Tie2, c-Kit/SCFR, EphB1), cytoplasmic protein kinases (FAK) phosphatases (SHPTP2), GTPases (Rand1), ligases (Nedd4), adaptor proteins (Shc) and other miscellaneous biomolecules such as caveolins, Netrin-1, FHL2, Hax-1, phosphoinositides.^{31,35,44,45} Though diverse and numerous, these are all upstream binding partners and as yet a downstream binding partner of Grb7 is to be identified.

Table 1.2: Binding partners of Grb7 protein

Binding partner	Recognition motif	domain
Growth factor receptors		
EGFR	not determined	SH2
EGFR2	PQPEpYVNQPD	SH2
EGFR3	EEYE pYMNRRR	SH2
EGFR4	not determined	SH2
PDGFR	YMAPpYDNYVP	SH2
FGF	not determined	SH2
IGF-1	not determined	SH2
Receptor tyrosine kinases		
IR	not determined	SH2 and BPS
Ret	not determined	SH2
Tek/Tie2	ERKTpYVNTTL	SH2
c-Kit/SCFR	TNHIpYSNLAN	SH2
EphB1	KMVQpYRDSFL	SH2
Cytoplasmic Protein kinases		SH2
FAK	ETDDpYAEIID	SH2
Protein Phosphatases		
SHPTP2	SARVpYENVGL	SH2
GTPases		
Rand1	YDN	SH2
Adaptor proteins		not determined
Shc	DDPSpYVNVQN	SH2
RNA	not determined	N-terminal
Miscellaneous		
Caveolin-1	EGHLpYTVPI	SH2
Netrin-1	not determined	N-terminal
FHL2	not determined	PH and RA
Hax-1	not determined	PH and RA
G6f	ELQVpYENIHL	SH2
3'-phosphoinositides	not determined	PH
HuR	not determined	N-terminal

Table 1.2 shows the various binding partners of Grb7, the domain of Grb7 involved and the recognition motif. Interestingly, most of the upstream binding partners of Grb7 are connected with a number of cancer cell properties.^{46,47} For example, the integrin pathway via FAK is important for cell migration.^{47,48} Besides, the various growth factor receptors are frequently implicated in growth and proliferation of cancer cells.⁴⁹ Indeed there are clinically available anticancer drugs in use that act on EGFR2 (also known as HER2 and ErbB2) such as Trastuzumab (Herceptin®),⁵⁰ Erlotinib (Tarceva®),⁵¹ and Gefitinib (Iressa®).⁵² Trastuzumab is a humanized monoclonal antibody that binds to the extracellular domain of EGFR2 whereas Gefitinib and Erlotinib are a small molecule drugs that bind to the ATP binding site of the intracellular kinase domain of the receptor. As the formation of EGFR2 and Grb7 signaling complex occurs in ErbB2 over expressing cancer cells, the availability of Grb7 inhibiting agents might provide an insight into the role and druggability of Grb7 in cancers. Apart from the above shown interaction partners of Grb7, a number of membrane bound macromolecules such as phosphoinositides are reported as important partners of Grb7 mediated signaling.⁵³

1.3. The molecular architecture of Grb7 protein

The human Grb7 protein is comprised of 532 amino acids. Its constituent residues are organized into a number of protein domains that serve different but complementary functions to the overall signaling role of Grb7.¹⁶ Grb7 domain components are well conserved across the mammalian species, and serve similar roles.^{35,16} The modular structure of Grb7 is composed of a proline rich domain, a Ras-associating domain, a pleckstrin homology (PH) domain, Src homology 2 (SH2) domain and a BPS domain (between the PH and SH2 domains).^{54,56} Fig. 1.2 illustrates the various domains of Grb7 together with the approximate amino acid residues.^{35,44} Our current knowledge of Grb7 domains will be described in greater detail under each heading.

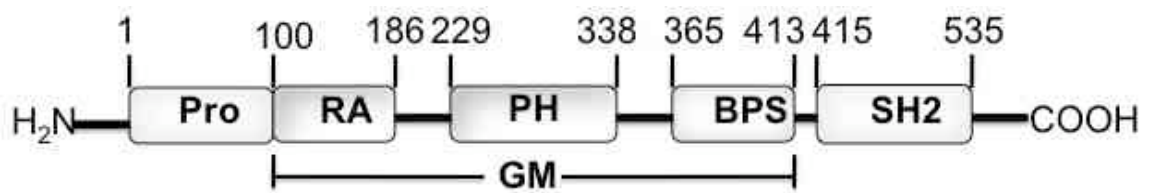


Figure 1.2. The modular organization of Grb7 protein. Numbers indicate the start and end residue number of the respective domains. Pro= proline rich domain; RA= Ras associating domain; PH= pleckstrin domain; BPS= between PH and SH2 domain; SH2 = Src Homology domain

1.3.1. The N-terminal Domain

The N-terminal domain of Grb7 represents the first 100 residues of the Grb7 protein. It is a motif comprising a conserved sequence rich in prolines and is likely to exist as an unstructured domain in the absence of a binding partner. Up until now little has been known as to the binding partners of Grb7 via its N-terminal domain.⁴⁰ Recently, however, experiments have come forth indicating novel potential binding partners for this part of the protein. For instance, mouse Grb7 has been shown to interact with HuR,⁵⁷ an RNA-binding protein important in regulation of nuclear-to-cytoplasmic shuttling of mRNA.⁵⁸ The Grb7-HuR interaction was found to be mediated by the N-terminal domain of Grb7.⁵⁷ Moreover, mouse Grb7 is also found to bind RNA via its proline rich N-terminal domain.⁵⁷ These interactions have yet to be verified for human Grb7 and their physiological function remain to be elucidated.

1.3.2. The Central GM region

The region of Grb7 bounded by the N- and C-terminal domains is what is referred to as the central GM, for Grb and Mig domains.³⁵ It consists of the longest stretch of Grb7 comprising about 300 amino acid residues. Its role in Grb7 signaling is much more studied and better understood than the N-terminal domain. It displays more than 50% sequence similarity with the *Caenorhabditis elegans* protein MIG-10^{59,60} from which it derives its name. MIG-10 (Migratory-10) is established to be critical for cell migration during embryogenesis.⁶¹ The presence of such a conserved sequence with known function lured researchers to investigate the role of Grb7 in cell migration, which predictably was subsequently verified. It is postulated that it is

because of this domain that Grb7 is an important cell migratory protein.^{39,42} The GM region is known to comprise three well conserved but non-contiguous domains: Pleckstrin homology (PH) domain, RA (Ras-associating) domain and a BPS (between PH and SH2) domains.^{16, 54}

The PH domain is 110 amino acids long and corresponds to residues 229-338 of Grb7. It is suggested to bind membrane bound phosphoinositides⁴² thereby assisting Grb7's association to these molecules. Moreover, it is found to interact with FHL2, a signaling protein associated with transcription regulation and cytoskeletal re-arrangement.³⁹ Recently it is also reported to interact with Hax-1 (Hs-1 Associated protein X-1), another protein important in cell migration and apoptosis, and to have a role in Grb7 dimerization in a head to tail manner.^{39,62} As a part of the GM region it is known to play a role in cell migration

The RA domain of Grb7 is 87 amino acids long stretching from 100 to 186 residues. Along with the PH domain, it is found to be important in the intramolecular dimerization of Grb7 by interacting with the SH2 domain, where the interaction is found to be of micromolar affinity.^{62,63} The phenomenon of dimerization is an important mechanism for the functioning of Grb7.⁶⁴ The RA domain is found in a number of proteins. It is also suggested to have a role in the involvement of Grb7 in the Ras signaling pathway and for cell proliferation.^{65,66} Together with the PH domain, the RA domain is reported to interact with the Hax-1 protein.⁶²

The BPS domain is a functional region of about 65 residues corresponding to residues 365-413 of Grb7. It is found between the PH and SH2 domain. The BPS region is thought to facilitate the interactions of SH2 domain to upstream partners of Grb7.⁶⁷ Moreover, it is suggested the BPS domain could contribute to the specificity of Grb7 binding to its partners.^{68,69} In the other Grb7 families such as Grb10 and Grb14, the BPS domains is found to interact with the activated IR and IGFR.⁷⁰ It displays up to 60% sequence similarity among the Grb7 family members, The BPS domain is found to be intrinsically unstructured,⁷¹ though a very short structured stretch of about 9 residues was identified for the Grb14 protein.⁷²

1.3.3. The C-terminal domain

By far the most widely thoroughly investigated region of Grb7 is the C-terminal Src homology 2 (SH2) domain.^{57,73} It corresponds to residues 415-535 of the Grb7 protein. SH2 domains are phosphopeptide-binding modules that are found in a number of related proteins.⁷⁴ Indeed, the discovery of Grb7 as adaptor protein was dependent on this property of SH2 domain. It is known to mediate the physical association Grb7 with a diverse array of membrane bound and cytoplasmic binding partners of Grb7.^{34,44} In particular, the SH2 domain is responsible for the recognition of specific phosphotyrosines (pTyr) residues via a well-described cationic pocket and surrounding peptide-binding cleft.^{74,69} The SH2 mediated association of Grb7 with its binding partners commences the first and, thus, a critical step in Grb7 dependent signal transduction. As such it forms an essential module for the variety of Grb7 mediated oncogenic transformations.^{44,46}

The binding specificity of the SH2 domain to upstream partners of Grb7 has been characterized at length.^{34,46} These studies have deciphered the sequence around the phosphorylated tyrosine recognized by Grb7 to be more or less conserved, from which a recognition motif of the sequence pYXN has been established. In other words, the presence of asparagine at the +2 position relative to the phosphorylated tyrosine (pY) is what the SH2 domain of Grb7 specifically demands of its binding partners.^{34,44} The position at +1 to the pY residue, indicated as X is where any amino acid would be tolerated. This condition for recognition by SH2 domain is found in the great majority of Grb7 binding partners with erbB2,⁷⁶ erbB3,⁷⁴ Tek,⁷⁷ c-Kit,⁷⁸ SHPTP,⁷⁹ Shc,¹⁹ PDGFR,²⁶ being the notable examples. However, some exceptions has been noted where the +2 Asparagine is not required as in FAK (pYAE),³⁵ EphB1 (pYRD),⁸⁰ cavelin (pYRD) ⁷⁵ or where even the tyrosine does not have to be phosphorylated as in RndI (YDN).⁸¹

1.3.4. The 3D-structure of Grb7 SH2 domain

The experimental structure of Grb7 SH2 domain has been solved both by NMR and X-ray crystallography.^{68,82} The crystal structure is solved to 2.1 Å resolution with an overall tetrameric assembly by our group (PDB ID: 2QMS). As shown in Fig. 1.3, the Grb7 SH2 domain comprises an anti-parallel β -sheet flanked by a pair of α -helices.^{63,68} Such a fold is a general feature of SH2 domain proteins.^{54,57} According to the accepted nomenclature,⁶⁸ the central anti-parallel β -sheet is formed by the β B, β C and β D loops where as the two α -helices are labeled α A and α B (see Fig. 1.3 for details) which implies that the domain fold of Grb7 could be described as α A β B β C β D α B.

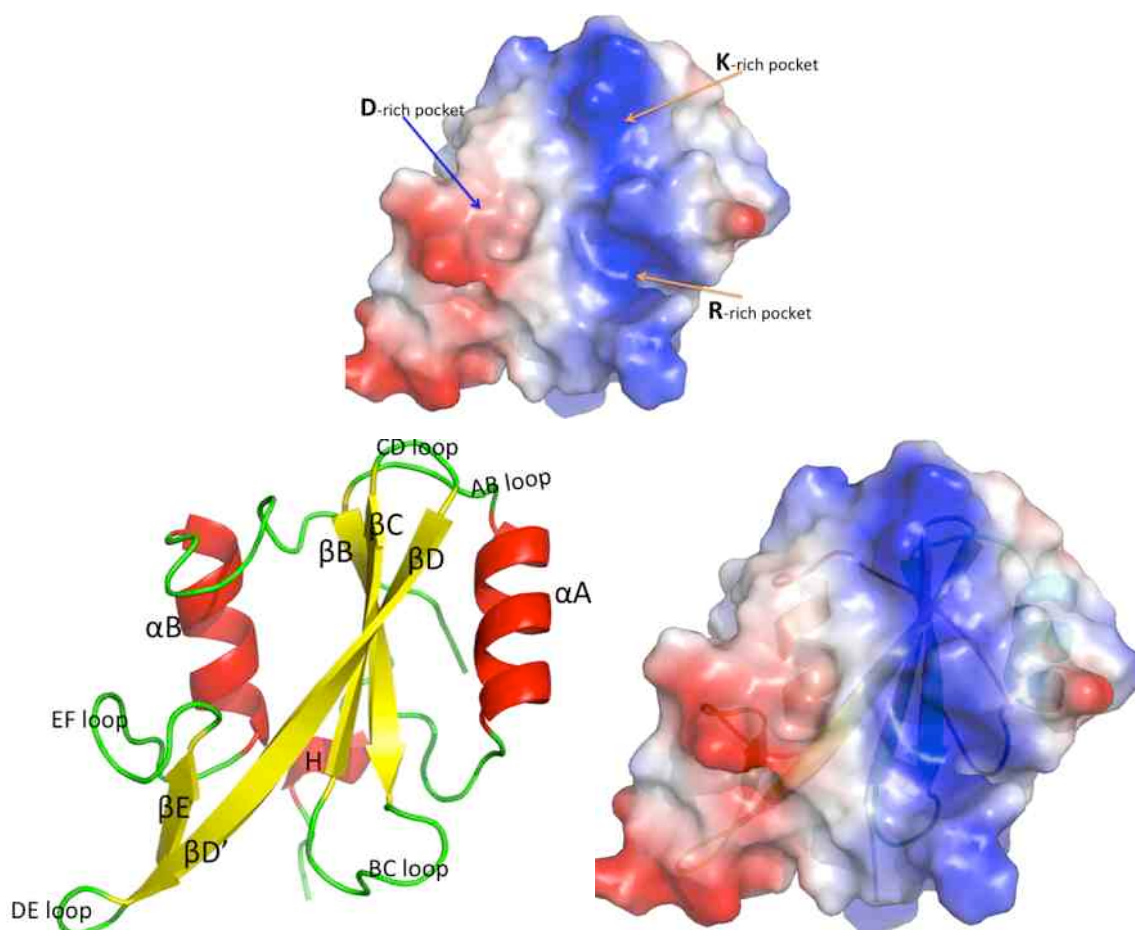


Figure 1.3. Domain fold of Grb7 SH2 protein. *Top*: vacuum electrostatic map showing the subpockets of the binding site as blue (positively charged); red (negatively charged); gray (neutral) regions. *Bottom left*: Cartoon representation of the Grb7 SH2 domain shown as helix (red); B-sheet (yellow) and loops (green) and the structural labeling. *Right*: superposition of the electrostatic map with the secondary structural elements.

The electrostatic map obtained for Grb7 SH2 apo structure reveals that the binding site is comprised of well defined, contiguous and distinct subpockets.^{40,68} Specifically, a positively charged phosphotyrosine binding pocket is noticed to comprise of arginine and lysine rich sub pockets. These are adjoined by an aspartic acid rich anionic pockets with each separated by a stretch of hydrophobic residues. In the crystal structure, the pTyr recognition pocket is seen to retain a sulfate residue from the crystallization conditions.⁶⁸ In the reported apo structure, a number of hydrogen bonding interactions between the sulfate ion and binding site residue atom on the BC and other loops are observed providing invaluable information for ligand design purposes.

1.4. The Potential of Grb7 as a Drug Target

Grb7 is found as a downstream effector of several signaling pathways.^{43,44,54} What is more, most of these pathways are previously known to be deregulated in human maladies, especially in cancer.^{83,84} This has prompted an investigation of the role of Grb7 in different properties of cancer cells such as migration, invasion and metastasis. Other disease states related with cell development and movement were also the center of investigation. In what follows, we provide a review of the role of Grb7 in different human maladies that has surfaced in the recent literature.

1.4.1. Grb7 and Breast Cancer

Breast cancer is one of the major types of adult tumors accounting for about 10 % of all cancer incidences among women and the fifth most common cause of cancer related death globally.⁸⁵ It is characterized by the levels of tumor size, stage, estrogen receptor sensitivity and lymph node involvement.⁸⁶ Gene amplification is a common mechanism of oncogenesis in breast cancer. Extensive histochemical and biochemical investigations are being conducted to unravel the specific genes and gene products that could be of use in the prognosis, prediction or a drug target in breast cancer patients.^{87,88}

Targeting Grb7 is thought to be of importance in the development of breast cancer on a number of grounds. First, Grb7 is found to be overexpressed in a number of

breast cancer cell lines, in particular, its co-overexpression and co-amplification with ErbB2 is widely investigated.^{16,31} This emanates from the fact that ErbB2 and Grb7 are found on the same chromosomal region at 17q12-q21, termed the erbB2 amplicon.^{89,90} Moreover, ErbB2 is already established target for clinically used drugs for breast cancer⁸⁹ such as the antibody Trusumutab⁵¹ and the small molecule anticancer agent Gefitinib.⁵³ Second, as described above, Grb7 and ErbB2 form a functional association in growth factor dependent signalling⁴⁵ and hence their importance in growth factor sensitive breast cancers. Third, as Grb7 is a downstream mediator of a number of oncogenic pathways parallel to the ErbB2 pathway, targeting Grb7 might provide an attractive additional alternative to turn off oncogenic pathways.

The mechanism of action of Grb7 in breast cancer cell lines has been widely researched. Grb7 has been shown to synergistically enhance tumor formation with ErbB2.^{76,91} The mechanism for Grb7 dependent tumor formation is described in a recent paper⁹² where activation of Grb7 is found to recruit and activate Ras-GTPases. This in turn is shown to promote phosphorylation of ERK1/2, thereby stimulating tumor growth. Moreover, co-overexpression of Grb7 and ErbB2 have also been associated with worse outcome in some set of breast cancer subjects.⁹³ The fact that Grb7 is found within the core of the ErbB2 amplicon at 17q12 is what explains most of the co-implications in breast cancer. However, a study conducted to identify the contribution of co-amplified genes has demonstrated that Grb7 alone may be a factor in breast cancer carcinogenesis. With the use of RNA interference technology, it is has been shown that Grb7 knockout SKBR3 and BT474 breast cancer cell lines possessed decreased cell proliferation and cell-cycle progression.⁹⁴ Moreover, recent experiments involving siRNA have shown that removal of Grb7 by RNA-interference reduced the viability of BT474 xenograft cancer cells and increased the activity of the antitumor drug lapatinib.⁹⁵

Breast cancer is commonly treated with estrogen competitive antagonists such as Tamoxifen and clomiphene and estrogen non-competitive antagonists like aromatase inhibitors. However, such drugs are effective only when the tumor is sensitive to the endogenous estrogen hormones. And in the late stage of breast

cancer the tumor is well known to advance into a resistant phenotype.⁹⁶ In this regard, a recent work has found Grb7 to be one of the genes involved in the transformation into estrogen-independent proliferating cells.⁹⁷ This investigation illustrates that the level of Grb7 could be a reason for treatment failure of estrogen antagonists and hence could be exploited to device the course of therapy in breast cancer patients.⁹⁸ In fact, related investigation have included Grb7 detection as a part of a commercially available kit used to assess risk status and prediction of prognosis for patients with breast cancer.⁹⁹

Finally there exist practical data demonstrating the amenability and relevance of Grb7 in breast cancer patients. To this effect, Pero et al. have showed that Grb7 could be inhibited with synthetic polypeptide antagonists which in turn were found to block the proliferation of four human breast cancer cell lines such as SK-BR-3, MDA-MB-231, MDA-MB-361, ZR-75-30 cells.¹⁰⁰ Moreover, adjuvant treatment of the peptide with known anticancer agents such as the antibody Herceptin and the antibiotics Doxorubicin was noted to reduce the IC₅₀ of Herceptin and Doxorubicin up to 84 % on the above breast cancer cells.¹⁰⁰

1.4.2. Grb7 and Gastrointestinal Cancer

Gastrointestinal cancer is one of the commonest forms of cancer.¹⁰¹ Gastric cancer is known to insidiously develop to its deadly advanced form with little chance of early detection and treatment.¹⁰² Recently, in research conducted to delineate the molecular mechanisms underlying the cause and development of gastrointestinal cancers,¹⁰² Grb7 was identified as one of the culprits. The study found that over expression of Grb7 was noted in as many as 31% of esophageal carcinomas and that the over expression was shown to strongly correlate with extra mucosal invasive potential of gastric tumors.¹⁰³ In a related study, more than 8-fold amplification and over expression of ErbB2 and Grb7 in primary gastric cancer cells was reported.¹⁰⁴ Furthermore, it was observed that such over expression was associated with the development of more aggressive gastric cancer phenotypes.¹⁰⁴ Another study on the quantitative estimation of Grb7 in gastrointestinal adenocarcinoma showed overexpression of Grb7 in up to 32% as compared to the normal Grb7 level in gastrointestinal cells.¹⁰⁵ The overexpression of Grb7 has been confirmed by an

independent study involving analysis of gene copy number and expression profiling of genes in upper gastrointestinal adenocarcinomas.¹⁰⁶ Finally, a related comparative genomic hybridization experiment has found Grb7 as one of the genes whose DNA copy number is highly correlated with its mRNA expression in gastric cancer.¹⁰⁷

1.4.3. Grb7 and Pancreatic Cancer

Pancreatic cancer is among the most aggressive and leading causes of cancer deaths worldwide.¹⁰⁸ The clinical relevance of Grb7 expression in pancreatic cancer was studied by Tanaka et. al. with the application of immunohistochemical analysis.¹⁰⁹ The study noted overexpression of Grb7 in 61% of pancreatic cancer cell lines as compared to non-cancerous samples.¹⁰⁹ In addition, the overexpression of Grb7 was shown to be elevated in pancreatic cancer patients with lymph node metastasis (ca. 77%) in contrast to those without the metastasis,¹⁰⁹ indicating a relationship between Grb7 level and metastatic potential of pancreatic tumors. Furthermore, related experiments have shown Grb7 and erbB2 co-overexpression in pancreatic cancer cells.¹¹⁰ A proof of concept in targeting Grb7 in pancreatic cancer has been provided by Tanaka et al, from Grb7 knockout experiments. They showed that the use of siRNA to knockdown Grb7 in pancreatic cell is associated with reduction of migratory potential of pancreatic cancer cell lines.¹⁰⁹ In a recent experiment, Furuyuma and co-workers have examined the significance of FAK in pancreatic cancer formation to discover that FAK was expressed in up to 48% of the studied cases and, importantly, its expression was found to relate to tumor size.¹¹¹ Since Grb7 is known to associate with and be activated by FAK, it might be the case that Grb7 has been co-implicated in the pancreatic tumor size. Genes on 17q12-q22 chromosomal region, which also includes the Grb7 locus, are noted to be amplified in some pancreatic tumors.¹¹² Finally, published data exist where the association of Grb7 with FAK in pancreatic cancer cells was disrupted with the use of synthetic polypeptide which in turn resulted in reduction of pancreatic cell migration and metastasis.¹⁰⁹

1.4.4. Grb7 and Oesophageal Cancer

Oesophageal cancer is a rarely curable with a low 5-year survival rate ranging from

5% to 30%.¹¹³ The development of an invasive and metastatic phenotype of the cancer is a huge risk factor.¹¹⁴ Grb7's role in esophageal cancer formation is well documented.¹¹⁵ For example, up to 45% Grb7 overexpression was noted in some esophageal carcinomas as compared to normal mucosa.¹¹⁶ In addition, Grb7 overexpression was directly related with the development of lymph node metastases¹⁰³ which suggest Grb7 overexpression as a major risk factor in such cancer populations. Epidermal growth factor and fibronectin stimulated tyrosine phosphorylation of Grb7 was noted in certain esophageal carcinoma cell lines. Such fibronectin-dependent phosphorylation of Grb7 was regulated by the integrin and FAK signaling system that was found to cause migration of esophageal carcinoma cells and transformation to the more invasive and metastatic phenotypes of esophageal tumour.³² Moreover, co-over expression of Grb7 with ErbB2 is reported in high grade dysplasia and gastric carcinoma.¹¹⁷

1.4.5. Grb7 and Hepatic Cancer

Hepatocellular cancer (HCC) is the fifth most frequent cancer in the world with associated high mortality and poor prognosis.¹¹⁸ The relationship between Grb7 overexpression and the development of hepatocellular carcinoma was extensively investigated by Itoh et al.¹¹⁹ They showed that Grb7 overexpression was correlated with the level of FAK in Hep3B cells and that such over expression was a cause for invasive and metastatic potential exhibited by the HCC cell lines. Moreover, the study demonstrated that the combined presence of high levels of Grb7 and FAK was associated with a poor prognosis as compared to negative controls.¹¹⁹ In addition, the druggability of Grb7 in HCC was investigated by a knockout experiment with the use of small interfering RNA and found that Grb7 knockout cancer cells had reduced invasive and migratory potential.¹¹⁹ Finally, suppression of Grb7 expression was noted to delay the onset of HCC tumor formation in mice.¹¹⁹ Taken together, these experiments demonstrate the potential of targeting Grb7 in hepatic cancer cells.

1.4.6. Grb7 and Ovarian Cancer

Undoubtedly, ovarian cancer represents one of the most deadly malignancies in women especially as it is mainly diagnosed after it has reached its late stage.¹²⁰ A recent study aimed to characterize the role of Grb7 and its splice variant Grb7v in

the ovarian carcinogenesis was conducted with application of immunohistochemical and western blotting analysis.¹²¹ The research showed up to a 40-fold increase in Grb7 overexpression in several ovarian cancer cell lines (SKOV3, OVCAR3, OVCA420, OVCA429, and OVCA433) while up to a 30-fold increase in the expression of Grb7v were reported. Moreover, such high level of overexpression was shown to correlate with high-grade ovarian cancers. Interestingly, differences in the role of Grb7 and its variant was noted where Grb7 was found to promote only cell proliferation, migration and invasion of ovarian cancer cell lines, whereas Grb7v was related only cell proliferation and anchorage-independent growth ability. Moreover, with the use of specific kinase inhibitors, the mechanistic detail of the tumorigenic function was delineated. It is showed that both Grb7 and Grb7v promoted cell proliferation through activating extracellular signal-regulated kinase, whereas Grb7 enhanced cell migration/invasion by activating c-Jun NH2 terminal kinase signaling. Further it is shown that the levels of phosphorylated JNK, phosphorylated ERK, and phosphorylated AKT were elevated by Grb7 overexpression whereas overexpression of Grb7v was found to increase the level of phosphorylated ERK.¹²¹

1.4.7. Grb7 and Testicular cancer

Testicular germ cell tumors (TGCTs) are common malignancies in the young whose incidence is on the rise.¹²² Research on the identification of proteins that are involved in TGCT carcinogenesis is shedding light on the molecular basis of TGCT development. In a recent study, the overexpression of Grb7 in TGCT is demonstrated with transcriptional profiling experiments.¹²³ Likewise, studies conducted on mutations, copy number and expression levels of genes in TCGT have shown Grb7 to be involved in the development TCGTs. The study noted that up to a 63 % increase in Grb7 expression was detected in primary TGCT tumor samples.¹²⁴ Interestingly, though Grb7 is known to co-amplify and co-express with ErbB2 in other cancers, such has not been the case in TCGT as the level of ErbB2 was not elevated in the TGCTs where high level of Grb7 is detected. This indicates that Grb7 alone may be independently contribute to TGCT tumor formation.¹²⁵ In other related experiments, increased Grb7 expression was found in various forms of TCGT such as intratubular germ cell neoplasia, seminoma and non-seminoma compared

with normal testicular samples.^{123,126} Additionally, Grb7 expression levels were found to positively correlate with RAS and KIT levels in TCGTs.¹²⁷

1.4.8. Grb7 and Blood cancer

Chronic lymphocytic leukemia (CLL) is a major form of blood cancer characterized by asymptomatic blood lymphocytosis and bone marrow failure.¹²⁸ Haran et al recently investigated the role of Grb7 in CCL and showed that Grb7 was not only overexpressed but its expression correlated with the severity of the CLL tumor. They showed that up to 88 % of Grb7 expression was detected in Stage IV as compared to 18 % in the Stage I of leukemia.¹²⁹ Moreover, corresponding increase in the migratory potential of cells at stage IV CLL was observed when compared to stage I cells,¹²⁸ indicating the role of Grb7 in transforming CCL to its deadly form. As the level of Grb7 is correlated with stages of CLL, the results from the study indicate that Grb7 level could potentially be employed as a prognostic marker to determine the status of leukemia and to guide the course of therapy in addition to its potential as drug target.¹²⁹

1.4.9. Grb7 and Rheumatoid arthritis

Grb7 overexpression has been associated with cellular diseases other than cancer. Rheumatoid arthritis (RA) is a chronic inflammatory disorder caused by the destruction of connective tissue of joints by the body's own immune system.¹³⁰ From experiments conducted to identify proteins involved in RA, Grb7 is reported as one of the proteins associated with antibodies isolated from RA synovial fluid along with Fibronectin, semaphorin 7A precursor and immunoglobulin μ .¹³¹ The fact that Fibronectin is also identified is interesting. In the esophageal carcinoma, for example, fibronectin is found to stimulate tyrosine phosphorylation of Grb7 which is regulated by integrin and FAK signaling system. Such Fibronectin-Integrin-FAK dependent activation of Grb7 was found to contribute to the migratory, metastatic and invasive potential of esophageal carcinoma cells.³² Moreover, since cell migration plays essential role in inflammation the involvement of Grb7 in rheumatoid arthritis could also arise from its general role in cell migration. By coupling NF-kappa-inducing kinase with erbB/EGFR family receptors, Grb7 is found to regulate inflammation.¹³²

1.4.10. Grb7 and Atopic dermatitis

Atopic dermatitis (AD) is a chronic inflammatory skin disease characterized by distributed eczematous skin lesions.¹³³ The role of Grb7 in this inflammatory disorder was investigated by considering the level of eosinophilia in AD patients.¹³⁴ Eosinophilia in AD patients occurs through an anti-apoptotic mechanism, where eosinophils exceed their normal lifespan and accumulate instead. Experiments to delineate the precise role of Grb7 in AD have showed that increased phosphorylation of Grb7 and FAK was detected in low viability eosinophils.¹³⁵ These results suggest that Grb7 phosphorylation may be one factor related with the anti-apoptosis mechanism of eosinophilia.¹³⁴ Further work detailing the precise role of Grb7 in AD and the possible connection with its role in carcinogenesis is awaited.

1.8.11. Grb7 and the Immune system

Controlled operation of signaling pathways is important for the proper functioning of the immune system.¹³⁶ The T-cell receptor (TCR) is plays a central role in the induction, co-ordination and production of immune responses.¹³⁷ In a study to identify the molecular mechanisms involving TCR signaling, it was found that Grb7 was expressed in lymphocytes and that this was related to TCR activation.¹³⁸ Moreover, Grb7 is known to bind to G6f protein, a trans membrane protein comprising the YXN recognition motif of Grb7.¹³⁹ G6f belongs to the immunoglobulin superfamily of proteins essential in the immune system. This is an indication that Grb7 has a role to play in the immune system.¹³⁹ Indeed, the level of Grb7 overexpression and its phosphorylation was noted to have stimulatory effect on the immune system. However, excessive and uncontrolled immunostimulation may be the factor that precipitates a number of autoimmune disorders such as RA and AD. Hence, further investigation of the role of immune stimulation by Grb7 is needed.

1.4.12. Grb7 and Arrhythmia

Ion channels are essential elements in the cellular process of the nervous system, cardiovascular system and musculoskeletal system.¹⁴⁰ Chemically, ion channels are formed by one or more pairs of trans membrane glycoproteins.¹⁴¹ The functional

role of many ion channels is regulated by ligand binding to their extracellular or intracellular domain.¹⁴¹ A recent study showed that Grb7 is one of the intracellular proteins important in the control of ion channel function. It is shown that Grb7 is co-expressed with a number of K-channels such as hERG, Kir1.1, Kv1.5, Kir2.2, Kir2.3, Kv4.3 and ROMK.¹⁴² Moreover, it is noted that over expression of Grb7 was noted to decrease the amplitude of most of the Kir channels in *Xenopus* oocytes.¹⁴³ Furthermore, it was shown that overexpression of Grb7 strongly decreases the activity of hERG, Kv1.5 and Kv4.3 potassium channels that are important in cardiac membrane excitability. Though the mechanism is not clear it is suggested that Grb7 may either hinder access of regulatory tyrosine kinases to the channel protein¹⁴² or the impact may be as a consequence of a direct protein–protein interaction. As most of these potassium channels are targets for clinically used anti-arrhythmic the precise role of Grb7 in arrhythmia is yet to be fully delineated.

1.4.13. Grb7 and Translation

One of the new roles of Grb7 being investigated is its effect on translation. Studies conducted on FAK interacting proteins such as Netrins has disclosed Grb7 as a new RNA-binding protein.⁴⁰ Netrins are extracellular proteins known to act via the FAK pathway to regulate neuronal migration and axonal growth.¹⁴⁴⁻¹⁴⁶ The work by Tsai et al showed that Grb7 upon stimulation by Netrin-1 could act as a translational repressor by binding to RNA targets via its amino-terminal domain. Interestingly, it was reported that its repressive activity was reversed by FAK-triggered hyper phosphorylation on its SH2 domain.⁴⁰ This looks consistent with the fact that FAK stimulated cancer and inflammatory cell migration. In a related paper, Grb7 was shown to function as a constitutive repressor for kappa opioid receptor (KOR), a receptor which is stimulated by Netrin-1 and known to act via the FAK pathway to stimulate cell migration.^{144,147}

1.4.14. Grb7 and Analgesia

A final role of Grb7 that is forthcoming is its possible involvement in analgesia, especially central analgesia. The finding that Netrin-1 stimulated kappa opioid receptor (KOR) translation in both P19 cell and DRG nerve cells and that that of

Grb7 expression in the DRG neuronal cell has led Tsai et al to suggest that Grb7 might have a role in analgesia. This is because KOR is known as a classical narcotic drug receptor and it has been found that its synthesis can be stimulated by Netrin-1 and mediated by Grb7.¹⁴⁷ Given the established pharmacological role for KOR in mediating the analgesic activity of opioid analgesics, future studies are proposed to investigate how the neuronal circuit of analgesia may be regulated by, or integrated with, growth factors.¹⁴⁷

1.5. The development of Grb7 antagonists

Grb7 has become a promising target in a variety of human disorders. As reviewed above it has an experimentally demonstrated role in a variety of cancers including breast, blood, hepatic, in inflammatory diseases such as rheumatoid arthritis, atopic dermatitis in immune system stimulation, RNA regulation, and many others. Moreover, Grb7 is a mediator of a diverse array of oncogenic and other signaling pathways.⁴⁵ From the viewpoint of multitarget selective drug development, Grb7 may represent an ideal target as it mediates a multitude of signal transduction pathways that operate in concert in the carcinogenic transformation of human cells.⁷³

For ligand design purposes, any of the Grb7 domains could theoretically be targeted to disrupt the role of Grb7 in the genesis of malignancies. In practice, the SH2 domain is especially interesting to target for a number of reasons. For one, the SH2 domain commences the first and hence the fate determining step in the entire process of Grb7 dependent signaling.⁴⁴ Moreover, it possesses a well defined and characterized binding pocket amenable to ligand design efforts.⁶⁴ Furthermore, as stated earlier, the SH2 domain of Grb7 is the most extensively studied domain where its interaction with a diverse array of signaling and non-signaling biomolecules is documented.⁴³⁻⁴⁶ In addition, the requirement of the SH2 domain to bind to Grb7's myriad upstream partners is generally conserved^{35,54} where a minimal recognition motif is established. These factors endow the SH2 domain as an attractive module in the development of Grb7 based therapeutic agents. Indeed, this has been demonstrated by the recent discovery of Grb7 antagonists that were specifically designed to act on the SH2 domain.^{100, 109}

Inspired by the conservative motif requirement of Grb7 SH2 domain to bind its upstream binding partners, Pero et al have conducted a PHAGE display experiment to identify the first polypeptide antagonist of Grb7. The peptide termed G7-18NATE was initially designed as a 19 residue polypeptide flanked by Cys residues at positions 1 and 11. Interestingly enough, it was shown that the peptide was inactive in its open form and cyclization was mandatory for activity against Grb7.^{109,148} To effect the cyclization, a disulfide linkage between the two Cys residues was introduced to close the ring. The original 19-residue structure was modified by removing residues outside the two Cys residues and the disulfide linkage was replaced with a thioether moiety to effect the ring closure which might provide stabilization in cellular environment. This 11 residue cyclic polypeptide-G7-18NATE (sequence: WFEGYDNTFPC)- was tested and proven to possess the same affinity as the larger disulfide containing form.¹⁴⁹ An important attribute of this lead peptide is its selective activity for Grb7 and the fact that it is non-phosphorylated makes it easier to be prepared and to transport across cell membranes. The chemical structure of G7-18NATE is displayed in Fig. 1.4. This G7-18NATE peptide is found to display low antagonist potency and was not investigated further.

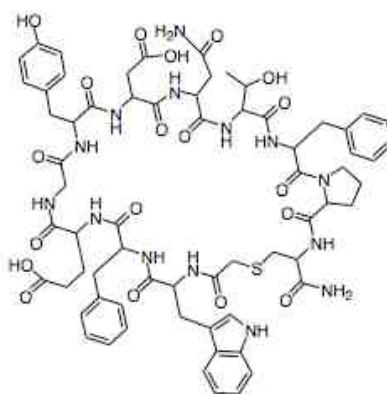


Figure 1.4: Chemical structures of G7-18NATE

The binding affinity of the G7-18NATE prototype peptide has been characterized extensively by isothermal titration calorimetry,^{64,149,150} surface plasmon resonance,¹⁵¹ and ELISA based assays.¹⁵² Such investigations provide invaluable information that should guide the further optimization of this lead polypeptide. The

three ITC experiments concur on the affinity of the peptide for Grb7 SH2 domain (34.5 μ M, 13.5 μ M, 35.7 μ M)^{64,149,150} indicating its binding with moderate affinity. Though this peptide represents an interesting breakthrough in Grb7 antagonist development, it is not of sufficient affinity to initiate animal experimentation. In other words, further optimization is necessary to transform the peptide into a clinical candidate. An important clue in this regard is afforded by isothermal titration calorimetry where deconvolution of the binding affinity into its components shows that the binding of G7-18NATE is enthalpically driven and entropically forbidden. This appears in line with the observation that the open form of G7-18NATE is devoid of any antagonistic activity.¹⁴⁹ This knowledge could be of assistance in the optimization of the lead peptide structure so as to improve the affinity, to convert the unfavorable entropy into a favorable one and possibly improve the enthalpic contribution as well.

Grb7 is an intracellular protein. Since G7-18NATE is a polypeptide, the plasma membrane represents a bottleneck for its use in cellular systems. However, this has been overcome by the use of other peptides known to assist in crossing biological membranes.¹⁵² For cellular experiments, G7-18NATE was synthesized with a 16 residues long sequence termed 'Penetratin' for *in vivo* studies (see Fig. 1.5). The cell proliferation and migration inhibition assay conducted with this cell permeable derivative (G7-18NATE-Penetratin) demonstrate the combined effect of membrane crossing (Penetratin) and Grb7 inhibition (G7-18NATE)¹⁴⁸ was encouraging as a moderate *in vivo* inhibitory effect was noted. Thus, the attachment of the 16-residue penetratin has extended the usefulness of G7-18NATE in living systems. Another arginine rich penetratin peptide with 11 residues sequence derived from the Tat sequence (G7-18NATE-Tat) was also investigated for its cell permeabilising ability where a positive effect is reported.¹⁴⁸ G7-18NATE-Penetratin as well as G7-18NATE-Tat systems have been used to assess the synergetic effect of G7-18NATE with Doxorubicin in breast cancer patients with a promising outcome.¹⁰⁰ A related experiment conducted on pancreatic cancer cell migration effect clearly established the potential of G7-18NATE in diverse cancer cell lines.^{100,109,147}

Other short phosphorylated peptides based on the consensus recognition motif

have been developed and tested,¹⁵³ see Fig.1.6. This includes peptides based on the sequence around the phosphotyrosine residue of ErbB1, ErbB2, ErbB3 and EphB1¹⁴⁹ Grb7 upstream binding partners. The phosphorylated peptides range from 6 to 11 residues with a dissociation equilibrium constant varying from 0.6 μ M to 366 μ M. The higher affinity of these peptides is ascribed to the phosphorylation of tyrosine.

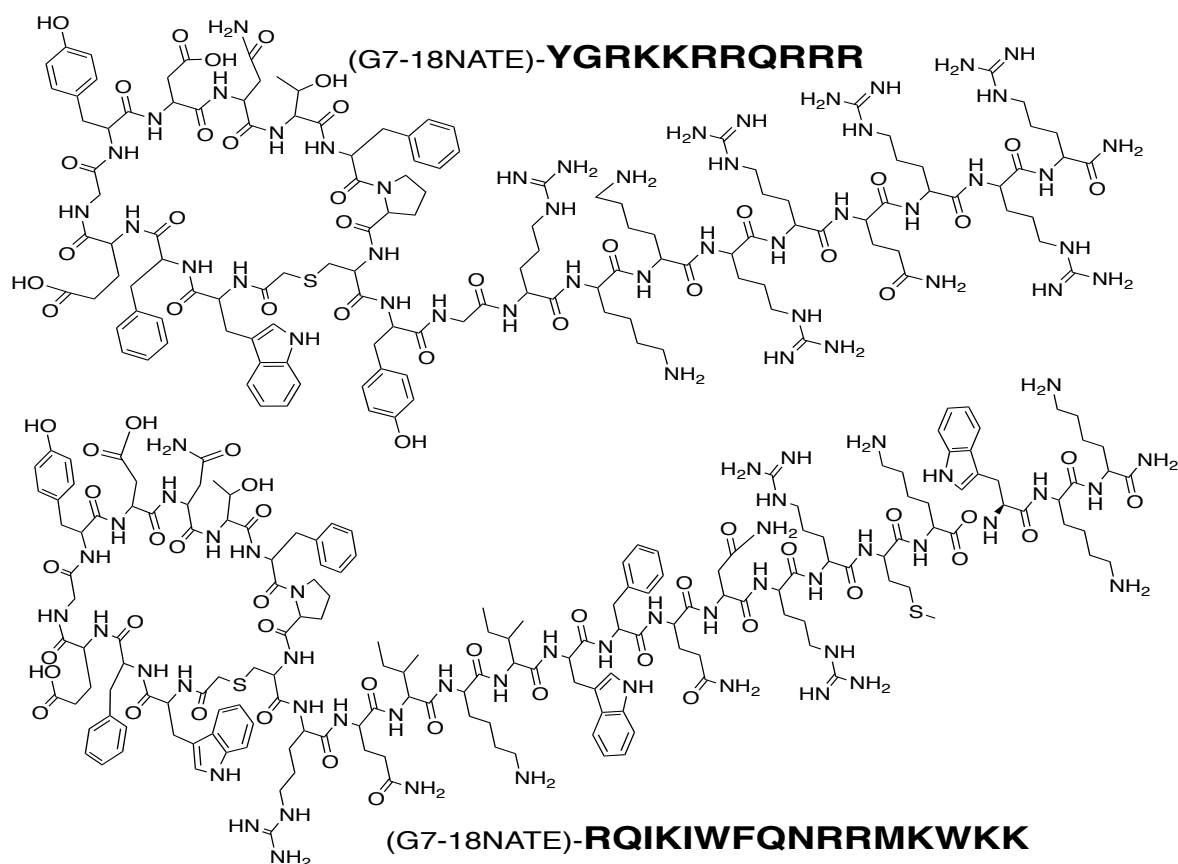


Figure 1.5: Sequence and chemical structures of cell permeable G7-18NATE derivatives. *Top*: G7-18NATE-Tat; *Bottom*: G7-18NATE-Penetratin. Single letter abbreviation of the penetratin residues is indicated in bold font.

Finally, peptides that were previously reported as Grb2 antagonists were tested for their inhibitory effect on Grb7 in a recent paper.¹⁵⁰ Interestingly, the result showed that not only do the peptides possess a Grb7 inhibitory effect, the activity rank is maintained on both Grb2 and Grb7 antagonism, i.e., the most potent peptide in Grb2 is found to be the most potent in Grb7 as well though a quantitative difference is observed.¹⁵⁰

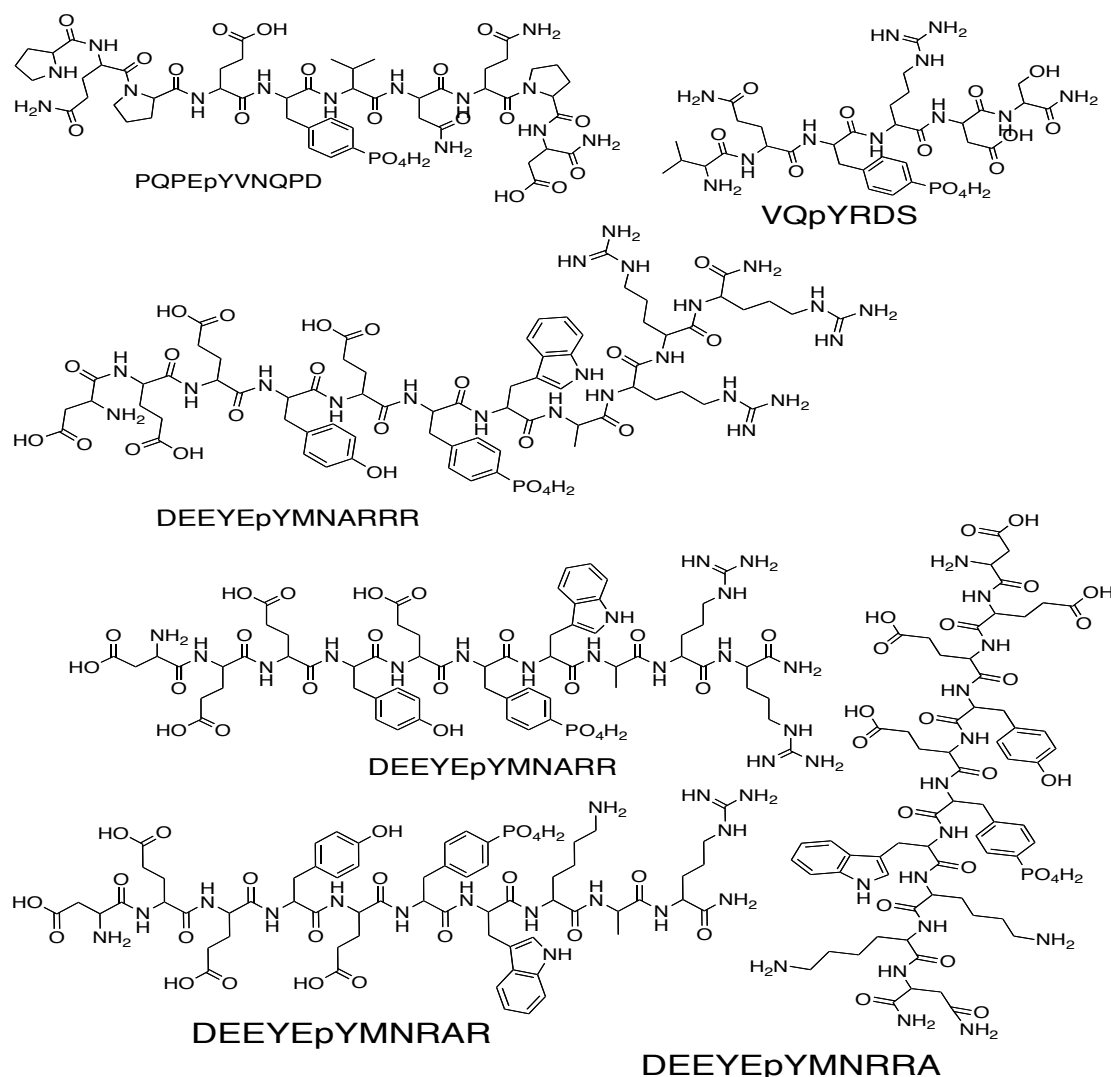


Figure 1.6: Sequence and chemical structure of phosphorylated peptide antagonists of Grb7

Finally, the crystal structure of G7-18NATE in complex with Grb7 SH2 has recently been solved in our laboratory. Analysis of the co-crystal structure provides the atomistic detail of the interaction between the peptide and Grb7 SH2 binding site. In particular, the number and types of peptide atom-receptor atom interaction, the preferred orientation and conformation of G7-18NATE on binding is known. In addition, key residues of the protein that participate in bonding interaction with the peptide could aid virtual screening experiments. Fig. 1.7 displays the complex structure of G7-18NATE with Grb7 SH2 domain. As can be seen the peptide appear to make less than optimal interaction especially with the all-important cationic pocket indicating the possibility for further affinity optimization.

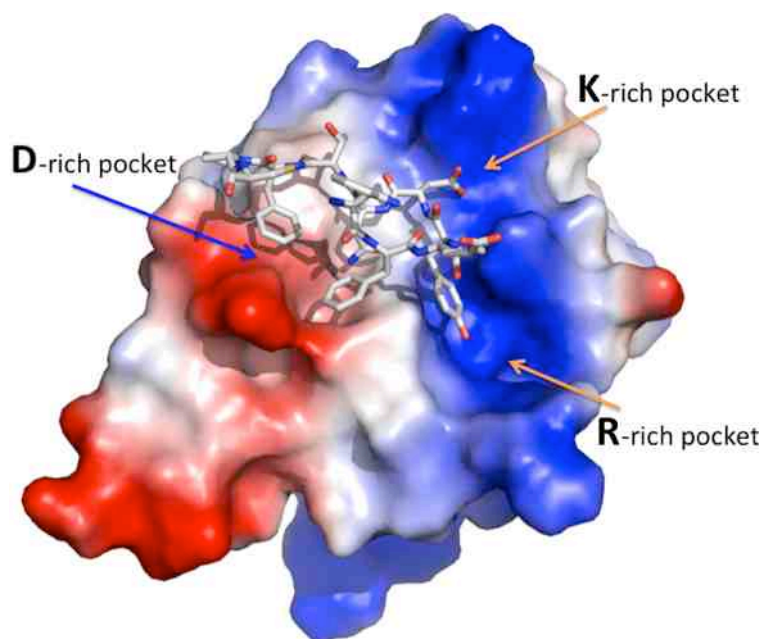


Figure 1.7. The Binding mode of G7-18NATE with Grb7 SH2 domain binding site. The peptide is displayed in sticks representation. The three sub pockets of the protein are indicated. The vacuum electrostatic map is created in PyMOL.

1.6. Conclusion and future outlook

Cancer remains mankind's leading health issue accounting for more than 10 million cases and over 5 million deaths annually.¹⁰¹ These figures are expected to rise exponentially as an attendant to the socioeconomic and life style revolution gripping the global populace. Even though more than 100 drugs are currently available on the market, the dwindling efficacy, high toxicity and the exorbitant cost means new agents with a novel mechanism of action are in big demand.

Advances in molecular sciences are accelerating the identification of novel drug targets in cancers and other human disorders. From the clinical standpoint, new targets provide novel drugs, novel mechanistic bases and potentially more efficacious means to treat diseases and a better understanding of the pathophysiological process underlying a given disease. From the commercial viewpoint, novel targets clearly present unexploited opportunity. Given its established role in various malignancies and the fact that there is no drug that acts on it, Grb7 based drug development is likely to be very promising endeavor in the

foreseeable future.

Grb7 is found in a diverse array of signaling events critical for carcinogenesis and inflammatory process. Its druggability is proven with the use of synthetic peptides. The major challenge, however, comes from its intracellular localization. Given the fact that many of the currently available drugs have intracellular drug targets such as the steroid agonist and antagonists, its mere localization should not be an obstacle. Indeed the recent development of cell permeable Grb7 antagonists is encouraging and illustrates that the permeability issue could be surmounted with little extra effort. Grb7 is especially suitable for a one drug-one target-multiple diseases effective drug design as it is found in numerous pathways. Though much has still to be studied, the data obtained so far are encouraging for the development of Grb7 as an antitumor therapeutic target.

1.7. References

- (1) Kiel, C.; Yus, E.; Serrano, L. Engineering signal transduction pathways. *Cell* **2010**, *140*, 33-47.
- (2) Lemmon, M. A.; Schlessinger, J. Cell signaling by receptor tyrosine kinases. *Cell* **2010**, *141*, 1117-1134.
- (3) Burz, C.; Berindan-Neagoe, I.; Balacescu, O.; Irimie, A. Apoptosis in cancer: key molecular signaling pathways and therapy targets. *Acta Oncol.* **2009**, *48*, 811-821.
- (4) Prenzel, N.; Fischer, O. M.; Streit, S.; Hart, S.; Ulrich, A. The epidermal growth factor receptor family as a central element for cellular signal transduction and diversification. *Endocr. Relat. Cancer* **2001**, *8*, 11-31.
- (5) Teti, A. Regulation of cellular functions by extracellular matrix. *J. Am. Soc. Nephrol.* **1992**, *2*, S83-S87.
- (6) Talapatra, S.; Thompson, C. B. Growth factor signaling in cell survival: implications for cancer treatment. *J. Pharmacol. Exp. Ther.* **2001**, *298*, 873-878.
- (7) Wang, Z.; Ahmad, A.; Li, Y.; Kong, D.; Azmi, A. S.; Banerjee, S.; Sarkar, F. H. Emerging roles of PDGF-D signaling pathway in tumor development and progression. *Biochim. Biophys. Acta.* **2010**, *1806*, 122-130.
- (8) Zwick, E.; Bange, J.; Ullrich, A. Receptor tyrosine kinase signaling as a target for cancer intervention strategies. *Endocr. Relat. Cancer* **2001**, *8*, 161-173.
- (9) Chikazawa, N.; Tanaka, H.; Tasaka, T.; Nakamura, M.; Tanaka, M.; Onishi, H.; Katano, M. Inhibition of Wnt signaling pathway decreases chemotherapy-

- resistant side-population colon cancer cells. *Anticancer. Res.* **2010**, *30*, 2041-2048.
- (10) Yoshida, T.; Zhang, G.; Haura, E. B. Targeting epidermal growth factor receptor: central signaling kinase in lung cancer. *Biochem. Pharmacol.* **2010**, *80*, 613-623.
 - (11) Korpai, M.; Kang, Y. Targeting the transforming growth factor-beta signaling pathway in metastatic cancer. *Eur. J. Cancer* **2010**, *46*, 1232-1240.
 - (12) Yang, L. TGF β and cancer metastasis: an inflammation link. *Cancer Metastasis Rev.* **2010**, *29*, 263-271.
 - (13) Gabay, C.; Lamacchia, C.; Palmer, G. IL-1 pathways in inflammation and human diseases. *Nat. Rev. Rheumatol.* **2010**, *6*, 232-241.
 - (14) Pawson, T.; Scott, J. D. Signaling through scaffold, anchoring, and adaptor proteins. *Science* **1997**, *278*, 2075-2080.
 - (15) Pawson, T.; Gish, G. D.; Nash, P. SH2 domains, interaction modules and cellular wiring. *Trends Cell Biol.* **2001**, *11*, 504-511.
 - (16) Margolis, B. The GRB family of SH2 domain proteins. *Prog. Biophys. Mol. Biol.* **1994**, *62*, 223-244.
 - (17) Songyang, Z.; Shoelson, S. E.; Chaudhuri, M.; Gish, G.; Pawson, T.; Haser, W. G.; King, F.; Roberts, T.; Ratnofsky, S.; Lechleider, R. J.; Neel, B. G.; Birge, R. B.; Fajard, J. E.; Chou, M. M.; Hanafusa, H.; Schaffhausen, B.; Cantley, L. C. SH2 domains recognize specific phosphopeptide sequences. *Cell* **1993**, *72*, 767-778.
 - (18) Songyang, Z.; Shoelson, S. E.; McGlade, J.; Olivier, P.; Pawson, T.; Bustelo, X. R.; Barbacid, M.; Sabe, H.; Hanafusa, H.; Yi, T.; Ren, R.; Baltimore, D.; Patnoffsky, S.; Feldman, R. A.; Cantley, L. C. Specific motifs recognized by the SH2 domains of Csk, 3BP2, fps/fes, GRB-2, HCP, SHC, Syk, and Vav. *Mol. Cell. Biol.* **1994**, *14*, 2777-2785.
 - (19) Frantz, J. D.; Giorgetti-Peraldi, S.; Ottinger, E. A.; Shoelson, S. E. Human GRB-IRbeta/ GRB10. Splice variants of an insulin and growth factor receptor-binding protein with PH and SH2 domains. *J. Biol. Chem.* **1997**, *272*, 2659-2667.
 - (20) Lim, M. A.; Riedel, H.; Liu, F. Grb10: more than a simple adaptor protein. *Front Biosci.* **2004**, *9*, 387-403.
 - (21) Cariou, B.; Bereziat, V.; Moncoq, K.; Kasus-Jacobi, A.; Perdureau, D.; Le Marcis, V.; Burnol, A. F. Regulation and functional roles of Grb14. *Front Biosci.* **2004**, *9*, 626-636.
 - (22) Holt, L. J.; Siddle, K. Grb10 and Grb14: enigmatic regulators of insulin action--and more? *Biochem. J.* **2005**, *388*, 393-406.
 - (23) Margolis, B.; Silvennoinen, O.; Comoglio, F.; Roonprapant, C.; Skolnik, E.; Ullrich, A.; Schlessinger, J. High-efficiency expression/cloning of epidermal growth factor-receptor-binding proteins with Src homology 2 domains. *Proc. Natl. Acad. Sci. U.S.A.* **1992**, *89*, 8894-8898.
 - (24) Skolnik, E. Y.; Margolis, B.; Mohammadi, M.; Lowenstein, E.; Fischer, R.; Drepps, A.; Ullrich, A.; Schlessinger, J. Cloning of PI3 kinase-associated p85 utilizing a

- novel method for expression/cloning of target proteins for receptor tyrosine kinases. *Cell* **1991**, 65, 83-90.
- (25) Lowenstein, E. J.; Daly, R. J.; Batzer, A. G.; Li, W.; Margolis, B.; Lammers, R.; Ullrich, A.; Skolnik, E. Y.; Barsagi, D.; Schlessinger, J. The SH2 and SH3 domain-containing protein GRB2 links receptor tyrosine kinases to ras signaling. *Cell* **1992**, 70, 431-442.
 - (26) Yokote, K.; Margolis, B.; Heldin, C. H.; Claesson-Welsh, L. Grb7 is a downstream signaling component of platelet-derived growth factor alpha- and beta-receptors. *J. Biol. Chem.* **1996**, 271, 30942-30949.
 - (27) Lucas-Fernández, E.; García-Palmero, I.; Villalobo, A. Genomic organization and control of the Grb7 gene family. *Curr. Genomics* **2008**, 1, 60-68.
 - (28) Kauraniemi, P.; Kallioniemi, A. Activation of multiple cancer-associated genes at the ERBB2 amplicon in breast cancer. *Endocr. Relat. Cancer* **2006**, 13, 39-49.
 - (29) Mano, M. S.; Rosa, D. D.; De Azambuja, E.; Ismael, G. F.; Durbecq, V. The 17q12-q21 amplicon: Her2 and topoisomerase-IIalpha and their importance to the biology of solid tumours. *Cancer Treat. Rev.* **2007**, 33, 64-77.
 - (30) Littman, B. H.; Williams, S. A. The ultimate model organism: progress in experimental medicine. *Nat. Rev. Drug Discov.* **2005**, 4, 631-668.
 - (31) Shen, T. L.; Guan, J. L. Grb7 in intracellular signaling and its role in cell regulation. *Front Biosci.* **2004**, 9, 192-200.
 - (32) Tanaka, S.; Mori, M.; Akiyoshi, T.; Tanaka, Y.; Mafune, K.; Wands, J. R.; Sugimachi, K. A novel variant of human Grb7 is associated with invasive esophageal carcinoma. *J. Clin. Invest.* **1998**, 102, 821-827.
 - (33) Fiddes, R. J.; Campbell, D. H.; Janes, P. W.; Sivertsen, S. P.; Sasaki, H.; Wallasch, C.; Daly, R. J. Analysis of Grb7 recruitment by heregulin-activated erbB receptors reveals a novel target selectivity for erbB3. *J. Biol. Chem.* **1998**, 273, 7717-7724.
 - (34) Stein, D.; Wu, J.; Fuqua, S.; Roonprapunt, C.; Yajnik, V.; D'Eustachio, P.; Moskow, J.; Buchberg, A.; Osborne, C.; Margolis, B. The SH2 domain protein GRB-7 is co-amplified, overexpressed and in a tight complex with HER2 in breast cancer. *EMBO J.* **1994**, 13, 1331-1340.
 - (35) Han, D. C.; Shen, T. L.; Guan, J. L. The Grb7 family proteins: structure, interactions with other signaling molecules and potential cellular functions. *Oncogene* **2001**, 20, 6315-6321.
 - (36) Han, D. C.; Guan, J. L. Association of focal adhesion kinase with Grb7 and its role in cell migration. *J. Biol. Chem.* **1999**, 274, 24425-24430.
 - (37) Han, D. C.; Shen, T. L.; Guan, J. L. Role of Grb7 targeting to focal contacts and its phosphorylation by focal adhesion kinase in regulation of cell migration. *J. Biol. Chem.* **2000**, 275, 28911-28917.
 - (38) Chu, P. Y.; Huang, L. Y.; Hsu, C. H.; Liang, C. C.; Guan, J. L.; Hung, T. H.; Shen, T. L. Tyrosine phosphorylation of growth factor receptor-bound protein-7 by

- focal adhesion kinase in the regulation of cell migration, proliferation, and tumorigenesis. *J. Biol. Chem.* **2009**, *284*, 20215-202126.
- (39) Siamakpour-Reihani, S.; Argiros, H. J.; Wilmeth, L. J.; Haas, L. L.; Peterson, T. A.; Johnson, D. L.; Shuster, C. B.; Lyons, B. A. The cell migration protein Grb7 associates with transcriptional regulator FHL2 in a Grb7 phosphorylation-dependent manner. *J. Mol. Recognit.* **2009**, *22*, 9-17.
- (40) Tsai, N. P.; Bi, J.; Wei, L. N. The adaptor Grb7 links netrin-1 signaling to regulation of mRNA translation. *EMBO J.* **2007**, *26*, 1522-15231.
- (41) Porter, C. J.; Wilce, M. C.; Mackay, J. P.; Leedman, P.; Wilce, J. A. Grb7-SH2 domain dimerization is affected by a single point mutation. *Eur. Biophys. J.* **2005**, *34*, 454-460.
- (42) Shen, T. L.; Han, D. C.; Guan, J. L. Association of Grb7 with phosphoinositides and its role in the regulation of cell migration. *J. Biol. Chem.* **2002**, *277*, 29069-29077.
- (43) Han, D. C.; Shen, T. L.; Guan, J. L. Role of Grb7 targeting to focal contacts and its phosphorylation by focal adhesion kinase in regulation of cell migration. *J. Biol. Chem.* **2000**, *275*, 28911-28917.
- (44) Daly, R. J. The Grb7 family of signaling proteins. *Cell Signal.* **1998**, *10*, 613-618.
- (45) Holt, L. J.; Daly, R. J. Adapter protein connections: the MRL and Grb7 protein families. *Growth Factors* **2005**, *23*, 193-201.
- (46) Pero, S. C.; Daly, R. J.; Krag, D. N. Grb7-based molecular therapeutics in cancer. *Expert. Rev. Mol. Med.* **2003**, *5*, 1-11.
- (47) Golubovskaya, V. M.; Kweh, F. A.; Cance, W. G. Focal adhesion kinase and cancer. *Histol. Histopathol.* **2009**, *24*, 503-510.
- (48) Zhao, J.; Guan, J. L. Signal transduction by focal adhesion kinase in cancer. *Cancer Metastasis Rev.* **2009**, *28*, 35-49.
- (49) Witsch, E.; Sela, M.; Yarden, Y. Roles for growth factors in cancer progression. *Physiology (Bethesda)*. **2010**, *25*, 85-101.
- (50) Roy, V.; Perez, E. A. Beyond trastuzumab: small molecule tyrosine kinase inhibitors in HER-2-positive breast cancer. *Oncologist* **2009**, *14*, 1061-1069.
- (51) Kim, T. E.; Murren, J. R. Erlotinib OSI/Roche/Genentech. *Curr. Opin. Investig. Drugs* **2002**, *3*, 1385-1395.
- (52) Velcheti, V.; Morgensztern, D.; Govindan, R. Management of patients with advanced non-small cell lung cancer: role of gefitinib. *Biologics* **2010**, *4*, 83-90.
- (53) Reiske, H. R.; Zhao, J.; Han, D. C.; Cooper, L. A.; Guan, J. L. Analysis of FAK-associated signaling pathways in the regulation of cell cycle progression. *FEBS Lett.* **2000**, *486*, 275-280.
- (54) Filippakopoulos, P.; Müller, S.; Knapp, S. SH2 domains: modulators of nonreceptor tyrosine kinase activity. *Curr. Opin. Struct. Biol.* **2009**, *19*, 643-649.

- (55) Haslam, R. J.; Koide, H. B.; Hemmings, B. A. Pleckstrin domain homology. *Nature* **1993**, *363*, 309-310.
- (56) Pawson, T. SH2 and SH3 domains in signal transduction. *Adv. Cancer Res.* **1994**, *64*, 87-110.
- (57) Tsai, N. P.; Ho, P. C.; Wei, L. N. Regulation of stress granule dynamics by Grb7 and FAK signalling pathway. *EMBO J.* **2008**, *27*, 715-726.
- (58) Doller, A.; Pfeilschifter, J.; Eberhardt, W. Signaling pathways regulating nucleo-cytoplasmic shuttling of the mRNA-binding protein HuR. *Cell Signal.* **2008**, *20*, 2165-2173.
- (59) Manser, J.; Roonprapunt, C.; Margolis, B. C. elegans cell migration gene mig-10 shares similarities with a family of SH2 domain proteins and acts cell nonautonomously in excretory canal development. *Dev. Biol.* **1997**, *184*, 150-164.
- (60) Ooi, J.; Yajnik, V.; Immanuel, D.; Gordon, M.; Moskow, J. J.; Buchberg, A. M.; Margolis, B. The cloning of Grb10 reveals a new family of SH2 domain proteins. *Oncogene* **1995**, *10*, 1621-1630.
- (61) Manser, J.; Wood, W. B. Mutations affecting embryonic cell migrations in *Caenorhabditis elegans*. *Dev. Genet.* **1990**, *11*, 49-64.
- (62) Siamakpour-Reihani, S.; Peterson, T. A.; Bradford, A. M.; Argiros, H. J.; Haas, L. L.; Lor, S. N.; Haulsee, Z. M.; Spuches, A. M.; Johnson, D. L.; Rohrschneider, L. R.; Shuster, C. B.; Lyons, B. A. Grb7 binds to Hax-1 and undergoes an intramolecular domain association that offers a model for Grb7 regulation. *J. Mol. Recognit.* **2010**, DOI: 10.1002/jmr.1062.
- (63) Depetris, R. S.; Wu, J.; Hubbard, S. R. Structural and functional studies of the Ras-associating and pleckstrin-homology domains of Grb10 and Grb14. *Nat. Struct. Mol. Biol.* **2009**, *16*, 833-839.
- (64) Porter, C. J.; Matthews, J. M.; Mackay, J. P.; Pursglove, S. E.; Schmidberger, J. W.; Leedman, P. J.; Pero, S. C.; Krag, D. N.; Wilce, M. C.; Wilce, J. A. Grb7 SH2 domain structure and interactions with a cyclic peptide inhibitor of cancer cell migration and proliferation. *BMC Struct. Biol.* **2007**, *7*:58.
- (65) Wojcik, J.; Girault, J. A.; Labesse, G.; Chomilier, J.; Mornon, J. P.; Callebaut, I. Sequence analysis identifies a ras-associating (RA)-like domain in the N-termini of band 4.1/JEF domains and in the Grb7/10/14 adapter family. *Biochem. Biophys. Res. Commun.* **1999**, *259*, 113-120.
- (66) Downward, J. Targeting RAS signalling pathways in cancer therapy. *Nat. Rev. Cancer* **2003**, *3*, 11-22.
- (67) Stein, E. G.; Gustafson, T. A.; Hubbard, S. R. The BPS domain of Grb10 inhibits the catalytic activity of the insulin and IGF1 receptors. *FEBS Lett.* **2001**, *493*, 106-111.
- (68) Stein, E. G.; Ghirlando, R.; Hubbard, S. R. Structural basis for dimerization of the Grb10 Src homology 2 domain. Implications for ligand specificity. *J. Biol. Chem.* **2003**, *278*, 13257-13264.

- (69) Scharf, P. J.; Witney, J.; Daly, R.; Lyons, B. A. Solution structure of the human Grb14-SH2 domain and comparison with the structures of the human Grb7-SH2/erbB2 peptide complex and human Grb10 SH2 domain. *Protein Sci.* **2004**, *13*, 2541-2546.
- (70) He, W.; Rose, D. W.; Olefsky, J. M.; Gustafson, T. A. Grb10 interacts differentially with the insulin receptor, insulin-like growth factor I receptor, and epidermal growth factor receptor via the Grb10 Src homology 2 (SH2) domain and a second novel domain located between the pleckstrin homology and SH2 domains. *J. Biol. Chem.* **1998**, *273*, 6860-6867.
- (71) Moncoq, K.; Broutin, I.; Larue, V.; Perdereau, D.; Cailliau, K.; Browaeys-Poly, E.; Burnol, A. F.; Ducruix, A. The PIR domain of Grb14 is an intrinsically unstructured protein: implication in insulin signaling. *FEBS Lett.* **2003**, *554*, 240-246.
- (72) Moncoq, K.; Broutin, I.; Craescu, C. T.; Vachette, P.; Ducruix, A.; Durand, D. SAXS study of the PIR domain from the Grb14 molecular adaptor: a natively unfolded protein with a transient structure primer? *Biophys. J.* **2004**, *87*, 4056-4064.
- (73) Daly, R. J. SH2 domain-containing signaling proteins in human breast cancer. *Breast Cancer Res. Treat.* **1995**, *34*, 85-92.
- (74) Janes, P. W.; Lackmann, M.; Church, W. B.; Sanderson, G. M.; Sutherland, R. L.; Daly, R. J. Structural determinants of the interaction between the erbB2 receptor and the Src homology 2 domain of Grb7. *J. Biol. Chem.* **1997**, *272*, 8490-8497.
- (75) Lee, H.; Volonte, D.; Galbiati, F.; Iyengar, P.; Lublin, D. M.; Bregman, D. B.; Wilson, M. T.; Campos-Gonzalez, R.; Bouzahzah, B.; Pestell, R. G.; Scherer, P. E.; Lisanti, M. P. Constitutive and growth factor-regulated phosphorylation of caveolin-1 occurs at the same site (Tyr-14) in vivo: identification of a c-Src/Cav-1/Grb7 signaling cassette. *Mol. Endocrinol.* **2000**, *14*, 1750-1775.
- (76) Stein, D.; Wu, J.; Fuqua, S. A.; Roonprapunt, C.; Yajnik, V.; D'Eustachio, P.; Moskow, J. J.; Buchberg, A. M.; Osborne, C. K.; Margolis, B. The SH2 domain protein GRB-7 is co-amplified, overexpressed and in a tight complex with HER2 in breast cancer. *EMBO J.* **1994**, *13*, 1331-1340.
- (77) Jones, N.; Master, Z.; Jones, J.; Bouchard, D.; Gunji, Y.; Sasaki, H.; Daly, R.; Alitalo, K.; Dumont, D. J. Identification of Tek/Tie2 binding partners. Binding to a multifunctional docking site mediates cell survival and migration. *J. Biol. Chem.* **1999**, *274*, 30896-308905.
- (78) Thömmes, K.; Lennartsson, J.; Carlberg, M.; Rönnstrand, L. Identification of Tyr-703 and Tyr-936 as the primary association sites for Grb2 and Grb7 in the c-Kit/stem cell factor receptor. *Biochem. J.* **1999**, *341*, 211-216.
- (79) Keegan, K.; Cooper, J. A. Use of the two hybrid system to detect the association of the protein-tyrosine-phosphatase, SHPTP2, with another SH2-containing protein, Grb7. *Oncogene* **1996**, *12*, 1537-1544.

- (80) Han, D. C.; Shen, T. L.; Miao, H.; Wang, B.; Guan, J. L. EphB1 associates with Grb7 and regulates cell migration. *J. Biol. Chem.* **2002**, *277*, 45655-45661.
- (81) Vayssière, B.; Zalcman, G.; Mahé, Y.; Mirey, G.; Ligensa, T.; Weidner, K. M.; Chardin, P.; Camonis, J. Interaction of the Grb7 adapter protein with Rnd1, a new member of the Rho family. *FEBS Lett.* **2000**, *467*, 91-96.
- (82) Ivancic, M.; Daly, R. J.; Lyons, B. A. Solution structure of the human Grb7-SH2 domain/erbB2 peptide complex and structural basis for Grb7 binding to ErbB2. *J. Biomol. NMR.* **2003**, *27*, 205-219.
- (83) Gullick, W. J. The role of the epidermal growth factor receptor and the c-erbB-2 protein in breast cancer. *Int. J. Cancer Suppl.* **1990**, *5*, 55-61.
- (84) Hu, X.; Stern, H. M.; Ge, L.; O'Brien, C.; Haydu, L.; Honchell, C. D.; Haverty, P. M.; Peters, B. A.; Wu, T. D.; Amler, L. C.; Chant, J.; Stokoe, D.; Lackner, M. R.; Cavet, G. Genetic alterations and oncogenic pathways associated with breast cancer subtypes. *Mol. Cancer Res.* **2009**, *7*, 511-522.
- (85) World Cancer Report **2008**. International Agency for Research on Cancer. http://www.iarc.fr/en/publications/pdfs-online/wcr/2008/wcr_2008 Retrieved on 04-09-2010
- (86) Ramsey, B.; Bai, T.; Hanlon, N. A.; Troxell, M.; Park, B.; Olson, S.; Keenan, E.; Luoh, S. W. GRB7 protein over-expression and clinical outcome in breast cancer. *Breast Cancer Res. Treat.* **2010**, DOI: 10.1007/s10549-010-1010-0.
- (87) Esteva, F. J.; Sahin, A. A.; Cristofanilli, M.; Arun, B.; Hortobagyi, G. N. Molecular prognostic factors for breast cancer metastasis and survival. *Semin. Radiat. Oncol.* **2002**, *12*, 3119-3128.
- (88) Jonkers, J.; Berns, A. Oncogene addiction: sometimes a temporary slavery. *Cancer Cell* **2004**, *6*, 535-538.
- (89) Glynn, R. W.; Miller, N.; Kerin, M. J. 17q12-21 - the pursuit of targeted therapy in breast cancer. *Cancer Treat. Rev.* **2010**, *36*, 224-229.
- (90) Kauraniemi, P.; Kallioniemi, A. Activation of multiple cancer-associated genes at the ERBB2 amplicon in breast cancer. *Endocr. Relat. Cancer* **2006**, *13*, 39-49.
- (91) Bai, T.; Luoh, S. W. GRB-7 facilitates HER-2/Neu-mediated signal transduction and tumor formation. *Carcinogenesis* **2008**, *29*, 473-479.
- (92) Chu, P. Y.; Li, T. K.; Ding, S. T.; Lai, I. R.; Shen, T. L. EGF-induced Grb7 recruits and promotes Ras activity essential for the tumorigenicity of Sk-Br3 breast cancer cells. *J. Biol. Chem.* **2010**, doi: 10.1074/jbc.C110.114124
- (93) Nadler, Y.; Gonzalez, A. M.; Camp, R. L.; Rimm, D. L.; Kluger, H. M.; Kluger, Y. Growth factor receptor-bound protein-7 (Grb7) as a prognostic marker and therapeutic target in breast cancer. *Ann. Oncol.* **2010**, *21*, 466-473.
- (94) Kao, J.; Pollack, J. R. RNA interference-based functional dissection of the 17q12 amplicon in breast cancer reveals contribution of coamplified genes. *Genes, Chromosomes & Cancer* **2006**, *45*, 761-769.
- (95) Nencioni, A.; Cea, M.; Garuti, A.; Passalacqua, M.; Raffaghello, L.; Soncini, D.; Moran, E.; Zoppoli, G.; Pistoia, V.; Patrone, F.; Ballestrero, A. Grb7 up regulation

- is a molecular adaptation to HER2 signaling inhibition due to removal of Akt-mediated gene repression. *PLoS One* **2010**, *5*, e9024.
- (96) Stockler, M.; Wilcken, N. R.; Gherzi, D.; Simes, R. J. Systematic reviews of chemotherapy and endocrine therapy in metastatic breast cancer. *Cancer Treat. Rev.* **2000**, *26*, 151-168.
- (97) van Agthoven, T.; Veldscholte, J.; Smid, M.; van Agthoven, T. L.; Vreede, L.; Broertjes, M.; de Vries, I.; de Jong, D.; Sarwari, R.; Dorssers, L. C. Functional identification of genes causing estrogen independence of human breast cancer cells. *Breast Cancer Res. Treat.* **2009**, *114*, 23-30.
- (98) van Agthoven, T.; Sieuwerts, A. M.; Meijer-vanGelder, M. E.; Look, M. P.; Smid, M.; Veldscholte, J.; Sleijfer, S.; Foekens, J. A.; Dorssers, L. C. Relevance of breast cancer antiestrogen resistance genes in human breast cancer progression and tamoxifen resistance. *J. Clin. Oncol.* **2009**, *27*, 542-549.
- (99) Paik, S.; Shak, S.; Tang, G.; Kim, C.; Baker, J.; Cronin, M.; Baehner, F. L.; Walker, M. G.; Watson, D.; Park, T.; Hiller, W.; Fisher, E. R.; Wickerhan, D. L.; Bryant, J.; Wolmark, N. A multigene assay to predict recurrence of tamoxifen-treated, node-negative breast cancer. *N. Engl. J. Med.* **2004**, *351*, 2817-2826.
- (100) Pero, S. C.; Shukla, G. S.; Cookson, M. M.; Flemer, S, Jr.; Krag, D. N. Combination treatment with Grb7 peptide and Doxorubicin or Trastuzumab (Herceptin) results in cooperative cell growth inhibition in breast cancer cells. *Br. J. Cancer.* **2007**, *96*, 1520-1525.
- (101) Ferlay, J.; Bray, F.; Pisani, P.; Parkin, D. GLOBOCAN 2002: cancer incidence, mortality and prevalence worldwide. IARC cancer baseno.5 version 2.0. Lyon: IARC Press, **2004**.
- (102) Yamada, T.; Koyama, T.; Ohwada, S.; Tago, K.; Sakamoto, I.; Yoshimura, S.; Hamada, K.; Takeyoshi, I.; Morishita, Y. Frame shift mutations in the MBD4/MED1 gene in primary gastric cancer with high-frequency microsatellite instability. *Cancer Lett.* **2002**, *181*, 115-120.
- (103) Tanaka, S.; Mori, M.; Akiyoshi, T.; Tanaka, Y.; Mafune, K.; Wands, J. R.; Sugimachi, K. Coexpression of Grb7 with epidermal growth factor receptor or Her2/erbB2 in human advanced esophageal carcinoma. *Cancer Res.* **1997**, *57*, 28-31.
- (104) Kishi, T.; Sasaki, H.; Akiyama, N.; Ishizuka, T.; Sakamoto, H.; Aizawa, S.; Sugimura, T.; Terada, M. Molecular Cloning of Human GRB-7 Co-amplified with CAB1 and c-ERBB-2 in Primary Gastric Cancer. *Biochem. Biophys. Res. Commun.* **1997**, *232*, 5-9.
- (105) Maqani, N.; Belkhiri, A.; Moskaluk, C.; Knuutila, S.; Dar, A. A.; El-Rifai, W. Molecular dissection of 17q12 amplicon in upper gastrointestinal adenocarcinomas. *Mol. Cancer Res.* **2006**, *4*, 449-455.
- (106) Myllykangas, S.; Junnila, S.; Kokkola, A.; Autio, R.; Scheinin, I.; Kiviluoto, T.; Karjalainen-Lindsberg, M. L.; Hollmén, J.; Knuutila, S.; Puolakkainen, P.; Monni, O. Integrated gene copy number and expression microarray analysis of gastric

- cancer highlights potential target genes. *Int. J. Cancer* **2008**, *123*, 817-825.
- (107) Yang, S.; Jeung, H. C.; Jeong, H. J.; Choi, Y. H.; Kim, J. E.; Jung, J. J.; Rha, S. Y.; Yang, W. I.; Chung, H. C. Identification of genes with correlated patterns of variations in DNA copy number and gene expression level in gastric cancer. *Genomics* **2007**, *89*, 451-459.
- (108) Bardeesy, N.; DePinho, R. A. Pancreatic cancer biology and genetics. *Nat. Rev. Cancer* **2002**, *2*, 897-909.
- (109) Tanaka, S.; Pero, S. C.; Taguchi, K.; Shimada, M.; Mori, M.; Krag, D. N.; Arii, S. Specific peptide ligand for Grb7 signal transduction protein and pancreatic cancer metastasis. *J. Natl. Cancer Inst.* **2006**, *98*, 491-498.
- (110) Safran, H.; Steinhoff, M.; Mangray, S.; Rathore, R.; King, T. C.; Chai, L.; Berzein, K.; Moore, T.; Iannitti, D.; Reiss, P.; Pasquariello, T.; Akerman, P.; Quirk, D.; Mass, R.; Goldstein, L.; Tantravahi, U. Overexpression of the HER-2/neu oncogene in pancreatic adenocarcinoma. *Am. J. Clin. Oncol.* **2001**, *24*, 496-499.
- (111) Furuyama, K.; Doi, R.; Mori, T.; Toyoda, E.; Ito, D.; Kami, K.; Koizumi, M.; Kida, A.; Kawaguchi, Y.; Fujimoto, K. Clinical Significance of Focal Adhesion Kinase in Resectable Pancreatic Cancer. *World J. Surg.* **2006**, *30*, 219-226.
- (112) Bashyam, M. D.; Bair, R.; Kim, Y. H.; Wang, P.; Hernandez-Boussard, T.; Karikari, C. A.; Tibshirani, R.; Maitra, A.; Pollack, J. R. Array-based comparative genomic hybridization identifies localized DNA amplifications and homozygous deletions in pancreatic cancer. *Neoplasia* **2005**, *7*, 556-562.
- (113) Koppert, L. B.; Wijnhoven, B. P.; van Dekken, H.; Tilanus, H. W.; Dinjens, W. N. The molecular biology of esophageal adenocarcinoma. *J. Surg. Oncol.* **2005**, *92*, 169-190.
- (114) Boonstra, J. J.; Dinjens, W. N.; Tilanus, H. W.; Koppert, L. B. Molecular biological challenges in the treatment of esophageal adenocarcinoma. *Expert. Rev. Gastroenterol. Hepatol.* **2007**, *1*, 275-286.
- (115) Tanaka, S.; Sugimachi, K.; Kawaguchi, H.; Saeki, H.; Ohno, S.; Wands, J. R. Grb7 signal transduction protein mediates metastatic progression of esophageal carcinoma. *J. Cell Physiol.* **2000**, *183*, 411-415.
- (116) Akiyama, N.; Sasaki, H.; Ishizuka, T.; Kishi, T.; Sakamoto, H.; Onda, M.; Hirai, H.; Yazaki, Y.; Sugimura, T.; Terada, M. Isolation of a candidate gene, CAB1, for cholesterol transport to mitochondria from the c-ERBB-2 amplicon by a modified cDNA selection method. *Cancer Res.* **1997**, *57*, 3548-3553.
- (117) Walch, A.; Specht, K.; Braselmann, H.; Stein, H.; Siewert, J. R.; Hopt, U.; Höfler, H.; Werner, M. Coamplification and coexpression of GRB7 and ERBB2 is found in high grade intraepithelial neoplasia and in invasive Barrett's carcinoma. *Int. J. Cancer.* **2004**, *112*, 747-753.
- (118) Bruix, J.; Lovet, J. M. Prognostic prediction and treatment strategy in hepatocellular carcinoma. *Hepatology* **2002**, *35*, 519-524.
- (119) Itoh, S.; Taketomi, A.; Tanaka, S.; Harimoto, N.; Yamashita, Y.; Aishima, S.; Maeda, T.; Shirabe, K.; Shimada, M.; Maehara, Y. Role of growth factor receptor

- bound protein 7 in hepatocellular carcinoma. *Mol. Cancer Res.* **2007**, *5*, 667-673.
- (120) Hoskins, W. J. Prospective on ovarian cancer: why prevent? *J. Cell Biochem. Suppl.* **1995**, *23*, 189-199.
- (121) Wang, Y.; Chan, D. W.; Liu, V. W.; Chiu, P.; Ngan, H. Y. Differential functions of growth factor receptor-bound protein 7 (GRB7) and its variant GRB7v in ovarian carcinogenesis. *Clin. Cancer Res.* **2010**, *16*, 2529-2539.
- (122) Horwich, A.; Shipley, J.; Huddart, R. Testicular germ-cell cancer. *Lancet* **2006**, *367*, 754-765.
- (123) Skotheim, R. I.; Abeler, V. M.; Nesland, J. M.; Fosså, S. D.; Holm, R.; Wagner, U.; Flørenes, V. A.; Aass, N.; Kallioniemi, O. P.; Lothe, R. A. Candidate genes for testicular cancer evaluated by in situ protein expression analyses on tissue microarrays. *Neoplasia* **2003**, *5*, 397-404.
- (124) McIntyre, A.; Summersgill, B.; Spendlove, H. E.; Huddart, R.; Houlston, R.; Shipley, J. Activating mutations and/or expression levels of tyrosine kinase receptors GRB7, RAS, and BRAF in testicular germ cell tumors. *Neoplasia* **2005**, *7*, 1047-1052.
- (125) Skotheim, R. I.; Monni, O.; Mousses, S.; Fosså, S. D.; Kallioniemi, O. P.; Lothe, R. A.; Kallioniemi, A. New insights into testicular germ cell tumorigenesis from gene expression profiling. *Cancer Res.* **2002**, *62*, 2359-2364.
- (126) Kraggerud, S. M.; Skotheim, R. I.; Szymanska, J.; Eknaes, M.; Fossa, S. D.; Stenwig, A. E.; Peltomaki, P.; Lothe, R. A. Genome profiles of familial / bilateral and sporadic testicular germ cell tumors. *Genes, Chromosomes & Cancer* **2002**, *34*, 168-174.
- (127) Goddard, N. C.; McIntyre, A.; Summersgill, B.; Gilbert, D.; Kitazawa, S.; Shipley, J. KIT and RAS signaling pathways in testicular germ cell tumors: new data and a review of the literature. *Int. J. Androl.* **2007**, *30*, 337-348.
- (128) Chiorazzi, N.; Ferrarini, M. B cell chronic lymphocytic leukemia: lessons learned from studies of the B cell antigen receptor. *Annu. Rev. Immunol.* **2003**, *21*, 841-894.
- (129) Haran, M.; Chebatco, S.; Flaishon, L.; Lantner, F.; Harpaz, N.; Valinsky, L.; Berrebi, A.; Shachar, I. Grb7 expression and cellular migration in chronic lymphocytic leukemia: a comparative study of early and advanced stage disease. *Leukemia* **2004**, *18*, 1948-1955.
- (130) Majithia, V.; Geraci, S. A. Rheumatoid arthritis: diagnosis and management. *Am. J. Med.* **2007**, *120*, 936-939.
- (131) Kim, C. W.; Cho, E. H.; Lee, Y. J.; Kim, Y. H.; Hah, Y. S.; Kim, D. R. Disease-specific proteins from rheumatoid arthritis patients. *J. Korean Med Sci.* **2006**, *21*, 478-484.
- (132) Pias, S.; Peterson, T. A.; Johnson, D. L.; Lyons, B. A. The Intertwining of Structure and Function: Proposed Helix-Swapping of the SH2 Domain of Grb7,

- A Regulatory Protein Implicated in Cancer Progression and Inflammation. *Crit. Rev. Immunol.* **2010**, *30*, 299-304.
- (133) Tokura, Y. Extrinsic and intrinsic types of atopic dermatitis. *J. Dermatol. Sci.* **2010**, *58*, 1-7.
- (134) Yoon, S. W.; Kim, T. Y.; Sung, M. H.; Kim, C. J.; Poo, H. Comparative proteomic analysis of peripheral blood eosinophils from healthy donors and atopic dermatitis patients with eosinophilia. *Proteomics* **2005**, *5*, 987-995.
- (135) An, J. J.; Kim, S. Y.; Lee, S. H.; Kim, D. W.; Ryu, H. J.; Yeo, S. I.; Jang, S. H.; Kwon, H. J.; Kim, T. Y.; Lee, S. C.; Poo, H.; Cho, S. W.; Lee, K. S.; Park, J.; Eum, W. S.; Choi, S. Y. Transduced PEP-1-Grb7 fusion protein suppressed LPS-induced COX-2 expression. *J. Biochem. Mol. Biol.* **2007**, *40*, 189-195.
- (136) Li, X.; Yu, M.; Zhu, M. Innate immune signaling pathways in animals: beyond reductionism. *Int. Rev. Immunol.* **2009**, *28*, 207-238.
- (137) Turner, S. J.; La Gruta, N. L.; Kedzierska, K.; Thomas, P. G.; Doherty, P. C. Functional implications of T cell receptor diversity. *Curr. Opin. Immunol.* **2009**, *21*, 286-290.
- (138) Chu, P.; Pardo, J.; Zhao, H.; Li, C. C.; Pali, E.; Shen, M. M.; Qu, K.; Yu, S. X.; Huang, B. C.; Yu, P.; Masuda, E. S.; Molineaux, S. M.; Kolbinger, F.; Aversa, G.; de Vries, J.; Payan, D. G.; Liao, X. C. Systematic identification of regulatory proteins critical for T-cell activation. *J. Biol.* **2003**, *2*:21.
- (139) De Vet, E. C.; Aguado, B.; Campbell, R. D. Adaptor signalling proteins Grb2 and Grb7 are recruited by human G6f, a novel member of the immunoglobulin superfamily encoded in the MHC. *Biochem. J.* **2003**, *375*, 207-213.
- (140) Di Resta, C.; Becchetti, A. Introduction to ion channels. *Adv. Exp. Med. Biol.* **2010**, *674*, 9-21.
- (141) Clare, J. J. Targeting ion channels for drug discovery. *Discov. Med.* **2010**, *9*, 253-60.
- (142) Ureche, O. N.; Ureche, L.; Henrion, U.; Strutz-Seeböhm, N.; Bundis, F.; Steinmeyer, K.; Lang, F.; Seeböhm, G. Differential modulation of cardiac potassium channels by Grb adaptor proteins. *Biochem. Biophys. Res. Commun.* **2009**, *384*, 28-31.
- (143) Bundis, F. Identifizierung und funktionelle Charakterisierung neuer Interaktionspartner des renalen ROMK-Kaliumkanals Doctoral thesis, 2006. Available from: <<http://deposit.ddb.de/cgi-bin/dokserv?idn=982481659>>.
- (144) Li, W.; Lee, J.; Vikis, H. G.; Lee, S. H.; Liu, G.; Aurandt, J.; Shen, T. L.; Fearon, E. R.; Guan, J. L.; Han, M.; Rao, Y.; Hong, K.; Guan, K. L. Activation of FAK and Src are receptor-proximal events required for netrin signaling. *Nat. Neurosci.* **2004**, *7*, 1213-1221.
- (145) Liu, G.; Beggs, H.; Jürgensen, C.; Park, H. T.; Tang, H.; Gorski, J.; Jones, K. R.; Reichardt, L. F.; Wu, J.; Rao, Y. Netrin requires focal adhesion kinase and Src family kinases for axon outgrowth and attraction. *Nat. Neurosci.* **2004**, *7*, 1222-1232.

- (146) Ren, X. R.; Ming, G. L.; Xie, Y.; Hong, Y.; Sun, D. M.; Zhao, Z. Q.; Feng, Z.; Wang, Q.; Shim, S.; Chen, Z. F.; Song, H. J.; Mei, L.; Xiong, W. C. Focal adhesion kinase in netrin-1 signaling. *Nat. Neurosci.* **2004**, *7*, 1204-1212.
- (147) Tsai, N. P.; Tsui, Y. C.; Pinter, J. E.; Loh, H. H.; Wei, L. N. Kappa opioid receptor contributes to EGF-stimulated neurite extension in development. *Proc. Natl. Acad. Sci. U.S.A.* **2010**, *107*, 3216-3221.
- (148) Pero, S. C.; Oligino, L.; Daly, R. J.; Soden, A. L.; Liu, C.; Roller, P. P.; Li, P.; Krag, D. N. Identification of novel non-phosphorylated ligands, which bind selectively to the SH2 domain of Grb7. *J. Biol. Chem.* **2002**, *277*, 11918-11926.
- (149) Ambaye, N. D.; Lim, R. C.; Clayton, D. J.; Gunzburg, M. J.; Price, J. T.; Pero, S. C.; Krag, D. N.; Wilce, M. C.; Aguilar, M. I.; Perlmutter, P.; Wilce, J. A. Uptake of a cell permeable G7-18NATE construct into cells and binding with the Grb7-SH2 domain. *Biopolymers* **2010**, DOI: 10.1002/bip.21403.
- (150) Spuches, A. M.; Argiros, H. J.; Lee, K. H.; Haas, L. L.; Pero, S. C.; Krag, D. N.; Roller, P. P.; Wilcox, D. E.; Lyons, B. A. Calorimetric investigation of phosphorylated and non-phosphorylated peptide ligand binding to the human Grb7 SH2 domain. *J. Mol. Recognit.* **2007**, *20*, 245-252.
- (151) Gunzburg, M. J.; Ambaye, N. D.; Hertzog, J. T.; Del Borgo, M. P.; Pero, S. C.; Krag, D. N.; Wilce, M. C. J.; Aguilar, M. I.; Perlmutter, P.; Wilce, J. A. Use of SPR to Study the Interaction of G7-18NATE Peptide with the Grb7-SH2 Domain. *Int. J. Pept. Res. Therapeut.* **2010**, *16*, 177-184.
- (152) Howl, J.; Nicholl, I. D.; Jones, S. The many futures for cell-penetrating peptides: how soon is now? *Biochem. Soc. Trans.* **2007**, *35*, 767-769.
- (153) Luzy, J. P.; Chen, H.; Gril, B.; Liu, W. Q.; Vidal, M.; Perdureau, D.; Burnol, A. F.; Garbay, C. Development of binding assays for the SH2 domain of Grb7 and Grb2 using fluorescence polarization. *J. Biomol. Screen.* **2008**, *13*, 112-119.

1.8. Research Objectives

Grb7 is known to mediate a diverse spectrum of oncogenic pathways. Extensive research on different aspects of Grb7 carried over the years means it is now a promising antitumor drug target. Its druggability is demonstrated with the recent discovery of peptide antagonists. Apart from these early phase experimental antagonists, currently there exist no drug that is developed or known to act on Grb7. Moreover, the structure of Grb7SH2 domain both in apo form and in complex with a peptide antagonist is characterized. These studies have delineated the chemical features of the binding site and its requirement for effective interaction with potential antagonists. This project, thus, seeks to exploit the available background structural, biochemical and biophysical information to design, synthesize, test and optimize second-generation potent, selective, stable and cell permeable antagonists.

In particular the study aims to:

1. Design, synthesize and conduct binding studies of peptidic Grb7 antagonists

1.1. Cell Permeable G7-18NATE derivatives

1.2. G7-18NATE based analogue design

2. Structure based virtual screening

3. Structural characterization of the binding interaction using X-ray Crystallography and computational chemistry

The first part of the research focuses on the design of cell permeable forms of the lead G7-18NATE polypeptide, binding characterization as well as cellular uptake studies. This will be followed by the design of monocyclic and bicyclic G7-18NATE based second-generation polypeptides antagonists. In the structure based virtual screening part of the project, we seek to exploit the available structural information to discover novel antagonists of Grb7. In particular the in-house available co-crystal structure of G7-18NATE/Grb7 SH2 domain and a known potent tripeptide will be employed to initiate the virtual screening effort to identify small molecule antagonists. Finally, structural studies with the most promising lead candidates will be undertaken to further characterize the binding interaction.

Chapter 2

Sample Preparation and Crystallographic methods

This chapter describes the experimental procedures undertaken to prepare the peptide antagonists and the Grb7 SH2 domain protein used as a receptor for the *in vitro* binding and structural studies. The first section presents the details of solid phase peptide synthesis, purification and characterization strategies. The second section describes the overexpression and purification of the Grb7 SH2 domain protein. The last section details the crystallization and data processing procedures undertaken for the structural studies. Other methodologies utilized in the research undertaken for this thesis are described in the relevant chapters which have been prepared in manuscript format.

2.1. Solid Phase Peptide synthesis

2.1.1. Background

Solid phase peptide synthesis (SPPS)¹⁻³ is synthesis of peptides on an insoluble polymeric support (the solid). Introduced by Merrifield⁴⁻⁶ in the 60's, the principle of SPPS is extended to any chemical synthesis on a solid support and is generalized as a solid phase organic synthesis (SPOS).⁷ The practice of SPPS is typically undertaken in a sequence of chemical reactions termed *activation*, where the electrophilicity of the carbonyl carbon of amino acids is enhanced by the attachment of an electron withdrawing moiety;⁸ *coupling*, which refers to the actual amide bond forming reaction between the activated COOH of one amino acid and the amino (NH₂) of another amino acid; *deprotection* refers to the removal of amino or side chain protecting groups; and washing/filtration step used to get rid of excess or unused reactants and solvents. The entire procedure is cyclic where the aforementioned reactions are repeated till all of the residues are incorporated. Finally a *cleavage* reaction is effected to dislodge the peptide/protein from the insoluble support. Typically, the amino acids are N-terminally protected (temporary protection) with additional protection made on the side chain of the trifunctional amino acids (permanent protection). The N-terminal protecting group commonly utilized in SPPS are either the acid labile tert-butyloxycarbonyl (Boc) or base labile 9-fluorenylmethoxycarbonyl (Fmoc) which also serve to class SPPS as a Boc- or Fmoc based tactic.^{9,10} The development of activators, deprotection and protection schemes, cleavage cocktails and insoluble supports is an active area of research and there is a huge variety of each available to meet the desired level of orthogonality.¹⁰ Chemical peptide/protein synthesis is effected from C to N-terminal as opposed to the biological protein/peptide synthesis which runs from N to C-terminal.¹¹

Whereas the basic chemistry remains identical to the solution phase counterpart, solid phase synthesis has certain practical benefits such as (1) driving reactions to completion via the use of excess reagents; (2) use of simple washing and filtration to get rid of excess reagents and soluble by-products as compared to extraction and chromatographic separation, for example; (3) minimal losses of precious material as the product remains attached to the support throughout the synthesis.¹²

2.1.2. Synthesis of G7-18NATE analogue peptides

In this thesis, solid phase synthesis of the following peptides (see Fig. 2.1.) was carried out employing the Fmoc based chemistry stratagem. In what follows, the entire procedure will be described in detail.

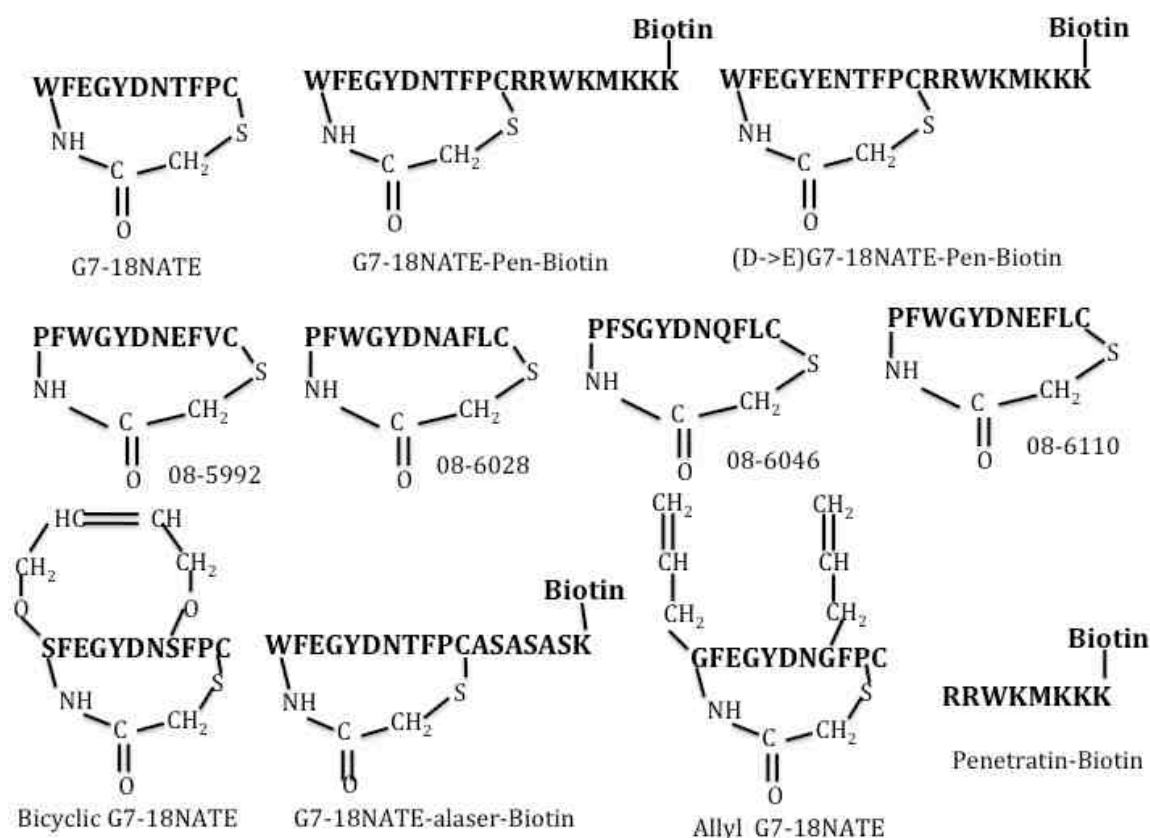


Figure 2.1. G7-18NATE and its Analogues. Peptides 08-6046, Bicyclic G7-18NATE and Allyl G7-18NATE were made manually using the Fmoc-strategy whereas the rest are synthesized in a semi automated manner. First row, G7-18NATE derivatives; second row, G7-18NATE Analogues; third row, Bicyclic G7-18NATE and control Peptides. Amino acid letters are shown in bold font.

The amino acids, protection and deprotection reagents, solvents, activators bases and coupling agents used are shown in Table 2.1.

Table 2.1: Amino Acids and reagents employed for peptides synthesis

Amino Acids:			
Fmoc-Trp (Boc)-OH	Fmoc-Asn (Trt)-OH	Fmoc-Glu (OtBu)-OH	Fmoc-Gly-OH,
Fmoc-Tyr (tBu)-OH	Fmoc-Thr (tBu)-OH	Fmoc-Asp (OtBu)-OH	Fmoc-Phe-OH
Fmoc-Pro-OH	Fmoc-Cys (Trt)-OH	Fmoc-Arg (Pbf)-OH	Fmoc-Met-OH
Fmoc-Lys(Mmt)-OH	Fmoc-Ser(tBu)-OH	Fmoc-Leu-OH	Fmoc-Val-OH
Fmoc-Lys(Boc)-OH	Fmoc-Ser(allyl)-OH	Fmoc-Allyl Gly-OH	
Deprotection: 20% Piperidine in DMF			
Solvents: Dichloromethane, Dimethylformamide, Acetone, Methanol N-methylpyrrolidone, Ethyl acetate, Diethyl Ether, Ethanol,			
Coupling Agents: Di-isopropyl ethylamine (DIPEA), HBTU, HATU, HoBt			
Cleavage Solution: Trifluoro acetic acid (TFA), Tri-isopropyl Silane (TIPS), Ethane dithiothritol (EDT), Water			

2.1.3. Resin Treatment

The solid support used throughout the synthesis was Rink amide resin¹³ (see Fig. 2.2). Hence all the peptides were synthesized as peptide amides. Rink amide resin is an acid labile resin commonly employed in the synthetic preparation of amides,¹³ amide derivatives, and other organic molecules.^{11,12} It is typically available as a 1-2% divinylbenzene cross-linked polystyrene possessing a mesh size of 200-400. It has a peptide loading capacity of up to 1.0 mmol/g and swells well in commonly used solvents in peptide synthesis

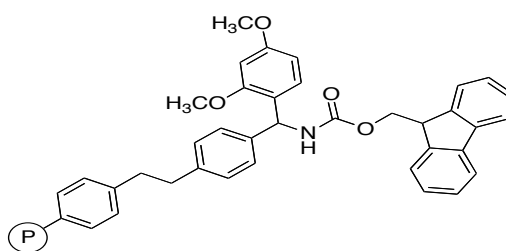


Figure 2.2: Rink Amide Resin. $\textcircled{\text{P}}$ represents the cross-linked polymeric support.

The scale of the synthesis followed in all cases was 0.1 mmole. And hence in every case 100 mg of rink amid resin was taken to serve as an insoluble support. As the swelling properties of polystyrene based resins vary depending on solvents and is crucial for exposing coupling sites, the resin was swelled for 30 min in DMF added

to about three times the resin volume. For some peptides where poor coupling was noticed, swelling in a 1:1 mixture of DCM/DMF was carried out.

Rink amide resin itself is available as Fmoc-derivatized co-polymer.¹³ Following swelling, the resin Fmoc-removal was achieved using a deprotection solution of 20%(v/v) piperidine in synthetic grade DMF. The deprotection solution was added in three times resin volume and the reaction was effected at room temperature for 30 min with occasional stirring. This was followed by resin washing successively with DMF (once, 3x resin volume), DCM (once, 3x resin volume) and DMF (twice, 3x resin volume). The wash time was about 2 min in each case and vacuum was applied to effect immediate filtration. The mechanism of Fmoc-removal is displayed in Fig. 2.3.

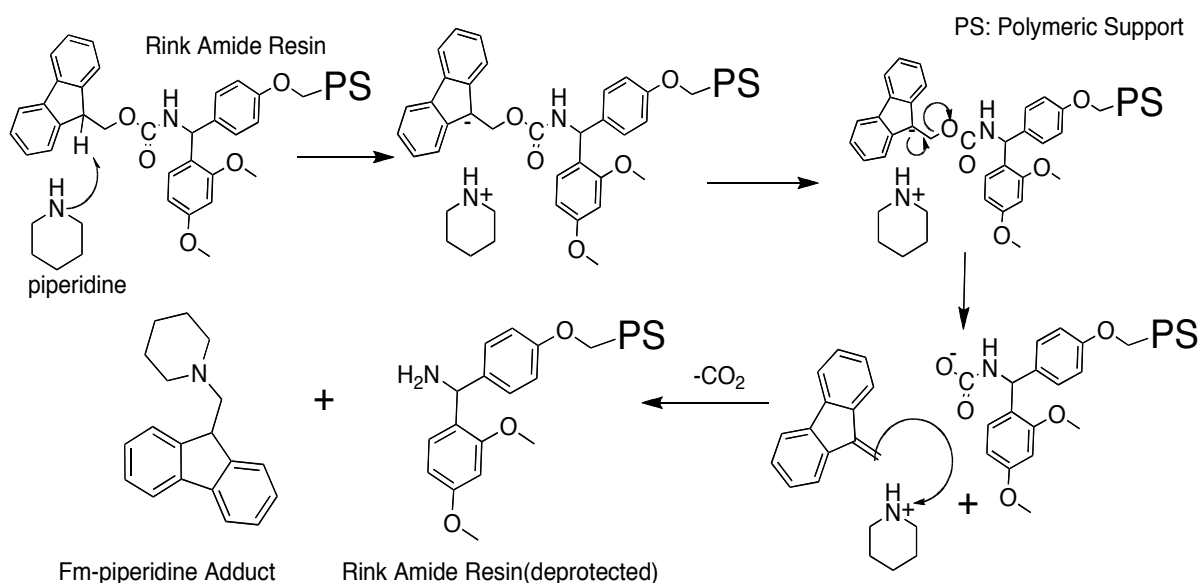


Figure 2.3: The resin Fmoc removal reaction.

2.1.4. Kaiser Test

The successes of deprotection and manual coupling reactions were checked using Kaiser's ninhydrin based color reaction.¹⁶ After washing the deprotected/coupled resin, a few resin beads were taken out, washed with 70% (v/v) ethanol/H₂O. To the dried deprotected/coupled resin 15 μ l of Reagent A, 30 μ l of Reagent B and 15 μ l of Reagent C were added and the reaction mixture incubated at 110 °C for 5-10 min. The absence or presence of deep blue color was used as a confirmation of coupling or deprotection respectively, Fig. 2.4. Table 2.2 displays the composition of reagents used in Kaiser test.

Table 2.2: Composition of Kaiser's test Reagents

Reagent	Composition	Strength
A	Ninhydrin/Ethanol	5% (w/v)
B	KCN/Pyridine	20 μ M
C	Phenol/Ethanol	76%(w/v)

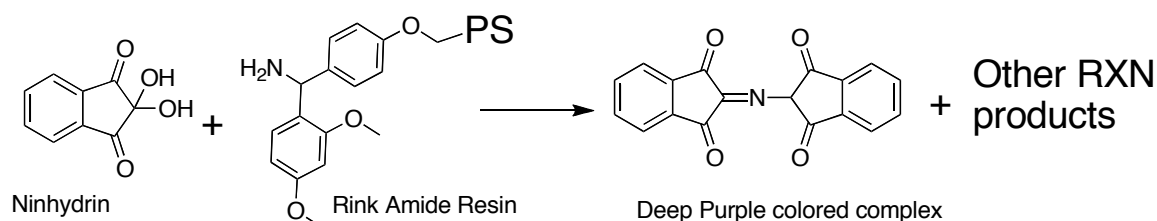


Figure 2.4. Kaiser's ninhydrin based color reaction used to check the success of Fmoc removal and residue coupling reactions. After treating few washed resin beads with the ninhydrin reagents, the appearance of deep blue color is taken to indicate the removal of Fmoc group from the resin.

2.1.5. First residue coupling to the resin

As is the case with the standard Fmoc-synthetic strategy, the synthesis direction was from C-to-N terminus and hence in all the peptide amides made, the first residue to be loaded was either Fmoc-Cys (trt)-OH or Fmoc-Lys (Biotin)-OH. All the Fmoc-amino acids were preactivated by reaction with the activating and coupling agents.¹¹ The coupling agent used was HBTU (*O*-benzotriazol-1-yl-*N,N,N',N'*-tetramethyluronium hexafluorophosphate).^{17,18} As the scale of the synthesis is 0.1 mmole, 0.3 mmole (3.0 fold excess) of each amino acid and 2.9 mmole (2.9-fold excess) coupling agents were used. The concentration of amino acids and the coupling agent was set at 0.5 M in the first residue manual coupling and 0.2 M in the automated microwave peptide synthesizer. The activating agent and neutralizing agent employed was 100 μ l of di-isopropyl ethylamine (DIEPA). Specifically the manual pre-activation reaction was carried out by dissolving 113.7 mg of HBTU in 550 μ l of synthetic grade DMF which in turn was used to dissolve the residues fully. 100 μ l of DIEPA was added to the mixture and full dissolution was effected and a preactivation time of 2 min was allowed. Fig. 2.5 illustrates the mechanism for the preactivation reaction of Fmoc-Cys(trt)-OH. All the amino acid preactivation reactions follow the same mechanism.

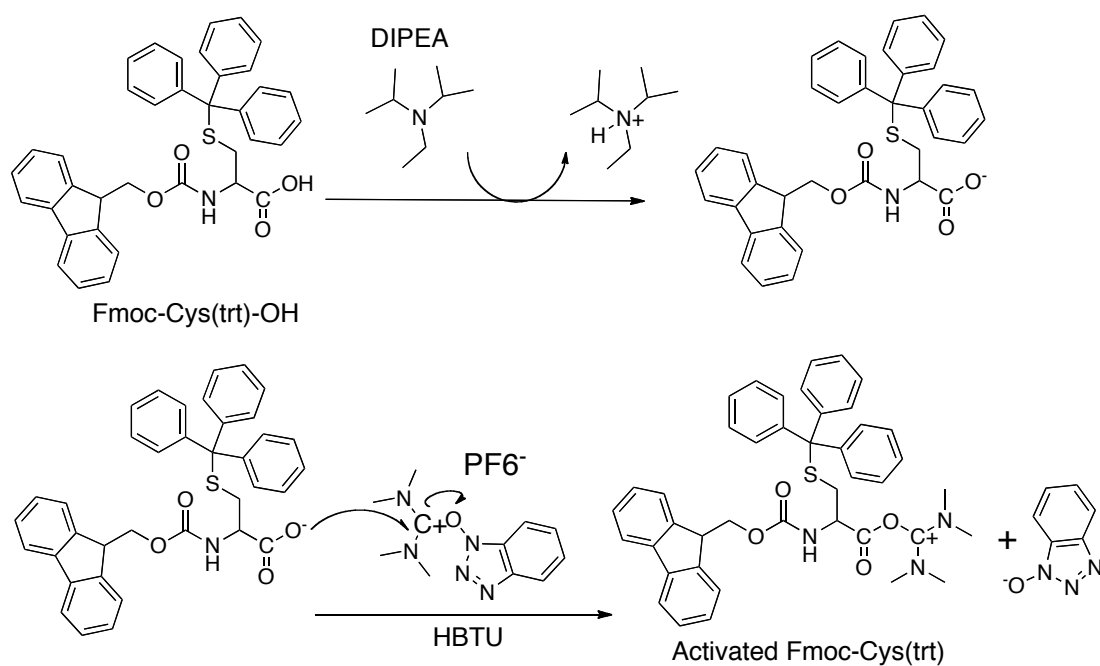


Figure 2.5: The preactivation of Fmoc-Cys (trt)-OH by HBTU and DIPEA.

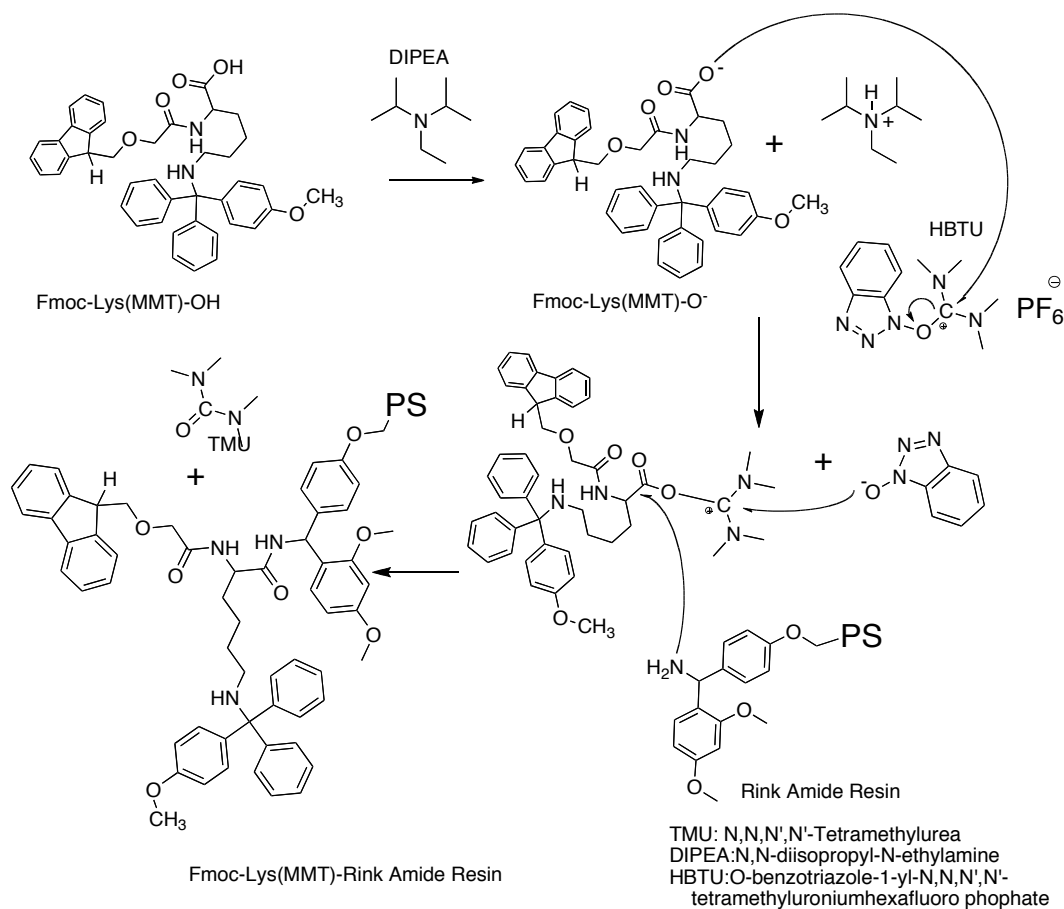


Figure 2.6: The pre-activation and coupling of Fmoc-Lys (Mmt) to rink amide resin. PS indicates the resin polymeric support

Following 2 min of activated ester formation time, the activated Fmoc-cysteine or Fmoc-Lys (Biotin) was added to the swollen deprotected resin to effect coupling/loading at RT and allowed to react for 30 min. The success of coupling was checked using ninhydrin based Kaiser's test (see Fig. 2.6) which should be colorless. In case of less-than optimal coupling, double coupling and/or increasing the coupling time or use of more powerful coupling agents such as HATU was made as alternative to effect full coupling reaction.¹⁹

2.1.6. The biotinylation reaction

In case of biotinylated polypeptides, the synthesis was effected with the use of a biotinylated lysine residue as a C-terminal residue. The first residue, Fmoc-Lys (Mmt), was preactivated using HBTU and DIPEA and then loaded manually to the deprotected resin in a similar way described for the Fmoc-Cys (trt) coupling. The monomethoxytrityl (Mmt) side chain protecting group was selectively removed with a cocktail of 10% acetic acid, 20% trifluoro-ethanol, and 70% dichloromethane. The reaction was completed in 45 min at RT.

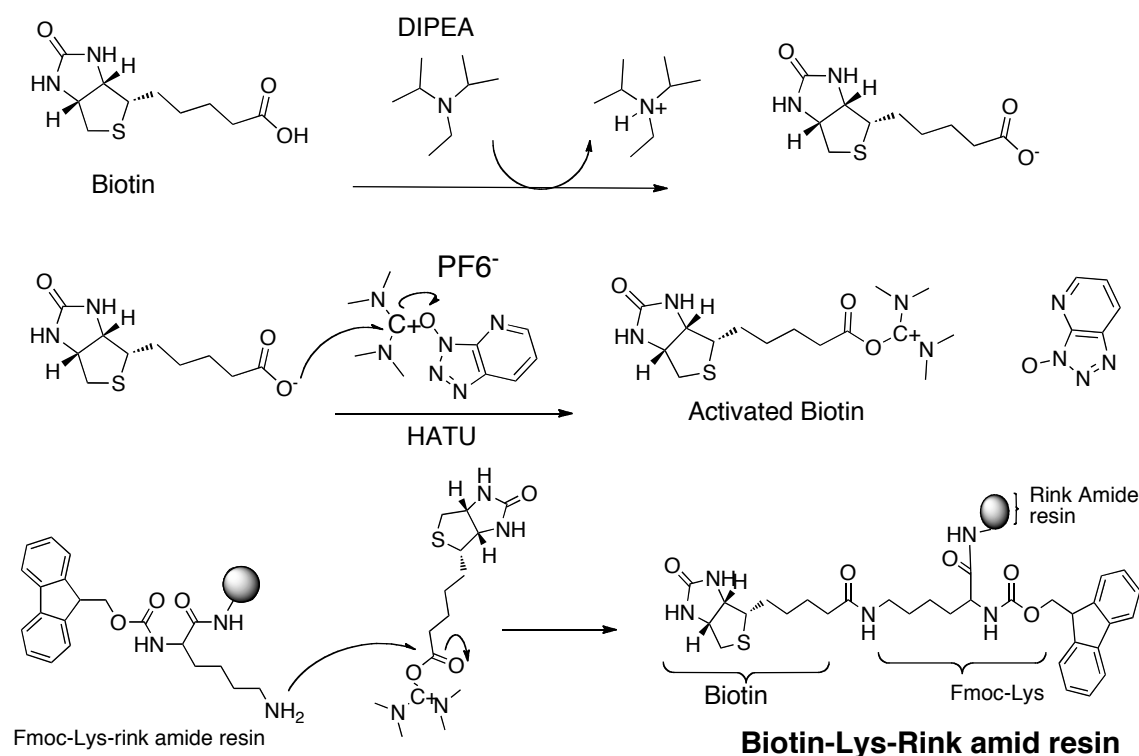


Figure 2.7. The coupling of biotin to resin bound Fmoc-Lys residue

Biotin was then coupled in a six-fold molar excess (0.6 mmole) using 2-(7-Aza-1H-benzotriazole-1-yl)-1,1,3,3-tetramethyluronium hexafluorophosphate (HATU) as coupling agents in anhydrous dimethylsulphoxide (DMSO) while DIEPA was used as activating agent. Biotinylation reaction was carried out for 60 min at RT. The success of the biotin coupling was checked using Kaiser's test¹³ as described above. The biotinylation reaction is depicted in Fig. 2.7.

2.1.7. Synthesis on automated peptide synthesizer

A Liberty's automated peptide synthesizer was used to continue the synthesis from the first C-terminal residue.²⁰ The system uses microwave energy to drive coupling and deprotection reactions to completion faster than conventional heating methods.²¹ Liberty employs a circular cavity reaction vessel and utilizes a single-mode cavity that focuses a homogenous microwave energy field on the sample.²² A method was devised based on the scale of synthesis and sequence of each peptide on the PepDriver software²⁰ of the synthesizer. The usage utilities module was then used to calculate the amount of amino acids and coupling agents. The concentration of amino acids and coupling agents was set to 0.2 M. Besides, 0.1 M HoBt²³ was added to the deprotection solution-20% piperidine in synthetic grade DMF-to suppress aspartamide formation during deprotection of Asp, Glu, Gln and Asn residues. The coupling agent was either HBTU or HATU containing 0.1 M of HoBt. The activator based used was DIEPA in N-methyl pyrrolidone (NMP). Residues known to be difficult to incorporate such as Arg, Trp, Phe, Asn, Thr were double coupled and double coupling time was allowed to ensure full incorporation. All the amino acids and the coupling agent were dissolved in synthetic grade DMF. The microwave synthesizer was flashed and calibrated as the case may be and the synthesis was started with the N-terminal amino acid deprotected but with no cleavage from the resin option effected.

2.1.8. Chloroacetylation reaction

Following incorporation of the residues by the microwave synthesizer, the N-terminal amino group was capped manually. To this end, manual chloro-acetylation was effected as follows at RT. The peptide resin was transferred to a fresh reaction

vessel (either syringe or glass) and was put under vacuum. A successive wash with DMF and DCM was carried out and the resin-peptide was dried at room temperature. The capping reagent used was chloroacetic acid anhydride. For the 0.1 mmole peptide synthesis, a 171 mg of chloro acetic acid anhydride was dissolved in 2 ml synthesis grade DMF to which 80ul of DIPEA base was added. The mixture was transferred to the resin and capping reaction was effected for 30 min. The reaction is shown in Fig. 2.8. Kaiser's test was used to check the success of capping. The resin-peptide was then washed successively with DMF and DCM and dried for 60 min at RT.

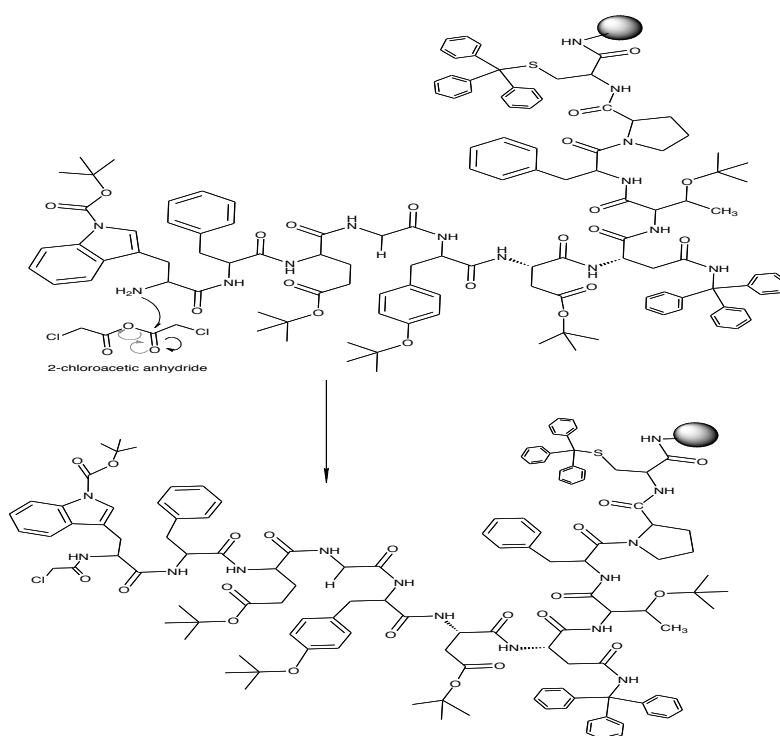


Figure 2.8: The Chloroacetylation reaction in the synthesis of G7-18NATE and related peptides. Chloroacetic acid anhydride is used to acetylate the N-terminal amino group while the crude peptide is on the rink amide resin with all the side chain protecting groups undetached from the residues. The same reaction is followed for the synthesis of the rest peptides. Electron pushing arrows are presented so as to work in sequel.

2.1.9. Ring closing metathesis

The bicyclic G7-18NATE peptide was designed so as to make the original G7-18NATE peptide²⁴ more rigid by introducing another ring onto it. This additional ring was formed using the principle of ring closing metathesis where two olefin moieties participate in intramolecular reaction to yield cycloalkene derivative and ethene.²⁵ The catalyst Hoveyda-Grubbs second generation used was used in a 20

mol% concentration.²⁶ Cyclization of peptides is a general strategy to reduce the flexibility of a peptide and thus increase the affinity toward a receptor.²⁷ The ring closing metathesis reaction is shown in Fig. 2.9.

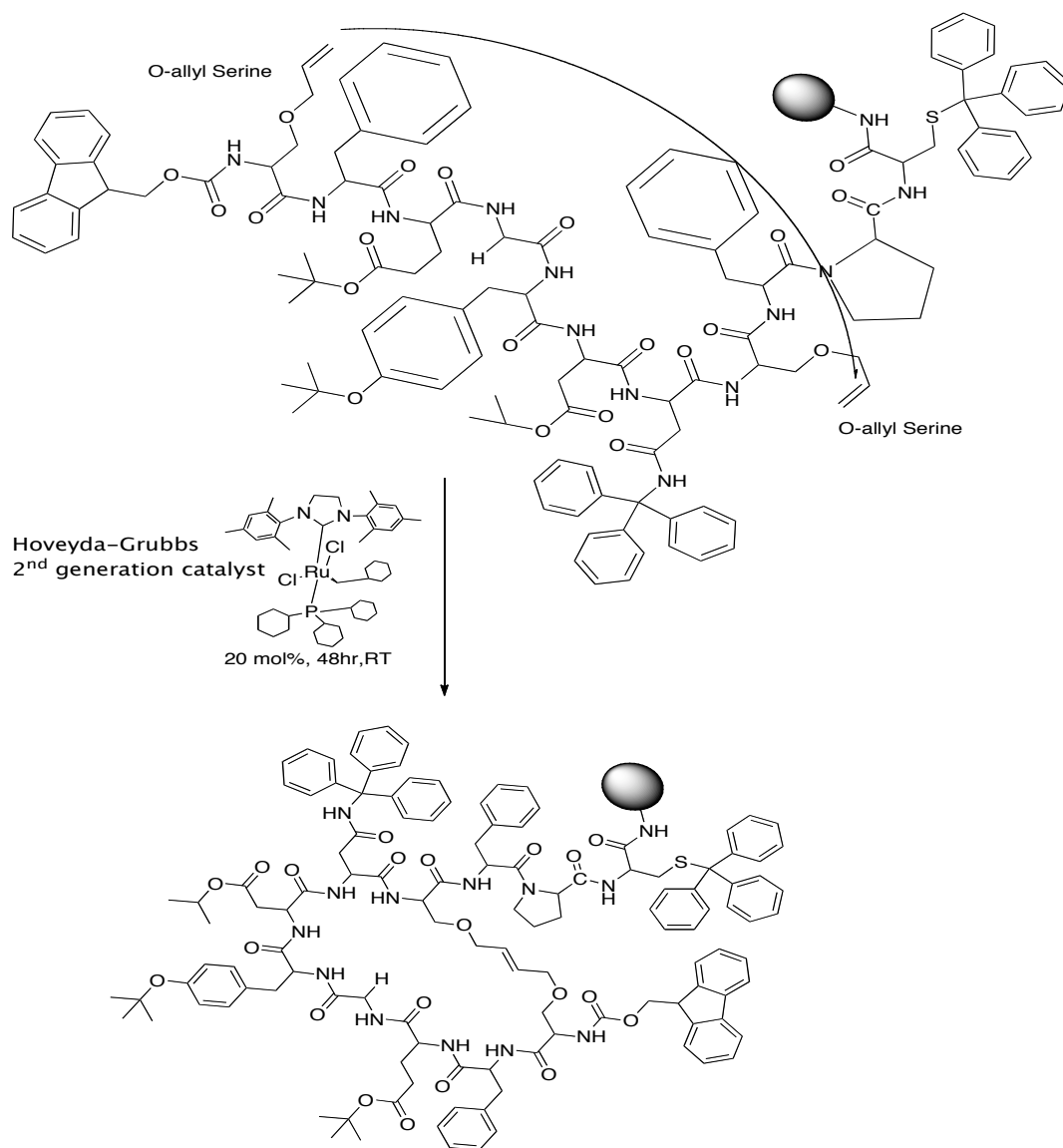


Figure 2.9. The ring closing metathesis reaction

After manual incorporation of the residues, 20 mol% excess of the second generation Hoveyda-Grubbs catalyst over the expected peptide weight of the resin bound protected peptide was dissolved in DMSO and the reaction allowed to run for 48 hrs at RT.

2.1.10. Cleavage, Precipitation and Dissolution of Peptides

Cleavage and deprotection reactions are one of the most crucial steps in peptide synthesis. There exist several procedures describing a variety of cleavage and deprotection methods for peptides synthesized with an Fmoc strategy.^{28,29} Most of these techniques are TFA-based, and differ primarily in the final concentration of TFA, types of scavengers used, and reaction times which in turn is mainly dictated by the amino acid composition of the peptide to be cleaved. In the present case, the washed and dried resin-peptide was subjected to the cleavage reaction as follows. The total dry weight of resin-peptide was noted and volume of cleavage solution required was computed based on the dry mass to be 20 ml of cleavage solution per gram of peptide-resin (20 μ l/mg). The composition of the cleavage solution used was 94.5%TFA/2.5%TIPS/2.5%MQ H₂O/0.5% EDT and the cleavage time was 3-4 hrs. After this 3-4hrs of cleavage time, TFA was evaporated under stream of nitrogen gas till the resin is dried. Figure 2.10 displays the cleavage reaction.

Peptide precipitation was achieved using ca. 50 ml cold diethyl ether in a 50 ml plastic tube kept in ice. Precipitation time was set for ca. 30 min on ice. The peptide was filtered with a sinter glass filter. The sintered-glass filter was washed successively with H₂O, DMF, DCM, Acetone, DCM and finally with diethyl ether and dried briefly over oven. The peptides were dissolved and filtered with successive small volumes of 50% ACN/H₂O (three 2 ml and two 3 ml while dissolving/mixing for about 2 minutes before filtration during each additions) into small round bottom flask. The filtrate was freeze-dried using dry ice/acetone mixture and lyophilized overnight or over the weekend.

2.1.11. Removal of CO₂ adduct

Tryptophan containing peptides are notorious for forming adduct with CO₂. This was evidently present when analytical reverse phase high performance chromatography showed unresolved peak. The strategy followed to get rid of the adduct was to treat the crude peptides with 10% acetic acid 50% acetonitrile in water solution at 2 mg/ml peptide strength. The adduct removal solution was carried out for 1 hr at room temperature. Following this treatment, the peptide solution was freeze-dried and lyophilized.

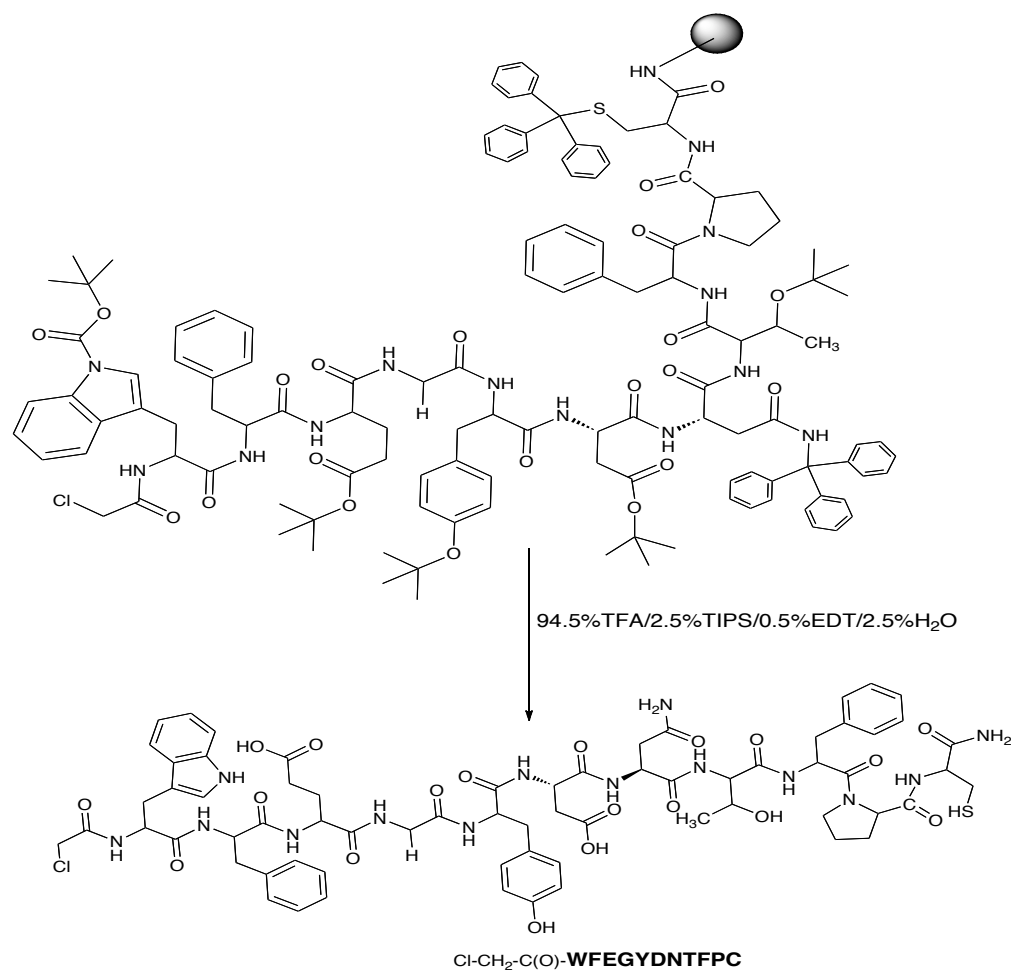


Figure 2.10: The cleavage reaction. This rxn removes all the side chain protecting groups and is used to dislodge the peptide off the resin.

2.1.12. Thioether formation

Thioether formation reaction was conducted on the fully deprotected peptide by exploiting the unique property of thiols to easily get deprotected to thiolates above pK_a of 8.0. To generate the thiolate ion, the crude lyophilized peptides were dissolved in folding buffer of 50 mM NH_4HCO_3 in 50% ACN/ H_2O , pH 8.0 at a strength of 2 mg/ml. Thioether formation was achieved in 1 hr. reaction at RT (Fig. 2.11). The folding buffer was prepared first as 100 mM NH_4HCO_3 (197.5 mg) in 25 ml of MQ water, pH 8.0 that was subsequently diluted with another 25 ml of 100 % acetonitrile to yield 50 mM buffer solution.

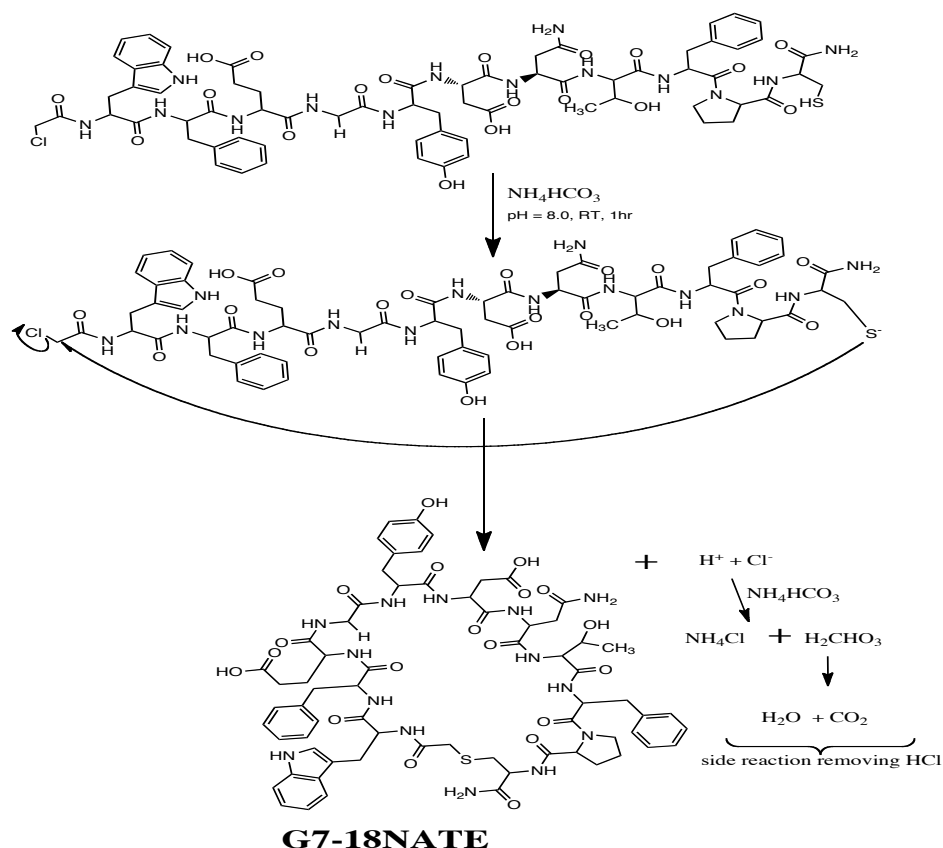


Figure 2.11: The Ring forming Reaction. Rxn of G7-18NATE formation is shown as an example. The thiolate ion participates in nucleophilic displacement of chlorine atom from the crude peptide to form the thioether ring. NH_4HCO_3 also removes the HCl produced into CO_2 and water.

As with the adduct removal treatment, when there is an insolubility problem a 2 to 4.0 M urea was used to effect complete dissolution. At the end of 1 hr. folding, the completion of the reaction was checked with Mass spectroscopy and HPLC. Additional 30-45 min was waited in case there is incomplete cyclization reaction.

2.1.13. Peptide purification

Peptide purification was conducted using HPLC (Agilent, Australia) on C18 reverse phase preparative columns (2.2cm×25cm, Vydac28TP1022). The mobile phase A contained 0.1%TFA/Water while mobile phase B comprised 0.1%TFA 80% acetonitrile in water. All buffers were filtered using 0.45 μM filter. The lyophilized peptides were dissolved in 1.5 equivalents of MQ H_2O /0.1%TFA/20%ACN and 2 M urea as needed to aid in solubility. A linear gradient was developed and purification on 20-80% acetonitrile/0.1% TFA over 60 min on an equilibrated HPLC column

with a flow rate of 6 ml/min. Detection was performed at 214 and 280 nm and fractions were collected by hand. Experiments were carried out at a flow rate of 6 mL/min, at ambient temperature. The appropriate fractions were pooled and lyophilized. Fractions collected were confirmed by electrospray mass spectrometry and analytical reverse phase HPLC.

2.1.14. Mass spectrometry analysis

The progress and success of capping and folding reaction and also the final identity of preparative HPLC collected fraction and the final peptide purity was conformed with electrospray mass spectrometry (Agilent, Australia) in conjunction with reverse phase analytical HPLC. Negative ion mode of ion generation was employed for G7-18NATE and a positive ion mode was pursued for the penetratin containing peptides. For the negative ion mode, an amount of peptide enough to form a 0.5 mg/ml solution was dissolved in 10 mM NH_4OOCH_3 /50%ACN solution while for a positive ion mode the solvent used was 0.1%TFA/50% ACN/ H_2O .

2.1.15. Results and Discussion of peptide synthesis

The synthetic outcome of the peptides is summarized in Table 2.1.3. As shown in the table, the synthetic yield varied from 2 to 17 % based on the theoretical outcome expected on the scale of the synthesis taken. These figures may not be strictly applied since up to 6-fold excess of reactants were used in some instances, as is typically the case in peptide synthesis. Nevertheless, it provides a comparative assessment of the outcome of the synthetic effort. In particular, it is to be noted that the penetratin and peptides with containing the penetratin tail are found to be associated with poor yield. This appears to be the result of the sequence composition of penetratin-a contiguous sequence of positively charged residues. Such a motif is termed as a “difficult sequence” in peptide synthesis^{30,31} for the fact that such amino acids are hard to incorporate. Different strategies such as the use of excess reagent amino acids, use of more powerful coupling agents such as HATU in lieu of HBTU and doubling the coupling time have been attempted.³²

Table 2.3. Synthetic yield of peptides

S.No.	Peptide	Molecular Mass		Yield		
		Expected	Observed	Actual (mg)	Theoretical (mg)	Percent
1	G7-18NATE	1417.6	1417.1	22	141.7	15.53
2	G7-18NATE-Pen-Biotin	2787.2	2786.5	5.8	278.6	2.1
3	(D->E)G7-18NATE-Pen-Biotin	2798.6	2798.8	7.0	279.6	2.5
4	Penetratin-Biotin	1385.02	1385.1	6.5	138.5	4.69
5	08-5992	1415.0	1415.4	11.2	141.5	7.92
6	08-6028	1370.6	1370.8	18.3	137.06	13.35
7	08-6110	1428.6	1429.0	25.0	142.86	17.50
8	08-6046	1328.5	1328.8	10.0	132.85	7.53
9	G7-18NATE-alaser-Biotin	2245.3	2245.6	10.0	224.53	4.45
10	Bicyclic G7-18NATE	1355.5	1355.1	4.1	135.55	3.02
11	Allyl G7-18NATE	1323.5	1323.6	5.5	132.35	4.16

Of the polypeptides made, 08-6046, bicyclic G7-18NATE and Allyl G7-18NATE were prepared entirely by hand. The polypeptide 08-6046 was made manually for the synthesizer was down for some time. The reason for the other two peptides manual synthesis was different, however. It was because the O-allyl serine residue was considered to be unstable under microwave condition. After incorporation of the residues by hand or machine, chloracetylation was effected prior to cleavage from resin. This was important as potential chloracetylation sites exist such as NH₂ and other nucleophilic sites on other residues. The ring closing metathesis was effected on resin so as to avoid poisoning of the catalyst by thiols and NH₂ groups of residues. In what follows the mass spectra and the analytical LC chromatogram confirming the identity and purity of the peptides made will be presented.

2.2. Expression and Purification of Grb7 SH2 domain

The SH2 domain of Grb7 corresponding to residues 415-532 was used as a receptor for *in vitro* binding and crystallization experiments. The expression and purification of the Grb7 SH2 domain will be presented below.

2.2.1. Transformation of Grb7 SH2 domain

The pGex2T plasmid encoding human Grb7-SH2 domain corresponding to the residues 415–532 as well as Glutathione-S-Transferase (GST) gene as a fusion protein for purification purpose was obtained from Roger Daly.³² The strain of *E. coli* used as the expression host was BL21 (DE3) pLysS DH5 α .³³ The pGex2T plasmid paper containing the Grb7 SH2 domain gene was cut and soaked with 5 μ l HEPES buffer pH 7.4 in a 1.7 ml falcon tube. The mixture was vortexed for 1 min and then kept at RT for 2 min to ensure full extraction of the plasmid. This was followed by centrifugation for 1 min with 5000rpm at 4 °C on a desktop Eppendorf centrifuge (<http://www.eppendorf.com.au>). The 5 μ l plasmid solution was then transferred to 50 μ l of the competent BL21 (DE3) pLysS DH5 α *E. coli* cell strain³³ with a subsequent incubation on ice for 30 min. The mixture was heat shocked at 42 °C using warm water for 45 seconds. Further incubation on ice for 2 min was effected afterwards. The cell mixture was subsequently added to 350 μ l of sterile LB broth media containing no antibiotics and incubated for 1 hr. at 37 °C, 250 rpm. Table 2.2.1 shows the composition of the culture medias. 200 μ l of the transformation mixture was then plated onto LB agar plates containing selective antibiotics (100 μ g/ml of Ampicillin and 100 μ g/ml of Chloramphenicol). The LB agar plate was prepared near a hot flame area previously cleansed with a spray of 100 % ethanol. 30 ml of the melted LB agar media was obtained to which both Ampicillin and Chloramphenicol were added to obtain desired final antibiotic concentration of 100 μ g/ml. Following this, the LB agar media containing the antibiotics were poured to the plates and spread to cover the whole surface and allowed to stand for 1 hr at room temperature. The prepared agar plates were used to incubate the 200 μ l of the transformation mixture overnight at 37 °C in Ratek orbital mixer incubator (<http://www.ratek.com.au/>).

Table 2.2.1. Culture Media Composition for 1L culture

Constituent	Culture (gram)	
	LB Broth	LB Agar
Tryptone	10	10
Yeast Extract	5	5
NaCl	10	10
Glucose	1	1
Agar	-----	15

2.2.2. Over expression of Grb7 SH2 domain

Grb7 SH2 domain is over-expressed as fusion protein with the GST tag³⁴ as follows. The medium used for the overexpression was the LB broth and was prepared in a batch of 4L culture media. After dissolving the components into a 4L beaker, the solution was divided and transferred to four 1L flasks. 100 ml of the same media was also made and the five flasks with their contents were autoclaved. Following this, the flasks were brought to room temperature. 100 µl of 100 mg/ml of Ampicillin and Chloramphenicol was added to the 100 ml flask LB media at the flame area to get a final antibiotic concentration of 100 µg/ml. A single colony from the previous transformation culture was inoculated into the 100ml culture media. Incubation was carried out on an incubator-shaker overnight at 37 °C at 250 rpm. In the event of growth failure, a regrowth was initiated: 40 ml sterile LB broth media was taken to which a single colony from the stored plates or scratch from the glycerol stock was inoculated and incubation carried out in the incubator-shaker at 37 degrees at 250 rpm overnight. When the overnight culture was successful, 10 ml of it was inoculated into each of the four 1L sterile LB culture media previously prepared. This was followed by incubation at 37 degrees at 250 rpm on orbital mixer incubator (Ratek, <http://www.ratek.com.au/>). After ca. 3 hours of the optical density was checked by measuring the absorbance at 600 nm using 1 ml culture solutions from one of the flasks. When the absorbance reading was close to 0.6, cell induction with isopropyl β-D-1-thiogalactopyranoside (IPTG) was effected as follows. The flasks were taken out of the shaker-incubator and cooled to room temperature for 30 min and 400 µl of 1M IPTG was added to each flask to have a final IPTG concentration of 400 µM. Then, cell growth was continued at 28 °C for 41/2 hours with Innova®44 refrigerated incubator shaker (News Brunswick,

<http://www.nbsc.com>) shaking at 250 rpm speed. The contents of the flasks were transferred into six 800 ml rubber centrifuge tubes. Cells were harvested by centrifugation (5000 rpm, 20 min, 4 °C) on SORVALL Evolution centrifuge (Thermo scientific, <http://www.thermoscientific.com>) with SLC-6000 rotor. The supernatant was discarded. The cell pellets were resuspended in ice cold PBS and transferred to 50 ml falcon tubes. The cell pellets were re-centrifuged (15000 rpm, 15 min, 4 °C) on SORVALL Evolution centrifuge with SS-34 rotor. The supernatant was discarded and the cell pellets stored in -80 °C till desired.

2.2.3. Cell Lysis

The cell pellets from the previous 2L culture was resuspended to homogeneity with about 50 ml cell lysis buffer on ice. The cell lysis buffer has the following composition prepared from the corresponding stock solution as given in Table 2.2.2. and Table 2.2.3.

Table 2.2.2. Composition of cell lysis buffer (250mL)

Component	Required stock solution
1 x PBS	25 mL 10 x PBS
2 mM EDTA	1 mL 0.5M EDTA
0.5% Triton-X 100	1.25 mL 100% Triton-X 100
1 mM DTT	250 µl 1M DTT

Note: PBS = phosphate buffer saline; DTT = dithiothritol;
EDTA = ethylenediamine tetra acetic acid

Table 2.2.3. Composition of the 10 X PBS buffer

Component	Amount
1.36 M NaCl	80 g
27 mM KCl	2 g
0.1 M Na ₂ HPO ₄	14.4 g
18 mM KH ₂ HPO ₄	2.4 g
MQ H ₂ O	to 1L

This was followed by sonication on ice for 6x10 seconds with 30 seconds cooling period on SoniPrep 150 plus bench top Sonicator (<http://www.mseuk.co.uk>). For some of the purification steps, EmulsiFlex-05 high-pressure homogenizer (<http://www.avestin.com/>) was used to break up the cells with four to five passages through the homogenizer at a pressure of about 1500 psi. The cells were

then spanned at 15,000 rpm, 4 °C for 45 min at a previously cooled SORVALL Evolution centrifuge (<http://www.thermoscientific.com>). The supernatant was retained and filtered via a 0.20 µM Millipore Steritop™ Filters (www.millipore.com). A succession of chromatographic separation/purifications was made to get the final pure Grb7SH2 domain as described below.

2.2.4. Affinity chromatography separation

The first stage in purification was running an affinity chromatography. A Glutathione-S-Transferase column (GE health care, www.gelifesciences.com) was used to separate GST-Grb7 fusion protein from any other impurities or degradation products in an affinity based separation.³⁵ The 5 ml column was attached to peristaltic pump P-1 (www.gelifesciences.com) system and was equilibrated by washing successively with 30 ml of MQ water, 30 ml of wash buffer and 30 ml of cell lysis buffers. All buffers and the MQ water were filtered through a 0.2 µM filter prior to use. The protein was loaded at a flow rate of 1 ml/min. The buffers used for affinity chromatograph purification have the composition indicated in Table 2.2.4.

Table 2.2.4. Composition of wash and elution buffers used

Wash Buffer		Elution Buffer, pH 7.4 (100ml)	
Composition	Quantity	Composition	Quantity
1 x PBS	25 ml	1 x PBS	10 ml
0.5% Triton-X 100	1.25 ml 100% Triton-X 100	0.5% Triton-X 100	0.5 mL 100% Triton-X 100
1 mM DTT	250 µl of 1M DTT	1 mM DTT	100 µl of 1M DTT
MQ-Water	to 250 ml	10 mM GSH	0.3072 g GSH
		MQ-Water	to 100 ml

Following the equilibration, the filtered supernatant solution was bound to the GST column (www.gelifesciences.com) at a flow rate of 1 ml/min. A wash with 10 ml of cell lysis buffer was effected prior to elution. The solution as well as the eluent fractions flows through and washes were all collected/kept on ice. Elution was effected using 45 ml of the elution buffer. Three to four 10 ml eluent fractions were

collected. Following elution the column re-equilibrated by washing with 30 ml of MQ water, 30 ml of wash buffer and 30 ml of cell lysis buffer. The flow through collected from the first binding was rebound to the column and elution was effected as described above. After collecting another three 15 ml eluent fractions from the second rebinding, the collected six fractions and the washes as well as the soluble and insoluble components from the cell lysis centrifugations were checked by carrying out electrophoresis on a 15 % SDS-PAGE gel.³⁶ Fractions that contain the target fusion protein were combined and cleaved with thrombin overnight at cold room on a rotator. 75 units of thrombin³⁷ were used for 50 ml of GST-Grb7SH2 fusion protein.

2.2.5. SDS-PAGE Gel Electrophoresis

Sodium dodecyl sulphate-polyacrylamide gel electrophoresis (SDS-PAGE) was used to monitor the success of over expression and purification protocols.^{38,39} SDS-PAGE was carried out with Mini-PROTEAN Tetra Cell apparatus (<http://www.bio-rad.com>).

Table 2.2.5: Buffer composition for the SDS-PAGE Electrophoresis

Running Buffer (1L)		Stacking Gel (5 ml)		Resolving Gel (10%, 10 ml)	
Component	Quantity	Component	Quantity	Component	Quantity
Glycine	72 g	40% Acrylamide	0.5 ml	40% Acrylamide	4.5 ml
Tris	15 g	MQ H ₂ O	2.65 ml	MQ H ₂ O	3 ml
SDS	5 g	0.5 M Tris, pH 6.6	1.75 ml	0.5MTris,pH 6.6	2.5 ml
MQ H ₂ O	to 1 L	10% SDS	50 µl	10% SDS	100 µl
		10% APS	50 µl	10% APS	100 µl
		TEMED	5 µl	TEMED	10 µl

Note: SDS= sodium dodecyl sulphate; Tris= tris (hydroxymethyl) amino methane; APS= ammoniumpersulphate; TEMED= Tetraethylmethylenediamine

1.5 mm thick gels were prepared. 5 µl of Mark 12™ low molecular weight protein standards were run per gel as a reference standard. The stacking and resolving gel and buffer composition pursued for preparation is given in Table 2.2.5 of the gel and running buffer. The SDS run was effected as follows: 10 µl of protein fractions were mixed with 1 µl of Coomassie Brilliant blue dye. The mixture was denatured at ca. 100 °C for 5 min and was centrifuged for 1 min. 10 µl of the denatured fractions

were loaded to the gel wells. Gels were electrophoresed at 200 V and 400 mA for 45 min. Following this, gels were stained for 20 min and de-stained thereafter for another 20 min. Table 2.2.6 depicts the composition of the staining and destaining buffers. The appearance of peaks corresponding to the expected molecular weight of either GST-Grb7 SH2 (M.wt. ca. 38, 672) or Grb7 SH2 (M.wt. = 13, 672) was watched.

Table 2.2.6: Staining and de-staining buffer composition

Staining Buffer		Distaining Buffer	
Component	Quantity	Component	Quantity
100% Ethanol	450 ml	Methanol	2.25 L
Glacial acetic acid	100 ml	Glacial acetic acid	500 ml
Commassie Blue	2.5 g	MQ H ₂ O	2.25 L
MQ H ₂ O	to 1L		

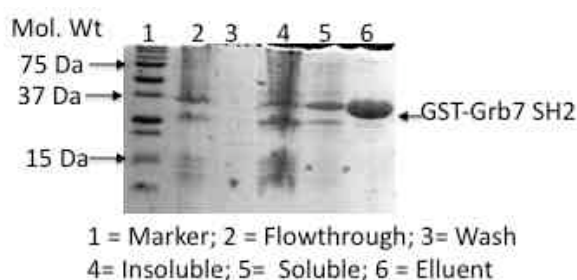


Figure 2.2.1. SDS-PAGE of Grb7SH2 from affinity chromatography separations

2.2.6. Dialysis

The next stage in the Grb7 SH2 purification was dialysis.⁴⁰ The solution from the overnight thrombin cleavage at cold room was dialyzed first into 1 L of ion exchange buffer A for three hours and then into the another 1 L ion exchange buffer overnight. The dialysis was carried out in dialysis membrane of MWCO 3500 (www.eppendorf.com). The ion exchange buffers were cooled at cold room for 1 hr prior to use. The dialysis was effected at 4 °C in a cold room with the buffer being stirred continuously using a magnetic stirrer. The composition of the ion exchange and size exclusion buffers used is shown in Table 2.2.7.

Table 2.2.7. Compositions of cation exchange and size exclusion buffers

Ion Exchange Buffer A	Quantity (500 mL)	Quantity (1L)
20 mM HEPES, pH 7.4	10 mL 1M HEPES	20 mL 1M HEPES
20% Glycerol	100 mL	200 mL
1 M DTT	500 µl	1 ml
MQ H ₂ O	to 500 ml	to 1 L
Ion Exchange Buffer B	Quantity (500 mL)	Quantity (1L)
20 mM HEPES, pH7.4	10 mL 1M HEPES	20 ml 1M HEPES
20% glycerol	100 mL	200 ml
1 M NaCl	29.22 g	58.4 g
1 mM DTT	500 µl	1 ml
MQ H ₂ O	to 500 ml	to 1 L
Size exclusion buffer	Quantity (500 mL)	Quantity (1L)
50 mM Mes, pH 6.6	4.88 g	9.76 g
100 mM NaCl	2.92 g	5.844 g
1 mM DTT	500 µl	1 ml
MQ H ₂ O	to 500 ml	to 1 L

2.2.7. Cation Exchange Chromatography

After extensive dialysis, cation exchange chromatography⁴¹ purification was used to separate Grb7 SH2 from GST, degradation products and other contaminants. It was carried using 5 ml HiTrap cation exchange column (GE healthcare, www.gelifesciences.com) connected to BioLogic Duo Flow chromatography system (Bio-Rad laboratories, www.bio-rad.com). All buffers were 0.2 µm filtered prior to use. The HiTrap column was equilibrated as follows: 30 ml of MQ water at a flow rate of 1.5 ml/min, 30 ml of ion exchange buffer A, 10 ml of Ion exchange buffer B and then 45 ml of ion exchange buffer A.

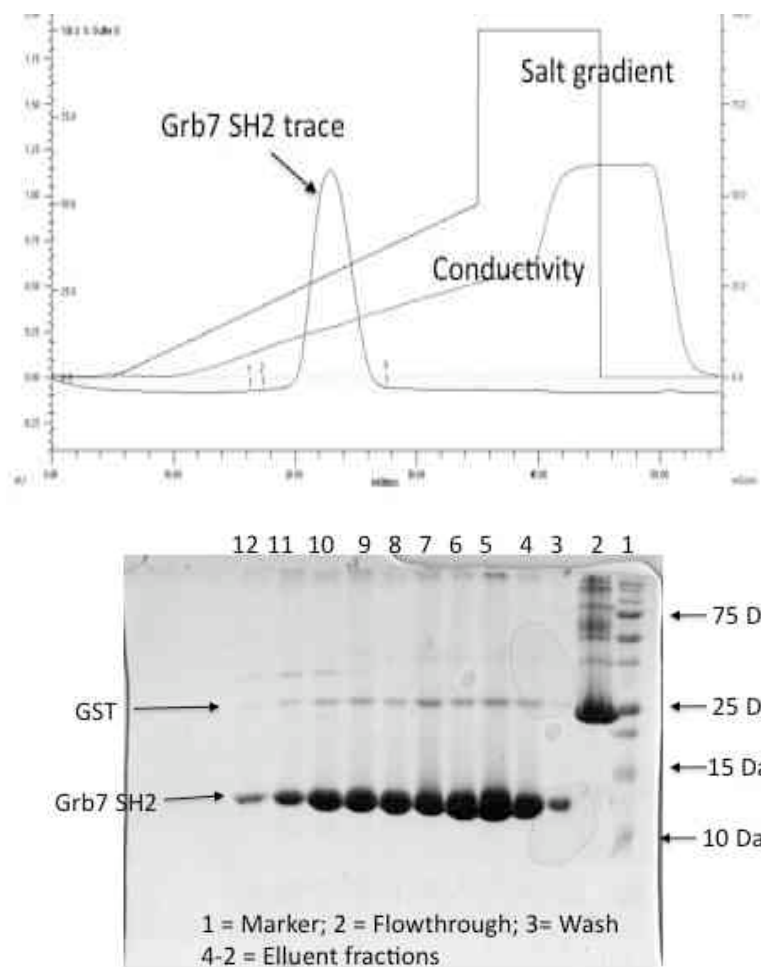


Figure 2.2.2. SDS-PAGE of Grb7SH2 (top) and the Chromatogram from Ion Exchange chromatography purification (bottom)

The dialysate was bound to the HiTrap column at a rate of 1.0 ml/min. The column was attached to the BioLogic's fast protein liquid chromatography (FPLC) system. The FPLC tubing's were purged with about 5 ml of ion exchange buffer A. Peak elution was monitored at 280 nm and fractions were collected and analyzed using the 18 % SDS-PAGE electrophoresis. Fractions containing the Grb7 SH2 domain were pooled and dialyzed into size exclusion buffer for 3 hrs and then overnight at cold room (4 °C). The SDS-Gels and cation exchange chromatogram is shown in Fig. 2.2.2.

2.2.8. Size Exclusion Chromatography

The last stage in the purification strategy was carrying out a size based chromatographic separation/purification.⁴² Size exclusion chromatography was used to further cleanup any remaining contaminants. First the dialysate was concentrated to 5 ml using bench top Eppendorf centrifuge and Amicon® Ultra-4 Centrifugal concentrators with MWCO 3500 (<http://www.millipore.com>). The size exclusion chromatography was conducted on Superdex™ 75 10/300 GL column (<http://www.gelifesciences.com>) connected to a BioLogic Duo Flow chromatography system (Bio-Rad laboratories). The column was pre-equilibrated with MQ water and size exclusion buffer at a flow rate of 0.5 ml/min. The absorbance of the protein at 280 nm was followed and fractions collected. The purity of collected fractions was determined using the SDS-PAGE electrophoresis. Fractions containing pure SH2 domain were pooled and concentrated. The concentrated Grb7 SH2 domain was kept in the fridge till desired. The SDS-Gels and Size exclusion chromatogram is shown in Fig. 2.2.3.

2.2.9. Protein concentration determination

Cary 100 UV-Vis spectrophotometer (<http://www.varianinc.com>) was used to determine the concentration of Grb7 SH2 domain with the wavelength of absorbance set at 280 nm. Beer-Lambert formula was used to get concentration from the absorbance reading of the spectroscopy as follows:

$$A = \epsilon \cdot c \cdot l$$

Where

A = measured absorbance at 280 nm

ε = Theoretical absorptivity co-efficient at 280nm (8480 M⁻¹cm⁻¹)

C = concentration in molarity, and

l = the path length in cm

The molar absorptivity co-efficient was computed from the primary sequence of the Grb7SH2 domain.⁴³

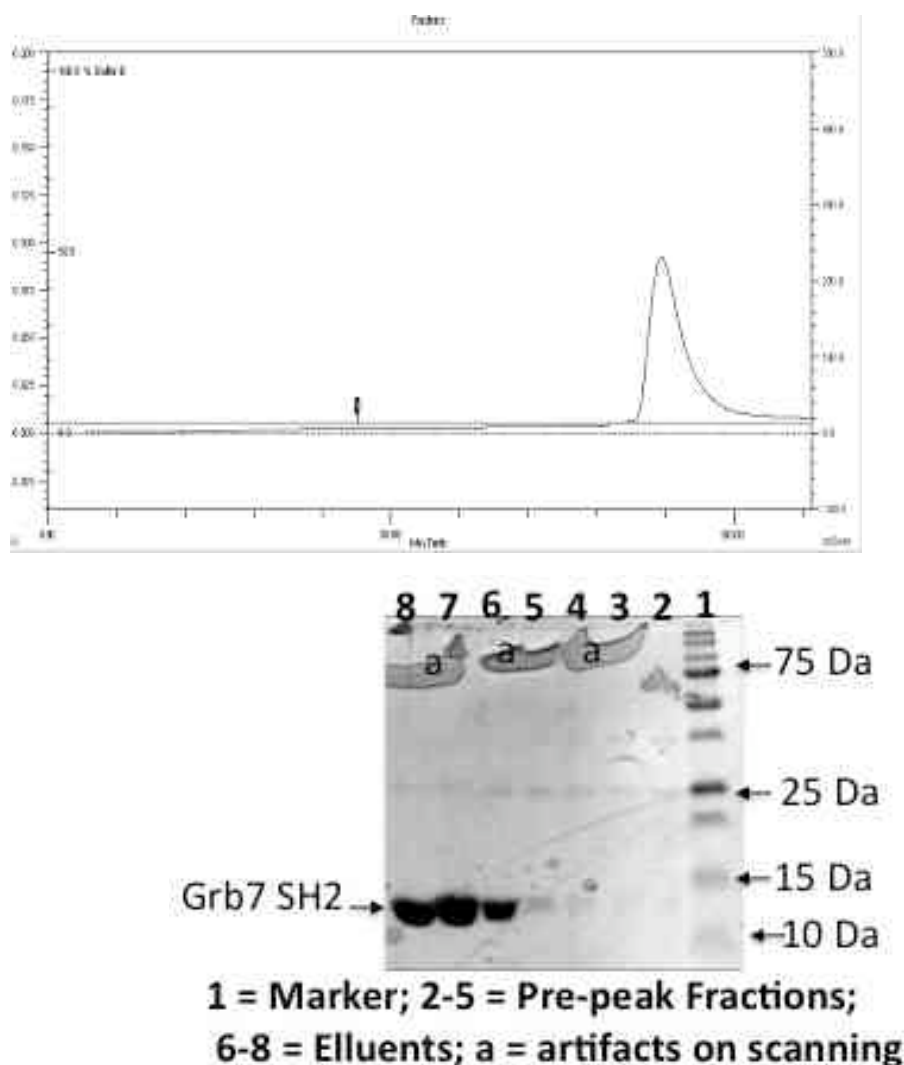


Figure 2.2.3. Size Exclusion chromatography purification. *Top*: Chromatogram showing the elution peak of Grb7 SH2 domain. *Bottom*: SDS-PAGE of Grb7SH2 domain

2.2.10. Results of Grb7 SH2 domain preparation

The protocol for Grb7 SH2 domain overexpression and purification is well established. In this thesis, it and the F511R Grb7 SH2 mutant in one, was used for in vitro binding (isothermal titration calorimetry and ThermoFluor based denaturation experiment) and for structural studies (X-ray crystallography). The over all yield of Grb7 SH2 domain expression and purification was in the region of 5-18 mg from a 2 L culture media.

2.3. Crystallography methods

2.3.1. Crystallization

The purified protein sample was concentrated using Eppendorf concentrator of MWCO of 3500 cutoff at 4 °C to 7 mg/ml corresponding to about 511 μ M in molarity. The crystallization set up was conducted for both the apo and holo forms of Grb7 SH2. The hanging drop vapor diffusion method was used to set up the crystallization trials with 24 well tissue culture plates.^{44,45} First, a layer of vaseline/grease was applied around the top edge of the wells. The wells were then filled with 500 μ l of precipitant solution. For the apo form of Grb7 SH2, 1 μ l of the protein was mixed with 1 μ l of the reservoir solution to make a final drop of size 2 μ l. For the co-crystallization trials, 1.5:1 molar ratio of the bicyclic peptide with Grb7 SH2 domain was prepared first. The prepared complex solutions were mixed with the reservoir in a 1:1 ratio to form 2 μ l drops. The cover slip on which the drop was deposited was sealed afterwards. All the protein and protein/peptide complex solutions were filtered prior to making the drops. A variety of commercially available screens such as Hamptons and SIGMA screens were tried. All the crystallization set-ups were carried out at room temperature and kept and monitored in temperature controlled room at 20 °C.

2.3.2. Crystal Optimization

Once initial crystals were obtained and confirmed to be protein by diffraction measurements, crystal optimization was effected by micro and macro-seeding experiments.^{46,47} Typically, the crystallization condition that produced the first crystal was prepared by hand and filled into 4-6 wells. The apo and complex drops were made as described above. Micro seeding experiment was conducted by the use of a cat whisker to streak seed the microcrystal into the newly setup drop over the reservoir condition.⁴⁶

2.3.3. Data Collection

Diffraction data were collected using a Rigaku RU-200 rotating anode Cu K α source (40kV, 100 mA); equipped with an R-axis IV++ detector (Rigaku, TX, USA). Data was also collected at the Australian Synchrotron to get better diffraction using the

Macromolecular Crystallography (MX2) beam line. Crystals were soaked briefly in a cryoprotectant composed of 20 % v/v glycerol/mother liquor prior to data collection. The crystals were then flash frozen in liquid nitrogen. Crystal diffraction experiments were conducted at 100 K maintained by stream of N₂ gas.

2.3.4. Data Reduction

The diffraction data collected at the Australian Synchrotron was indexed by XDS⁴⁸ while XDSCALE and XDSCONV functionalities were used respectively to scale and convert the reflections data to a format suitable for subsequent processing packages. Diffraction data collected at the in-house Rigaku detector were processed with MOSFLM⁴⁹ and scaled by SCALA.⁵⁰ In both cases, the data were scaled to a resolution so that average I/σ value in the highest resolution bin was greater than 2.0. 5% reflections were flagged for cross-validation during refinement at random. Following scaling, the number of protein molecules and the water content of asymmetric unit was estimated using Matthew's analysis.⁵¹ The Matthews coefficient (V_m) was determined by dividing the volume of the asymmetric unit by the molecular weight of the protein in the asymmetric unit in the CCP4i suite.⁵¹ The number of protein molecules in the asymmetric unit was estimated to be a value which gave a V_m between 1.6 and 3.5 Å³/Da, about 50 % water content and a higher probability.⁵²

2.3.5. Phasing

Experimental phasing was effected by molecular replacement as the crystal structure of the apo form of Grb7 SH2 was already published (PDB ID: 2QMS).⁵² The molecular replacement solution was determined using MOLREP⁵³ or PHASER⁵⁴ from Collaborative Computational Project Number 4 (CCP4).⁵⁵ MOLREP and PHASER estimates the position of the unknown structure in the asymmetric unit by positioning a known structure of the homologous protein within the asymmetric unit and assessing how well the calculated structure factors agree with observed structure factors. The template structure⁵² was available as a tetrameric complex and hence pre-treated by removing its water molecules and the other three chains. The MOLREP experiment was effected by applying the multicopy search option. For

PHASER run, the similarity to the input structure was set to 0.8. Molecular replacement was carried out in the space group determined from data processing and scaling. In addition the number of molecules per asymmetric unit searched for during molecular replacement was based upon the results of the Matthews analysis. The solutions obtained from the molecular replacement were then subsequently submitted for refinement and further processing.

2.3.6. Refinement

Following data reduction, scaling and phasing, structure refinement was carried out using REFMAC5⁵⁶ in the CCP4 suite. During refinement the co-ordinate parameters were minimized to satisfy a maximum likelihood target on amplitudes.⁵⁷ Initially rigid body refinement was applied with no prior phase information. This was followed by restrained refinement. Temperature factors were refined isotropically and TLS refinement was made in sequel. The test reflections set aside previously were used as a cross validation set to calculate R_{free} .⁵⁸ A typical ARP_WATERS cycle was applied using the default parameters to analyze solvent models and the removal of poorly fitting atoms. The added water molecules were subsequently analyzed using COOT^{59,60} and some water molecules were removed depending on the shape of the electron density. Following refinement, $m|F_o|-D|F_c|$ and $2m|F_o|-D|F_c|$ maps, where m is the figure of merit and D is an estimate of error in the structure based on co-ordinate errors, were generated using REFMAC5 from the CCP4i suite and read into COOT for model building.

2.3.7. Model Building

Manual model building was undertaken in COOT^{59,60} using the electron density maps generated during the REFMAC5 refinement. The model building cycle involved building into both $2m|F_o|-|F_c|$ contoured at 1.0σ , and $m|F_o|-|F_c|$ electron maps contoured at 3.0σ . During the building process, side chain groups that did not fit to the electron density were fit using the rotamer conformation that best fit the environment immediately surrounding the side chain. In the final stages of model building, water molecules were built manually into regions of spherical and positive electron density that were within hydrogen bonding distance of protein or other

water atoms. Any regions of potential ligand density were also identified and manually built into. Ramachandran plot, rotamer, geometry and density fit analyses were utilized to aid the model building process. Finally, PROCHECK⁶¹ was used to assess the quality of the model and adjustments were made to residues that were described as having bad contacts, Ramachandran outliers or had bond lengths or angles greater than two standard deviations away from the mean. The refinement and manual building cycle was continued until peaks no greater than 4σ or less than -4σ were present in the $|F_o|-|F_c|$ map.

The methods were used to solve the structure of the Grb7 SH2 domain apo and in complex with the peptide to high resolution.

2.3.8. References

- (1) Merrifield, B. Concept and early development of solid-phase peptide synthesis. *Methods Enzymol.* **1997**, *289*, 3-13.
- (2) Wade, J. D.; Tregear, G. W. Solid phase peptide synthesis: recent advances and applications. *Australas. Biotechnol.* **1993**, *3*, 332-336.
- (3) White, P. D.; Chan, W. C. Basic Principles. In *Fmoc Solid Phase Peptide Synthesis: A Practical Approach*, Chan, W.C., White, P.D., Eds.; Oxford University Press, Oxford, 2000, pp.9-40.
- (4) Merrifield, R. B. Solid phase synthesis. II. The synthesis of bradykinin. *J. Am. Chem. Soc.* **1964**, *86*, 304-305.
- (5) Merrifield, R. B. Solid-phase synthesis. III. An improved synthesis of bradykinin. *Biochemistry* **1964**, *3*, 1385-1390.
- (6) Merrifield, R.B. Solid phase synthesis. IV. The synthesis of methionyl-lysyl-bradykinin. *J. Org. Chem.* **1964**, *29*, 3100-3102.
- (7) Sewald, N.; Jakubke, H. D. *Peptides: Chemistry and Biology*. Wiley-VCH Verlag GmbH & Co. KGaA: Darmstadt, 2003; pp.135-267.
- (8) Sheehan, J. C.; Hess, G. P. A new method of forming peptide bonds. *J. Am. Chem. Soc.* **1955**, *77*, 1067-1068.
- (9) Schnolzer, M. A. P.; Jones, A.; Alewood, D.; Kent, S. B. H. In Situ Neutralization in Boc-chemistry Solid Phase Peptide Synthesis. *Int. J. Peptide Res. Therap.* **2007**, *13*, 31-44.
- (10) Chang, C. D.; Meienhofer, J. Solid-phase synthesis using mild base cleavage of $N\alpha$ -fluorenylmethoxycarbonylamino acids, exemplified by a synthesis of dihydrosomatostatin. *Int. J. Pept. Prot. Res.* **1978**, *11*, 246-249.
- (11) Nilsson, B. L.; Soellner, M. B.; Raines, R. T. Chemical Synthesis of Proteins. *Annu. Rev. Biophys. Biomol. Struct.* **2005**, *34*, 91-118.
- (12) Hermkens, P. H. H.; Ottenheijm, H. C. J.; Rees, D. C. Solid-phase organic reactions II: A review of the literature Nov95-Nov 96. *Tetrahedron* **1997**, *53*, 5643-

5678.

- (13) Rink, H. Solid-phase synthesis of protected peptide fragments using a trialkoxy-diphenyl-methylester resin. *Tetrahedron Lett.* **1987**, *28*, 3787-3790.
- (14) Mellor, S. L.; Chan, W. C. 4-[2,4-Dimethoxyphenyl (*N*-fluoren-9-ylmethoxy carbonyl-*N*-alkylaminooxy)-methyl] phenoxymethyl polystyrene: a multiple solid-phase approach to *N*-alkylhydroxamic acids. *J. Chem. Soc., Chem. Commun.* **1997**, 2005-2006.
- (15) Garigipati, R. S. Reagents for combinatorial organic synthesis: preparation and uses of Rink-chloride. *Tetrahedron Lett.* **1997**, *38*, 6807-6810.
- (16) Kaiser, E.; Colescott, R. L.; Bossinger, C. D.; Cook, P. I. Color test for detection of free terminal amino groups in the solid-phase synthesis of peptides. *Anal. Biochem.* **1970**, *34*, 595-598.
- (17) Dourtoglou, V.; Ziegler, J.-C.; Gross, B. L'hexafluorophosphate de *O*-benzotriazolyl-*N,N*-tetramethyluronium hexafluorophosphate: a new and efficient peptide coupling reagent. *Tetrahedron Lett.* **1978**, *19*, 1269-1272.
- (18) Dourtoglou, V.; Gross, B.; Lambropoulou, V.; Zioudrou, C. *O*-Benzotriazolyl-*N,N,N',N'*-tetramethyluronium hexafluorophosphate as coupling reagent for the synthesis of peptides of biological interest. *Synthesis* **1984**, *7*, 572-574.
- (19) Reid, G. E.; Simpson, R. S. Automated solid-phase peptide synthesis: use of 2-(1*H*-ben-zotriazol-1-yl)-1,1,3,3-tetramethyluronium tetrafluoroborate for coupling of *tert*-butyloxycarbonyl amino acids. *Anal. Biochem.* **1992**, *200*, 301-309.
- (20) CEM Corporation, 3100 Smith Farm Rd, North Carolina, USA, 28106
- (21) Mavandadi, F.; Lidström, P. Microwave assisted chemistry in drug discovery. *Curr. Top. Med. Chem.* **2004**, *4*, 773-792.
- (22) Van der Eycken, E.; van der Eycken, J. Microwaves in combinatorial and high-throughput synthesis. *QSAR Comb. Sci.* **2004**, *23*, 825-926.
- (23) König, W.; Geiger, R. A new method for the synthesis of peptides: activation of the carboxyl group with dicyclohexylcarbodiimide and 1-hydroxybenzotriazoles. *Chem. Ber.* **1970**, *103*, 788-798.
- (24) Pero, S. C.; Oligino, L.; Daly, R. J.; Soden, A. L.; Liu, C.; Roller, P. P.; Li, P.; Krag, D. N. Identification of novel non-phosphorylated ligands, which bind selectively to the SH2 domain of Grb7. *J. Biol. Chem.* **2002**, *277*, 11918-11926.
- (25) Astruc, D. The metathesis reactions: from a historical perspective to recent developments. *New J. Chem.* **2005**, *29*, 42-56.
- (26) Vougioukalakis, G. C.; Grubbs, R. H. Ruthenium-based heterocyclic carbene-coordinated olefin metathesis catalysts, *Chem. Rev.* **2010**, *110*, 1746-1787.
- (27) Adang, A. E. P.; Hermkens, P. H. H.; Linders, J. T. M.; Ottenheijm, H. C. J.; van Staveren, C. J. Case Histories of Peptidomimetics: Progression from Peptides to Drugs. *Recl. Trav. Chim. Pays-Bas.* **1994**, *113*, 63-78.
- (28) Lloyd-Williams, P.; Albericio, F.; Giralt, E. *Chemical Approaches to the Synthesis of Peptides and Proteins*, CRC Press, Boca Raton, Florida, 1997.

- (29) Fields, G. B.; Noble, R. L. Solid phase peptide synthesis utilizing 9-fluorenylmethoxycarbonyl amino acids. *Int. J. Pept. Protein Res.* **1990**, *35*, 161-214.
- (30) Lukszo, J.; Patterson, D.; Albericio, F.; Kates, S. A. 3-(1-Piperidinyl)alanine formation during the preparation of C-terminal cysteine peptides with the Fmoc/t-Bu strategy. *Lett. Pept. Sci.* **1996**, *3*, 157-166.
- (31) Milton, R. C. L.; Milton, S. C. F.; Adams, P. Prediction of difficult sequences in solid-phase peptide synthesis. *J. Am. Chem. Soc.* **1990**, *112*, 6039-6046.
- (32) Tam, J. P.; Lu, Y. A. Coupling Difficulty Associated with Interchain Clustering and Phase Transition in Solid Phase Peptide Synthesis. *J. Am. Chem. Soc.*, **1995**, *117*, 12058-12063.
- (32) Janes, P. W.; Lackmann, M.; Church, W. B.; Sanderson, G. M.; Sutherland, R. L.; Daly, R. J. Structural determinants of the interaction between the erbB2 receptor and the Src homology 2 domain of Grb7. *J. Biol. Chem.* **1997**, *272*, 8490-8497.
- (33) Davanloo, P.; Rosenberg, A. H.; Dunn, J. J.; Studier, F. W. Cloning and expression of the gene for bacteriophage T7 RNA polymerase. *Proc. Natl. Acad. Sci. U. S.*, **1984**, *81*, 2035-2039.
- (34) Frangoni, J.V.; Neel, B. G. Solubilization and purification of enzymatically active glutathione-S-transferase (GEX) fusion proteins. *Anal. Biochem.* **1993**, *210*, 179-187.
- (35) Urh, M.; Simpson, D.; Zhao, K. Affinity chromatography: general methods. *Methods Enzymol.* **2009**, *463*, 417-438.
- (36) Klepárník, K.; Bocek, P. Electrophoresis today and tomorrow: Helping biologists' dreams come true. *Bioessays* **2010**, *32*, 218-226.
- (37) Smith, D. B.; Johnson, K. S. Single-step purification of polypeptides expressed in *Escherichia coli* as fusions with glutathione S-transferase. *Gene* **1988**, *67*, 31-40.
- (38) Laemmli, U. K. Cleavage of structural proteins during the assembly of the head of bacteriophage T4. *Nature* **1970**, *227*, 680-685.
- (39) Schagger, H.; von Jagow, G. Tricine-sodium dodecyl sulfate-polyacrylamide gel electrophoresis for the separation of proteins in the range from 1 to 100 kDa, *Anal. Biochem.* **1987**, *166*, 368-379.
- (40) van Reis, R.; Zydney, A. Membrane separations in biotechnology. *Curr. Opin. Biotechnol.* **2001**, *12*, 208-211.
- (41) Jungbauer, A.; Hahn, R. Ion-exchange chromatography. *Methods Enzymol.* **2009**, *463*, 349-371.
- (42) Barth, H. G.; Boyes, B. E.; Jackson, C. Size exclusion chromatography. *Anal. Chem.* **1994**, *66*, 595R-620R.
- (43) Gill, S. C.; von Hippel, P. H. Calculation of protein extinction coefficients from amino acid sequence data. *Anal Biochem.* **1989**, *182*, 319-326.
- (44) Chayen, N. E.; Saridakis, E. Protein crystallization: from purified protein to diffraction-quality crystal. *Nat. Methods* **2008**, *5*, 147-53.

-
- (45) McPherson, A. Introduction to protein crystallization. *Methods* **2004**, *34*, 254-265
- (46) Sweeney, A. M.; D'Arcy, A. Seeding. In *Protein Crystallization*, 2nd ed.; Bergfors T., Ed.; International University Line, La Jolla, California, 2009; pp. 95-113
- (47) Bergfors, T. Succeeding with Seeding: Some Practical Advice. In *Evolving Methods for Macromolecular Crystallography*, Read, R. J., Sussman, J.L., Eds.; Springer, Dordrecht, 2007; pp.1-10
- (48) Kabsch, W. Automatic processing of rotation diffraction data from crystals of initially unknown symmetry and cell constants. *Appl. Cryst.* **1993**, *26*, 795-800.
- (49) Leslie, A.G.W. Joint CCP4 + ESF-EAMCB Newsletter on Protein Crystallography, **1992**, No. 26.
- (50) Evans, P. R. Data Collection and Processing. In *Proceedings of the CCP4 Study Weekend*, Sawyer, L., Isaacs, N., Bailey, S., Eds.; Daresbury Laboratory: Warrington, **1993**; pp. 114-122..
- (51) Matthews, B. W. Solvent content of protein crystals. *J. Mol. Biol.* **1968**, *33*, 491-497.
- (52) Porter, C. J.; Matthews, J. M.; Mackay, J. P.; Pursglove, S. E.; Schmidberger, J. W.; Leedman, P. J.; Pero, S. C.; Krag, D. N.; Wilce, M. C.; Wilce, J. A. Grb7 SH2 domain structure and interactions with a cyclic peptide inhibitor of cancer cell migration and proliferation. *BMC Struct. Biol.* **2007**, *7*:58.
- (53) Vagin, A.; Teplyakov, A. MOLREP: an Automated Program for Molecular Replacement. *J. Appl. Cryst.* **1997**, *30*, 1022-1025.
- (54) McCoy, J.; Grosse-Kunstleve, R. W.; Adams, P. D.; Winn, M. D.; Storoni, L. C.; Read R. J. Phaser crystallographic software. *J. Appl. Cryst.* **2007**, *40*, 658-674.
- (55) The CCP4 Suite: Programs for Protein Crystallography. *Acta Cryst.* **1994**, *D50*, 760-763.
- (56) Murshudov, G. N.; Vagin, A. A.; Dodson, E. J. Refinement of macromolecular structures by the maximum-likelihood method. *Acta Crystallogr. D Biol. Crystallogr.* **1997**, *53*, 240-255.
- (57) Murshudov, G.; Vagin, A.; Dodson, E. Application of Maximum Likelihood Refinement in the Refinement of Protein structures. *Proceedings of Daresbury Study Weekend*, **1996**
- (58) Brünger, A. T. Free R-value: a novel statistical quantity for assessing the accuracy of crystal structures. *Nature* **1992**, *355*, 472-475.
- (59) Emsley, P.; Cowtan, K. Coot: model-building tools for molecular graphics. *Acta Crystallogr. D Biol. Crystallogr.* **2004**, *60*, 2126-2132.
- (60) Emsley, P.; Lohkamp, B.; Scott, W.G.; Cowtan, K. Features and development of Coot. *Acta Crystallogr. D Biol. Crystallogr.* **2010**, *66*, 486-501.
- (61) Laskowski, R. A.; MacArthur, M. W.; Moss, D. S.; Thornton, J. M. PROCHECK: a program to check the stereochemical quality of protein structures. *J. Appl. Cryst.*, **1993**, *26*, 283-291.

**JOHN WILEY AND SONS LICENSE
TERMS AND CONDITIONS**

Dec 03, 2010

This is a License Agreement between Nigus D Ambaye ("You") and John Wiley and Sons ("John Wiley and Sons") provided by Copyright Clearance Center ("CCC"). The license consists of your order details, the terms and conditions provided by John Wiley and Sons, and the payment terms and conditions.

All payments must be made in full to CCC. For payment instructions, please see information listed at the bottom of this form.

License Number	2561410274918
License date	Dec 03, 2010
Licensed content publisher	John Wiley and Sons
Licensed content publication	Biopolymers
Licensed content title	Uptake of a cell permeable G7-18NATE construct into cells and binding with the Grb7-SH2 domain
Licensed content author	Nigus D. Ambaye,Reece C.C. Lim,Daniel J. Clayton,Menachem J. Gunzburg,John T. Price,Stephanie C. Pero,David N. Krag,Matthew C.J. Wilce,Marie-Isabel Aguilar,Patrick Perlmutter,Jacqueline A. Wilce
Licensed content date	Jan 1, 2010
Start page	n/a
End page	n/a
Type of use	Dissertation/Thesis
Requestor type	Author of this Wiley article
Format	Print and electronic
Portion	Full article
Will you be translating?	No
Order reference number	
Total	0.00 USD

[Terms and Conditions](#)**TERMS AND CONDITIONS**

This copyrighted material is owned by or exclusively licensed to John Wiley & Sons, Inc. or one of its group companies (each a "Wiley Company") or a society for whom a Wiley Company has exclusive publishing rights in relation to a particular journal (collectively "WILEY"). By clicking "accept" in connection with completing this licensing transaction, you agree that the following terms and conditions apply to this transaction (along with the billing and payment terms and conditions established by the Copyright Clearance Center Inc., ("CCC's Billing and Payment terms and conditions"), at the time that you opened your Rightslink account (these are available at any time at <http://myaccount.copyright.com>).

Terms and Conditions

1. The materials you have requested permission to reproduce (the "Materials") are protected by copyright.
2. You are hereby granted a personal, non-exclusive, non-sublicensable, non-transferable,

worldwide, limited license to reproduce the Materials for the purpose specified in the licensing process. This license is for a one-time use only with a maximum distribution equal to the number that you identified in the licensing process. Any form of republication granted by this license must be completed within two years of the date of the grant of this license (although copies prepared before may be distributed thereafter). Any electronic posting of the Materials is limited to one year from the date permission is granted and is on the condition that a link is placed to the journal homepage on Wiley's online journals publication platform at www.interscience.wiley.com. The Materials shall not be used in any other manner or for any other purpose. Permission is granted subject to an appropriate acknowledgement given to the author, title of the material/book/journal and the publisher and on the understanding that nowhere in the text is a previously published source acknowledged for all or part of this Material. Any third party material is expressly excluded from this permission.

3. With respect to the Materials, all rights are reserved. No part of the Materials may be copied, modified, adapted, translated, reproduced, transferred or distributed, in any form or by any means, and no derivative works may be made based on the Materials without the prior permission of the respective copyright owner. You may not alter, remove or suppress in any manner any copyright, trademark or other notices displayed by the Materials. You may not license, rent, sell, loan, lease, pledge, offer as security, transfer or assign the Materials, or any of the rights granted to you hereunder to any other person.

4. The Materials and all of the intellectual property rights therein shall at all times remain the exclusive property of John Wiley & Sons Inc or one of its related companies (WILEY) or their respective licensors, and your interest therein is only that of having possession of and the right to reproduce the Materials pursuant to Section 2 herein during the continuance of this Agreement. You agree that you own no right, title or interest in or to the Materials or any of the intellectual property rights therein. You shall have no rights hereunder other than the license as provided for above in Section 2. No right, license or interest to any trademark, trade name, service mark or other branding ("Marks") of WILEY or its licensors is granted hereunder, and you agree that you shall not assert any such right, license or interest with respect thereto.

5. WILEY DOES NOT MAKE ANY WARRANTY OR REPRESENTATION OF ANY KIND TO YOU OR ANY THIRD PARTY, EXPRESS, IMPLIED OR STATUTORY, WITH RESPECT TO THE MATERIALS OR THE ACCURACY OF ANY INFORMATION CONTAINED IN THE MATERIALS, INCLUDING, WITHOUT LIMITATION, ANY IMPLIED WARRANTY OF MERCHANTABILITY, ACCURACY, SATISFACTORY QUALITY, FITNESS FOR A PARTICULAR PURPOSE, USABILITY, INTEGRATION OR NON-INFRINGEMENT AND ALL SUCH WARRANTIES ARE HEREBY EXCLUDED BY WILEY AND WAIVED BY YOU.

6. WILEY shall have the right to terminate this Agreement immediately upon breach of this Agreement by you.

7. You shall indemnify, defend and hold harmless WILEY, its directors, officers, agents and employees, from and against any actual or threatened claims, demands, causes of action or proceedings arising from any breach of this Agreement by you.

8. IN NO EVENT SHALL WILEY BE LIABLE TO YOU OR ANY OTHER PARTY OR ANY OTHER PERSON OR ENTITY FOR ANY SPECIAL, CONSEQUENTIAL, INCIDENTAL, INDIRECT, EXEMPLARY OR PUNITIVE DAMAGES, HOWEVER CAUSED, ARISING OUT OF OR IN CONNECTION WITH THE DOWNLOADING, PROVISIONING, VIEWING OR USE OF THE MATERIALS REGARDLESS OF THE FORM OF ACTION, WHETHER FOR BREACH OF CONTRACT, BREACH OF WARRANTY, TORT, NEGLIGENCE, INFRINGEMENT OR OTHERWISE (INCLUDING, WITHOUT LIMITATION, DAMAGES BASED ON LOSS OF PROFITS, DATA, FILES, USE, BUSINESS OPPORTUNITY OR CLAIMS OF THIRD PARTIES), AND WHETHER OR NOT THE PARTY HAS BEEN ADVISED OF THE POSSIBILITY OF SUCH DAMAGES. THIS LIMITATION SHALL APPLY NOTWITHSTANDING ANY FAILURE OF ESSENTIAL PURPOSE OF ANY LIMITED REMEDY PROVIDED HEREIN.

9. Should any provision of this Agreement be held by a court of competent jurisdiction to be illegal, invalid, or unenforceable, that provision shall be deemed amended to achieve as nearly as possible the same economic effect as the original provision, and the legality, validity and enforceability of the remaining provisions of this Agreement shall not be affected or impaired thereby.

10. The failure of either party to enforce any term or condition of this Agreement shall not constitute a waiver of either party's right to enforce each and every term and condition of this Agreement. No breach under this agreement shall be deemed waived or excused by either party

unless such waiver or consent is in writing signed by the party granting such waiver or consent. The waiver by or consent of a party to a breach of any provision of this Agreement shall not operate or be construed as a waiver of or consent to any other or subsequent breach by such other party.

11. This Agreement may not be assigned (including by operation of law or otherwise) by you without WILEY's prior written consent.

12. These terms and conditions together with CCC's Billing and Payment terms and conditions (which are incorporated herein) form the entire agreement between you and WILEY concerning this licensing transaction and (in the absence of fraud) supersedes all prior agreements and representations of the parties, oral or written. This Agreement may not be amended except in a writing signed by both parties. This Agreement shall be binding upon and inure to the benefit of the parties' successors, legal representatives, and authorized assigns.

13. In the event of any conflict between your obligations established by these terms and conditions and those established by CCC's Billing and Payment terms and conditions, these terms and conditions shall prevail.

14. WILEY expressly reserves all rights not specifically granted in the combination of (i) the license details provided by you and accepted in the course of this licensing transaction, (ii) these terms and conditions and (iii) CCC's Billing and Payment terms and conditions.

15. This Agreement shall be governed by and construed in accordance with the laws of England and you agree to submit to the exclusive jurisdiction of the English courts.

16. Other Terms and Conditions:

BY CLICKING ON THE "I ACCEPT" BUTTON, YOU ACKNOWLEDGE THAT YOU HAVE READ AND FULLY UNDERSTAND EACH OF THE SECTIONS OF AND PROVISIONS SET FORTH IN THIS AGREEMENT AND THAT YOU ARE IN AGREEMENT WITH AND ARE WILLING TO ACCEPT ALL OF YOUR OBLIGATIONS AS SET FORTH IN THIS AGREEMENT.

V1.2

Gratis licenses (referencing \$0 in the Total field) are free. Please retain this printable license for your reference. No payment is required.

If you would like to pay for this license now, please remit this license along with your payment made payable to "COPYRIGHT CLEARANCE CENTER" otherwise you will be invoiced within 48 hours of the license date. Payment should be in the form of a check or money order referencing your account number and this invoice number RLNK10894058.

Once you receive your invoice for this order, you may pay your invoice by credit card. Please follow instructions provided at that time.

**Make Payment To:
Copyright Clearance Center
Dept 001
P.O. Box 843006
Boston, MA 02284-3006**

If you find copyrighted material related to this license will not be used and wish to cancel, please contact us referencing this license number 2561410274918 and noting the reason for cancellation.

Questions? customercare@copyright.com or +1-877-622-5543 (toll free in the US) or +1-978-646-2777.

Declaration for Thesis Chapter [3]

Declaration by candidate


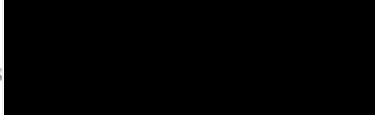
In the case of Chapter [3], the nature and extent of my contribution to the work was as follows:

Nature of contribution

Synthesized the peptides, conducted ITC binding experiment, prepared the receptor protein and contributed towards manuscript preparation.

Contribution (%) Signature

The following co-authors contributed to the work. Co-authors who are students at Monash University must also indicate the extent of their contribution in percentage terms:

Name	Nature of contribution	Signature
Renee C Lim ¹	Conducted the cell permeability experiments	
Daniel J Clayton ¹	Participated in peptide synthesis	
Alanachem J Gunzburg ¹	Participated in protein expression/purification	
John T Price ¹	Contributed in data interpretation	
Stephanie C Pero ³	Contributed in data interpretation	
David N Krag ³	Contributed in data interpretation	
Matthew CJ Wilce ¹	Contributed in data interpretation	
Abdel I Aguilar ¹	Contributed data interpretation and peptide synthesis	
Patrick Perlmutter ²	Oversaw the synthesis of peptides	
Jaqueline A Wilce ¹	Planned and supervised the overall experiments and oversaw the reporting of the results	

¹Department of Biochemistry and Molecular Biology, Monash University, VIC 3800, Australia; ²Department of Chemistry, Monash University, VIC 3800, Australia; ³Department of Surgery and Vermont Cancer Center, University of Vermont, Burlington, VT, USA

Declaration by co-authors

I hereby certify that:

- (1) the above declaration correctly reflects the nature and extent of the candidate's contribution to this work, and the nature of the contribution of each of the co-authors.
- (2) they meet the criteria for authorship in that they have participated in the conception, execution, or interpretation, of at least that part of the publication in their field of expertise;
- (3) they take public responsibility for their part of the publication, except for the responsible author who accepts overall responsibility for the publication;
- (4) there are no other authors of the publication according to these criteria;
- (5) potential conflicts of interest have been disclosed to (a) granting bodies, (b) the editor or publisher of journals or other publications, and (c) the head of the responsible academic unit; and
- (6) the original data are stored at the above location(s) and will be held for at least five years from the date indicated below:

Chapter 3

Uptake of a cell permeable G7-18NATE construct into cells and binding with Grb7-SH2 domain

This chapter describes the design of cell permeable derivatives of G7-18NATE. A short cell permeablising sequence was identified, attached on the N-terminus of G7-18NATE and its impact on in vitro binding affinity of G7-18NATE investigated by ITC. Finally, cellular uptake studies were conducted to see its ability to shuttle G7-18NATE across cell membrane.

Uptake of a Cell Permeable G7-18NATE Construct Into Cells and Binding With the Grb7-SH2 Domain

Nigus D. Ambaye¹, Reece C. C. Lim¹, Daniel J. Clayton², Menachem J. Gunzburg¹, John T. Price¹, Stephanie C. Pero³, David N. Krag³, Matthew C. J. Wilce¹, Marie-Isabel Aguilar¹, Patrick Perlmutter², Jacqueline A. Wilce¹

¹Department of Biochemistry and Molecular Biology, Monash University, VIC 3800, Australia

²Department of Chemistry, Monash University, VIC 3800, Australia

³Department of Surgery and Vermont Cancer Center, University of Vermont, Burlington, VT

Received 14 December 2009; revised 24 January 2010; accepted 25 January 2010

Published online 00 Month 2010 in Wiley InterScience (www.interscience.wiley.com). DOI 10.1002/bip.21403

ABSTRACT:

Grb7 is an adapter protein found to be overexpressed in several breast and other cancer cell types along with ErbB2. Grb7 is normally an interaction partner with focal adhesion kinase and in cancer cells also aberrantly interacts with ErbB2. It is thus implicated in the migratory and proliferative potential of cancer cells. Previous studies have shown that the phage display-derived cyclic nonphosphorylated inhibitor peptide, G7-18NATE, when linked to Penetratin[®], is able to interfere with the interaction of Grb7 with its upstream binding partners and to impact on both cell migration and proliferation. Here we report the synthesis of a biotinylated G7-18NATE covalently attached to just the last seven residues of Penetratin[®] (G7-18NATE-P-Biotin). We demonstrate that this construct is taken up efficiently into MDA-MB-468 breast cancer cells and colocalizes with Grb7 in the cytoplasm. We also used isothermal titration calorimetry to determine the binding affinity of G7-18NATE-P-Biotin to the Grb7-SH2

domain, and showed that it binds with micromolar affinity ($K_d = 14.4 \mu\text{M}$), similar to the affinity of G7-18NATE ($K_d = 35.4 \mu\text{M}$). Together this shows that this shorter G7-18NATE-P-Biotin construct is suitable for further studies of the antiproliferative and antimigratory potential of this inhibitor. © 2010 Wiley Periodicals, Inc. *Biopolymers (Pept Sci)* 00: 000-000, 2010.

Keywords: Grb7 adapter protein; SH2 domain; non-phosphorylated cyclic peptide; peptide inhibitor; penetratin; cell uptake; co-localisation; breast cancer cells

This article was originally published online as an accepted preprint. The "Published Online" date corresponds to the preprint version. You can request a copy of the preprint by emailing the Biopolymers editorial office at biopolymers@wiley.com

INTRODUCTION

Human growth factor receptor bound protein 7 (Grb7) is a 532-amino acid protein that was originally identified as a binding partner for activated epidermal growth factor receptor (EGF-R).¹ Grb7 is a member of a family of proteins that includes two other homologous proteins, Grb10 and Grb14.^{2,3} These proteins share a conserved multidomain structure with domains that mediate both protein–protein and protein–lipid interactions. These domains include an N-terminal proline rich domain, a Ras-associating-like (RA) domain, a pleckstrin homology (PH) domain, a C-terminal src-homology 2

Correspondence to: Dr. Jacqueline A. Wilce, Biochemistry and Molecular Biology, Monash University, Wellington Road, VIC 3800, Australia; e-mail: jackie.wilce@med.monash.edu.au
Contract grant sponsors: Australian Research Council Project Grant (to J.A.W. and D.N.K.) and Monash University Graduate Scholarship (to N.D.A.)

© 2010 Wiley Periodicals, Inc.

(SH2) domain, and a region between the PH and SH2 domains termed the BPS domain.³ Notably, these proteins share a region with sequence homology to the Mig-10 *C. elegans* gene required for migration of neuronal cells in embryonic development, suggesting a role for the Grb7 family in cell migration.⁴

AQ3

Grb7-family proteins function as adaptors, coupling activated tyrosine kinase receptors to downstream signaling pathways. Grb7 upstream binding partners include the members of the ErbB (also known as HER) receptor family^{5,6} and focal adhesion kinase (FAK)⁷ whose activities play a critical role in the regulation of cell proliferation and migration,^{8,9} and interactions with other tyrosine kinases have also been reported.^{10,11} Although a large number of binding partners functioning upstream of Grb7 have been identified, the precise downstream events leading to cell proliferation and migration are not yet elucidated.

Studies have shown that Grb7 is involved in cancer cell progression. Although Grb7 normally binds to the cytoplasmic domain of the ErbB3 receptor, in cancer cells it has been found in tight association with the ErbB2 receptor that plays a major role in cancer cell proliferation.⁶ Grb7 is tightly coamplified with ErbB2 in breast cancer cell lines, and there is also a strong correlation between ErbB2 and Grb7 overexpression in oesophageal and gastric carcinoma.^{12,13} A role for Grb7 in the transition from low-grade to high-grade tumor has also been reported. Coamplification and coexpression of Grb7 and ErbB2 is found in high-grade invasive Barrett's carcinoma, but not in less aggressive tumors.¹⁴ Similarly, Grb7 expression is increased markedly in high-grade but not in low-grade chronic lymphocytic leukemia.¹⁵ There is also compelling evidence that implicates Grb7 in cancer cell migration. Grb7 is found in focal adhesions in association with FAK¹⁶ and plays a key role in integrin-mediated signal transduction in cell migration.¹⁷ Overexpression of Grb7 has been shown to enhance cell migration, whereas inhibition of the Grb7 resulted in the inhibition of cell migration.⁷ Taken together, these studies have made the Grb7 an attractive target in the development of anticancer therapeutics.

The interaction between Grb7 and its partners is mediated by the SH2 domain (residues 416-532) of Grb7.⁶ This domain therefore constitutes a good target for the inhibition of Grb7 with its upstream binding partners. To this end, a non-phosphorylated peptide inhibitor was developed using a phage-displayed peptide library method.¹⁸ This peptide contains 10 amino acids flanked by two terminal cysteines (seq: CWFEGYDNTFPC) to create a cyclic peptide through disulfide linkage. The peptide was then synthesized as a redox-stable thioether bridged analog, referred to as G7-18NATE. The

cyclic nature of the peptide was found to be necessary for binding to Grb7-SH2 domain, as also seen for Grb2-SH2 domain interaction with its YXN motif peptide targets. The G7-18NATE peptide, however, binds with high specificity (does not bind to the Grb2 or the closely related Grb14) and has been shown to specifically inhibit the association of Grb7 with ErbB2.

Cellular studies with the G7-18NATE peptide have shown that it is able to interfere with both cell proliferation and cell migration.^{19,20} Since peptides of the size and composition of G7-18NATE are generally impermeable to the cell membrane, cell permeable forms of the peptide were constructed by the covalent attachment of carrier peptides Penetratin[®] or Tat. Cell permeable G7-18NATE was shown to inhibit proliferation in several breast cancer cell lines that overexpress Grb7 and not nonmalignant breast cells.¹⁹ It was shown that cotreatment of cell permeable forms of G7-18NATE with Doxorubicin or Trastuzumab (Herceptin) results in enhanced antiproliferation of breast cancer cells. Furthermore, in a recent breakthrough study, a cell permeable form of the G7-18NATE peptide was shown to successfully block the Grb7 interaction with FAK and inhibit cell migration of a pancreatic cancer cell line.²⁰ Such a peptide, which binds Grb7 without the need for phosphotyrosine, represents a particularly attractive starting point for targeting Grb7 because phosphate groups are intrinsically unstable chemical moieties and reduce cell wall permeability.

Cellular studies of the effects of G7-18NATE on cell proliferation showed that Penetratin[®] effected the uptake of G7-18NATE into cells more efficiently than Tat.¹⁹ Penetratin[®] is a 17-amino acid residue sequence derived from the third domain of the antennapedia homeodomain.²¹ Fischer et al. have previously shown that the last seven residues of Penetratin[®] are sufficient to confer cell permeability to a cargo, though uptake is reduced compared with full length Penetratin[®].²² In this study, we have sought to determine whether this shorter region of Penetratin[®] would be sufficient to effect cellular uptake of G7-18NATE, and also whether the presence of this cell permeabilization sequence impacts on the binding of the peptide to its target. We thus report the synthetic strategy utilized for the preparation of G7-18NATE synthesized with a short Penetratin[®] sequence and a biotin label for cellular uptake studies (G7-18NATE-P-Biotin). We show that this cell permeabilization sequence does not interfere with the interaction of G7-18NATE with the Grb7-SH2 domain target and that the construct is efficiently taken up into cells. Together this shows that this shorter G7-18NATE-P-Biotin construct is suitable for further studies of the antiproliferative and antimigratory potential of this inhibitor.

EXPERIMENTAL PROCEDURES

Preparation of G7-18NATE and G7-18NATE-P-Biotin Peptides

G7-18NATE (cyclo-(CH₂CO-WFEGYDNTFPC)-amide) and G7-18NATE-P-Biotin (cyclo-(CH₂CO-WFEGYDNTFPCRR MKWKKK(Biotin))-amide) were synthesized as peptide amide using the Fmoc based solid phase peptide synthesis strategy on a Rink amide resin (1.0 mmol/g).²³ The resin swelling was conducted as pre-treatment for 30 minutes in dimethyl formamide (DMF) in three times the resin volume followed by treatment with 30% v/v piperidine in DMF for 30 minutes at room temperature (RT) to effect removal of the 9-fluorenylmethoxycarbonyl (Fmoc) group from the Rink amide resin. The successful removal of Fmoc was checked with a ninhydrin based Kaiser's test.²⁴ All amino acids were coupled as their Fmoc-derivatives. The first residue was preactivated using *O*-benzotriazol-1-yl-*N,N,N',N'*-tetramethyluronium hexafluorophosphate (HBTU) and di-isopropyl ethylamine (DIPEA) and then loaded manually to the deprotected resin and coupled at RT for 30 minutes. A CEM Liberty automated synthesizer (Ai Scientific, Australia) was then used to incorporate the remaining residues. The system uses microwave energy to drive coupling and deprotection reactions to completion. The coupling agent was HBTU containing hydroxybenzotriazole (HoBt) and the activator base employed was diisopropylethylamine (DIEPA) in *N*-methyl pyrrolidone (NMP). Double couplings were carried out for Met, Lys, Arg, Phe, Trp, Thr, and Asn residues.

In the case of the G7-18NATE-P-Biotin peptide, the C-terminal Lys side chain was protected with the monomethoxytrityl (Mmt), which could be selectively removed with a cocktail of 10% acetic acid, 20% trifluoro-ethanol, and 70% dichloromethane. Biotin was then coupled at sixfold molar excess using 2-(7-aza-1H-benzotriazole-1-yl)-1,1,3,3-tetramethyluronium hexafluorophosphate (HATU) as a coupling agent in anhydrous dimethylsulphoxide (DMSO) while DIEPA was used as activating agent. The biotinylation reaction was carried out for 60 minutes at room temperature. The success of the biotin coupling was checked using Kaiser's test.²⁴

Following incorporation of the residues using the microwave synthesizer, chloroacetylation was carried out manually as at room temperature. Briefly, chloroacetic acid anhydride was used to cap the N-terminal amino moiety manually at room temperature and the reaction was effected for about 30 minutes. The peptide was then fully cleaved from the resin and fully deprotected using a 94.5% trifluoroacetic acid (TFA)/2.5% triisopropylsilane (TIPS)/2.5% H₂O/0.5% etha-

nedithiothreitol (EDT) cleavage cocktail with a 20-fold excess volume over dry weight of resin-peptide for 3 hours at room temperature. The TFA was evaporated under a stream of nitrogen gas and the resin dried at room temperature. This was followed by precipitation of peptide in cold diethylether. Finally, the peptide was dissolved and extracted with successive small volumes of 50%ACN/H₂O and lyophilized overnight. Thioether formation was effected by dissolving the lyophilized peptide at 2 mg/ml in 50 mM NH₄HCO₃ in 50%ACN/H₂O of pH 8.0. The cyclized peptide was freeze-dried and purified using preparative RP HPLC and finally homogeneity and identity of the prepared peptide was confirmed by analytical reverse phase HPLC and electron-spray mass spectroscopy as presented below.

Peptide Purification by Reverse Phase HPLC

Peptide purification was conducted using HPLC (Agilent, Australia) on a C18 reverse phase preparative columns (2.2 cm × 25 cm, Vydac 28TP1022). The mobile phase A contained 0.1%TFA/water while mobile phase B comprised 0.1%TFA 80% acetonitrile in water. All buffers were filtered using 0.45 μM filter. The lyophilized peptides were dissolved in 1.5 equivalents of MQ H₂O/0.1%TFA/20%ACN and 2M urea as needed to aid in solubility. A linear gradient was developed and purification on 20% to 80% acetonitrile/0.1% TFA over 60 minutes on an equilibrated HPLC column with a flow rate of 6 ml/min. Detection was performed at 214 and 280 nm and fractions were collected by hand. Experiments were carried out at a flow rate of 6 ml/min, at ambient temperature. The appropriate fractions were pooled and lyophilized. Fractions collected were confirmed by electrospray mass spectrometry and analytical reverse phase HPLC.

Structure Confirmation by Mass Spectrometry

The progress and success of capping and folding reaction and also the final identity of preparative HPLC collected fraction and the final peptide purity was conformed with electrospray mass spectrometry (Agilent, Australia) in conjunction with reverse phase analytical HPLC. Negative ion mode of ion generation was employed for G7-18NATE and a positive ion mode was pursued for G7-18NATE-P-Biotin. For the negative ion mode, an amount of peptide enough to form a 0.5 mg/ml solution was dissolved in 10 mM NH₄OOCH₃/50%ACN solution while for a positive ion mode the solvent used was 0.1%TFA 50% ACN/H₂O. (G7-18NATE: [M-H]⁻ *m/z* = 1417.6 (calculated), 1417.1 (observed); G7-18NATE-P-Biotin: [M+H]⁺ *m/z* = 2787.2 (calculated), 2786.5 (observed)).

Preparation of Grb7-SH2 Domain

The pGex2T plasmid containing the Grb7-SH2 insert (encoding residues 415–532 of human Grb7) was obtained from Dr. Roger Daly.²⁵ Grb7-SH2 was expressed as a GST fusion protein in *Escherichia coli* strain BL21(DE3).pLysS as previously described.²⁶ The cells were resuspended in phosphate buffer saline (PBS) with 2 mM EDTA and 0.5% Triton-X 100 and lysed by sonication. GST-Grb7-SH2 was purified by glutathione affinity chromatography, using a GSTrap FF column (GE) and eluted with PBS containing 0.5% Triton-X100, 10 mM glutathione, and 1 mM DTT. The Grb7-SH2 fusion protein was cleaved with thrombin liberating free Grb7-SH2, which was purified by cation exchange chromatography using a HiTrap SH HP column (GE), after dialysis into 20 mM HEPES pH 7.4, 20% glycerol, and 1 mM DTT, and eluted with a gradient from 0 to 0.5M NaCl. Peak fractions were dialyzed into 50 mM MES pH 6.6, 100 mM NaCl and 1 mM DTT and further purified by size exclusion chromatography using a sephadex 75 XK 16/60 column (GE). Grb7-SH2 domain was concentrated and stored at 4°C. The final concentration was determined spectrophotometrically at A_{280} using an extinction coefficient of 8480 M^{-1} .²⁷

Isothermal Titration Calorimetry (ITC)

ITC binding experiments were performed on a VP-ITC microcalorimeter (Microcal, Northampton, MA) at 25°C.^{28,29} Grb7-SH2 domain was dialyzed extensively against 50 mM NaOOCCH₃ (pH 6.6), 100 mM NaCl, and 1 mM DTT at 4°C overnight. Lyophilized G7-18NATE was dissolved in appropriate volume of filtered dialysate buffer. The concentration of Grb7-SH2 was determined by recording its absorbance at 280 nm whereas that of the peptides was determined from their mass obtained with an analytical balance and dissolution in the required volume. The peptide and protein solutions were degassed and thermostated at 20°C for 5 minutes using the ThermoVac of the VP-ITC microcalorimeter. The reference power of the experiment was set to 20 $\mu\text{Cal/sec}$ and the cell contents were stirred continuously at 307 rpm throughout the titrations. The feedback mode gain was set to high with fast and autoequilibrations options applied. The reference cell was filled with Milli-Q water. The peptides of 0.70 to 1.3 mM concentrations were titrated into Grb7-SH2 solutions of 50 to 70 μM concentrations in 10 μl injections with a 3-minute delay between each injection. A binding isotherm was generated by plotting the heat change evolved per injection against the molar ratio of peptides to Grb7-SH2 domain receptor. A blank determination in which the peptides were titrated against the buffer was carried out to account for heats of dilution and mixing which was then

subtracted from the binding data. The corrected data was then employed to fit to a single binding site model using a nonlinear least squares with the Origin (Microcal Software, Northampton, MA). All of the ITC fitting parameters were kept floating.

Cell Uptake and Visualization Experiments

MDA-MB-468 breast cancer cells were seeded on sterilized glass coverslips (13 mm diameter) in 24-well plate and grown in DMEM with 10% FBS to 60% to 70% confluence. G7-18NATE-P-Biotin (1 mg/ml in MilliQ water) was diluted in culture medium and applied to the cells at a final concentration of 10 μM . After 30 minutes of incubation with the peptide at 37°C, cells were washed with medium (500 μl per well) twice and continued to incubate for an additional 30 minutes, after which the cells were washed twice (500 μl /well, 1 \times PBS: 140 mM NaCl, 10 mM Na₂HPO₄, 2.7 mM KCl, 1.8 mM KH₂PO₄, 1 mM CaCl₂, and 0.5 mM MgCl₂) and fixed (4% paraformaldehyde in 1 \times PBS, 300 μl per well, 20 minutes). Cells were then permeabilized (0.5% Tween-20 in 1 \times PBS, 500 μl per well, 20 minutes), blocked (3% bovine serum albumin, BSA, in 1 \times PBS, 500 μl per well, 30 minutes), and treated with Streptavidin, Alexa Fluor[®] 594 conjugate (Molecular Probe, 10 $\mu\text{g/ml}$ in 0.1% BSA, 30 μl per coverslip) for 1 hour at room temperature in the dark and then washed twice with 1 \times PBS. For detection of Grb7, fixed cells were treated with rabbit polyclonal anti-Grb7 (H-70) (Santa Cruz sc-13954, 1:1000 in 0.1% BSA, 30 μl per coverslip) in humid chamber overnight at 4°C and then washed three times with 1 \times PBS before treated with goat antirabbit IgG-FITC (Molecular Probe, 1:50 in 0.1% BSA, 30 μl per coverslip) for 1 hour at room temperature. Cells were washed three times with 1 \times PBS. For double immunostaining, both Streptavidin, Alexa Fluor[®] 594 conjugate and goat anti-rabbit IgG-FITC were treated together on Grb7 immunolabeled cells. After mounting on glycerol-based mounting medium, slides were stored with minimal light exposure before viewing by confocal microscopy (Olympus FV1000), using a 100 \times oil-objective lens.

RESULTS

Synthesis of G7-18NATE and G7-18NATE-Penetratin-Biotin

The sequences of G7-18NATE and G7-18NATE-P-Biotin are displayed in Figure 1. The prototype peptide G7-18NATE, which was identified using the phage display technique by Pero et al.¹⁸ is interesting for its selective antagonist potential

F1

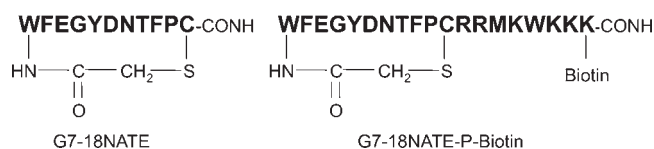


FIGURE 1 Peptides synthesized for the current study. One letter code for amino acids are shown in bold.

for Grb7, having minimal or no activity against the closely related adaptor proteins such as Grb2, Grb10, and Grb14. The synthesis of both peptides was effected utilizing a standard solid phase peptide synthesis based on Fmoc chemistry. Specifically, amino acids were all preactivated using the HBTU/DIPEA reagents before coupling. In both cases, the first residue was coupled manually at room temperature and chloroacetylation was conducted at the final residue. The selective deprotection of the C-terminal lysine side chain facilitated its biotinylation at the start of the G7-18NATE-P-Biotin synthesis. Thioether formation between the cysteine side chain and the N-terminus of both peptides was achieved in aqueous solution subsequent to their cleavage from the resin. The thiolate anion of the cysteine forms at pH 8 and acts as a nucleophile to displace the chloride ion from the N-terminal chloroacetyl group to form the thioether ring. A yield of about 15.5% for G7-18NATE and about 2.5% for

G7-18NATE-P-Biotin was achieved. The lower yield obtained for G7-18NATE-P-Biotin likely reflects the number of extra coupling and deprotection steps and, most importantly, the poor coupling efficiencies of sequential Lys and Arg residues in the Penetratin[®]-derived sequence despite the use of double couplings.

ITC Binding for G7-18NATE and G7-18NATE-P-Biotin Binding to Grb7-SH2

In order to check whether the presence of the Penetratin-derived sequence would interfere, or otherwise, with the G7-18NATE/Grb7-SH2 domain interaction, their *in vitro* association was analyzed using ITC. The determination of the thermodynamic parameters for the formation of ligand-receptor complexes offers a helpful description of such associations.²⁹ The ITC enthalpic readout gives a direct measure of the binding contribution from the formation or breakage of noncovalent bonds in the system while the entropic data gives quantitative value for the change in order of the system as a result of conformational and/or solvation changes. The precise determination of both these terms along with the number of binding sites (*N*) and binding constant (*K_b*) from the experiment makes ITC an invaluable tool for a clearer

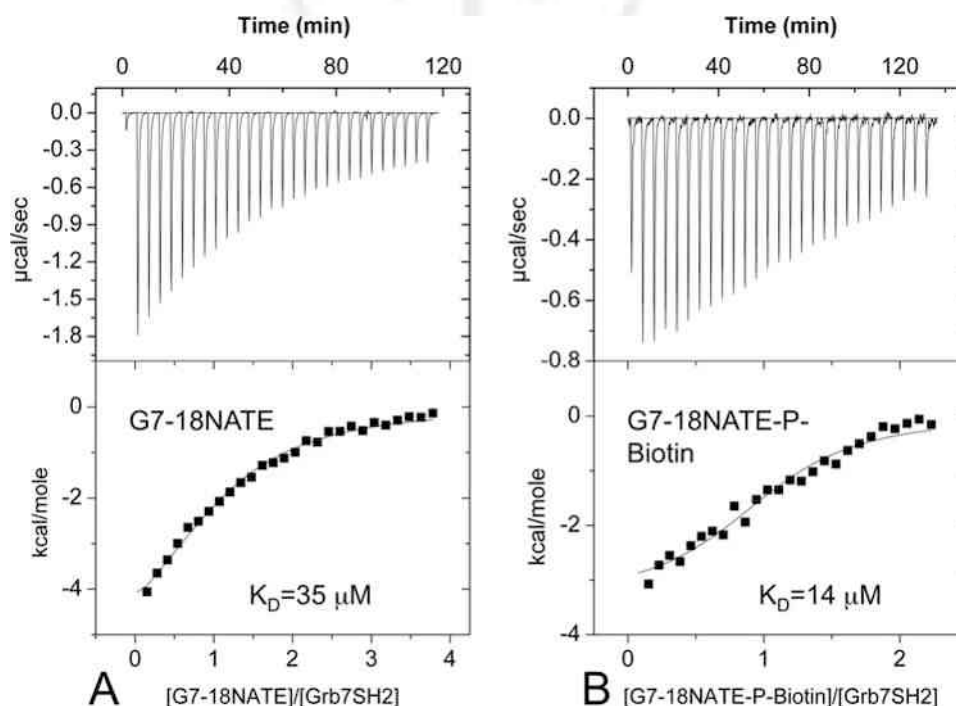


FIGURE 2 ITC Thermograms obtained from the isothermal titration of (A) G7-18NATE and (B) G7-18NATE-P-Biotin peptides against the Grb7-SH2 domain. The upper panel show raw data obtained from 10 μl injections of peptides at 25°C. The lower panels in both figures display plots of integrated total energy exchanged (as kcal/mol of injected peptides) as a function of molar ratio of the peptide to the Grb7-SH2 domain.

Table 1 Thermodynamic Binding Parameters of the G7-18NATE Peptides

Binding Parameter	$K_b (M^{-1})$	ΔH (Cal/mol)	ΔS (Cal/mol/°K)	ΔG (Cal/mol)	N	K_d (μM)
G7-18NATE	$2.89E4 \pm 0.44E4$	-6404 ± 889	-1.05	-6090	1.05 ± 0.11	35.4 ± 5
G7-18NATE-P-Biotin	$7.27E4 \pm 1.49E4$	-3583 ± 222	10.2	-6627.7	1.10 ± 0.04	14.4 ± 3

understanding of important attributes of ligand-receptor associations. Figure 2 displays the thermograms of the G7-18NATE and its cell penetrable variant, G7-18NATE-P-Biotin, titrated against the SH2 domain of Growth factor receptor bound protein 7 (Grb7). Table I shows the in vitro binding thermodynamics data analysis.

The ITC experiments show that every titration injection for both peptides is associated with a release of heat and hence the binding phenomenon is exothermic. Moreover, the binding in both cases can be explained as enthalpically driven, whereas the contribution of entropy to the over all binding is minimal (G7-18NATE-P-Biotin) or even negative (G7-18NATE). From these data, the G7-18NATE-P-Biotin binds with slightly higher affinity ($K_d = 14.4 \mu M$) than G7-18NATE ($K_d = 35.4 \mu M$). Though the enthalpic component of binding for G7-18NATE-Penetratin-Biotin is about half that of G7-18NATE, its entropic contribution is more than 10 times higher resulting in its relatively higher affinity.

Uptake of G7-18NATE-P-Biotin and Colocalization With Grb7

To demonstrate whether G7-18NATE-P-Biotin is spontaneously taken up into cultured cells, subcellular localization of the peptide was examined in our cell line of interest, human breast cancer cells MDA-MB-468. The cells were treated with G7-18NATE-P-Biotin at $10 \mu M$ or untreated. After 30-minute incubation with the peptide, the cells were examined for their uptake of the biotinylated peptide using a fluorescently-labeled streptavidin that binds biotin. After 30 minutes, cells showed incorporation of the G7-18NATE-P-Biotin throughout the cytoplasm of the cells as well as fainter nuclear localization (Figure 3C). Cells with no treatment do not show detectable fluorescence (Figure 3A). This indicates that the peptide had indeed spontaneously traversed the cell membrane from the culture medium into the cells.

As G7-18NATE is able to bind to the SH2 domain of Grb7 as shown previously, colocalization of the peptide with Grb7 was examined. The cells, treated with G7-18NATE-P-Biotin or untreated, were double stained for Grb7 and biotin. Grb7 was found to be distributed throughout the cytoplasm and to be excluded from the nucleus of the cells (Figure 3B). Thus, Grb7 and G7-18NATE-P-Biotin both appear to be

present throughout the cytoplasm, providing the opportunity for these molecules to interact (Figure 3D).

DISCUSSION

The G7-18NATE peptide is an important lead for the study of the effect of Grb7 inhibition in cells and for the potential development of inhibitors of Grb7 where it is aberrantly overexpressed in cancer. The peptide provides the specificity required for Grb7 inhibition, an attribute that is unlikely to be mimicked by a small molecule antagonist. It suffers, however, as do most peptides, in its requirement for both aqueous solubility and sufficient lipid solubility. Aqueous solubility is required for easy transport across biological fluids, whereas sufficient lipid solubility is mandatory for molecules to cross the myriads of membrane layers before they reach the target site. Inability to strike a balanced aqueous and lipid solubility can be linked to problems ranging from safety, efficacy, and manufacturability to difficulty of discovering a new chemotypes. The membrane permeability issue is particularly demanding for the exploitation of intracellular targets. The requirement is especially pronounced for charged and polar molecules such as peptides. Cell permeabilizing cargoes such as Penetratin[®] therefore represent attractive vehicles for the transport of otherwise cell-impermeable candidates and exploration of the potential of novel intracellular molecules as drug targets.

The G7-18NATE peptide has previously been transported into cells by the use of the full Penetratin[®] sequence to demonstrate biological activity in cells.^{19,20} Here, we sought to determine the utility of a shortened version of Penetratin[®] because the last seven residues have been shown to be sufficient for effective uptake of peptides into cells.²² We were interested to check that the G7-18NATE peptide interaction with the Grb7-SH2 domain was not detrimentally affected by the presence of the short Penetratin[®]-derived sequence, and that uptake into the cell for interaction with the Grb7 molecule in vivo was effected. To these ends we prepared G7-18NATE (as previously reported³⁰) and G7-18NATE with the seven Penetratin[®]-derived residues synthesized as a C-terminal extension and an extra C-terminal biotinylated lysine to facilitate intracellular detection (G7-18NATE-P-Biotin). Both peptides were successfully synthesized and cyclized for the current studies.

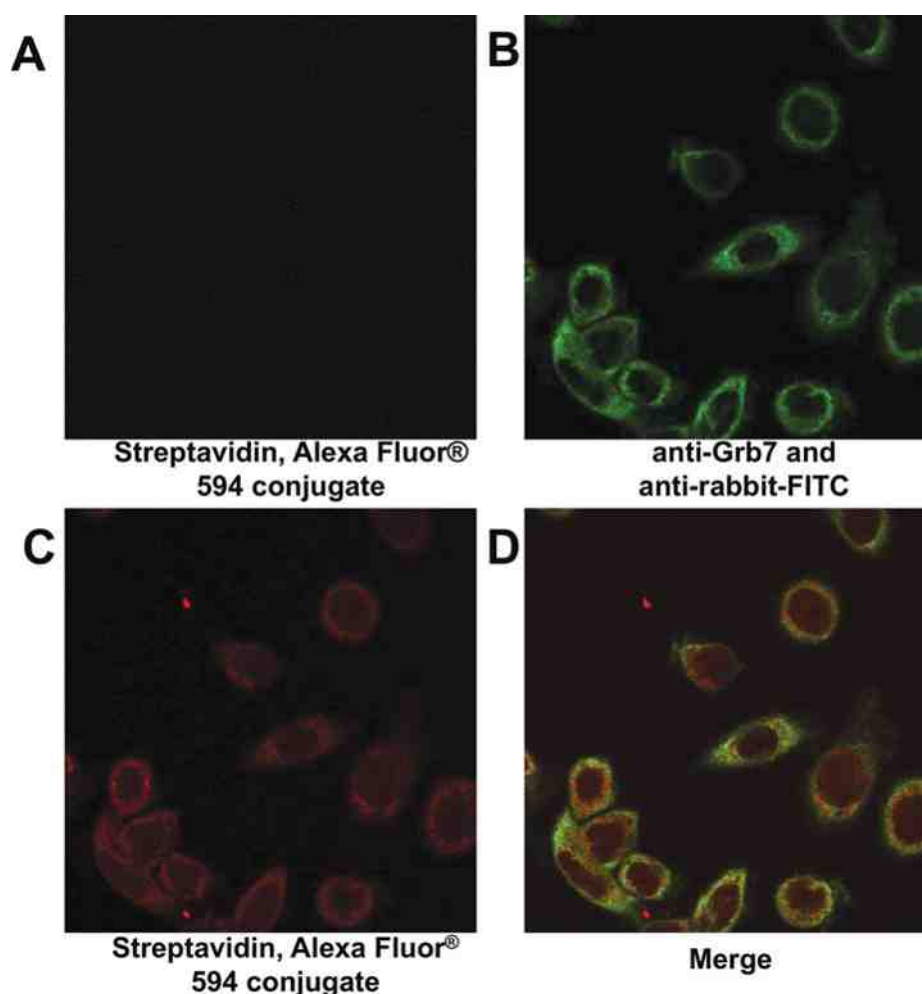


FIGURE 3 Localization of G7-18NATE-P-Biotin in MDA-MB-468 breast cancer cells. The cells were exposed to 10 μM G7-18NATE-P-Biotin for 30 minutes before being fixed and permeabilized. (A) The no peptide control shows no staining by the Streptavidin, Alexa Fluor[®] 594 conjugate. (B) Grb7 was localized using anti-Grb7 and anti-rabbit-FITC. (C) The biotinylated peptide was localized using Streptavidin, Alexa Fluor[®] 594 conjugate and (D) shows the merged images.

A comparison of the peptide interactions with the Grb7-SH2 domain was undertaken using ITC. The affinity of G7-18NATE-P-Biotin (14.4 μM) and that of G7-18NATE (35.4 μM) for the Grb7-SH2 domain were found to be of the same order of magnitude. The affinity of G7-18NATE is comparable to previously reported values of 35.7 μM and 13.2 μM ^{30,31} where the differences are likely to reflect differences in the experimental conditions such as buffer type and composition, peptide and protein concentrations. Interestingly, the slightly higher affinity estimated for the G7-18NATE-P-Biotin peptide is a reflection not of an increased enthalpic contribution to binding, but rather appears to be due to a larger increase in entropy of the system. Considering the structures of the peptides, the structure of G7-18NATE-P-Biotin would be expected to display greater flexibility, and to display a more

entropically unfavorable binding than the seemingly more rigid G7-18NATE. However, entropy is a combined effect of both conformational and solvation/desolvation phenomena. In the present case, given the highly charged nature of the Penetratin[®]-derived tail, it is likely to be highly solvated and thus produce a compensatory favorable entropy via desolvation during the binding event. The two peptides exhibit a similar stoichiometry of 1:1 for their binding to the Grb7-SH2 domain. Overall, this study shows that the impact of the Penetratin[®]-derived sequence on the binding of G7-18NATE to Grb7-SH2 domain is minimal and, most importantly, that the Penetratin[®]-derived sequence does not interfere or negatively impact the binding of G7-18NATE to its target.

The G7-18NATE-P-Biotin peptide was found to be readily taken up by cells in culture, similar to other peptides cova-

lently attached to the full-length Penetratin[®] construct.^{32,33} This was as expected from studies of the cellular permeability of different sequences derived from Penetratin[®],²² but has not been previously demonstrated for the G7-18NATE peptide nor shown, to the best of our knowledge, using confocal microscopy for this sequence. Furthermore, the G7-18NATE was found to be mainly localized in the cytoplasm that is also where Grb7 was shown to reside in the human MDA-MB-468 breast cancer cells. Whilst the cell rupture and fixation processes required for the detection of biotin with streptavidin and the detection of Grb7 with antibodies may impact on the fine detail of molecular localization in the cell, their colocalization in the cytoplasm suggests that this construct is suitable for studies of the effect of G7-18NATE/Grb7 interactions in cells.

Together these studies have demonstrated the suitability of the Penetratin[®]-derived sequence for the delivery of G7-18NATE to cells for interaction with Grb7. These studies have confirmed that the interaction of the G7-18NATE with the Grb7 SH2 domain occurs with micromolar affinity, and that this is not detrimentally impacted on by the addition of the Penetratin[®]-derived cell penetrating sequence. Future derivatives of the G7-18NATE peptide, which are currently sought with improved affinity for Grb7, are also likely to be assisted in their delivery into cells using this strategy.

REFERENCES

- Margolis, B.; Silvennoinen, O.; Comoglio, F.; Roonprapunt, C.; Skolnik, E.; Ullrich, A.; Schlessinger, J. *Proc Natl Acad Sci USA* 1992, 89, 8894–8898.
- Ooi, J.; Yajnik, V.; Immanuel, D.; Gordon, M.; Moskow, J. J.; Buchberg, A. M.; Margolis, B. *Oncogene* 1995, 10, 1621–1630.
- Daly, R. J.; Sanderson, G. M.; Janes, P. W.; Sutherland, R. L. *J Biol Chem* 1996, 271, 12502–12510.
- Manser, J.; Roonprapunt, C.; Margolis, B. *Dev Biol* 1997, 184, 150–164.
- Fiddes, R. J.; Campbell, D. H.; Janes, P. W.; Sivertsen, S. P.; Sasaki, H.; Wallasch, C.; Daly, R. J. *J Biol Chem* 1998, 273, 7717–7724.
- Stein, D.; Wu, J.; Fuqua, S. A.; Roonprapunt, C.; Yajnik, V.; D'Eustachio, P.; Moskow, J. J.; Buchberg, A. M.; Osborne, C. K.; Margolis, B. *EMBO J* 1994, 13, 1331–1340.
- Han, D. C.; Guan, J. L. *J Biol Chem* 1999, 274, 24425–24430.
- Feldner, J. C.; Brandt, B. H. *Exp Cell Res* 2002, 272, 93–108.
- McLean, G. W.; Carragher, N. O.; Avizienyte, E.; Evans, J.; Brunton, V. G.; Frame, M. C. *Nat Rev Cancer* 2005, 5, 505–515.
- Yokote, K.; Margolis, B.; Heldin, C. H.; Claesson-Welsh, L. *J Biol Chem* 1996, 271, 30942–30949.
- Han, D. C.; Shen, T. L.; Miao, H.; Wang, B.; Guan, J. L. *J Biol Chem* 2002, 277, 45655–45661.
- Tanaka, S.; Mori, M.; Akiyoshi, T.; Tanaka, Y.; Mafune, K.; Wands, J. R.; Sugimachi, K. *Cancer Res* 1997, 57, 28–31.
- Kishi, T.; Sasaki, H.; Akiyama, N.; Ishizuka, T.; Sakamoto, H.; Aizawa, S.; Sugimura, T.; Terada, M. *Biochem Biophys Res Commun* 1997, 232, 5–9.
- Walch, A.; Specht, K.; Braselmann, H.; Stein, H.; Siewert, J. R.; Hopt, U.; Hofler, H.; Werner, M. *Int J Cancer* 2004, 112, 747–753.
- Haran, M.; Chebatco, S.; Flaishon, L.; Lantner, F.; Harpaz, N.; Valinsky, L.; Berrebi, A.; Shachar, I. *Leukemia* 2004, 18, 1948–1950.
- Han, D. C.; Shen, T. L.; Guan, J. L. *J Biol Chem* 2000, 275, 28911–28917.
- Shen, T. L.; Guan, J. L. *FEBS Lett* 2001, 499, 176–181.
- Pero, S. C.; Oligino, L.; Daly, R. J.; Soden, A. L.; Liu, C.; Roller, P. P.; Li, P.; Krag, D. N. *J Biol Chem* 2002, 277, 11918–11926.
- Pero, S. C.; Shukla, G. S.; Cookson, M. M.; Flemer, S., Jr.; Krag, D. N. *Br J Cancer* 2007, 96, 1520–1525.
- Tanaka, S.; Pero, S. C.; Taguchi, K.; Shimada, M.; Mori, M.; Krag, D. N.; Arii, S. *J Natl Cancer Inst* 2006, 98, 491–498.
- Derossi, D.; Joliot, A. H.; Chassaing, G.; Prochiantz, A. *J Biol Chem* 1994, 269, 10444–10450.
- Fischer, P. M.; Zhelev, N. Z.; Wang, S.; Melville, J. E.; Fahraeus, R.; Lane, D. P. *J Pept Res* 2000, 55, 163–172.
- White, P. D.; Chan, W. C. In *Fmoc Solid Phase Peptide Synthesis: A Practical Approach*; Chan, W. C.; White, P. D., Eds.; Oxford University Press: Oxford, 2000; pp 9–37.
- Kaiser, E.; Colecott, R. L.; Bossinger, C. D.; Cook, P. I. *Anal Biochem* 1970, 34, 595–598.
- Janes, P. W.; Lackmann, M.; Church, W. B.; Sanderson, G. M.; Sutherland, R. L.; Daly, R. J. *J Biol Chem* 1997, 272, 8490–8497.
- Porter, C. J.; Wilce, M. C.; Mackay, J. P.; Leedman, P.; Wilce, J. A. *Eur Biophys J* 2005, 34, 454–460.
- Pace, C. N.; Vajdos, F.; Fee, L.; Grimsley, G.; Gray, T. *Prot Sci* 1995, 4, 2411–2423.
- Perozzo, R.; Folkers, G.; Scapozza, L. *J Recept Signal Transduct Res* 2004, 24, 1–52.
- Ward, W. H.; Holdgate, G. A. *Prog Med Chem* 2001, 38, 309–376.
- Porter, C. J.; Matthews, J. M.; Mackay, J. P.; Pursglove, S. E.; Schmidberger, J. W.; Leedman, P. J.; Pero, S. C.; Krag, D. N.; Wilce, M. C.; Wilce, J. A. *BMC Struct Biol* 2007, 7, 58.
- Spuches, A. M.; Argiros, H. J.; Lee, K. H.; Haas, L. L.; Pero, S. C.; Krag, D. N.; Roller, P. P.; Wilcox, D. E.; Lyons, B. A. *J Mol Recognit* 2007, 20, 245–252.
- Derossi, D.; Chassaing, G.; Prochiantz, A. *Trends Cell Biol* 1998, 8, 84–87.
- Hodoniczky, J.; Sims, C. G.; Best, W. M.; Bentel, J. M.; Wilce, J. A. *Biopolymers* 2008, 90, 595–603.

Chapter 4

Synthesis and Thermodynamic Characterization of Second Generation G7-18NATE Analogues

This chapter reports the solid phase synthesis and binding characterization of G7-18NATE analogue peptides. The synthesis and affinity data for eight polypeptides is described. The in vitro binding affinities were determined to be in the range of $K_d = 0.67\text{-}60\ \mu\text{M}$. The impact of buffer and pH composition as well as the dimerization status on the binding characteristics of G7-18NATE and its derivatives is presented.

Abstract

Growth factor receptor bound protein-7 (Grb7) is an intracellular adaptor protein known to mediate oncogenic signaling pathways. The amplification and over-expression of the Grb7 gene has been connected with cancer cell proliferation, migration and metastasis. The present work reports the design, synthesis and binding affinity characterization of second generation peptide antagonists of Grb7. Specifically, through the application of a phage display technology on a deliberately biased peptide library containing the YXN recognition motif, a set of four peptides were identified as potential antagonists of Grb7. The experimental binding affinity was determined by ITC and was found to be of moderate strength ranging from 57 μ M to 18 μ M. All the peptides were found to bind with favorable enthalpy and entropy. Moreover cell permeable and non-permeable derivatives of G7-18NATE were designed and tested in acetate and phosphate buffers. Peptides tested in phosphate buffer were found to have a higher affinity than those in acetate (4.8 μ M vs 35 μ M). Finally, investigation of the effect of dimerization status of Grb7 SH2 domain on G7-18NATE peptide binding has shown that the peptide binds both to both the monomeric and dimeric forms with equal affinity and 1:1 stoichiometry with the Grb7 SH2 domain. Taken together, the study could help expedite the rational development of Grb7 based anticancer therapeutics agents.

Keywords: Grb7, adapter protein, SH2 domain, G7-18NATE; cancer cells, ITC, PHAGE display

Introduction

Growth factor Receptor Bound protein 7 (Grb7) is an adapter protein that mediates a variety of membrane bound and cytoplasmic receptors to effect downstream signaling events.^{1,2} The growing understanding of the molecular mechanisms involved in signal transduction has rendered Grb7 as a central protein in several pathways affecting processes such as cell growth, migration, angiogenesis, inflammation and proliferation. Research available on different aspects of Grb7 means it is now of great interest as a therapeutic target in a variety of human cancers such as breast,³ blood,⁴ pancreatic,⁵ esophageal,⁶ ovarian,⁷ hepatic,⁸ testicular,⁹ gastric carcinomas,¹⁰ and in inflammatory disorders such rheumatoid arthritis,¹¹ and atopic dermatitis.¹² Especially, the relevance of Grb7 in cancer has been widely investigated by a comparative analysis of the characteristics of Grb7 over-expressing and Grb7 knockout cancer cells where it is found to be critical for the life of different cancer cells.^{5,13} Finally, Grb7 is demonstrated to be a druggable protein that can be blocked by synthetic agents resulting in a significant reduction of cancer cell viability.¹⁴ Put together, these investigations make Grb7 an attractive target for the development of therapeutics that may have a potential in cancers and inflammations.

Grb7 is composed of 532 residues that are arranged in well-conserved protein domains including a Ras-associating domain, a pleckstrin homology (PH) domain, a C-terminal Src homology 2 (SH2) domain. Grb7 has an N-terminal domain rich in prolines and another domain termed BPS domain (for between the PH and SH2 domains).^{1,15} Each domain is characterized to make separate but complementary contributions to the overall signaling function of Grb7. Specifically, the role and attributes of the SH2 domain of Grb7 is widely investigated. The SH2 domain is crucial to link Grb7 to its upstream binding partners and it is known to bear a cationic pocket that serve as a docking site for phosphorylated tyrosines of Grb7 binding partners. The selectivity of recognition of binding SH2 domain hangs upon the sequence surrounding the phosphotyrosine residue.¹⁵ Interestingly enough, the SH2 domain is found in a number of Grb7 related and other adaptor proteins.¹⁶ As the first step in the involvement of Grb7 in growth factor dependent and related pathways is the binding of Grb7 to its upstream partners via its SH2 domain, this domain forms an essential module for the variety of Grb7 mediated oncogenic

transformations. Also the availability of the experimental structure of Grb7-SH2 domain is an asset for inhibitor development via computational and biochemical studies.¹⁷

The Phage display technique is a useful tool to identify peptide based receptor antagonists.^{18,19} Usually, peptides obtained from the phage display are subjected to a plethora of optimization approaches so as to transform them into clinical candidates.^{20,21} Recently, using random peptide libraries, a PHAGE display experiment was applied to identify the first cyclic phosphorylated polypeptide antagonist of Grb7-the G7-18NATE.¹⁴ It was found that the peptide possessed remarkable selectivity for Grb7 with little cross reactivity against the related Grb2. The binding affinity of the peptide for the Grb7 SH2 domain, however, was found to only be micromolar which is suboptimal for cellular studies. The present work was inspired by this observation and was designed to further explore the YXN motif recognized by the Grb7 oncoprotein and reports the design, synthesis and binding affinity characterization of second-generation antagonists of Grb7. Moreover, in carrying out NMR experiments with the lead peptide, we accidentally discover that in the phosphate buffer used for the NMR enhanced the binding interaction. These observations lead us to extend and investigate the impact of pH and buffer composition for the other peptide as well. In line with this, we report the design, synthesis and binding studies on cell permeable and non-permeable G7-18NATE derivatives. Finally, the effect of dimerization status of the Grb7 SH2 domain on binding to G7-18NATE is investigated with expression and purification of the monomeric form of Grb7 SH2 domain.

Materials and methods

Solid phase synthesis of G7-18NATE Analogues

Following the identification of G7-18NATE analogue structures by the PHAGE display technique, solid phase synthesis was effected to prepare the peptides for the binding studies. The G7-18NATE peptide analogues were synthesized as peptide amides using the Fmoc based solid phase peptide synthesis strategy on a rink amide resin (1.0mmol/g).²² Following resin swelling for 30 min in dimethyl form amide (DMF), the protecting group on the resin, 9-flourenyl methoxy carbonyl (Fmoc), was

removed with 20% v/v piperidine/DMF for 45 min at room temperature. Kaiser's ninhydrin based colortest²³ was employed to check the success of Fmoc removal. The first residue, Fmoc-Cys (trt)-OH, was coupled manually at RT for 45 min in three fold excess and the success of coupling was checked by Kaiser's test. In cases where less than efficient coupling was noted as indicated by the Kaiser's color reaction, the coupling time was increased up to 1 hr and HATU was employed as a coupling agent instead of HBTU. Following, successful coupling of the Fmoc-Cys (trt) residue, the resin was transferred to the Liberty's peptide synthesizer (www.chemie.de) to incorporate the remaining residues. The coupling and activating system used were HBTU/HoBt/DIEPA. Double couplings were employed for residues Phe, Tyr, Trp, Thr and Asn and the coupling time was doubled. Following incorporation of the residues using the microwave synthesizer, the N-terminal Fmoc group was removed and chloroacetylation was carried out on the protected and resin-bound peptide with chloroacetic acid anhydride (171 mg, 2 ml DMF, 100µl DIPEA) at RT for about 30 min. The dried peptide was then cleaved and fully deprotected using a cocktail of 94.5% TFA/2.5%TIPS/2.5%H₂O/0.5%EDT in a 20-fold excess volume over dry weight of resin-peptide for 3-4 hours at RT. TFA evaporation and resin drying was effected with a stream of nitrogen gas. This was followed by precipitation of peptide in ice-cold diethyl ether. Finally the crude peptides were dissolved and extracted with successive small volumes of 50% ACN/H₂O and were lyophilized overnight. Thioether formation was effected by dissolving the lyophilized peptide at 2 mg/ml in 50 mM NH₄HCO₃ in 50% acetonitrile/H₂O of pH 8.0 for 11/2 hrs at RT. The success of cyclization was followed by mass spectrometry. The cyclized peptides were freeze-dried and purified using preparative RP HPLC. Finally homogeneity and identity of the synthesized peptides was confirmed by analytical reverse phase HPLC and electron-spray ionization mass spectroscopy in negative ion mode, as described in chapter 2.

Binding studies by Isothermal Titration Calorimetry

ITC binding experiments were performed on a VP-ITC Micro calorimeter (Microcal, Northampton, MA, USA) at 25 °C.²⁴ The Grb7 SH2 domain was dialyzed extensively against 50 mM NaOOCCH₃ (pH 6.6), 100 mM NaCl and 1 mM DTT at 4 °C overnight. Lyophilized peptides were dissolved in appropriate volume of filtered dialysate

buffer. The concentration of Grb7 SH2 was determined by recording its absorbance at 280 nm whereas that of the peptides was determined by a mass obtained with an analytical balance and dissolution in the required volume. The peptide and protein solutions were degassed and thermostated at 20 °C for 5 min using the ThermoVac of the VP-ITC Micro calorimeter. The reference power of the experiment was set to 20 μ Cal/sec and the cell contents were stirred continuously at 307 rpm throughout the titrations. The feedback mode gain was set to high with fast and auto equilibration options applied. The reference cell was filled with MQ water. The peptides of 0.70-1.55 mM concentrations were titrated into Grb7 SH2 solutions of 55-85 μ M concentrations in 10 μ L injections with a 3-4 min delay between each injection. A binding isotherm was generated by plotting the heat change evolved per injection against the molar ratio of peptides to the Grb7 SH2 domain receptor. A blank determination in which the peptides were titrated against the buffer was carried out to account for heats of dilution and mixing which was then subtracted from the binding data. The corrected data was then employed to fit to a single binding site model using a non-linear least squares with the Origin (Microcal Software, Northampton, MA, USA). All of the ITC fitting parameters were kept floating during the fitting procedure. The ITC studies in phosphate buffer (100 mM Sodium phosphate, pH 6.0, 1 mM DTT) were done analogously.

Expression and purification of Grb7-SH2 domain

The SH2 domain of Grb7 was used as a receptor for the ITC binding experiments was purified as described in chapter 2. Briefly, the pGex2T plasmid containing the Grb7-SH2 insert encoding residues 415-532 of human Grb7 protein was expressed in *E. coli* expression system as a GST fusion protein in BL21 (DE3) pLysS strains.^{25,26} Cell induction was achieved with a 400 μ M isopropyl β -D-1-thiogalactopyranoside. The final concentration was determined with UV-Visible spectroscopy.²⁷ The F511R mutant of Grb7 SH2 domain was expressed and purified analogously.

Results

A. Synthesis and binding studies of G7-18NATE analogue peptides obtained by PHAGE display

The discovery of G7-18NATE as a selective antagonist of Grb7 has stimulated the further exploration of its structure in a bid to identify analogues with activity against the Grb7 oncoprotein.¹⁴ The cyclic peptides shown in Fig. 4.1 were identified using a phage display technique that is biased towards the YXN recognition motif present in most of Grb7 binding partners. That biased system has resulted in conservative substitutions of G7-18NATE and generation of the four polypeptides shown above as potential Grb7 antagonists as determined by our collaborators in the University of Vermont, USA.

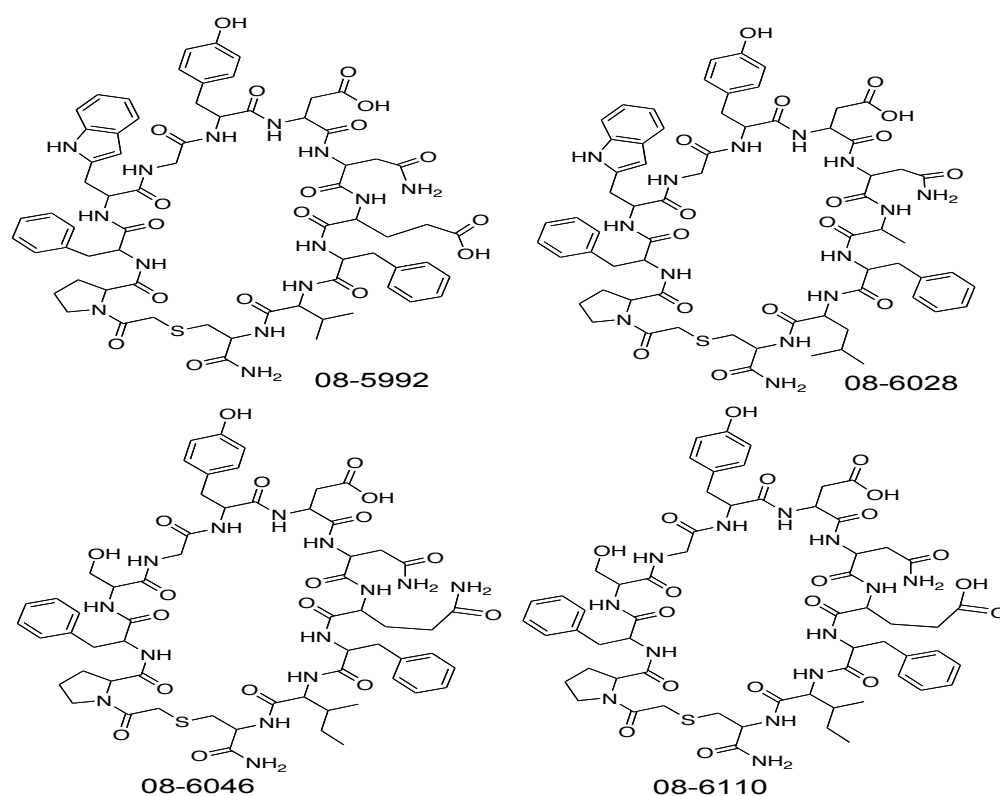


Figure 4.1. Chemical structure of the second-generation Grb7 antagonist polypeptides

The chemical synthesis of peptides was effected utilizing standard solid phase peptide synthesis based on Fmoc chemistry. Specifically, amino acids were all pre-activated using the HBTU/DIPEA or HATU/DIPEA in the presence of HoBt as an

additive. In all cases the first residue was coupled manually at room temperature and chloroacetylation was conducted at the N-terminal residues while the crude peptide was still on the resin. Ring closure was achieved with thioether bond formation between the cysteine side chain and the chloroacetylated N-terminus of peptides in aqueous solution. Thioether formation was made possible by exploiting the property of thiol groups to get deprotected at pH 8.0 and thereby to act as a nucleophile to displace the chloride ion from the chloroacetylated N-terminal amino group. The synthetic outcome of the peptides is summarized in Table 4.1. As indicated a yield of 7.92% for peptide 08-5992, 13.32% for 08-6028, 17.49% for 08-6110 and 7.52% for 08-6046 was obtained based on the theoretical outcome expected on the scale of the synthesis taken. These figures may not be strictly applied, however, since up to 6-fold excess of reactants were used in cases of the double coupling of residues (Phe, Tyr, Trp, Thr and Asn) so as to achieve efficient coupling, as is typically the case in peptide synthesis.²⁸

Table 4.1: Synthetic yield of G7-18NATE analogue peptides

S.No.	Peptide	Molecular Mass			Yield	
		Expected	Observed	Actual (mg)	Theoretical (mg)	Percent
1.	08-5992	1415.0	1415.4	11.2	141.5	7.92
2.	08-6028	1370.6	1370.8	18.3	137.1	13.36
3.	08-6110	1428.6	1429.0	25.0	142.86	17.50
4.	08-6046	1328.5	1328.8	10.0	132.85	7.52

The determination of thermodynamic binding parameters for the interaction between ligand and receptor is useful to gain an insight into the molecular mechanism of complex formation.²⁹ In that regard, ITC binding measurements are invaluable as they afford a quantitative description of the interaction in a detailed manner.²⁶ For example, ITC enthalpic readout gives a direct measure of the binding contribution from the formation or breakage of non-covalent bonds while the entropic data provides a quantitative value for changes in order of the system associated with the conformational and/or solvation phenomenon during ligand-receptor complex formation. The precise determination of both these parameters

along with the number of binding sites (N) and dissociation constant (K_d) contributes to a clearer understanding of the overall attributes of ligand-receptor associations under investigation.^{24,29}

The binding thermodynamics of the four G7-18NATE analogues (08-5992, 08-6110, 08-6046 and 08-6028) were characterized with ITC. The experimental measurements were conducted under identical experimental conditions including identical buffer composition, pH, titration schedule, receptor preparation and instrumentation so as not to introduce any systematic bias. Fig. 4.2 shows the binding isotherm for the analogues titrated against the SH2 domain of Growth factor receptor bound protein 7 (Grb7) as a receptor representing Grb7.

In common with the lead G7-18NATE interaction with the Grb7 SH2 domain,²⁷ all the peptides characteristically bound with evolution of heat, i.e., through exothermic binding. This is clearly evident from the over all thermogram displayed in Fig. 4.2. Such an interaction has also been noted for other analogues of G7-18NATE²⁸ and for cell permeable derivatives of G7-18NATE.³⁰ Moreover, the stoichiometry of binding is also similar to the parent peptide at a 1:1 ratio indicating the peptides and lead structure bind to a single binding site on the SH2 domain. Interestingly, the equilibrium dissociation constant (K_d) obtained is similar for the four peptides being 57.8 μM for 08-5992, 44.5 μM for 08-6110, 18.1 μM for 08-6046, and 52.36 μM for 08-6028, see Table 4.2 for details. This is also very similar to that of the parent G7-18NATE ($K_d = 34.6 \mu\text{M}$).

This might reflect the chemical make up of the peptides; very similar both in sequence, composition and over all size. Even though the affinity and over all thermograms looks similar, there appears to be subtle differences in the relative contribution of the components of binding to the overall affinity. Specifically, with the exception of peptide 08-6110, the other analogue peptides seem to interact through a more or less identical enthalpy of binding.

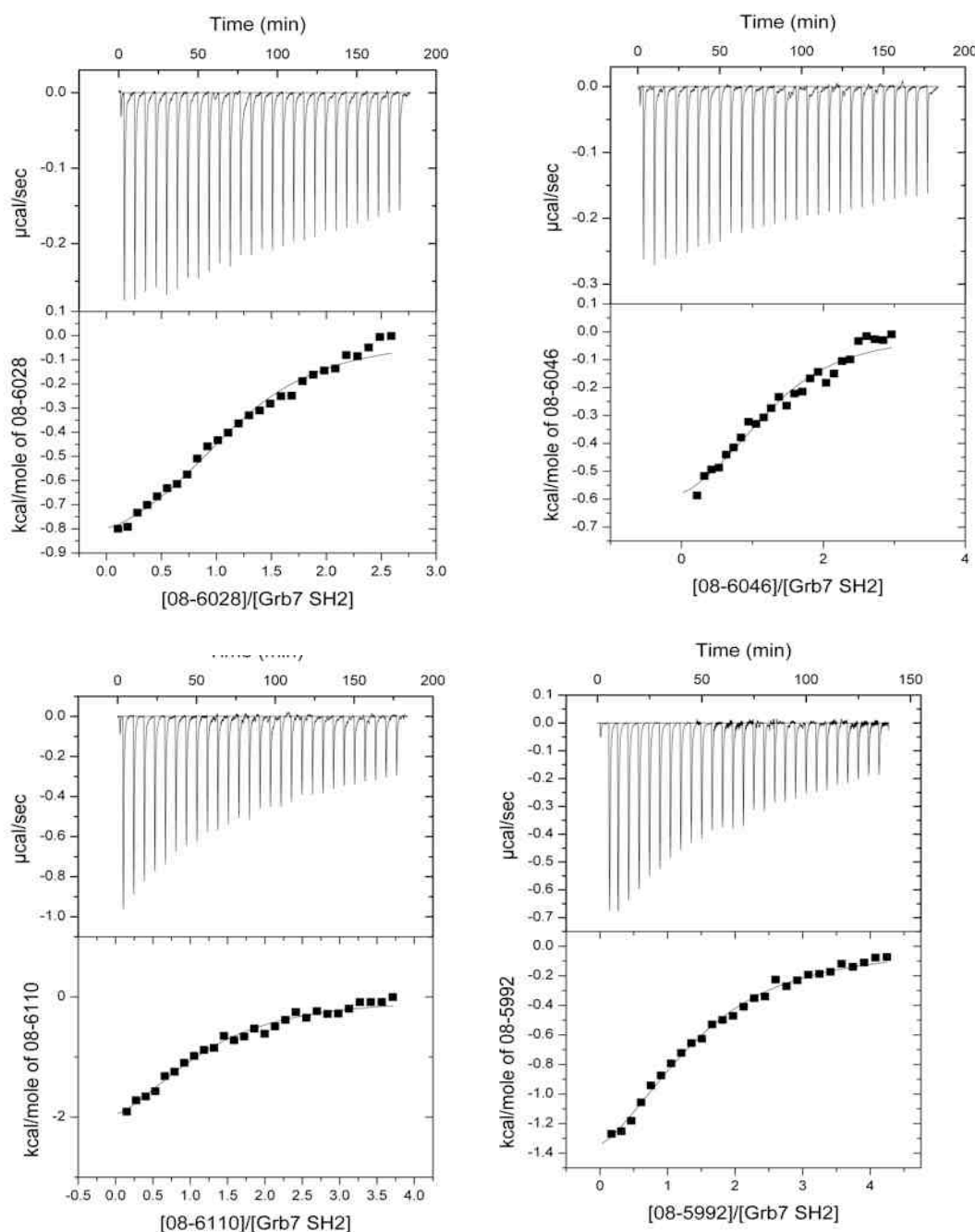


Figure 4.2. ITC Thermograms obtained from the isothermal titration of G7-18NATE analogues against Grb7SH2 domain. The upper panel show raw data obtained from 10 μl injections of peptides at 25 $^{\circ}\text{C}$. The lower panels in both figures display plots of integrated total energy exchanged (as kcal/mol of injected peptides) as a function of molar ratio of the peptides to the Grb7 SH2 domain

Even then, the binding enthalpy of peptide 08-6110 is only slightly higher than the other analogues and it is observed to bind in almost equivalent enthalpy and entropy of associations. In the entropic component of binding to the SH2 domain, however, there exist appreciable differences among the analogues. It is apparent

from the table that the entropic component ($T\Delta S$) is predominating as compared to the enthalpic part of the binding interaction (08-5992, 08-6028, 08-6046). Specifically the entropic contribution of analogues 08-5992 and 08-6028 peptides is about twice its binding enthalpy where as it is more than thrice for peptide 08-6046. This observation could potentially aid the further optimization of the affinities of these analogues peptide antagonists. Despite the relative enthalpy/entropy contribution differences, the gross binding affinities found remain similar and this is tempting to suggest that there is entropy-enthalpy compensation at work especially as the K_d values remain virtually unaffected.

Table 4.2: Thermodynamic binding parameters of G7-18NATE analogues

Binding Parameter	08-5992	08-6110	08-6046	08-6028
N	1.2 ± 0.18	1.13 ± 0.09	1.31 ± 0.08	1.05 ± 0.162
$K(10^4 M^{-1})$	1.73 ± 0.23	2.26 ± 0.47	5.53 ± 0.14	1.91 ± 0.40
ΔH (kcalmole ⁻¹)	-1.92 ± 0.37	-2.89 ± 0.33	-1.64 ± 0.06	-1.60 ± 0.33
ΔS (calmole ⁻¹ K ⁻¹)	12.85	10.23	19.55	14.2
$-T\Delta S$ (kcalmole ⁻¹)	-3.83	-3.05	-5.83	-4.23
ΔG (kcalmole ⁻¹)	-5.75 ± 0.37	-5.94 ± 0.33	-6.48 ± 0.06	-5.84 ± 0.33
K_d (μM)	58.8 ± 7.8	46.3 ± 9.6	18.1 ± 0.5	54.8 ± 11.5

When compared to the binding thermodynamics of the parent G7-18NATE peptide,³⁰ though the overall thermogram looks similar to that of the parent G7-18NATE peptide and the affinity is in the same range, the enthalpic/entropic contribution to the overall free energy of binding is very different. In the case of G7-18NATE binding, the enthalpic part is pronounced and is observed to be almost the sole contributor to the overall affinity where as its entropic contribution is found to be unfavorable or negative contributor.^{30,31} The amino acid composition of the analogues is generally similar to that of parent G7-18NATE peptide except for some slight changes in sequence. In all of the four analogues, however, there is proline at the N-terminal position and proline is known to affect protein/peptide architectures.³² Because of its placement at the N-terminal position and the fact that the ring is formed via proline's ring nitrogen atom, it is tempting to suggest that it might have forced the system to be somehow more restricted system and thereby

improving the entropic contribution of interaction. However, this has to be clarified experimentally. The overall conclusion is that the amino acids that vary between these peptides do not look to confer significant impact on the binding interactions with the Grb7-SH2 domain. Nevertheless, these analogues could serve as starting point for further optimization efforts.

B. Thermodynamic characterization of G7-18NATE derivatives

This section describes the thermodynamic characterization of G7-18NATE derivatives shown in Fig. 4.3. After briefly describing the design concepts behind the peptides, the results and interpretation made will be presented.

The G7-18NATE-Penetratin-Biotin peptide was designed to test whether a shorter cell permeable sequence would be sufficient to transport G7-18NATE into cells. The cell permeability sequence was selected on the basis of the study by Fischer et. al.³³ In the study, a series of cell permeablising peptides were synthesized and tested. It was shown that just the last 7 residues of this 17 residues peptide were efficiently translocated into cells. Since the synthesis of a shorter peptide is easier and less expensive than the long one, it was of interest to test its suitability for the delivery of G7-18NATE. In addition a C-terminal lysine was added to the sequence that could be used to attach a biotin group. This could allow the detection of the peptide in cells via fluorescent streptavidin treatment of cells and also potentially permit attachment to a streptavidin chip for SPR based *in vitro* affinity determination. Furthermore, if taken into cells the peptide could also be used to test the bioactivity of G7-18NATE in a cellular system. Chapter 3 reports the successful uptake of this peptide into cells and also the ITC based affinity measurement that confirms that the G7-18NATE retains its ability to bind to its target in the presence of the appended penetratin based sequence. In anticipation of the G7-18NATE-Penetratin-Biotin peptide being a useful construct to test both in cellular and in vitro assays, an analogue was designed in which the aspartic acid at residue 6 was replaced by a glutamic acid. This was based on the early modeling studies¹⁷ and analysis of the structure determination of the G7-18NATE/Grb7 SH2 domain co-crystal structure, where it is suggested that Glu than Asp may make favorable electrostatic interaction. It was thus of interest to test this peptide ((D->E) G7-18NATE-

Penetratin-Biotin) for both in affinity to Grb7 SH2 domain and, potentially, for its bioactivity in cells.

Table 4.3. Synthetic yield of G7-18NATE analogue peptides

S.No.	Peptide	Molecular Mass		Yield		
		Expected	Observed	Actual (mg)	Theoretical (mg)	Percent
1.	G7-18NATE	1417.6	1417.1	22	141.7	15.53
2.	G7-18NATE-Pen-Biotin	2787.2	2786.5	5.8	278.6	2.1
3.	(D->E) G7-18NATE-Pen-Biotin	2798.6	2798.8	7.0	279.6	2.5
4.	Allyl G7-18NATE	1323.5	1323.6	5.5	132.35	4.16

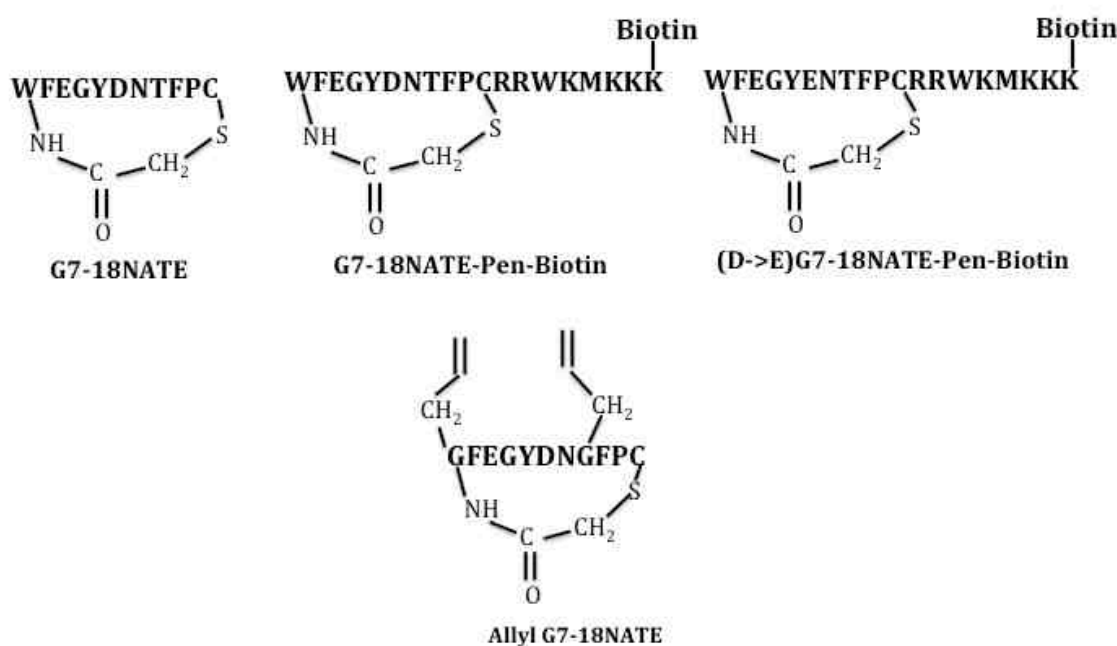


Figure 4.3. Sequence structure of Grb7 antagonists investigated in the present study. Amino acid abbreviations are indicated in bold letters.

Structural analysis of the binding geometry of the G7-18NATE peptide in complex with the Grb7 SH2 domain and our molecular dynamics simulation (not part of this thesis) revealed that residues Trp1 and Thr8 were not involved in significant bond formation with the Grb7 SH2 binding site. Thus, these two residues were replaced with allyl-glycine residue which carries moieties that could also be used for further

optimization by cyclization. The resulting derivative termed Allyl G7-18NATE was prepared and tested in phosphate buffer to investigate the impact of such amino acids replacements on the binding affinity of the parent G7-18NATE.

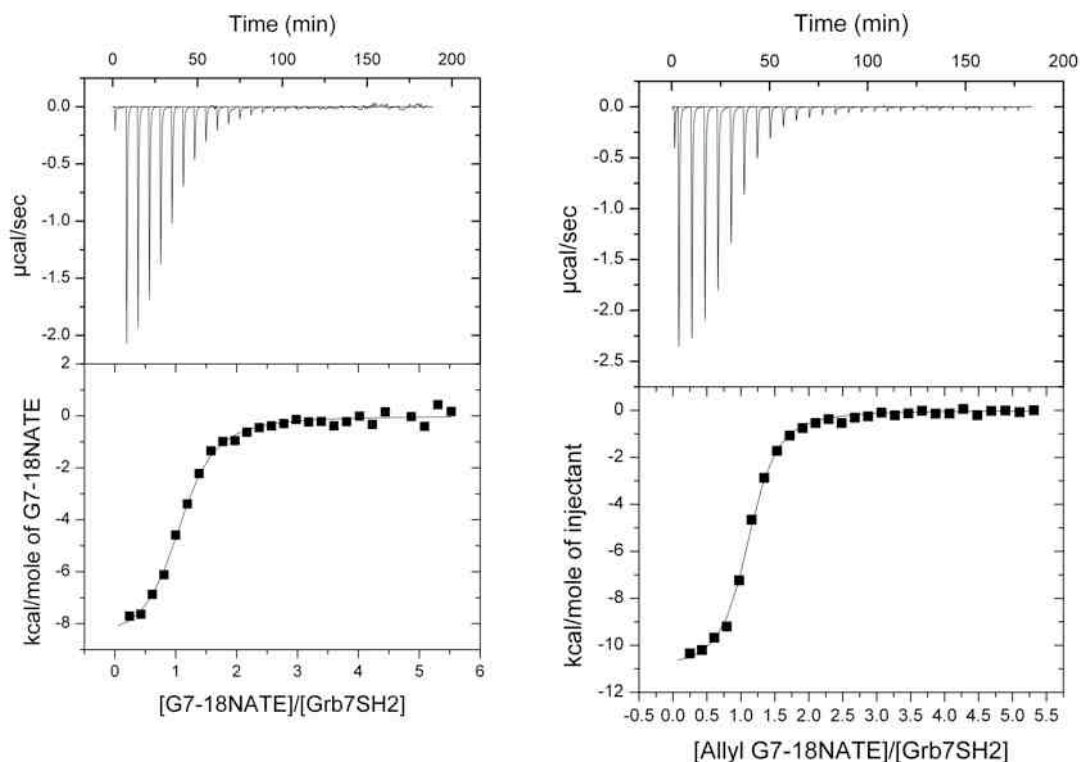


Figure 4.4. ITC thermograms obtained for the binding of G7-18NATE and Allyl G7-18NATE in phosphate buffer. The upper panel show raw data obtained from 10 μ l injections of peptides at 25 $^{\circ}$ C. The lower panels in both figures display plots of integrated total energy exchanged (as kcal/mol of injected peptides) as a function of molar ratio of the peptides to the Grb7 SH2 domain.

The chemical synthesis of the G7-18NATE derivatives was effected utilizing standard solid phase peptide synthesis based on Fmoc chemistry. The synthetic outcome of the peptides is summarized in Table 4.3. As indicated a yield of 15.53% for peptide G7-18NATE, 2.1% for G7-18NATE-Penetratin-Biotin, 2.5% for (D->E) G7-18NATE-Penetratin-Biotin and 4.2% for the allyl G7-18NATE was obtained based on the theoretical outcome expected on the scale of the synthesis taken.

Thermodynamics of G7-18NATE and allyl G7-18NATE in phosphate buffer

The binding affinity of G7-18NATE and Allyl G7-18NATE were conducted in phosphate buffer pH 6.0 (since the peptides had been subjected to characterization

by NMR spectroscopy in this buffer). The binding of G7-18NATE is described extensively.^{30,31} This study was intended to evaluate the impact of pH and buffer composition on the binding characteristics of G7-18NATE. For that we chose to study the effect on the phosphate buffer of pH 6.0 as compared to the previous study on sodium acetate at pH 6.6.^{30,31} As indicated in Fig. 4.4, the thermograms produced on using phosphate buffer were close to the ideal sigmoid curve expected in ITC titration experiments. Without changing the concentration of reactants as compared to previous ITC experiment with acetate buffer, the interaction in the present study was noted to clearly reach full saturation. Importantly, the immediate outcome of such thermograms is that it is much easier to fit such curves and derive the thermodynamic parameters with little ambiguity/difficulty. This is because the non-linear curve fitting routines implemented in the ITC data analysis packages assume perfect sigmoidal relationships between the power consumed/released and the amount of the interacting species as well as full saturation of binding event. This, in turn, could translate into more accuracy and reliability of the binding parameters obtained in such scenarios.

The equilibrium dissociation constant obtained for G7-18NATE is found to be 4.8 μM as which is compared to that of the previous report on sodium acetate buffer ($K_d = 34.6 \mu\text{M}$).³⁰ See Table 4.4. Though the pH might not be close enough to the physiological pH, but the buffer actually is. This is especially so for Grb7 SH2 domain as it is intracellular protein where phosphate is major buffer. Nevertheless, the G7-18NATE was found to bind with unfavorable entropy and favorable enthalpy, i.e., in the qualitative sense the pH and buffer changes had little effect on the enthalpic/entropic components of the affinity. This is in agreement with previous studies in sodium acetate buffer.³⁰ As such it is seen that the enthalpic part of binding (-8.067 kcal/mole) is the only force deriving the association with Grb7 SH2 as the entropic part ($T\Delta S = -0.89 \text{ kcal/mol}$) is found to negatively affect binding event. Over all, the effect of changes in the pH and buffer composition seems on the quality of the thermogram, the ease of fitting procedure and quantitative estimates of the binding parameters without affecting/altering the overall mechanistic basis of binding. The study reveals that the experimental conditions for ITC binding measurement can greatly impact quality and reliability of the thermodynamic data.

The binding thermodynamics for the allyl G7-18NATE was found to be similar to that of the parent G7-18NATE though the dissociation constant is slightly improved ($K_d = 1.42 \mu\text{M}$, compared to $K_d = 4.8 \mu\text{M}$). This modified peptide is found to bind with unfavorable entropy ($T\Delta S = -3.1 \text{ kcal/mol}$) and with favorable entropy ($\Delta H = -11.1 \text{ kcal/mole}$). As with the G7-18NATE, the enthalpic part remains the predominant factor to binding to the Grb7 SH2 domain. This experiment confirms that the two residues-Trp1 and Thr8- do not have an important role in bond formation to the binding site. As such structures contain groups important for ring formation these two residues could be well utilized in ring closing metathesis and hence potentially aid the further optimization of the affinities of these peptide antagonists.

Table 4.4: Binding parameters of G7-18NATE derivatives

Binding Parameter	G7-18NATE	G7-18NATE-Pen-Biotin	(D->E)G7-18NATE-Pen-Biotin*	Allyl G7-18NATE
Stoichiometry	1.04 ± 0.02	0.97 ± 0.01	1.08 ± 0.11	1.06 ± 0.01
K (10^5M^{-1})	2.08 ± 0.06	14.9 ± 1.28	0.26 ± 0.03	7.03 ± 0.57
$\Delta H(\text{kcalmol}^{-1})$	-8.07 ± 0.23	-7.09 ± 0.06	-3.37 ± 0.41	-11.1 ± 0.13
$-T\Delta S(\text{kcalmol}^{-1})$	0.89	-1.34	-2.65	3.10
$\Delta G(\text{kcalmol}^{-1})$	-7.18 ± 0.23	-8.43 ± 0.06	6.02 ± 0.41	-8.00 ± 0.13
$K_d (\mu\text{M})$	4.81 ± 0.04	0.69 ± 0.01	38.98 ± 4.51	1.34 ± 0.09

Binding Thermodynamics of cell permeable derivatives of G7-18NATE

One of the bottlenecks in the development of peptides as drugs is the barrier presented by membranes, especially so when the target is an intracellular protein like Grb7. To alleviate this problem, other peptides are being developed that have the ability to ferry peptide drugs across biological membranes. We recently identified the shorter penetrating tail that was shown to possess the peptide translocating property in cells.³⁰ As an attempt to further explore the potential of such a short permeablizing sequence, it was synthesized in the form of a fusion polypeptide as G7-18NATE-Penetratin-Biotin and its impact on the binding of G7-18NATE to Grb7 SH2 domain was characterized using ITC. In this case, the phosphate buffer system was utilized. Also a modified cell permeable analogue, (D-

>E) G7-18NATE-Penetratin-Biotin was synthesized and its binding investigated in acetate buffer conditions.

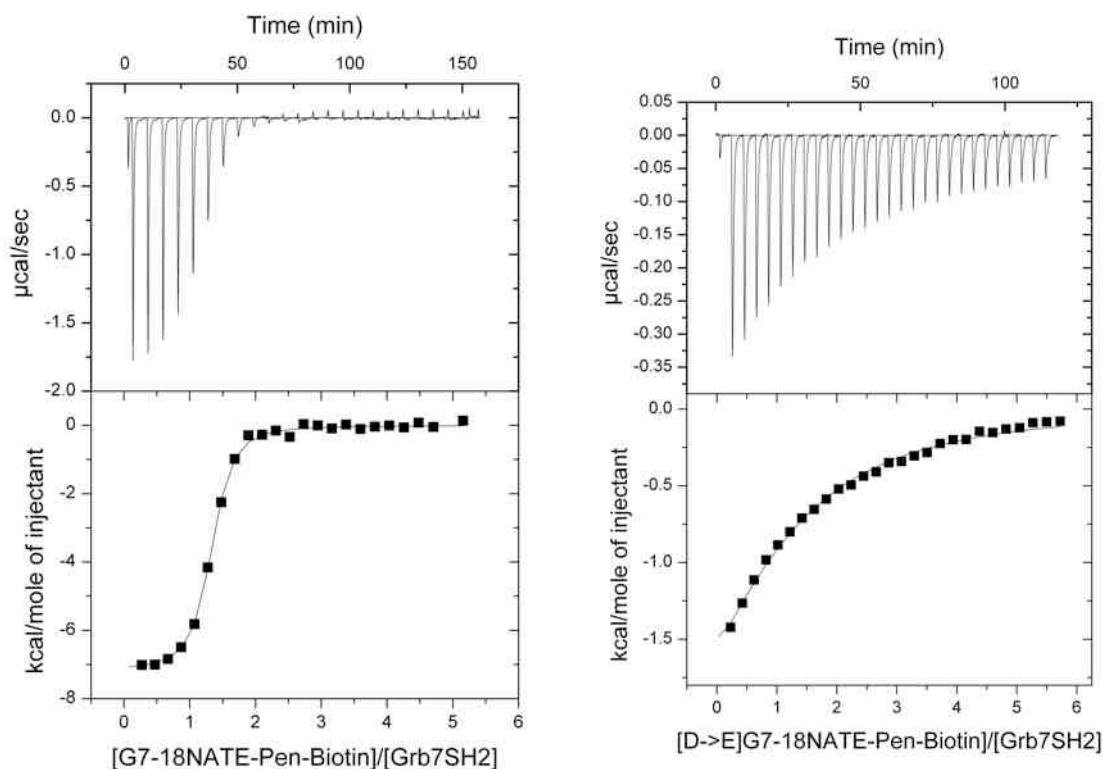


Figure 4.5. ITC Thermograms obtained from the isothermal titration of cell permeable G7-18NATE analogues against Grb7SH2 domain. *Left*: G7-18NATE-penetratin-Biotin; *Right*: (D->E) G7-18NATE-Penetratin-Biotin. The upper panel show raw data obtained from 10 μ l injections of peptides at 25 °C. The lower panels in both figures display plots of integrated total energy exchanged (as kcal/mol of injected peptides) as a function of molar ratio of the peptides to the Grb7 SH2 domain.

As shown in Fig. 4.5, both G7-18NATE-Penetratin-Biotin and (D->E) G7-18NATE-penetratin-biotin bind with the release of heat. Moreover, the stoichiometry of binding is also similar to the non-cell permeable counter parts, being at 1:1.^{30,31} The equilibrium dissociation constant obtained for the G7-18NATE-Penetratin-Biotin in phosphate buffer is 0.69 μ M. This is compared to a K_d of 14.42 μ M in acetate buffer pH 6.6,³⁰ indicating a significant improvement as in the case of G7-18NATE. The phosphate ion in the buffer seems to enhance the binding of both G7-18NATE and its cell permeable form-the G7-18NATE-Penetratin-Biotin. The thermograms obtained for G7-18NATE-Penetratin-Bioitn in phosphate buffer appear nicely sigmoidal which makes deriving the binding parameters easier and reliable. The thermogram of the (D-E>) G7-18NATE-Penetratin-Biotin in acetate buffer was not

sigmoidal. The K_d obtained for this peptide was 38.9 μM in acetate buffer, as shown in Table 4.4. This is comparable to the 14.42 μM K_d of the G7-18NATE³⁰ obtained under similar buffer and experimental conditions, suggesting the conservative nature of the substitution. The major observation is that irrespective of the buffer composition, both the cell permeable derivatives are seen to interact with Grb7 Sh2 domain with favorable enthalpy and entropy. This is in contrast to the parent peptide where it was found to bind in unfavorable entropy of binding. This looks counter intuitive when considering the sequence/structures of the peptides, the cell permeable peptides would be expected to display greater flexibility, and to display a more entropically unfavorable binding than the parent G7-18NATE peptide. However, entropy is a combined effect of both conformational and solvation/desolvation phenomena and given the highly charged nature of the permeablising tail, it is likely to be highly solvated and thus produce a compensatory favorable entropy via desolvation during binding event. All in all, the most important conclusion is that the penetratin tail does not negatively interfere in the binding process both in the G7-18NATE-penetratin-Biotin and (D->E)G7-18NATE-Penetratin-Biotin and the peptides could well be used in the further development of cell permeable analogues.

C. Impact of dimerization status of Grb7 SH2 domain to binding to G7-18NATE

Protein dimerization is an important control mechanism in the control of protein function.³⁴ Grb7 dimerization is considered critical for the regulation of Grb7 dependent signal transduction events.³⁴ As such it was found interesting to investigate the impact of dimerization on the impact of peptide binding. For that purpose, a mutant form of Grb7 SH2 domain (F511R) was prepared which was previously known to exist as a monomer only.³⁵ The ITC binding study was conducted in similar way as described above for the other analogues on the wild type Grb7 SH2 domain in sodium acetate buffer of pH 6.6.

Table 4.5. Binding parameters of G7-18NATE on the mutant Grb7 SH2 domain

Stoichiometry	$K(10^4\text{M}^{-1})$	ΔH (kcalmol ⁻¹)	ΔS (calmol ⁻¹ K ⁻¹)	$T\Delta S$ (kcalmol ⁻¹)	ΔG (kcalmol ⁻¹)	K_d (μM)
1.25±0.06	2.79±0.39	-2.09±0.141	13.3	3.965	-6.06±0.14	35.84

The ITC thermogram obtained is shown in Fig. 4.6 and it is in agreement with that of G7-18NATE and its analogues on the wild type Grb7 SH2 domain in that the binding exhibited an exothermic with the release of heat and a 1:1 stoichiometry, see Table 4.5. The dissociation constant obtained was 35.84 μM . This agrees well with previous report of G7-18NATE binding with Grb7 SH2 domain ($K_d = 34.5 \mu\text{M}$) on the wild type Grb7 SH2 domain.^{17,30} Taken together, the data suggests that mutation to alter the dimerization status does not look to have impact on its ability to bind Grb7 antagonists. This may originate from the fact that the dimerization interface and binding site are located on the opposite ends of the Grb7 structure.²³ Moreover, the stoichiometry found from studies on the wild type protein is 1:1 suggesting that Grb7 SH2 has a single binding site per monomer^{17,30,31} irrespective of its existence as a dimer. Taking the position of the dimer interface, the observed binding affinity and stoichiometry, the present study suggest that the wild type and the mutant Grb7 SH2 domains bind in a similar fashion and hence the monomeric form could equally be well exploited in the further development of Grb7 antagonists especially when the dimerization status may be of an interference in other experimental studies. A point of difference that is noticed is in the relative contribution of enthalpy and entropy to the overall affinity.

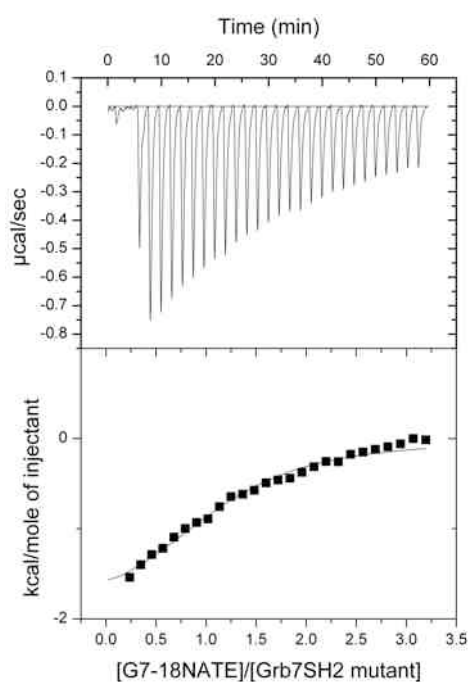


Figure 4.6. ITC Thermograms for the isothermal titration of G7-18NATE against F511R mutant Grb7 SH2 domain. The upper panel show raw data obtained from 10 μl injections of peptides at 25 $^{\circ}\text{C}$. The lower panels in both figures display plots of integrated total energy exchanged (as kcal/mol of injected G7-18NATE) as a function of molar ratio of the peptide to the Grb7 SH2 domain.

The data in Table 4.5 shows that the binding to the mutant monomeric form is favorable by both enthalpy ($\Delta H = -2.1$ kcal/mol) and entropic components ($T\Delta S = -3.97$ kcal/mol), indicating that the entropic part is not only favorable but also the predominant contributor (about twice) to binding. The physical meaning and value of this observation awaits further investigation.

Discussion

Grb7 is found as downstream mediator of several oncogenic pathways¹ and is established to have a definitive role in cell migration, progression, invasion and metastasis.³⁶ This has rendered Grb7 an interesting novel target for the development of potential therapeutic agents in different cancers and inflammatory disorders.³⁶ As yet there is no drug that acts on Grb7, even though its clinical relevance is well appreciated. Hence, the identification of experimental antagonist of Grb7 is expected to lay the groundwork for the development of clinical candidates molecules that act on this novel target protein. Moreover, as the downstream effectors of Grb7 have yet to be elucidated, molecular agents would have a potential as tool to be used to investigate the detail-signaling network to which Grb7 is involved.

Binding studies of G7-18NATE analogues obtained by the PHAGE display experiment shows the peptides bind in a similar affinity and mechanism to the parent G7-18NATE. This might be a reflection of the conservative nature of the amino acid substitution in these peptides, especially as the all-important YDN motif remains unaltered in all the peptide antagonists. Nevertheless, the fact that all the four peptides bind in a similar affinity might be important to derive a common feature for further optimization studies.

We have discovered a very interesting phenomenon in the case of the G7-18NATE/Grb7 SH2 domain interaction. It appears that binding is enhanced in phosphate buffer pH 6 compared to acetate buffer. The present work clearly suggests that careful and judicious selection of experimental parameters can produce a better thermogram that reaches clear saturation and hence a more reproducible and reliable binding parameters could be obtained. It is interesting to note that qualitatively the obtained thermogram data remain similar as to that

obtained in different experimental setting indicating^{17,30} that such changes do not affect the underlying mechanisms involved in the association event.

In agreement with previous report on the lead G7-18NATE, Allyl G7-18NATE was noticed to interact with favorable enthalpy and unfavorable entropy.^{17,30,31} The study shows that Trp1 and Thr8 of G7-18NATE could be easily removed and replaced with no significant impact on binding. Furthermore, the use of the cell permeablising sequence was investigated in different buffer/pH systems and peptides to find out similar result. This indicates that cell permeable derivatives of G7-18NATE (G7-18NATE-Penetratin-Biotin and (D->E) G7-18NATE-Penetratin-Biotin) could be used in real time cellular or animal experimentation studies. Finally, the experiment on the monomeric Grb7 SH2 mutant form demonstrates that dimerization status has little effect on the binding ability of Grb7 SH2 domain. This was evident and in agreement with the observed stoichiometry in this study and previously.^{17,30}

In conclusion, through a combined study involving antagonist design, chemical synthesis and binding studies the potential of the polypeptide antagonists of Grb7 is highlighted. The importance of setting the right experimental conditions for the ITC measurements is emphasized. Investigation on the mutant form also establishes that the monomeric form of Grb7 SH2 domain behaves in identical manner as the wild type counterpart. Through a combined phage display and chemical synthesis, a total of four polypeptide antagonists of Grb7 are proposed. The experimentally measured binding affinity is of moderate affinity being in low micro molar range. It is anticipated that these polypeptides could serve as additional tools in the further development of Grb7 based anticancer therapeutics and to further probe the functional and structural studies of Grb7 protein.

References

- (1) Han, D. C.; Shen, T. L.; Guan, J. L. The Grb7 family proteins: structure, interactions with other signaling molecules and potential cellular functions. *Oncogene* **2001**, *20*, 6315-6321.
- (2) Margolis, B.; Silvennoinen, O.; Comoglio, F.; Roonprapunt, C.; Skolnik, E.; Ullrich, A.; Schlessinger, J. High-efficiency expression/cloning of epidermal growth factor-receptor-binding proteins with Src homology 2 domains. *Proc. Natl. Acad. Sci. USA*, **1992**, *89*, 8894-8898.
- (3) Stein, D.; Wu, J.; Fuqua, S. A.; Roonprapunt, C.; Yajnik, V.; D'Eustachio, P.; Moskow, J. J.; Buchberg, A. M.; Osborne, C. K.; Margolis, B. The SH2 domain protein GRB-7 is co-amplified, overexpressed and in a tight complex with HER2 in breast cancer. *EMBO J.* **1994**, *13*, 1331-1340.
- (4) Haran, M.; Chebatco, S.; Flaishon, L.; Lantner, F.; Harpaz, N.; Valinsky, L.; Berrebi, A.; Shachar, I. Grb7 expression and cellular migration in chronic lymphocytic leukemia: a comparative study of early and advanced stage disease. *Leukemia* **2004**, *18*, 1948-1950.
- (5) Tanaka, S.; Pero, S. C.; Taguchi, K.; Shimada, M.; Mori, M.; Krag, D. N.; Arii, S. Specific peptide ligand for Grb7 signal transduction protein and pancreatic cancer metastasis. *J. Natl. Cancer Inst.* **2006**, *98*, 491-498.
- (6) Dahlberg, P. S.; Jacobson, B. A.; Dahal, G.; Fink, J. M.; Kratzke, R. A.; Maddaus, M. A.; Ferrin, L. J. ERBB2 amplifications in esophageal adenocarcinoma. *Ann. Thorac. Surg.* **2004**, *78*, 1790-1800.
- (7) Wang, Y.; Chan, D. W.; Liu, V. W.; Chiu, P.; Ngan, H. Y. Differential functions of growth factor receptor-bound protein 7 (GRB7) and its variant GRB7v in ovarian carcinogenesis. *Clin. Cancer Res.* **2010**, *16*, 2529-2539.
- (8) Itoh, S.; Taketomi, A.; Tanaka, S.; Harimoto, N.; Yamashita, Y.; Aishima, S.; Maeda, T.; Shirabe, K.; Shimada, M.; Maehara, Y. Role of growth factor receptor bound protein 7 in hepatocellular carcinoma. *Mol. Cancer Res.* **2007**, *5*, 667-673.
- (9) Goddard, N. C.; McIntyre, A.; Summersgill, B.; Gilbert, D.; Kitazawa, S.; Shipley, J. KIT and RAS signaling pathways in testicular germ cell tumors: new data and a review of the literature. *Int. J. Androl.* **2007**, *30*, 337-348.
- (10) Kishi, T.; Sasaki, H.; Akiyama, N.; Ishizuka, T.; Sakamoto, H.; Aizawa, S.; Sugimura, T.; Terada, M. Molecular cloning of human GRB-7 co-amplified with CAB1 and c-ERBB-2 in primary gastric cancer. *Biochem. Biophys. Res. Commun.* **1997**, *232*, 5-9.
- (11) Kim, C. W.; Cho, E. H.; Lee, Y. J.; Kim, Y. H.; Hah, Y. S.; Kim, D. R. Disease-specific proteins from rheumatoid arthritis patients. *J. Korean. Med. Sci.* **2006**, *21*, 478-84.
- (12) Yoon, S. W.; Kim, T. Y.; Sung, M. H.; Kim, C. J.; Poo, H. Comparative proteomic analysis of peripheral blood eosinophils from healthy donors and atopic dermatitis patients with eosinophilia. *Proteomics* **2005**, *5*, 1987-1995.
- (13) Pero, S. C.; Shukla, G. S.; Cookson, M. M.; Flemer, S.; Krag, D. N. Combination treatment with Grb7 peptide and Doxorubicin or Trastuzumab (Herceptin)


- results in cooperative cell growth inhibition in breast cancer cells. *Br. J. Cancer* **2007**, *96*, 1520-1525.
- (14) Pero, S. C.; Oligino, L.; Daly, R. J.; Soden, A. L.; Liu, C.; Roller, P. P.; Li, P.; Krag, D. N. Identification of novel non-phosphorylated ligands, which bind selectively to the SH2 domain of Grb7. *J. Biol. Chem.* **2002**, *277*, 11918-11926.
- (15) Pero, S. C.; Daly, R. J.; Krag, D. N. Grb7-based molecular therapeutics in cancer *Expert. Rev. Mol. Med.* **2003**, *5*, 1-11.
- (16) Pawson, T.; Gish, G. D.; Nash, P. SH2 and SH3 domains in signal transduction. *Adv. Cancer Res.* **1994**, *64*, 87-110.
- (17) Porter, C. J.; Matthews, J. M.; Mackay, J. P.; Pursglove, S. E.; Schmidberger, J. W.; Leedman, P. J.; Pero, S. C.; Krag, D. N.; Wilce, M. C.; Wilce, J. A. Grb7 SH2 domain structure and interactions with a cyclic peptide inhibitor of cancer cell migration and proliferation. *BMC Struct. Biol.* **2007**, *7*:58
- (18) Zwick, M. B.; Shen, J.; Scott, J. K. Phage-displayed Peptide Libraries. *Curr. Opin. Biotechnol.* **1998**, *9*, 427-436.
- (19) Scott, J. K.; Craig, L. Random Peptide Libraries. *Curr. Opin. Biotechnol.* **1994**, *5*, 40-48.
- (20) Nilsson, F.; Tarli, L.; Viti, F.; Neri, D. The use of phage display for the development of tumour targeting agents. *Adv. Drug Deliv. Rev.* **2000**, *43*, 165-196.
- (21) Smith, G. P. Filamentous fusion phage: novel expression vectors that display cloned antigens on the viron surface. *Science* **1985**, *228*, 1315-1317.
- (22) White, P. D.; Chan, W.C., Basic Principles, In *Fmoc Solid Phase Peptide Synthesis: A Practical Approach*, Chan, W.C.; White, P.D., Eds.: Oxford University Press, Oxford, **2000**, 9-37.
- (23) Kaiser, E.; Colescott, R. L.; Bossinger, C. D.; Cook, P. I Color test for detection of free terminal amino groups in the solid-phase synthesis of peptides. *Anal. Biochem.* **1970**, *34*, 595-598.
- (24) Ward, W. H.; Holdgate, G. A. Isothermal titration calorimetry in drug discovery. *Prog. Med. Chem.* **2001**, *38*, 309-376.
- (25) Janes, P. W.; Lackmann, M.; Church, W. B.; Sanderson, G. M.; Sutherland, R. L.; Daly, R. J. Structural determinants of the interaction between the erbB2 receptor and the Src homology 2 domain of Grb7. *J. Biol. Chem.* **1997**, *272*, 8490-8497.
- (26) Porter, C. J.; Wilce, M. C.; Mackay, J.P.; Leedman, P.; Wilce, J. A. Grb7-SH2 domain dimerisation is affected by a single point mutation. *Eur. Biophys. J.* **2005**, *34*, 454.
- (27) Pace, C. N.; Vajdos, F.; Fee, L.; Grimsley, G.; Gray, T. How to measure and predict the molar absorption coefficient of a protein. *Protein Sci.* **1995**, *4*, 2411.
- (28) Sabatino, G.; Papini, A. M. Advances in automatic, manual and microwave-assisted solid-phase peptide synthesis. *Curr. Opin. Drug Discov. Devel.* **2008**, *11*, 762-770.
- (29) Freyer, M. W.; Lewis, E. A. Isothermal titration calorimetry: experimental design, data analysis, and probing macromolecule/ligand binding and kinetic interactions. *Methods Cell Biol.* **2008**, *84*, 79-113.

- (30) Ambaye, N. D.; Lim, R. C.; Clayton, D. J.; Gunzburg, M. J.; Price, J. T.; Pero, S. C.; Krag, D. N.; Wilce, M. C.; Aguilar, M. I.; Perlmutter, P.; Wilce, J. A. Uptake of a cell permeable G7-18NATE construct into cells and binding with the Grb7-SH2 domain. *Biopolymers* **2010**, DOI: 10.1002/bip.21403
- (31) Spuches, A. M.; Argiros, H. J.; Lee, K. H.; Haas, L. L.; Pero, S. C.; Krag, D. N.; Roller, P. P.; Wilcox, D. E.; Lyons, B. A. Calorimetric investigation of phosphorylated and non-phosphorylated peptide ligand binding to the human Grb7-SH2 domain. *J. Mol. Recognit.* **2007**, 20, 245-252.
- (32) MacArthur, M. W.; Thornton, J. M. Influence of proline residues on protein conformation. *J. Mol. Biol.* **1991**, 218, 397-412.
- (33) Fischer, P. M.; Zhelev, N. Z.; Wang, S.; Melville, J. E.; Fåhræus, R.; Lane, D. P. Structure-activity relationship of truncated and substituted analogues of the intracellular delivery vector Penetratin. *J. Pept. Res.* **2000**, 55, 163-172
- (34) Marianayagam, N. J.; Sunde, M.; Matthews, J. M. The power of two: protein dimerization in biology. *Trends Biochem. Sci.* **2004**, 29, 618-625.
- (35) Porter, C. J.; Wilce, M. C.; Mackay, J. P.; Leedman, P.; Wilce, J. A. Grb7-SH2 domain dimerization is affected by a single point mutation. *Eur. Biophys. J.* **2005**, 34, 454-460.
- (36) Pero, S. C.; Daly, R. J.; Krag, D. N. Grb7-based molecular therapeutics in cancer *Expert. Rev. Mol. Med.* **2003**, 5, 1-11

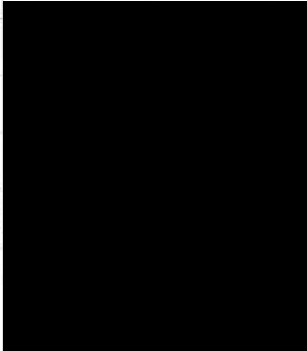
Declaration for Thesis Chapter [5-6-7]

Declaration by candidate

In the case of Chapter [5],[6] and [7] the nature and extent of my contribution to the work was as follows:

Nature of contribution	Contribution (%)	Signature
Conducted virtual screening, ThermoFluor and ITC binding experiment, prepared the receptor protein and contributed towards manuscript preparation	90%	

The following co-authors contributed to the work. Co-authors who are students at Monash University must also indicate the extent of their contribution in percentage terms:

Name	Nature of contribution	Signature
Reece C Lim ¹	Conducted the cell based assay	
Menachem J Gunzburg ¹	Participated in protein expression/purification	
Matthew CJ Wilce ¹	Contributed to data interpretation	
John T Price ¹	Contributed to data interpretation	
Jacqueline A Wilce ¹	Planned and supervised the overall experiments and oversaw the reporting of the results	

¹Department of Biochemistry and Molecular Biology, Monash University, VIC 3800, Australia;

Declaration by co-authors

I hereby certify that:

- (1) the above declaration correctly reflects the nature and extent of the candidate's contribution to this work, and the nature of the contribution of each of the co-authors.
- (2) they meet the criteria for authorship in that they have participated in the conception, execution, or interpretation, of at least that part of the publication in their field of expertise;
- (3) they take public responsibility for their part of the publication, except for the responsible author who accepts overall responsibility for the publication;
- (4) there are no other authors of the publication according to these criteria;
- (5) potential conflicts of interest have been disclosed to (a) granting bodies, (b) the editor or publisher of journals or other publications, and (c) the head of the responsible academic unit; and
- (6) the original data are stored at the above location(s) and will be held for at least five years from the date indicated below:

Chapter 5

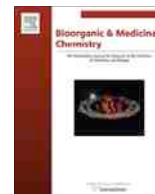
Benzopyrazine derivatives: a novel class of Growth factor receptor bound protein 7 antagonists

This chapter reports the virtual and experimental screening strategies pursued to design small molecular antagonists of Grb7 protein. Starting from a known tripeptide antagonist, computational tools ranging from shape based similarity searches, conformational analysis, molecular docking to 2D-similarity searches were effected to identify and optimize benzopyrazine based antitumor candidates. Detailed binding characterization by ThermoFluor based thermal denaturation and isothermal titration calorimetry was made to discover a novel class of Grb7 antagonists possessing low molecular affinity is reported.



Contents lists available at ScienceDirect

Bioorganic & Medicinal Chemistry

journal homepage: www.elsevier.com/locate/bmc

Benzopyrazine derivatives: A novel class of growth factor receptor bound protein 7 antagonists

Nigus D. Ambaye, Menachem J. Gunzburg, Reece C. C. Lim, John T. Price, Matthew C. J. Wilce[†],
Jacqueline A. Wilce^{*,†}

Department of Biochemistry and Molecular Biology, Monash University, Wellington Road, Victoria 3800, Australia

ARTICLE INFO

Article history:

Received 30 July 2010

Revised 8 October 2010

Accepted 12 October 2010

Available online xxx

Keywords:

Grb7

Adapter protein

SH2 domain

Benzopyrazines

Cancer cells

Similarity search

Virtual screening

ITC

Thermofluor

Melting point shift assay

Cellular growth assay

ABSTRACT

Growth factor receptor bound protein 7 (Grb7) is an adapter protein that functions as a downstream effector of growth factor mediated signal transduction. Over-expression of Grb7 has been implicated in a variety of cancers such as breast, blood, pancreatic, esophageal, and gastric carcinomas. Inhibition of Grb7 has been shown to reduce the migratory and proliferative potential of these cancers, making it an attractive therapeutic target. Starting with a known peptide antagonist, the present work reports the application of a succession of computational ligand design tools comprising a ligand shape based similarity search, molecular docking and a 2D-similarity search to identify small molecular antagonists of the Grb7-SH2 domain from the NCI chemical database. Binding to the Grb7-SH2 domain was then experimentally tested using melting point shift assays and isothermal titration calorimetry. Overall, a total of 11 benzopyrazine based small molecular antagonists were identified with affinity for the Grb7-SH2 domain. Representative compounds tested using ITC were revealed to possess moderate binding affinity in the low micromolar range. Finally, the lead compound (NSC642056) was found to reduce the growth of a Grb7-expressing breast cancer cell line with an IC_{50} of 86 μ M. It is expected that the identified antagonists will be useful additions to further explore the function of Grb7 and for the development of inhibitors with therapeutic potential.

© 2010 Published by Elsevier Ltd.

1. Introduction

Growth factor Receptor Bound protein 7 (Grb7) is an adapter protein that mediates signals from tyrosine kinases to effect downstream events.¹ Grb7 is of great interest as a therapeutic target in cancers in which it is aberrantly overexpressed with HER2 and impacts on cell proliferation and migration.² Grb7 co-overexpression has been implicated in a variety of human cancers such as breast,³ blood,⁴ pancreatic,⁵ esophageal⁶ and gastric carcinomas.⁷ Moreover, the level of Grb7 over-expression is shown to correlate with severity of Barrett's carcinoma⁸ and lymphocytic leukemia.⁴ In addition to growth factor dependent signaling, Grb7 is also known to associate with focal adhesion kinase⁹ and to be a component of integrin-mediated signal transduction which is an important pathway in cancer cell migration.¹⁰ The importance of Grb7 in cancer has been established by a comparative analysis of the characteristics of Grb7 over-expressing and Grb7 knockout cancer cells.^{11,12} Finally, Grb7 has been demonstrated to be a targetable protein that can be blocked by synthetic agents resulting in a significant reduction of cancer cell viability.⁵ Put together, these investigations

make Grb7 a highly attractive target for the design of anti-cancer agents.

Grb7 is a multi-domain protein composed of a proline rich N-terminal domain, a Ras-associating domain, a plekstrin homology (PH) domain, a C-terminal Src homology 2 (SH2) domain and a BPS domain (between the PH and SH2 domains).^{13,14} Each domain serves a distinct role that contributes to the overall signaling function of Grb7.¹⁵ The physical association of Grb7 with its activated upstream binding partners is predominantly mediated by the C-terminal SH2 domain of Grb7. The SH2 domain bears a cationic pocket that is the binding site of phosphorylated tyrosines. Specific phosphotyrosines are recognized based upon the sequence surrounding the phosphotyrosine residue.¹⁵ The SH2 domain is also found in a number of Grb7-related and other adaptor proteins guiding their specific interactions with upstream binding partners.^{16–18} This step is the most critical event in growth factor dependent Grb7 mediated signal transduction. As such, the SH2 domain forms an essential module for Grb7 mediated oncogenic signaling. Since the Grb7-SH2 domain is readily produced and its crystal structure is available, it provides a clear opportunity for inhibitor development via computational and biochemical studies.¹⁹

Virtual screening has been developed as a powerful tool for the acceleration of drug discovery, specifically in the early part of lead compound design.^{20,21} Ligand based virtual screening, a broad sub-

* Corresponding author. Tel.: + 61 3 9902 9226; fax: +61 3 9902 9500.

E-mail address: jackie.wilce@monash.au (J.A. Wilce).

[†] Co-senior authors.

category of virtual screening, is based on the principle that similar structures produce similar effects.²² Depending on the representation and description of lead structures, several approaches exist that transform such information into a model that can be used to scan compound repositories.^{22,23} Most commonly, chemical similarity measures based on two or three-dimensional structure or molecular shape are employed in ligand based virtual screening efforts^{24,25} as well as in optimization tools such as quantitative structure–activity relationship,^{26,27} molecular docking²⁸ and pharmacophore mapping.^{29,30}

There have been numerous reports of the design and optimization of peptide-derived agents geared towards inhibition of the broad class of growth factor receptor bound adaptor proteins, via their SH2 domains.^{31,32} A variety of tactics ranging from phosphorylation³³ macrocyclization³⁴ conformational restriction³⁵ and use of amino acid surrogates³⁶ have been exploited to optimize the binding affinity of the lead peptides. Indeed, this has remarkably resulted in the development of effective inhibitors³⁷ and contributed to a better understanding of the structural and functional investigations of the SH2 domains. More specifically, Pero et al. have utilized a phage display techniques to discover an 11-residue non-phosphorylated polypeptide (termed G7-18NATE) antagonist of Grb7.^{5,38} This peptide does not possess a rigid structure in solution but interacts with the Grb7-SH2 domain with micromolar affinity in a predicted turn-structure at the phosphotyrosine binding site.^{19,39} Cell-permeable forms of this peptide have been shown to maintain their binding to Grb7-SH2 and to have anti-proliferative and anti-migratory activity in cancer cell lines.^{5,40,41} Together this demonstrates the potential for non-phosphorylated compounds to bind to the Grb7-SH2 domain and to possess anti-cancer activity. Experiments conducted in vitro on G7-18NATE and other phosphorylated peptides demonstrate the potential for peptides to be modified to enhance their affinity for Grb7-SH2.^{42,43} However, almost all the identified antagonists to date belong to a single chemical class, that is, peptides, and thus are subject to issues inherent to peptidic structures such as bioavailability, permeability and stability that remain a stumbling block for the application of these molecules in vivo. Most presumably due to these bottlenecks, to date there has not been a single peptide that has progressed to the development of a useful therapeutic agent targeting Grb7 and related growth factor binding proteins, despite extensive efforts.³¹ With this in mind, the present work was initiated as a first step in the development of a potent, selective and stable small molecular antagonist of the Grb7 oncoprotein. To the authors' knowledge this is the first time a small molecular antagonist is reported to bind to the Grb7-SH2 domain. This work reports a shape based virtual screening, molecular docking, 2D-similarity search, melting point shift assay and isothermal titration calorimetric study carried out to identify a novel structural class of Grb7 antagonist. We finally report a preliminary functional study carried out with the lead compound that demonstrates its growth inhibitory effects in a breast cancer cell line.

2. Results

2.1. Shape based query using known antagonist of the Grb7-SH2 domain

Given the limited number and lack of structural diversity in the so far reported antagonists of Grb7, a shape based virtual screening was undertaken as a starting point to identify a novel lead. Structural studies of SH2 domains in complex with peptide-based ligands and numerous binding studies of modified peptide ligands have revealed the common features of their interactions.¹⁸ Thus, as a starting point to the filtering of compounds, a shape based

query was generated using a tripeptide (*m*-aminobenzoyl-pY(α -Me)pYN-NH₂) shown previously to be the most potent antagonist of growth factor bound adaptor 2 (Grb2) and Grb7 proteins and also the smallest and simplest of the known antagonists.⁴⁴ As the experimental conformation of the tripeptide in complex with the Grb7-SH2 domain was not available, a conformational search strategy was pursued to establish possible bioactive conformations. To this end, the MacroModel⁴⁵ conformation search⁴⁶ engine in Schrodinger⁴⁷ was employed to generate stable conformers for interrogation.

In order to select the conformer that may represent the optimum shape for the shaped-based query, a test database of known antagonists of Grb7-SH2 with determined comparative experimental affinities⁴³ was prepared using the Maestro interface of Schrodinger.⁴⁷ Since the lowest energy conformer is not necessarily the bioactive conformer,⁴⁶ all of the top five conformers of the query tripeptide were evaluated for their suitability as a shape based query model by considering their ability to rank-order the known antagonists. This assumes that all the known antagonists bind at the same site on the same receptor as the query tripeptide. The program PHASE⁴⁸ was employed to carry out a shape based virtual screening experiment.

Table 1 indicates the shape similarity coefficient obtained using the top five stable conformers of the tripeptide as shape based queries against the mini-database of known Grb7 antagonists. The correlation coefficient obtained between the shape based similarity indices of the antagonists and their pIC₅₀ values depict the strength of the relationship. The best correlation obtained is 0.93, corresponding to conformer 5. Thus, although the differences in the peptide affinities for their target do not span a wide range, which limits the significance of the correlation, conformer 5 was selected as the basis for the shape based query in the subsequent lead identification procedure.

2.2. Virtual screening of the NCI chemical database

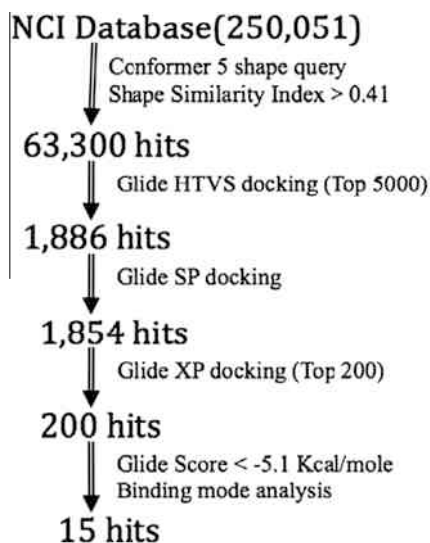
A schematic representation of the virtual screening flowchart used is displayed in Figure 1. The tripeptide conformer 5 was used as a shape based query to screen the National Cancer Institute (NCI) database (which contained 250,251 structures at the time of this work) [<http://dtp.nci.nih.gov/>]. This returned a total of 63,300 hits when the similarity score cut-off was set at 0.41. The top hits from the shape based search were further screened using the Glide based molecular docking protocol.^{49,50} The top 5000 from the search were docked using Glide's high-throughput virtual screening (Glide HTVS) docking routine. This initial crude docking protocol resulted in 1886 successfully docked hits. All of the 1886 hits were subsequently re-docked using the more accurate Glide standard precision (Glide SP) docking procedure. Inspection of the failed structures revealed that the rejects were either simple or polycyclic hydrocarbons that met the shape based criteria. The Glide SP docking experiment resulted in 1854 of the 1886 hits being successfully re-docked. The top 200 from the Glide SP docking were finally docked with the extra precision Glide (Glide XP) docking routine. The molecular docking protocol was the same throughout the computational experiment. Of the 200 hits identified, 15 potential candidates with favorable Glide SP or Glide XP docking scores, and with good predicted surface complementarity and interactions at the target Grb7-SH2 domain surface upon examination, were selected. The compounds identified and their docking scores are shown in Table 2.

2.3. Predicted binding mode of hit NSC642056

An example of a compound selected by the above criterion, a benzopyrazine numbered NSC642056, is shown in its docked

Table 1Shape similarity index of known Grb7 antagonists using the top five conformers of the *m*-aminobenzoyl-pY(α -Me)pYN-NH₂ tripeptide as a query

S. No	Known antagonist	pIC ₅₀ ^a	Shape similarity index ^b				
			Conf. 1	Conf. 2	Conf. 3	Conf. 4	Conf. 5
1	PEpYVNQ-NH ₂	5.96	0.54	0.50	0.48	0.39	0.47
2	Ac-pYVNQ-NH ₂	5.47	0.51	0.46	0.39	0.43	0.35
3	EpYVNQ-NH ₂	5.815	0.51	0.48	0.43	0.45	0.45
4	pYVNQ-NH ₂	5.45	0.45	0.48	0.43	0.41	0.38
Correlation coefficient ^c			0.58	0.62	0.63	0.04	0.93

^a The pIC₅₀ values were obtained from the reported IC₅₀ value⁴³ using the equation pIC₅₀ = -logIC₅₀.^b Conf. 1–5 represent the top five conformers of the query tripeptide used in the virtual screening experiment.^c The correlation coefficient indicates the correlation between the pIC₅₀ value and the shape similarity value for each conformer.**Figure 1.** Schematic representation of the virtual screening experiment conducted based on *m*-aminobenzoyl (α -Me)pY-NH₂ tripeptide as shape based query.

geometry in Figure 2. NSC642056 is predicted to form a number of specific binding interactions with the binding site of the Grb7-SH2 domain. The phenyl ring of the benzoyl moiety is appropriately positioned to make favorable hydrophobic/van der Waals interactions with the side chains of Leu481 and Tyr480 within the binding site. A potential hydrophobic/van der Waals bond with the side chains of Val468 and His479 is also apparent with the aromatic system of the hit. In addition, the hit also forms multiple hydrogen

bonding interactions with the Grb7-SH2 domain binding site. The carbonyl adjacent to the ester moiety is observed to make two hydrogen bonding interactions with the guanidine group of Arg458. Moreover two other hydrogen bonding contact pairs occur between each of the di-oxo moieties on the anilino benzene carboxamide with the backbone NHs of Arg462 and Asn461 residues. Finally the carboxamide amino moiety is involved in a hydrogen bonding interactions with the Gln463 of Grb7-SH2 binding site.

2.4. Experimental pre-screening with melting point shift assay

Out of the top 15 potential hits, five were available at the time of this work and kindly provided by the NCI Developmental and Therapeutic program unit of the USA (Drug synthesis and Chemistry branch, <http://dtp.nci.nih.gov/>) (indicated in Table 2). These were subjected to in vitro binding studies, as supplied by the NCI without further characterization. Experimental pre-screening of these compounds was carried out using a ThermoFluor based thermal shift assay.^{52,53} This assay is based upon the increased melting temperature of a protein induced by ligand binding. The compounds were dissolved in 1% DMSO/buffer solution and their effect on the melting temperature of the Grb7-SH2 domain was determined. One of out of the five tested compounds, NSC642056, produced a positive melting point shift (Table 3). Interestingly, the finding that hit NSC642056 interacts with the Grb7-SH2 domain correlates with its better shape based similarity coefficient and glide docking score relative to those of the four structures that turned out to be false hits. Indeed, NSC642056 occurs in the top 5 of the priority list while the negative hits were in the bottom 5 of the 15 hits suggested from the combined virtual screening experiment. The change in melting point produced by the hit

Table 2

Final hits identified based on the tripeptide based shape search

Rank	Hit ID.	Shape similarity index	Glide SP docking		Glide XP docking	
			Glide score	Emodel	Glide score	Emodel
1	NSC677186	0.433	-6.348	-79.584	-5.130	-95.586
2	NSC677177	0.463	-6.337	-84.217	-4.790	-62.836
3	NSC677184	0.429	-5.883	-73.463	-4.190	-89.924
4	NSC633047	0.480	-5.792	-68.058	-3.420	-79.200
5	NSC642056*	0.457	-5.749	-71.077	-4.900	-81.612
6	NSC677147	0.437	-5.716	-69.901	-3.200	-77.713
7	NSC677176	0.427	-5.484	-72.001	-3.310	-80.790
8	NSC713163	0.413	-5.368	-44.324	-3.760	-45.198
9	NSC677174	0.427	-5.318	-63.131	-3.560	-74.519
10	NSC100787	0.428	-5.277	-63.580	-4.550	-84.740
11	NSC129843*	0.435	-5.264	-75.089	-3.780	-83.889
12	NSC642057*	0.436	-5.256	-67.214	-3.540	-76.789
13	NSC344032	0.441	-5.252	-64.706	-3.220	-77.365
14	NSC687783*	0.426	-5.241	-65.861	-3.750	-68.422
15	NSC657678*	0.458	-5.223	-61.619	-3.870	-74.176

* Indicates hits that are tested experimentally.

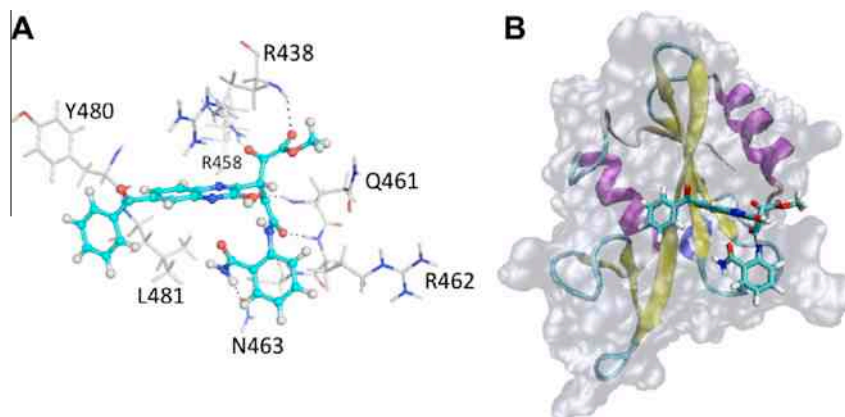


Figure 2. Binding mode of lead NSC642056. (A) The specific interaction between the ligand and Grb7-SH2 domain. The ligand is displayed in ball and stick format while binding site residues are shown in line format. The yellow dotted lines represent hydrogen bonds between the hit and Grb7 binding site; the figure was produced in Maestro of Schrodinger suite. (B) The overall fold of Grb7-SH2 domain depicting its surface, secondary structural elements and the relative positioning of the lead compound. The figure was produced by virtual molecular dynamics (VMD) visualization program.⁵¹

Table 3
Tanimotto similarity coefficient and melting point shift data for benzopyrazine derivatives

S. No.	Hit code	Tanimotto similarity coefficient (%)	ΔT_m^a (°C)	
			100 μ M	200 μ M
1	NSC642040	97	0.45	0.95
2	NSC648605	98	0.05	0.55
3	NSC644743	92	0.95	0.95
4	NSC648607	97	0.45	1.45
5	NSC644745	90	1.30	1.30
6	NSC644750	94	0.45	0.85
7	NSC644770	94	0.45	0.55
8	NSC646820	90	1.20	0.95
9	NSC646823	95	1.00	0.70
10	NSC648589	92	0.90	0.60
A	NSC642056	100	0.60	1.10
B	G7-18NATE	Not applicable	1.35	1.85

^a The change in melting point (ΔT_m) are obtained from duplicate experiments after the melting point of Grb7-SH2 apo ($T_m = 49.0^\circ\text{C}$) was subtracted from that of the hit bound form. NSC642056 was the lead compound while G7-18NATE is the reference polypeptide concurrently run in the melting shift assay.

was 0.6°C at $100\ \mu\text{M}$ and 1.1°C at $200\ \mu\text{M}$ which were slightly lower than that produced by a peptide-based (G7-18NATE)³⁸ Grb7-SH2 inhibitor control (1.35°C at $100\ \mu\text{M}$ and 1.85°C at $200\ \mu\text{M}$). Thus, hit NSC642056 was able to effect stabilization comparable to the known G7-18NATE-based polypeptide inhibitor which suggests that the compound may have potential as an antagonist of Grb7.

2.5. Lead discovery using 2D-similarity searches and binding studies

In an effort to discover further compounds with affinity for Grb7-SH2, structures related to NSC642056 were sought. To this end, analogues of the hit were screened using a two-dimensional (2D) structure based similarity search.²³ The 2D-search was undertaken against the same NCI database using the SMILES⁵⁴ description of the lead structure as an input. The use of the lead NSC642056 as a 2D-query returned 22 benzopyrazine hits of which 15 were available at the time of this work from the NCI developmental and Therapeutic program. The 15 compounds were then assessed using the melting point shift assay as described above. The result, shown in Table 3, revealed that out of the 15 structural analogues tested 10 were able to produce a positive melting point shift. The change in melting point induced by the analogues was

found to be comparable to that of the lead NSC642056 compound (Fig. 3). The structures of the 10 leads identified in addition to the starting structure are shown in Figure 4. The 10 identified compounds were sub-classified into di-substituted benzopyrazines (NSC644743, NSC646820, NSC646823, and NSC648589), tri-substituted benzopyrazines with benzoyl substituent (NSC642040, NSC648607, and NSC648605) and tri-substituted benzopyrazines with a nitro substituent (NSC644750, NSC644770, and NSC644745). Though these are analogues of NSC642056, the virtual screening criteria adopted in the initial shape based search might have prevented these structures from showing up within the top 15 of the shape based hits.

2.6. Confirmation of binding by ITC

Further characterization of these interactions was undertaken using isothermal titration calorimetry (ITC).⁵⁵ ITC measures the amount of heat absorbed or released as one interacting species is titrated into the other. From this, the equilibrium dissociation constant, free energy, enthalpy, entropy and stoichiometry of binding

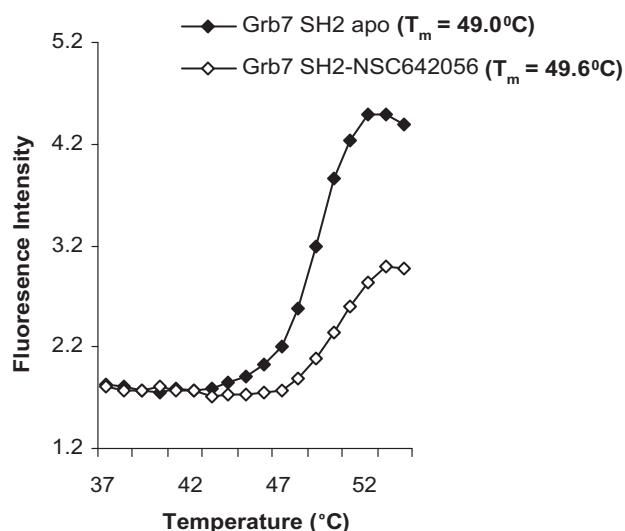


Figure 3. Unfolding curve of Grb7-SH2 domain obtained from thermal melting experiment. The filled square curve corresponds to the apo form of Grb7 ($T_m = 49.0^\circ\text{C}$) while the open square curve represents that of Grb7-NSC642056 complex ($T_m = 49.6^\circ\text{C}$).

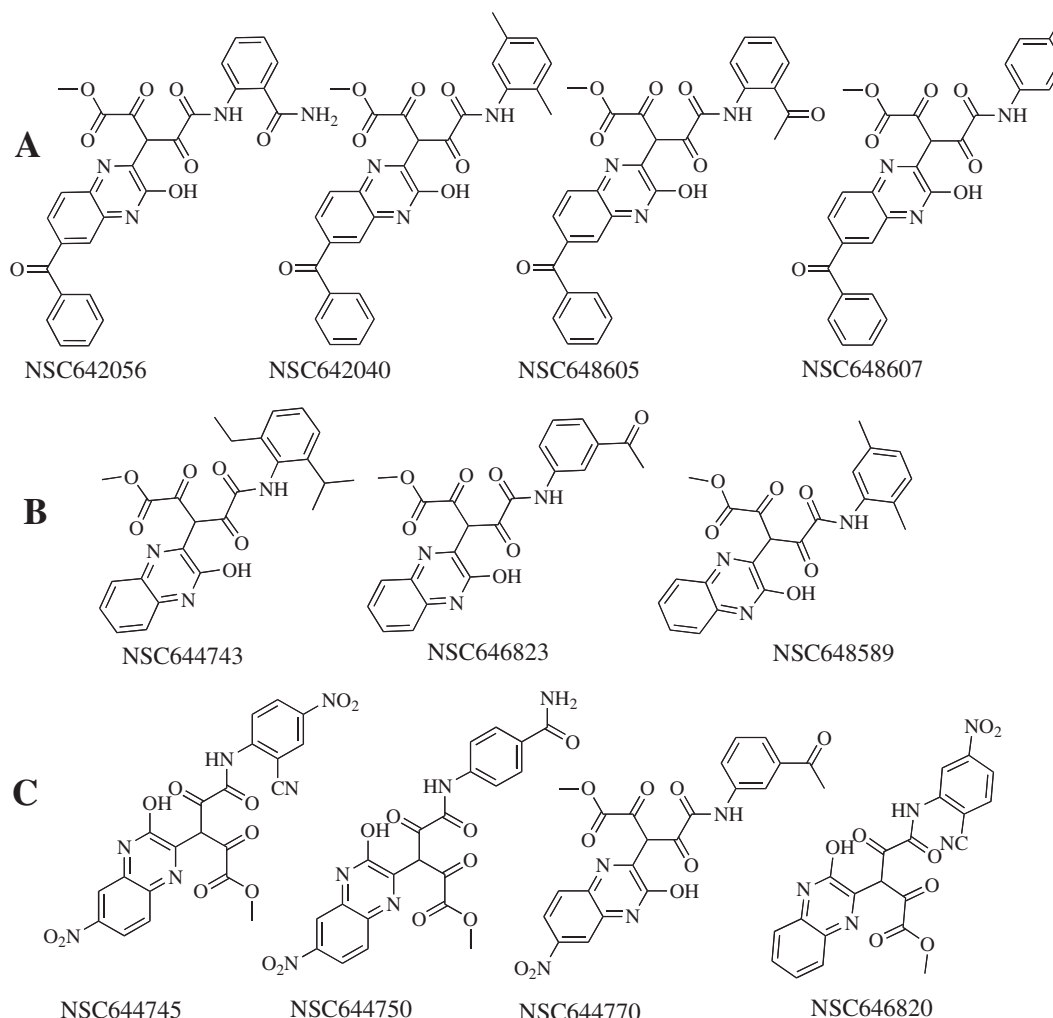


Figure 4. Chemical structures of the benzopyrazine derivatives. (A) Tri-substituted benzopyrazines with benzoyl substituent. (B) Di-substituted benzopyrazine derivatives. (C) Tri-substituted benzopyrazines with a nitro substituent.

can be determined.⁵⁶ The binding of NSC642056 as well as 5 representative compounds from three classes of substituted benzopyrazines, identified by the Grb7-SH2 domain melting point assay, were determined by ITC. As shown in Table 4, the equilibrium dissociation constant for hit NSC642056 was found to be 17.15 μM . This not only confirms the binding but demonstrates that it occurs with a moderate affinity. The binding data shows that the compounds interact with favorable enthalpy and unfavorable entropy with a 1:1 binding stoichiometry. In a similar vein, the analogue structures (representative structures from each subclass—NSC642040, NSC644745, NSC644743, NSC646823, and NSC648607)—were subjected to the ITC binding assay. Figure 5 shows the ITC binding isotherm for one of the analogues tested.

Each of the compounds characteristically bound with evolution of heat, that is, through exothermic binding similar to the lead NSC642056 (Table 4). The experimental affinities were found to be of moderate values ranging from $K_d = 3.06 \mu\text{M}$ for NSC646807 to $K_d = 17.15 \mu\text{M}$ for NSC642056 lead. Though the free energy of binding is in a very close range (ca. -7 kcal/mol), deconvolution into its constituents reveals subtle differences in the entropic and enthalpic contributions to binding. In the case of NSC648607 and NSC644743, the enthalpic contribution to binding is greater than the entropic part. However, for leads NSC644745 and NSC646823 the enthalpic/entropic ratio is reversed. The fact that the gross binding affinities remained virtually unaffected despite the differences in the relative contribution of the constituent parts suggests

Table 4
Thermodynamic binding parameters for the benzopyrazine derivatives

Lead	NSC642040	NSC644745	NSC646823	NSC644743	NSC646807	NSC642056
Stoichiometry	1.11 \pm 0.03	1.14 \pm 0.03	1.04 \pm 0.11	1.06 \pm 0.03	1.04 \pm 0.02	1.09 \pm 0.04
K_b (10^5 M^{-1})	2.06 \pm 0.42	1.58 \pm 0.35	1.41 \pm 0.10	1.85 \pm 0.46	3.48 \pm 0.87	0.60 \pm 0.10
ΔH (Kcal/mol)	-2.94 ± 0.11	-1.33 ± 0.05	-0.74 ± 0.09	-6.11 ± 0.32	-5.54 ± 0.19	-10.23 ± 0.51
ΔS (cal/mol/K)	14.35	19.3	21.1	3.61	6.89	-12.5
$T\Delta S$ (Kcal/mol)	4.28	5.75	6.29	1.08	2.05	-3.73
ΔG (Kcal/mol)	-7.21 ± 0.11	-7.08 ± 0.05	-7.03 ± 0.09	-7.19 ± 0.32	-7.56 ± 0.19	-6.50 ± 0.51
K_d (μM)	5.06 \pm 1.03	6.57 \pm 1.20	7.12 \pm 0.50	5.76 \pm 1.40	3.06 \pm 0.77	17.15 \pm 2.97

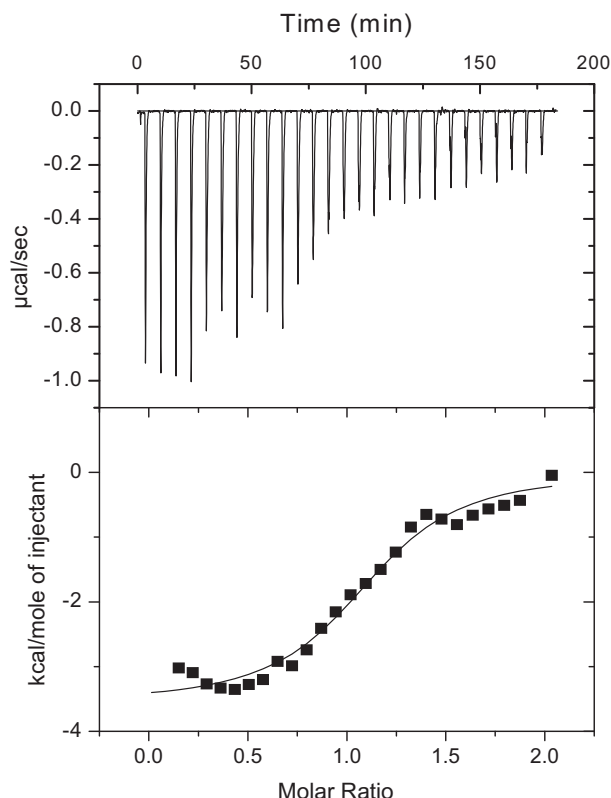


Figure 5. ITC thermogram of a benzopyrazine derivative, NSC642040. The upper panel show raw data obtained from 10 μ l injections of compound at 25 $^{\circ}$ C. The lower panel display plots of integrated total energy exchanged (as kcal/mol of injected compound) as a function of molar ratio of the compound to the Grb7-SH2 domain (squares). Solid lines indicate the fit to a single-site saturation model.

that entropy–enthalpy compensation phenomenon taking place. This is commonly observed in ligand–receptor binding studies.⁵⁷

2.7. Cellular growth inhibitory assay

Finally, a cellular growth assay was conducted using the MDA-MB-468 breast cancer cell line to determine whether the lead compound would display activity in an in vivo system. To this effect, the impact of compound NSC642056 on these Grb7-expressing cancer cells was investigated. The result, as shown in Figure 6, shows that the lead compound impacts on the growth of the cells in a concentration dependent manner. The in vivo IC_{50} determined for the cell growth inhibition is found to be 86.0 μ M. This is compared to the in vitro K_d of 17.3 μ M, and thus suggests a correlation between the inhibitor binding affinity for the Grb7 target and the concentration required for cell growth inhibition. Future investigations, using both cells in which Grb7 is knocked out using RNAi and knocked back in, will allow us to identify the extent to which the inhibitor action is indeed occurring through binding and inhibition of Grb7.

3. Discussion

Few antagonists of Grb7 have previously been identified. Those reported include the polypeptide G7-18NATE^{5,38,39} identified through phage display and found to be selective for Grb7 with minimal activity against related proteins. Other short peptides are also reported to bind to the Grb7-SH2 domain in vitro.⁴³ Being peptidic in nature, however, the potential for their in vivo use is restricted until major issues such as the limited bioavailability, in vivo insta-

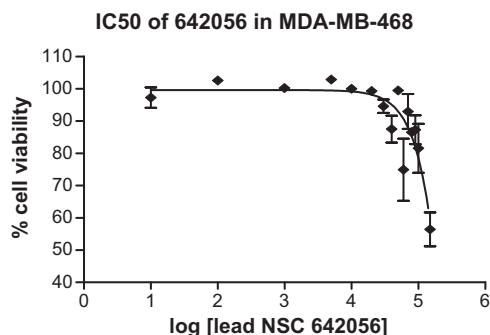


Figure 6. Cellular growth inhibition curve obtained for MDA-MB-468 breast cancer cells treated with the lead NSC642056. The IC_{50} was found to be 86 μ M.

bility, cell impermeability and high synthetic costs of peptides are resolved.⁵⁸ Here we identify compounds of the benzopyrazine class that have an equivalent affinity for the Grb7-SH2 domain as the previously reported peptides (i.e., moderate to low micromolar binding affinity), and suggest that these may offer an alternative scaffold for the development of potent inhibitors of Grb7. Similarly to the in vivo activity of the peptide-based Grb7 inhibitor, G7-18NATE, inhibition of the growth of cancer cells is observed.⁴⁰ Future experiments will be required to demonstrate whether the mode of action is specifically via Grb7 inhibition, or also/alternatively through other pathways. The current studies do not establish whether these compounds possess intrinsic specificity for the Grb7-SH2 domain. Being predicted to bind to the peptide recognition surface of the Grb7-SH2 domain, however, we propose that they would be amenable to modification to improve their affinity, pharmacological properties and potentially to confer specificity for Grb7. The compounds would not be the target of proteases, which is a major obstacle for the use of peptides as drugs, and their relatively smaller size is predicted to improve their bioavailability to their intracellular target.

Benzopyrazines from the NCI database were identified in the current study owing to their ability to adopt a structurally similar shape to a known peptide-based inhibitor of the Grb7-SH2 domain. The present work effectively exploited the molecular similarity principle that shape based similarity can reflect similarity in potential binding interactions.^{59,60} The shape based virtual screening experiment was able to identify moderate affinity lead candidates, as confirmed by a Thermofluor binding assay. The identification of a substituted benzopyrazine (NSC642056) prompted a 2D-similarity search, resulting in the identification of further benzopyrazines with potential for binding to the Grb7-SH2 domain. Binding to the target was confirmed experimentally using both melting point assays and ITC. Overall, the computational experiments attest to the usefulness of the application of a succession of virtual screening tools in lead compound identification.

The Thermofluor binding assay proved an effective experimental method to confirm ligand binding. It is a rapid and inexpensive assay that does not utilize very much material. Thermofluor exploits the concept of protein stabilization upon ligand binding. Only a one degree change in the melting temperature of the protein was observed upon interaction with the lead compounds. This relatively low value is typical for ligands binding with micromolar affinity and may represent the limit of detection of the method.^{54,55,61} Similar thermal shift values were measured for a known peptide inhibitor of the Grb7-SH2 domain that binds with micromolar affinity. ITC was used to confirm the interactions, measure the affinity and also provided insight into the entropic versus enthalpic contributions to binding. Though the identified benzo-

pyrazines bound with only micromolar binding these small molecule antagonists could be useful for the experimental and clinical investigations of Grb7 and related proteins.

In conclusion, starting with a known peptide antagonist, the present work reported the successful application of a succession of computational ligand design tools comprising ligand shape based similarity search, molecular docking and 2D-similarity search to identify a novel class of small molecular antagonists of Grb7. Experimental binding studies with a melting point shift assay and ITC confirmed the interactions and shed some light on the thermodynamic aspects of the binding interactions. That the lead NSC642056 antagonist reduced the growth of breast cancer cells was confirmed in the MDA-MB-435 cell line. Further work will be required to determine whether the mode of action is, indeed, via Grb7 inhibition. It is expected that the newly identified benzopyrazine scaffolds will be useful additional agents to further explore and accelerate functional studies of Grb7 and potentially lead to the development of novel therapeutics.

4. Experimental section

4.1. Generation of the shape based query

MacroModel's⁴⁵ conformation search⁴⁶ engine in Schrodinger⁴⁷ was employed to generate stable conformers of the *m*-aminobenzoyl-pY(α -Me)pYN-NH₂ peptide, previously shown to be a potent inhibitor of the Grb7-SH2 domain.⁴³ The optimal potential for liquid simulation force field with a distance dependent dielectric constant was used during the conformation search. Partial charges were computed using the force field. Geometry optimization was effected with maximum iteration of 5000 and a gradient convergent criterion was applied with a threshold of 0.05. The systematic torsional sampling option was employed to generate representative conformations of the tripeptide reference query. Unless specifically mentioned, all other conformation search parameters were kept at their default value.

4.2. Shape based similarity virtual screening

The program PHASE⁴⁸ was employed to carry out shape based virtual screening experiments. The atom type used for volume scoring was set to none so as not to bias the search towards a particular hit class particularly for the subsequent database screening. The conformer that produced the best correlation between the shape based similarity index and the biological activities of the peptides in the mini-database was then employed to serve as a query to search the enhanced National Cancer Institute (NCI) database. The average similarity index of the known antagonist was then used as a cut-off during the NCI screening.

4.3. Molecular docking

The program Glide was used to perform Grb7-SH2 domain docking studies for top hits from the shape based search. Glide comprises three docking routines that are designed to suit different stages of chemical database screening.^{49,50} The PDB file for the Grb7-SH2 domain was read into Maestro in Schrodinger and the protein preparation wizard used to set up the protein including addition of hydrogen atoms and deletion of water molecules beyond 5 Å from protein atoms. Hydrogen bond assignment was effected with the exhaustive sampling option and the system was subsequently relaxed with geometry minimization. A grid of size 12 × 12 × 12 Å was defined using the peptide binding surface about the phosphotyrosine pocket to define the binding site. All the other docking parameters were kept at their default values.

4.4. Expression and purification of Grb7-SH2 domain

The SH2 domain of Grb7 was used as a receptor for the thermal shift and ITC binding experiments. The pGex2T plasmid containing the Grb7-SH2 insert encoding residues 415–532 of human Grb7 protein was expressed in *Escherichia coli* expression system as a GST fusion protein in BL21(DE3)pLysS host strains.^{62,63} Cell induction was achieved with 400 μ M isopropyl β -D-1-thiogalactopyranoside. Cell resuspension was carried out in ice-cold phosphate buffer saline with 2 mM EDTA, 0.5% Triton-X 100 and lysis by sonication. The fusion protein was purified by glutathione affinity chromatography (GE Healthcare) and cleaved with thrombin. Purification using cation exchange chromatography was then effected using a HiTrap SP column (GE) after an overnight dialysis into 20 mM HEPES pH 7.4, 20% glycerol, and 1 mM DTT at 4 °C. This was followed by dialysis into 50 mM MES pH 6.6, 100 mM NaCl, and 1 mM DTT and final purification by size exclusion chromatography using a Sephadex 75 XK 16/60 column (GE). Grb7-SH2 domain was concentrated and stored at 4 °C. Its purity was verified using SDS-PAGE. The final concentration was determined with UV-vis spectroscopy.⁶⁴

4.5. ThermoFluor based melting point shift assay

The thermoFluor based melting point shift assay relies on an increase in melting point of the target protein as an indication of compound binding.^{52,53} The dye Sypro Orange is used to detect the melting transitions through its binding to exposed hydrophobic regions of the unfolding protein. The melting point of the Grb7-SH2 domain was determined with the use of Quiagen's quantitative RT-PCR instrument (www.qiagen.com). The wavelength of excitation/emission was set to 470/555 and 470/610 nm. A heating rate of at 1 °C per min was programmed over a 30–80 °C temperature range with a holding time of 60 s. The buffer used was 50 mM MES, 100 mM NaCl, pH 6.6, 1 mM dithiothreitol (DTT). The purified Grb7-SH2 domain was added to each tube to yield a final concentration of 20 μ M. The protein concentration was established using UV-vis spectrophotometer at 280 nm and a molar extinction coefficient of 8480 M⁻¹ cm⁻¹. All the compounds were dissolved in 1% DMSO/buffer solution and a final concentration of 100 μ M and 200 μ M was added to the protein. After mixing, 25 μ l of the protein/hit solution was transferred to the PCR tubes for the melting experiment. A known peptide inhibitor³⁸ was also tested as a positive control. Each denaturation experiment was conducted in duplicate and in each case the average melting temperature was taken for analysis. The Rotor-Gene 3000 software was used to set up the experiment and analyze the results.

4.6. Isothermal titration calorimetry

ITC binding experiments were performed on a VP-ITC Microcalorimeter (Microcal, Northampton, MA, USA) at 25 °C.^{55,56} The Grb7-SH2 domain was dialyzed against 2 L of 50 mM NaOOCCH₃ (pH 6.6), 100 mM NaCl, and 1 mM DTT. The concentration of Grb7-SH2 and hits was determined as described in the melting experiment. The hit and protein solutions were degassed and thermostated at 20 °C for 5 min using the ThermoVac of the VP-ITC Microcalorimeter. The reference power of the experiment was set to 20 μ Cal/s and the cell contents were stirred continuously at 307 rpm throughout the titrations. The feedback mode gain was set to high with fast and auto equilibrations options applied. The reference cell was filled with MQ water. The hits at concentrations in the range of 500–950 μ M were titrated into Grb7-SH2 solutions of 50–85 μ M concentrations in 7–10 μ l injections with a 3–6 min delay between each injection. A binding isotherm was generated by plotting the heat change evolved per injection against the molar

ratio of the leads to Grb7-SH2 domain receptor. A blank determination in which the compounds were titrated against the buffer was then subtracted from the binding data. The corrected data was then fitted by a single binding site model using a non-linear least squares with the Origin (Microcal Software, Northampton, MA, USA).

4.7. Lead optimization by 2D-similarity search

Two-dimensional structure based similarity^{22,23} searches of the National Cancer Institute database (<http://dtp.nci.nih.gov/>) were conducted using the SMILES⁵³ description of chemical structure using the lead NSC642056 as input. The SMILES string was generated using the enhanced NCI database browser platform. The maximum number of hits was set to 1000. Hits with Tanimotto similarity coefficients above 90% were obtained for further subsequent experimental investigation.

4.8. Cellular growth inhibitory studies

To determine the effects of the compounds on cellular growth, MDA-MB-468 breast cancer cells were resuspended at 5×10^4 cells/mL and 100 μ L of this cell suspension was plated in 96 well plates (BD Biosciences, California, USA). The following day cells were treated with a range of concentration of the compounds, each concentration with triplicates wells. Cells were incubated under standard growth conditions with 10% fetal bovine serum over a 4-day period (0–4 days). Adherent cell cultures were fixed in situ after 4 days by the addition of 25 μ L of cold 50% trichloroacetic acid solution (Sigma–Aldrich, Missouri, USA) and incubated for 60 min at 4 °C. The supernatant was then discarded and the plate was washed five times with running distilled water before being dried overnight. Fixed cells were stained by the addition of 100 μ L of sulforhodamine B (SRB) sodium salt solution (0.4% (w/v) in 1% acetic acid; Sigma–Aldrich, Missouri, USA) and incubated for 10 min at room temperature. Unbound SRB solution was removed by washing five times with 1% acetic acid after which the plates were air-dried overnight. The following day, the bound stain was solubilized with 100 μ L of 10 mM Tris buffer (pH 10.5) and the absorbance of the eluted dye was read on the spectrophotometric BMG PolarStar Optima plate reader (BMG Labtech, Offenburg, Germany) at 540 nm. SRB is a total protein stain, which directly correlates with cell number and is used routinely to measure cell growth rate. The Nonlinear regression analysis of the concentration–response plot was conducted using GraphPad Prism software.

Acknowledgments

This work was funded by an Australian Research Council Project Grant awarded to J.A.W. and D.N.K. and a Monash University Graduate Scholarship awarded to N.D.A. M.C.J.W. and J.T.P. are the recipients of a Senior Research Fellowship and a R.D. Wright Fellowship respectively from the National Health and Medical Research Council of Australia. We thank the Drug Synthesis and Chemistry Branch of National Cancer Institute of the USA for providing the compounds used in the screening and testing. The Victorian partnership for advanced computing (VPAC) is acknowledged for granting us access to the computational facility employed in the study.

References and notes

- Shen, T. L.; Guan, J. L. *Front Biosci.* **2004**, 9, 192.
- Nencioni, A.; Cea, M.; Garuti, A.; Passalacqua, M.; Raffaghello, L.; Soncini, D.; Moran, E.; Zoppoli, G.; Pistoia, V.; Patrone, F.; Ballestrero, A. *PLoS One* **2010**, 5, e9024.
- Stein, D.; Wu, J.; Fuqua, S. A.; Roonprapunt, C.; Yajnik, V.; D'Eustachio, P.; Moskow, J. J.; Buchberg, A. M.; Osborne, C. K.; Margolis, B. *EMBO J.* **1994**, 13, 1331.
- Haran, M.; Chebatco, S.; Flaishon, L.; Lantner, F.; Harpaz, N.; Valinsky, L.; Berrebi, A.; Shachar, I. *Leukemia* **2004**, 18, 1948.
- Tanaka, S.; Pero, S. C.; Taguchi, K.; Shimada, M.; Mori, M.; Krag, D. N.; Arii, S. *J. Natl. Cancer Inst.* **2006**, 98, 491.
- Tanaka, S.; Mori, M.; Akiyoshi, T.; Tanaka, Y.; Mafune, K.; Wands, J. R.; Sugimachi, K. *Cancer Res.* **1997**, 57, 28.
- Kishi, T.; Sasaki, H.; Akiyama, N.; Ishizuka, T.; Sakamoto, H.; Aizawa, S.; Sugimura, T.; Terada, M. *Biochem. Biophys. Res. Commun.* **1997**, 232, 5.
- Walch, A.; Specht, K.; Braselmann, H.; Stein, H.; Siewert, J. R.; Hopt, U.; Höfler, H.; Werner, M. *Int. J. Cancer* **2004**, 112, 747.
- Han, D. C.; Shen, T. L.; Guan, J. L. *J. Biol. Chem.* **2000**, 275, 28911.
- Shen, T. L.; Guan, J. L. *FEBS Lett.* **2001**, 499, 176.
- Itoh, S.; Taketomi, A.; Tanaka, S.; Harimoto, N.; Yamashita, Y.; Aishima, S.; Maeda, T.; Shirabe, K.; Shimada, M.; Maehara, Y. *Mol. Cancer Res.* **2007**, 5, 667.
- Bai, T.; Luoh, S. W. *Carcinogenesis* **2008**, 29, 473.
- Margolis, B. *Prog. Biophys. Mol. Biol.* **1994**, 62, 223.
- Han, D. C.; Shen, T. L.; Guan, J. L. *Oncogene* **2001**, 20, 6315.
- Holt, L. J.; Daly, R. J. *Growth Factors* **2005**, 23, 193.
- Pero, S. C.; Daly, R. J.; Krag, D. N. *Expert. Rev. Mol. Med.* **2003**, 10, 1.
- Bradshaw, J. M.; Waksman, G. *Adv. Protein Chem.* **2002**, 61, 161.
- Pawson, T. *Adv. Cancer Res.* **1994**, 64, 87.
- Porter, C. J.; Matthews, J. M.; Mackay, J. P.; Pursglove, S. E.; Schmidberger, J. W.; Leedman, P. J.; Pero, S. C.; Krag, D. N.; Wilce, M. C.; Wilce, J. A. *BMC Struct. Biol.* **2007**, 7, 58.
- Bleicher, K. H.; Bohm, H. J.; Muller, K.; Alanine, A. I. *Nat. Rev. Drug Disc.* **2003**, 2, 369.
- Oprea, T. I.; Matter, H. *Curr. Opin. Chem. Biol.* **2004**, 8, 349.
- Martin, Y. C.; Kofron, J. L.; Traphagen, L. M. *J. Med. Chem.* **2002**, 45, 4350.
- Nikolova, N.; Jaworska, J. *QSAR Comb. Sci.* **2004**, 22, 1006.
- Ebalunode, J. O.; Ouyang, Z.; Liang, J.; Zheng, W. *J. Chem. Inf. Model.* **2008**, 48, 889.
- Putta, S.; Lemmen, C.; Beroza, P.; Greene, J. J. *Chem. Inf. Comput. Sci.* **2002**, 42, 1230.
- Cramer, R. D., III; Patterson, D. E.; Bunce, J. D. *J. Am. Chem. Soc.* **1988**, 110, 5959.
- Verli, H.; Albuquerque, M. G.; Bicca de Alencastro, R.; Barreiro, E. J. *Eur. J. Med. Chem.* **2002**, 37, 219.
- Goldman, B. B.; Wipke, W. T. *Proteins* **2000**, 38, 79.
- Ebalunode, J. O.; Dong, X.; Ouyang, Z.; Liang, J.; Eckenhoff, R. G.; Zheng, W. *Bioorg. Med. Chem.* **2009**, 17, 5133.
- Masek, B. B.; Merchant, A.; Matthew, J. B. *J. Med. Chem.* **1993**, 36, 1230.
- Burke, T. R. *Int. J. Pept. Res. Ther.* **2006**, 12, 33.
- Fretz, H.; Furet, P.; Garcia-Echeverria, C.; Schoepfer, J.; Rahuel, J. *Curr. Pharm. Des.* **2000**, 6, 1777.
- Liu, W. Q.; Vidal, M.; Olszowy, C.; Million, E.; Lenoir, C.; Dhôtel, H.; Garbay, C. J. *Med. Chem.* **2004**, 47, 1223.
- Shi, Z. D.; Wei, C. Q.; Lee, K.; Liu, H.; Zhang, M.; Araki, T.; Roberts, L. R.; Worthy, K. M.; Fisher, R. J.; Neel, B. G.; Kelley, J. A.; Yang, D.; Burke, T. R., Jr. *J. Med. Chem.* **2004**, 47, 2166.
- Oishi, S.; Karki, R. G.; Kang, S. U.; Wang, X.; Worthy, K. M.; Bindu, L. K.; Nicklaus, M. C.; Fisher, R. J.; Burke, T. R., Jr. *J. Med. Chem.* **2005**, 48, 764.
- Kang, S. U.; Choi, W. J.; Oishi, S.; Lee, K.; Karki, R. G.; Worthy, K. M.; Bindu, L. K.; Nicklaus, M. C.; Fisher, R. J.; Burke, T. R., Jr. *J. Med. Chem.* **2007**, 50, 1978.
- García-Echeverria, C. *Curr. Med. Chem.* **2001**, 8, 1589.
- Pero, S. C.; Oligino, L.; Daly, R. J.; Soden, A. L.; Liu, C.; Roller, P. P.; Li, P.; Krag, D. N. *J. Biol. Chem.* **2002**, 277, 11918.
- Porter, C. J.; Wilce, J. A. *Biopolymers* **2007**, 88, 174.
- Pero, S. C.; Shukla, G. S.; Cookson, M. M.; Flemer, S., Jr.; Krag, D. N. *Br. J. Cancer* **2007**, 96, 1520.
- Ambaye, N. D.; Lim, R. C.; Clayton, D. J.; Gunzburg, M. J.; Price, J. T.; Pero, S. C.; Krag, D. N.; Wilce, M. C.; Aguilar, M. I.; Perlmutter, P.; Wilce, J. A. *Biopolymers* **2010**. doi:10.1002/bip.21403.
- Spuches, A. M.; Argiros, H. J.; Lee, K. H.; Haas, L. L.; Pero, S. C.; Krag, D. N.; Roller, P. P.; Wilcox, D. E.; Lyons, B. A. *J. Mol. Recognit.* **2007**, 20, 245.
- Luzy, J. P.; Chen, H.; Gril, B.; Liu, W. Q.; Vidal, M.; Perdureau, D.; Burnol, A. F.; Garbay, C. J. *Biomol. Screen.* **2008**, 13, 112.
- Liu, W. Q.; Vidal, M.; Gresh, N.; Roques, B. P.; Garbay, C. J. *Med. Chem.* **1999**, 42, 3737.
- Mohamadi, F.; Richard, N. G. J.; Guida, W. C.; Liskamp, R.; Lipton, M.; Caufield, C.; Chang, G.; Hendrickson, T.; Still, W. C. *J. Comput. Chem.* **1990**, 11, 440.
- Leach, A. R. In *Reviews in Computational Chemistry*; Lipkowitz, K. B., Boyd, D. B., Eds.; Wiley-VCH, Inc., 1991; Vol. 2, pp 1–55.
- Schrodinger LLC, 120 West 45th Street, New York, New York.
- Dixon, S. L.; Smodyrev, A. M.; Rao, S. N. *Chem. Biol. Drug Des.* **2006**, 67, 370.
- Friesner, R. A.; Murphy, R. B.; Repasky, M. P.; Frye, L. L.; Greenwood, J. R.; Halgren, T. A.; Sanschagrin, P. C.; Mainz, D. T. *J. Med. Chem.* **2006**, 49, 6177.
- Friesner, R. A.; Banks, J. L.; Murphy, R. B.; Halgren, T. A.; Klicic, J. J.; Mainz, D. T.; Repasky, M. P.; Knoll, E. H.; Shelley, M.; Perry, J. K.; Shaw, D. E.; Francis, P.; Shenkin, P. S. *J. Med. Chem.* **2004**, 47, 1739.
- Humphrey, W.; Dalke, A.; Schulten, K. *J. Mol. Graphics* **1996**, 14, 33.
- Pantoliano, M. W.; Petrella, E. C.; Kwasnoski, J. D.; Lobanov, V. S.; Myslik, J.; Graf, E.; Carver, T.; Asel, E.; Springer, B. A.; Lane, P.; Salemme, F. R. *J. Biomol. Screen.* **2001**, 6, 429.
- Matulis, D.; Kranz, J. K.; Salemme, F. R.; Todd, M. J. *Biochemistry* **2005**, 44, 5258.

54. Weininger, D. J. *Chem. Inf. Comput. Sci.* **1988**, 28, 31.
55. Freyer, M. W.; Lewis, E. A. *Methods Cell Biol.* **2008**, 84, 79.
56. Perozzo, R.; Folkers, G.; Scapozza, L. J. *Recept. Signal Transduct. Res.* **2004**, 24, 1.
57. Eftink, M. R.; Anusiem, A. C.; Biltonen, R. L. *Biochemistry* **1983**, 22, 3884.
58. Danho, W.; Swistok, J.; Khan, W.; Chu, X. J.; Cheung, A.; Fry, D.; Sun, H.; Kurylko, G.; Rumennik, L.; Cefalu, J.; Cefalu, G.; Nunn, P. *Adv. Exp. Med. Biol.* **2009**, 611, 467.
59. Johnson, M. A.; Maggiora, G. M. *Concepts and Applications of Molecular Similarity*; John Wiley & Sons: New York, 1990.
60. Mezey, P. G. *Shape in Chemistry: An Introduction to Molecular Shape and Topology*; VCH: New York, 1993.
61. Cummings, M. D.; Farnum, M. A.; Nelen, M. I. J. *Biomol. Screen.* **2006**, 11, 854.
62. Janes, P. W.; Lackmann, M.; Church, W. B.; Sanderson, G. M.; Sutherland, R. L.; Daly, R. J. J. *Biol. Chem.* **1997**, 272, 8490.
63. Porter, C. J.; Wilce, M. C.; Mackay, J. P.; Leedman, P.; Wilce, J. A. *Eur. Biophys. J.* **2005**, 34, 454.
64. Pace, C. N.; Vajdos, F.; Fee, L.; Grimsley, G.; Gray, T. *Protein Sci.* **1995**, 4, 2411.

Chapter 6

The discovery of Phenylbenzamide derivatives as a novel class of Grb7 based antitumor agents

This chapter reports the virtual and experimental screening strategies pursued to design small molecular antagonists of Grb7 protein. Starting from experimentally determined co-crystal structure of a polypeptide antagonist of Grb7 (G7-18NATE), virtual screening experiments including shape based similarity searches, molecular docking and 2D-similarity searches were applied to discover and optimize potential structures. Detailed binding thermodynamics characterization was made by ThermoFluor based thermal denaturation and isothermal titration calorimetry. A novel structural class with moderate affinity against Grb7 is identified from the study.

The discovery of Phenylbenzamide derivatives as a novel class of Grb7 based anti-tumor agents

Nigus D. Ambaye, Menachem J. Gunzburg, Reece C.C. Lim, John T. Price, Matthew C.J. Wilce and Jacqueline A. Wilce#

Abstract

Human growth factor receptor bound protein-7 (Grb7) is a non-catalytic protein known to mediate mitogenic signal transduction. Grb7 over-expression has been associated with the proliferative and migratory properties of poor prognosis cancer cells. The present work reports the application of a succession of virtual screening experiments comprising shape based similarity search, molecular docking and 2D-similarity screening to identify novel scaffolds against this emerging oncogenic target. Experimental pre-screening with ThermoFluor based melting point shift assay followed by full thermodynamic characterization by isothermal titration calorimetry afforded the identification of 9 novel phenylbenzamide based antagonists. The experimental binding affinity found is in low micromolar, ranging from 47 μ M for lead NSC10499 to 1.1 μ M for lead NSC55148. Deconvolution of the affinity data into its thermodynamic components reveals differences in their binding mode-from being entropically driven binding (NSC104999) to enthalpically driven (NSC100874, NSC100877, NSC55158 and NSC55148) associations. Finally, in a cell growth assay the lead compound (NSC104999) was found to reduce the growth of a Grb7-expressing breast cancer cell line. It is expected that these structures will serve as novel leads in the further development of anticancer therapeutics and to further probe the functional, signaling and structural studies of Grb7 protein.

Keywords: Grb7, adapter protein, SH2 domain, phenylbenzamides; cancer cells, similarity search, virtual screening, ITC, ThermoFluor, melting point shift assay.

Introduction

Growth factors regulate many aspects of cell biology.¹ Growth factor receptors are transmembrane tyrosine kinases containing an extracellular growth factor binding domain and an intracellular domain with kinase activity. The first step in growth factor dependent signal transduction is growth factor binding initiated autophosphorylation of the kinase domain of receptor tyrosine kinases.^{2,3} The receptor phosphorylation is critical for the transfer of information from the growth factor to trigger intracellular events. One of the cytosolic proteins recruited to transmit the signaling information is Growth factor receptor bound protein 7 (Grb7) – so named for its original identification as a binding partner of epidermal growth factor receptor.⁴ It has since been found that Grb7 acts as an adapter for numerous tyrosine kinases, including cytosolic focal adhesion kinase that plays a role in cell migration.⁵

Grb7 has come to particular attention since its over-expression was found to be correlated with a variety of tumors ranging from breast,⁶ blood,⁷ pancreatic,^{8,9} esophageal^{10,11} to gastric carcinomas¹² and its involvement in the transformation of cancers to more aggressive and advanced phenotypes was established.^{13,14} Furthermore, investigative studies exist which demonstrate that the knock-down of expression or the inhibition of Grb7 results in the reduction of the proliferative and migratory properties of Grb7 expressing cancer cells.^{9,15} Taken together, these studies suggest that Grb7 is an emerging target in the development of anti-cancer molecular therapeutics.¹⁵

Grb7 is a 532-residue protein composed of a proline rich N-terminal domain, a Ras-associating domain, a pleckstrin homology domain, a C-terminal Src homology 2 (SH2) domain as well as a BPS (between the pleckstrin homology and SH2) domain.^{5,16} The binding of Grb7 to its upstream partners is primarily dictated by its SH2 domain.¹⁷ This domain is responsible for the recognition of specific phosphotyrosine (pTyr) via a well described cationic pocket and adjacent peptide binding cleft. Therefore this interaction poses a logical target for the development of drugs that interfere with Grb7 mediated pathways. Structural information for the Grb7-SH2 domain, and its interaction with binding peptides is available,¹⁸ potentially facilitating the rational development of potent inhibitor molecules that

can be used therapeutically. The present work thus makes use of the Grb7-SH2 domain for the cellular, biophysical and computational binding experiments.

Virtual screening of compound libraries is commonly employed to identify leads in early drug discovery projects.^{19,20} Depending on the chemical information available, either structure or ligand based virtual screening or a combination thereof is pursued. The availability of an experimentally determined structure is of particular utility in computational screening, as it can serve both as a source of query and a benchmark in hit screening and the validation process. The present project exploits the availability of an exclusive in-house solved structure of the Grb7-SH2 domain in complex with a lead peptide. Specifically, the experimentally determined conformation of the peptide could be used as shape query to filter hits from the virtual screening.

The search for Grb7 specific antagonists has already met with some success, with the discovery of peptide-based antagonists.^{21,22} However, problems inherent in bioactive peptide such as their lack of stability and cell permeability, has limited their use as therapeutics. This is particularly the case for intracellular targets such as Grb7. The current work was thus undertaken to discover a potent, cell permeable and stable small molecule antagonist of the Grb7 oncoprotein. This work reports shape based virtual screening, molecular docking, a 2D-similarity search, melting point shift assays and isothermal titration calorimetric binding measurements, resulting in the discovery of a novel structural class of Grb7 antagonist. The growth inhibitory effect of this class of antagonist is also demonstrated in a Grb7 expressing breast cancer cell line. It is hoped that these findings will help to advance the development of therapeutically useful Grb7 antagonists.

Results

Validation of the shape query

Virtual compound screening is a useful tool in lead identification. The lead peptide antagonist shown in Fig. 6.1 named, G7-18NATE²³ was used as reference shape query. It was chosen as it is the only peptide that has been specifically developed against the Grb7 oncoprotein and is reportedly selective for the Grb7-SH2 domain.

Furthermore we were able to utilize our exclusive X-ray structure of G7-18NATE in complex with the Grb7-SH2 domain (manuscript in preparation). Hence a G7-18NATE shape based database search was used as a starting point for the identification of potential small molecule antagonists of Grb7. This is based on the assumption that the best antagonists will bind at the same receptor site as the G7-18NATE reference structure. In order to put the use of G7-18NATE as a shape query to the test, a test database of Grb7 antagonists with known experimental affinity²⁴ was created in Schrodinger²⁵ to guide the computational experiment. The shape of G7-18NATE was then correlated with the shape of the known Grb7 antagonists.²⁴ This correlation was then considered with respect to its ability to reproduce the activity rank of the antagonists. Table 6.1 displays the relationship between the shape similarity coefficient and biological activities of the known antagonists.

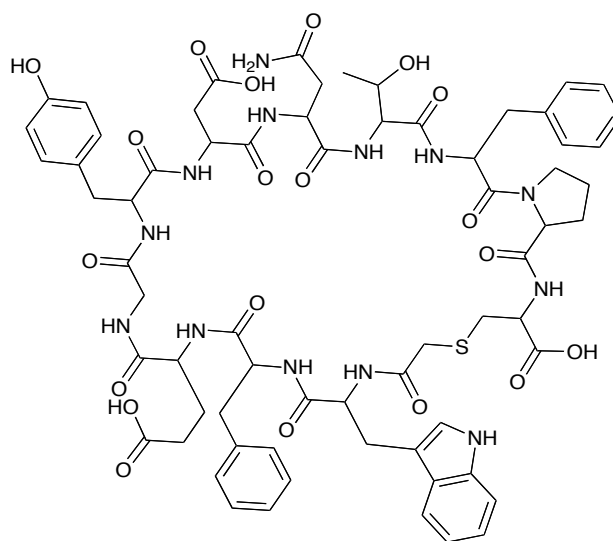


Figure 6.1. The chemical structure of G7-18NATE lead peptide used as a shape query. The peptide of amino acid sequence WFEGYDNTFPC is shown, cyclized with a thioether bond between the N-terminal residue and the side chain of the C-terminal cysteine

Table 6.1: Shape similarity index of Grb7 Antagonists used as test sets

Antagonist	pIC ₅₀ ^a	Shape Similarity Co-efficient
mAZ-pY(α -Me) pYN	6.523	0.249
PEpYVNQ	5.959	0.235
Ac-pYVNQ	5.469	0.231
EpYVNQ	5.815	0.229
pYVNQ	5.447	0.221
Correlation co-efficient		0.853

^apIC₅₀ is the negative log of the reported IC₅₀ value [24] using the equation $\text{pIC}_{50} = -\log \text{IC}_{50}$;

^bThe correlation co-efficient between is the pIC₅₀ values and the shape similarity indices obtained when using the G7-18NATE as a shape query.

The data are consistent with the existence of a relationship between the shape similarity index computed using G7-18NATE as a reference shape and the bioactivity of the reported antagonists. The most potent antagonist is indeed scored with a better shape similarity index and the least potent antagonist (lower pIC₅₀ value) is scored with one of the lowest similarity coefficients. This is also quantitatively expressed by the correlation coefficient calculated for these data. A correlation coefficient of 0.853 was obtained for the relationship between the shape similarity indices and the pIC₅₀ of the antagonists. This indicates the strength of the relationship and suggests that the bioactive shape of G7-18NATE may be used for the identification of potential small molecule candidates from chemical virtual databases. Furthermore, since the average of the similarity indices for the antagonists was 0.23, a hit with a similarity index of above this value was considered worthy of further investigation.

Virtual screening of the NCI chemical database

After its validation, the shape query method was applied to scan the NCI chemical database, which at the time of this work comprised some 250, 251 structures. A total of 16,521 hits were returned with a shape similarity coefficient better than 0.23. The top 5,000 were then submitted to the Glide virtual high throughput screening (Glide HTVS) docking routine.^{26,27}

This procedure resulted in 1007 hits that successfully passed the rapid computational binding test of Glide HTVS. Examination of the failed structures

revealed that the structures were either simple or polycyclic hydrocarbons and those that contain multiple compound structures that were able to meet the shape criteria. The 1007 hits were further docked using the Glide standard precision docking routine. This step produced 880 hits that were successfully redocked. Finally, the top 500 from the Glide SP were re-docked using the more accurate Glide extra precision docking routine. Using the criteria of a shape similarity cutoff of 0.23, a docking score of -5.5 kcal/mol in either Glide XP or SP and visual examination of the predicted binding mode of the structures, a total of 20 hits were considered as promising from the G7-18NATE shape based search. The hit codes, shape similarity index and docking scores (in kcal/mol) are shown in Table 2. The top hits vary from short peptides (NSC 710168, NSC 710170, NSC 710171, and NSC 710172) to small molecules belonging to different structural classes. An interesting observation is the presence of hit NSC708238, which is previously reported to be one of the most potent peptide based antagonist of the Grb2 SH2 domain,²⁸ which is a closely related to the Grb7 SH2 domain. This finding both lends confidence to the virtual screening protocol used and forewarns that ligand cross reactivity between Grb2 and Grb7 is possible.

Predicted Binding mode of lead NSC104999

The experimentally observed binding mode of G7-18NATE was used to guide the filtration of virtual screening hits. To this effect the binding geometry of the hits were analyzed and their binding to key residues of the Grb7 SH2 domain binding site was used as another criteria for hit acceptance. The predicted binding interaction of compound NSC104999 is displayed in Fig. 6.2. This compound is predicted to form a number specific binding interaction with the binding site of the Grb7 SH2 domain. Specifically, the imidazole nitrogen of the hit is predicted to form a hydrogen bond with the OH group of Tyr480. The phenyl ring containing the imidazole moiety of the hit is observed to be appropriately positioned to make a favorable hydrophobic/van der Waals interaction with another key residue of the binding site, Ile518. Furthermore, the phenyl ring of NSC104999 is positioned to form a potential hydrophobic bond with the side chain of Leu481. The carbonyl oxygen of the carboxamide moiety on the hit is also noted to make a hydrogen bond with guanidine moiety of Arg438.

Table 6.2: Shape similarity index and docking score of hits from G7-18NATE based virtual screening experiment

Hit ID.	Shape Sim.	Glide SP Dock score		Glide XP Dock score	
		GlideScore	Emodel	GlideScore	Emodel
NSC710170	0.286	-7.126	-89.238	-4.34	-90.77
NSC710168	0.269	-7.066	-89.879	-3.65	-96.61
NSC710171	0.269	-6.666	-93.185	-5.58	-93.99
NSC626667	0.247	-6.545	-87.522	-6.90	-89.31
NSC665676	0.231	-6.479	-38.235	-6.87	-40.37
NSC691697	0.232	-6.324	-98.863	-5.19	-105.49
NSC633031	0.231	-6.319	-70.609	-4.52	-79.67
NSC708238	0.235	-6.259	-77.895	-6.85	-81.83
NSC104999*	0.256	-5.808	-69.292	-4.79	-84.41
NSC710172	0.265	-5.784	-71.223	-5.30	-89.52
NSC677142	0.244	-5.776	-73.707	-4.60	-89.15
NSC705340	0.268	-5.754	-77.697	-7.99	-94.48
NSC677150	0.230	-5.750	-74.977	-4.18	-82.24
NSC677147	0.256	-5.717	-67.389	-4.53	-72.98
NSC641285*	0.270	-5.648	-68.491	-3.96	-77.80
NSC692905	0.240	-5.632	-50.521	-4.51	-30.89
NSC293553*	0.299	-5.618	-76.421	-4.22	-84.80
NSC408715*	0.291	-5.531	-51.460	-4.01	-65.76
NSC42067*	0.234	-5.467	-73.002	-9.50	-87.95
NSC141149*	0.348	-5.255	-78.457	-7.33	-96.22

Note: * indicates tested experimentally.

Finally, a pair of hydrogen bond exists between the side chain carbonyl of the hit and the side chain of Arg458. Overall, the hits shown in Table 6.2 were predicted to reproduce contacts also observed for a polypeptide antagonist of the Grb7-SH2 domain.

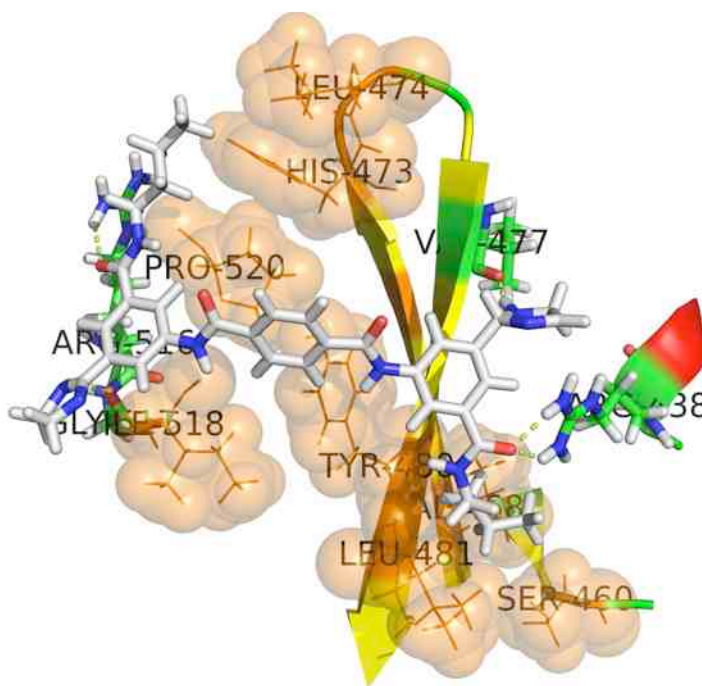


Figure 6.2: Binding mode of Hit NSC104999 predicted using Glide XP. The hit is displayed in ball and stick format. Hydrogenbonds are shown in broken line in lemon color. Grb7-SH2 domain binding site residues involved non-polar interactions with the hit are shown in line and transparent spheres. Binding site residues predicted to form a hydrogen bond are displayed in ball and stick (Carbon in green; Nitrogen in blue and Hydrogen in gray color)

Experimental pre-screening using a melting point shift assay

Experimental prescreening of the hits was carried out using a ThermoFluor based melting point shift method.^{29,30} Out of the top 20 potential hits, 6 were available at the time of this work and kindly provided by the NCI Developmental and Therapeutic program unit of the USA (Drug synthesis and Chemistry branch, <http://dtp.nci.nih.gov/>). The compounds were dissolved in 1-2% DMSO solution. The 6 hits, indicated in Table 8.2, were experimentally tested for their ability to increase the melting temperature of overexpressed and purified Grb7-SH2 domain using the ThermoFluor based thermal shift assay. From this prescreening, one hit NSC104999, produced a positive melting point shift (0.4 °C at 100 μ M and 0.7 °C at 200 μ M). Although these shifts were lower than those effected by a G7-18NATE-related peptide (0.65 °C at 100 μ M and 1.5 °C at 200 μ M), they were considered noticeable melting temperature shifts, possibly representing the binding of a weak antagonist. This data is shown in Table 6.3. Also shown in Table 6.3 are the melting point shifts and Tanimotto similarity coefficients of NSC104999 analogues. In sum,

the melting data for hit NSC104999 indicate that the values are comparable to that for the standard peptide and that further investigation is warranted.

Table 6.3: 2D-similarity, docking score and melting point shift for Phenylbenzamide derivatives

Hit	Tanimotto Similarity co-efficient (%)	Glide score		$\Delta T_m(^{\circ}\text{C})$	
		SP	XP	100 μM	200 μM
NSC55158	90	-3.50	-3.47	0.75	0.8
NSC57148	91	-3.87	-2.13	0.30	0.2
NSC63690	92	-3.29	-1.90	0.10	0.35
NSC70706	90	-3.55	-2.40	0.35	0.5
NSC100874	95	-4.29	-2.40	0.50	0.60
NSC100877	96	-5.02	-0.35	0.05	0.30
NSC59503	91	-3.92	-2.39	0.10	0.15
NSC50460	90	-4.08	-2.01	0.30	0.65
NSC104999	100	-4.73	-1.45	0.40	0.70
08-5992	Not applicable			0.65	1.50
Grb7SH2	Not applicable			$T_m = 51.5$	

^aThe change in melting point (ΔT_m) are obtained from duplicate experiments after the melting point of apo-Grb7-SH2 ($T_m = 51.5^{\circ}\text{C}$) was subtracted from that of the hit bound form. NSC10499 was the lead compound while the G7-18NATE related peptide is the reference polypeptide concurrently run in the melting shift assay.

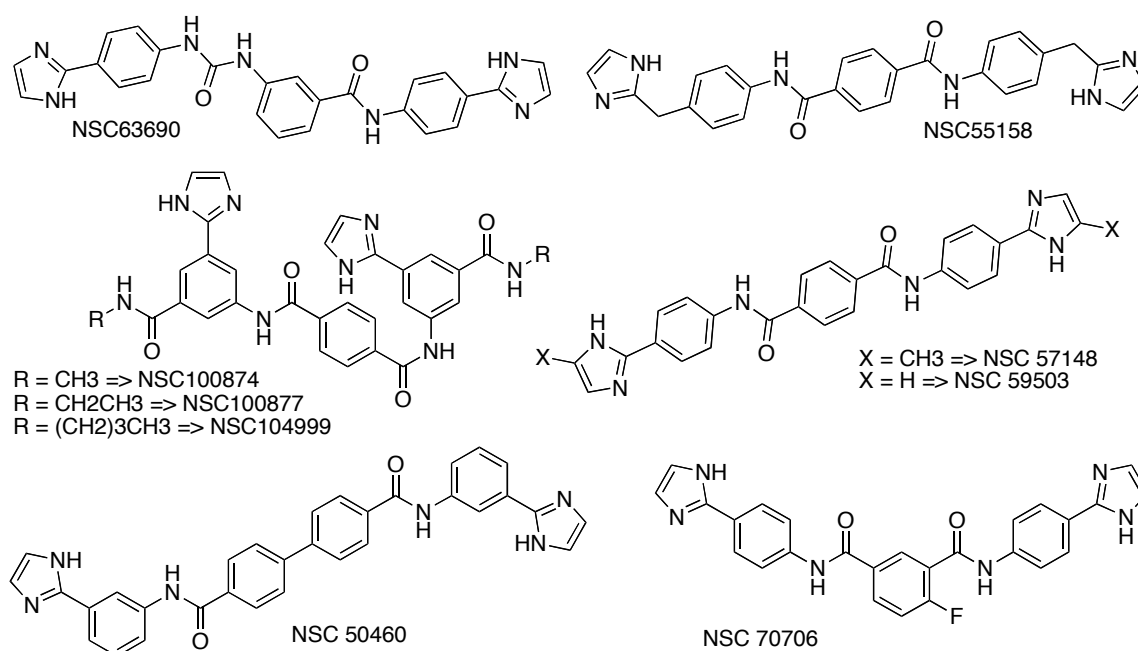


Figure 6.3: Chemical Structures of the Phenylbenzamide derivatives.

ITC binding study and 2D-similarity searches

Thermodynamic characterization of drug-receptor binding afforded by ITC is the gold-standard for the characterization of binding interactions in lead discovery and optimization studies.³¹ ITC relates the amount of heat absorbed or released to the amounts of the interacting species and provides parameters such as binding free energy, enthalpy, entropy and stoichiometry³¹ that can be used to characterize the molecular association event. The binding thermodynamics of hit NSC104999 that was identified by the melting experiment was determined by ITC. As shown in Table 6.4, ITC confirmed that the hit does indeed bind Grb7-SH2 domain with moderate affinity ($K_D = 47 \mu\text{M}$) and further provides detailed parameters of the binding. Thus, the combination of virtual and experimental investigation was able to identify a lead worthy of further exploration. With this goal, a 2D-similarity search was then pursued in order to identify analogues of NSC104999 with improved affinity. Use of the lead as a 2D-query returned 32 hits out of which 19 were available from the NCI Developmental and Therapeutic program at the time of this work. The 19 compounds were first assessed using the melting point shift assay as described above. The result, also shown in Table 6.3, revealed that, out of the 19 structural analogues tested, 8 were able to produce a positive melting point shift. This corresponds to about the 42% of the tested compounds which is a significant enrichment over the initial testing (ca. 16%). The structures of the 8 leads identified in addition to the starting structure are displayed in Fig. 6.3.

Following prescreening with the thermal shift assay the binding of four compounds from the 2D-similarity search to the Grb7-SH2 domain were characterized with ITC. The ITC experiment for NSC104999 and its analogues were determined under identical experimental conditions including identical buffer composition and titration schedules. Fig. 6.4 shows the ITC binding isotherm for NSC104999 and one of the analogues tested while Table 6.4 displays the values for the thermodynamic binding parameters. These data reveal a difference in the mode of association. Specifically, the parent lead was found to bind with absorption of heat while its analogues were found to interact with an evolution of heat energy. In all cases, the stoichiometry of binding was found to be close to a 1:1 ratio. The experimental affinity was found to be of moderate value ranging from $K_D = 1.1 \mu\text{M}$ for NSC55148 to $K_D = 47.12 \mu\text{M}$ for NSC104999.

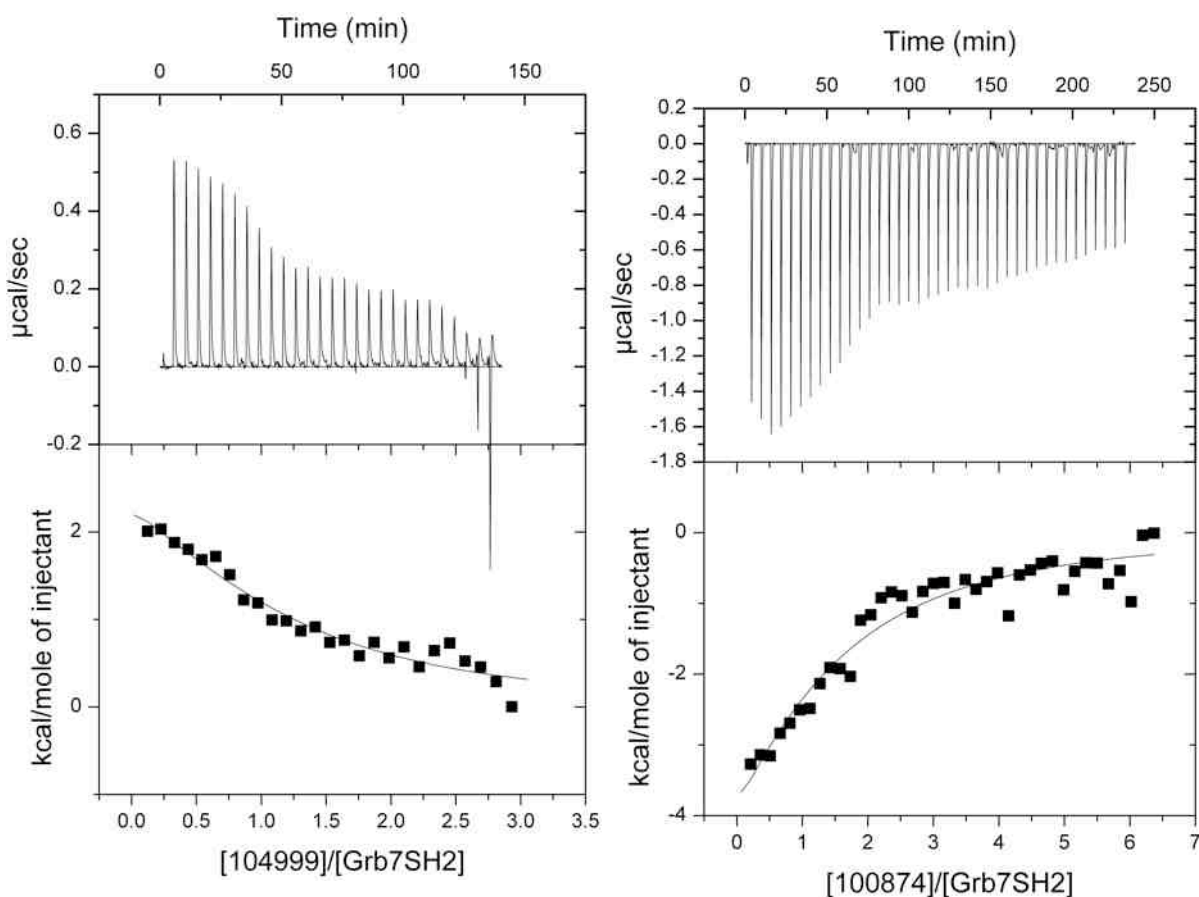


Figure 6.4. ITC thermograms of NSC104999 analogues. The upper panel show raw data obtained from 10 μ l injections of peptides at 25 °C. The lower panels in both figures display plots of integrated total energy exchanged (as kcal/mol of injectants) as a function of molar ratio of the compounds to the Grb7-SH2 domain: Data for NSC104999 is shown on the left and NSC100874 shown on the right. Solid lines show fit to a single site binding model.

This is an improvement over the starting lead structure. Though the overall free energy of binding (ΔG) is similar for these analogues (ca. -6 kcal/mole), deconvolution into entropic and enthalpic contributions reveals differences in these relative contributions. In the case of NSC104999 binding, the binding is a strongly entropically driven process. In contrast, the molecular mechanism underlying the binding of NSC100874 involves an unfavorable entropic component which is compensated by a large enthalpic contribution to binding. On the other hand, hits NSC55158 and NSC55148 bind through favorable enthalpic and entropic contributions.

The fact that the gross binding affinities remained virtually unaffected despite the differences in the relative contribution of the parts suggests entropy-enthalpy compensation phenomenon taking place. This is commonly observed in ligand-

receptor binding studies.³² Overall, the binding affinity of these small molecular leads is similar to the affinity of the query polypeptide ($K_D = 35 \mu\text{M}$).¹⁸

Table 6.4: Thermodynamic parameters for binding of Phenylbenzamide derivatives

Binding Parameter	NSC104999	NSC55158	NSC100874	NSC57148
Stoichiometry	1.02±0.2	1.07±0.04	1.08±0.03	1.04±0.03
K_A (10^4M^{-1})	2.42±0.86	7.91±0.13	5.56±0.26	91.2±3.1
ΔH (kcal/mol)	2.47 ± 0.74	-4.80± 0.35	-9.67± 0.39	-6.15± 0.74
ΔS (Cal/mol/K)	28.9	6.29	-11.2	2.4
$T\Delta S$ (kcal/mol)	8.62	1.88	-3.34	0.72
ΔG (kcal/mol)	-6.15 ±0.74	-6.68 ± 0.35	-6.33 ± 0.39	-6.86 ± 0.74
K_d (μM)	47.3 ±16	12.65±0.2	18.03±0.84	1.1 ±0.04

Cellular growth assay

Finally, a cellular growth assay was conducted using the MDA-MB-468 breast cancer cell line to determine whether the lead compound would display activity in an *in vivo* system. To this effect, the impact of lead NSC104999 on these Grb7 expressing cancer cells was investigated. The result, as shown in Fig. 6.5, shows that the lead compound impacts on the growth of the cells in a concentration dependent manner. The *in vivo* EC_{50} determined for the cell growth inhibition observed is $45.0 \mu\text{M}$. Interestingly, this correlates with the *in vitro* dissociation constant obtained by ITC (ca. $47.3 \mu\text{M}$). Thus the compound displays a growth inhibitory effect on the breast cancer cell line –though whether this is due in part or wholly to interaction with Grb7 is yet to be determined.

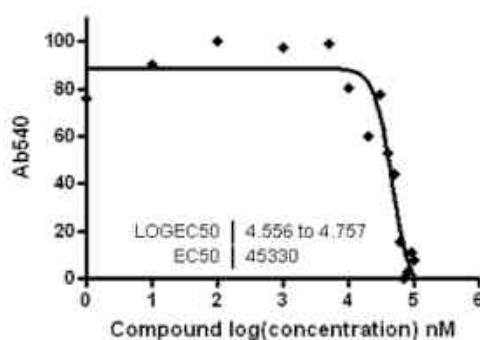


Figure 6.5: Cellular growth inhibition curve obtained for the lead NSC104999. The IC_{50} was found to be $45 \mu\text{M}$. The lead compound NSC104999 displayed growth inhibitory effects against MDA-MB-468 breast cancer cells. The IC_{50} obtained is $45 \mu\text{M}$, which closely relates the $K_d = 47.3 \mu\text{M}$ obtained by ITC on in vitro system.

Discussion

Grb7 is an emerging intracellular cancer target. This has been confirmed by a number of independent investigations over the years.^{9,15} So far, few antagonists have been specifically developed for Grb7 inhibition.^{23,24} Notably, the polypeptide-G7-18NATE,²³ that was identified through a phage display technique, showed promising anti-proliferative and anti-migratory activity in cancer cells.^{9,15} Since all the reported Grb7 antagonists are peptides, however, issues attributed to peptide structures such as poor membrane permeability, stability and bioavailability as well as manufacturing difficulty and the potential for immunogenicity make the current peptide based leads unattractive for pharmaceutical development. In contrast, small molecule Grb7 antagonists would have high potential for anti-cancer therapeutics development.³² Furthermore, since Grb7 is an intracellular protein whose downstream effectors are not yet elucidated, the availability of potent small molecular antagonists would help to elucidate the signaling and other cellular activities elicited by the Grb7 protein.

Shape complementarity has been recognized as an important concept in ligand receptor interaction.³⁴ Ligands that possess the most complementary shape to the binding groove of a receptor are expected to make the best-fit and maximum interaction with the receptor. Exploiting this concept in the current study, a shape based virtual screening experiment was able to identify a potential lead candidate from the NCI chemical database. It was found, however, that the shape searches alone were of limited use, as many of the best scoring hits from the shape similarity search did not achieve high docking scores. The application of a succession of virtual screening tools, however, was effective in yielding promising leads. As the search progressed from a gross shape based search to the more specific 2D-similarity search, an increase in hit rate was achieved. This is consistent with the similarity principle which states that structurally similar molecules are expected to be similar in their physicochemical and biological properties.³⁵ The virtual screening experiments attest to the usefulness of the application of a succession of virtual screening tools that can then be followed up with experimental screening approaches.

In the current study the ThermoFluor shift assay was used to rapidly test hits from the virtual screening experiments for binding to the Grb7-SH2 domain. The ThermoFluor shift assay is based on the principle that a protein will be stabilized upon ligand binding, resulting in an increased melting temperature. Furthermore, more potent ligands may be expected to result in a more significantly shifted protein melting temperature. Thus the observed change in melting temperature can be taken to be directly proportional to the potency of ligand binding. Indeed this principle has allowed workers to estimate the binding affinity of biomolecular associations²⁸ from thermal shift data alone. In the current study several hits gave rise to melting point shifts. The melting point shift data for the leads identified were similar to each other and this was also reflected in the binding affinity values obtained using ITC. Moreover, both the thermal shift values are comparable to that of the known peptide inhibitor, with all compounds binding in the low micromolar range. ITC also provided information as to the relative enthalpic and entropic contributions to binding. A surprising difference in these contributions was observed for the four hits analyzed using ITC, with one compound binding with a significant entropic contribution to binding, and the others binding with a predominantly enthalpic contribution. There is no clear reason why this should be the case from examination of the structures of these compounds. The potential for these small molecule ligands to bind with an entropic contribution to binding is in contrast to the binding observed for the G7-18NATE peptide ligand, which involves an entropic energy loss upon binding.³⁶ This is not unexpected given the more flexible nature of the reference polypeptide. Finally, when applied to a cell based assay, the lead compound was shown to have growth inhibition activity in a breast cancer cell line. Further work will be required to confirm whether this activity occurs in part or wholly due to Grb7 antagonism. Considering their non-peptidic structure and the moderate affinity values, the identified small molecular antagonists are expected to be good candidates for the further development of potent Grb7 antagonists.

In conclusion, starting with a co-crystal structure of a selective polypeptide antagonist, the present work reports the successful application of a succession of computational ligand design tools comprising a ligand shape based similarity search, molecular docking and a 2D-similarity search to identify a novel

phenylbenzamide class of small molecular antagonists of Grb7. Experimental binding studies with a melting-point shift assay and isothermal titration calorimetry has enabled the characterization of the interaction with the Grb7-SH2 domain and to shed some light on the mechanistic aspect of the binding interaction. That the phenylbenzamide based antagonists reduce the growth of breast cancer cells was confirmed in the MDA-MB-435 cell line, illustrating the potential of the antagonists in living systems. It is expected that the Identified scaffolds will be useful additional agents to further explore and accelerate the functional, signaling and structural studies of adaptor proteins.

Materials and Methods

Shape Similarity Search

The peptide conformation extracted from an in-house G7-18NATE/Grb7 SH2 co-crystal structure was used as a shape query. Hydrogen atoms were added to the extracted structure and the all atom conformation was then used as a shape query without any minimization. The program PHASE³⁷ was employed to carry out a shape based virtual screening experiment. The atom type used for volume scoring was set to none so as not to bias the search towards a particular hit class, particularly for the subsequent database screening. The National Cancer Institute (NCI) chemical database was used for virtual screening of potential antagonists. The average similarity index of the known antagonist was then used as a cut-off during the NCI database screening.

Molecular Docking

Molecular docking is a commonly employed tool for the prediction of binding affinity and geometry of ligands.^{38,39} The program Glide was used to perform docking studies for top hits from the shape search. Glide comprises three docking routines designed for virtual screening of chemical databases.^{26,27} The structure of the Grb7 SH2 domain solved in our laboratory was used as a receptor. The PDB file was read into Maestro in Schrodinger²⁴ and the protein preparation wizard was used to set up the protein including addition of hydrogen atoms and deletion of water molecules beyond 5 Å from protein atoms. Hydrogen bond assignment was

effected with exhaustive sampling option and the system was subsequently relaxed with geometry minimization. A grid of size 12 Å x 12 Å x 12 Å was defined using the peptide-binding surface about the phosphotyrosine pocket to define the binding site. All the other docking parameters were kept at their default values.

ThermoFluor Based Melting Point Shift Assay

Following identification of promising leads from virtual screening, experimental pre-screening with ThermoFluor was then conducted.^{29,30} ThermoFluor relies on melting point differences between apo and bound forms of proteins. An initial experiment was performed to establish the existence of a noticeable melting transition between the folded and unfolded states of the Grb7 SH2 domain. The environmentally sensitive dye Sypro Orange was used to detect the melting point transitions. The thermal shift experiment was conducted in Qiagen's quantitative RT-PCR instrument (www.qiagen.com). The wavelength of excitation/emission was set to 470/555 nm and 470/610 nm. A heating rate of at 1 °C/min was programmed over a temperature range of 30-80 °C. The buffer used was 50 mM MES, 100 mM NaCl, pH 6.6. The thermal denaturation was carried out in a reaction volume of 25 µl using a 72 tube rotor. The concentration of the Grb7 SH2 domain was determined using UV-VIS absorption spectroscopy at 280 nm. 20 µM of Grb7 SH2 domain with hit compounds of 100 µM and 200 µM concentrations were used for the melting experiment. A known G7-18NATE derived peptide inhibitor was also run at the same time to act as an internal control and for comparative purposes. Each denaturation experiment was conducted in duplicates and in each case the average melting temperature was taken for determination of the change in melting point. The Rotor-Gene 3000 software was used to set up experiment and analyze the results.

Binding Study with Isothermal Titration Calorimetry

ITC binding experiments were performed with the sensitive VP-ITC Microcalorimeter (Microcal, Northampton, MA, USA) at 25 °C.⁴⁰ The Grb7 SH2 domain was dialyzed overnight against 2 L of 50 mM NaOOCCH₃, pH 6.6, 100 mM NaCl and 1 mM DTT at 4 °C. Absorbance reading at 280 nm with a molar

absorptivity coefficient of $8480 \text{ cm}^{-1}\text{M}^{-1}$ was used to establish the Grb7-SH2 concentration. The concentrations of the hits were determined by dissolving an appropriately weighed sample in the required volume of filtered buffer. The hit and protein solutions were simultaneously degassed and thermostated at 20°C for 5 min using ThermoVac of the calorimeter. The reference power of the experiment was set to $25 \text{ }\mu\text{Cal/sec}$ and cell contents were stirred continuously at 307 rpm throughout the titrations. The feedback mode gain was set to high with fast and auto equilibrations options applied. The reference cell was filled with milliQ water. The concentration of the hits in range of 500-950 μM concentrations was titrated into Grb7 SH2 solutions of 50-85 μM concentrations in 7-10 μL injections with a 3-6 min delay time between each injection. A binding isotherm was generated by plotting the heat change evolved per injection against the molar ratio of the leads to Grb7-SH2 domain receptor. A blank determination in which the compounds were titrated against the buffer was carried out to account for heats of dilution and mixing which was subtracted from the binding data. The corrected data was then employed to fit to a single binding site model using a non-linear least squares with the Origin (Microcal Software, Northampton, MA, USA). All of the ITC fitting parameters were allowed to float.

Lead Optimization with 2D-Similarity Search

From the combination of virtual and experimental screening one compound, NSC104999, was determined to be a promising hit. It was then taken as a lead to further explore the structure in a bid to optimize the observed affinity. To this end, analogues of this compound were sought using a two-dimensional structure based similarity search. The 2D-search was pursued with the same NCI database using the SMILES representation⁴¹ of the lead compound. Hits with a Tanimotto similarity of above 90% were retained for subsequent investigation.

Expression and Purification of Grb7-SH2 domain

The SH2 domain of Grb7 was used as a receptor for the binding and computational experiments. It was expressed in an *E.coli* expression system. The pGex2T plasmid containing sequences corresponding to residues 415-532 of human Grb7 was

obtained from collaborators.⁴² Grb7-SH2 was expressed as a GST fusion protein in strain BL21 (DE3) pLysS of *E. coli*.⁴³ Cell induction was achieved with a 400 μ M Isopropyl β -D-1-thiogalactopyranoside. The cells were resuspended in ice-cold phosphate buffer saline with 2 mM EDTA and 0.5% Triton-X 100 and lysed by sonication. GST-Grb7-SH2 was purified by glutathione affinity chromatography (GE) and eluted with PBS containing 0.5% Triton-X100, 10 mM glutathione and 1 mM DTT. The Grb7-SH2 fusion protein was cleaved with thrombin liberating free Grb7-SH2, which was purified by cation exchange chromatography using a HiTrap SH HP column (GE), after dialysis into 20 mM HEPES pH 7.4, 20% Glycerol and 1 mM DTT, and eluted with a gradient from 0-0.5 M NaCl. Peak fractions were dialyzed into 50 mM MES pH6.6, 100 mM NaCl and 1 mM DTT and further purified by size exclusion chromatography using a Sephadex 75 XK 16/60 column (GE). The Grb7-SH2 domain was concentrated and stored at 4 °C. The final concentration was determined spectrophotometrically at 280 nm using an absorptivity coefficient of 8480 $\text{cm}^{-1}\text{M}^{-1}$.⁴⁴

Cellular growth studies

To determine the effects of the compounds on cellular growth, MDA-MB-468 breast cancer cells were resuspended at 5×10^4 cells/mL and 100 mL of this cell suspension was plated in 96 well plates (BD Biosciences, California, USA). The following day cells were treated with a range of various concentrations of the compounds, each concentration with triplicates wells. Cells were incubated under standard growth conditions with 10% fetal bovine serum over a four-day period (0-4 days). Adherent cell cultures were fixed *in situ* after 4 days by the addition of 25 ml of cold 50% trichloroacetic acid solution (Sigma-Aldrich, Missouri, USA) and incubated for 60 minutes at 4 °C. The supernatant was then discarded and the plate was washed five times with running distilled water before being dried overnight. Fixed cells were stained by the addition of 100 ml of sulforhodamine B (SRB) sodium salt solution (0.4% (w/v) in 1% Acetic Acid; Sigma-Aldrich, Missouri, USA) and incubated for 10 minutes at room temperature. Unbound SRB solution was removed by washing five times with 1% acetic acid after which the plates were air-dried overnight. The following day, the bound stain was solubilized with 100 ml of 10 mM Tris buffer (pH 10.5) and the absorbance of the eluted dye was read on the

spectrophotometric BMG PolarStar Optima plate reader (BMG Labtech, Offenburg, Germany) at 540 nm. SRB is a total protein stain, which directly correlates with cell number and is used routinely to measure cell growth rate. The Nonlinear regression analysis of the concentration-response plot was conducted using GraphPad Prism software.

Acknowledgements

This work was funded by an Australian Research Council Project Grant awarded to JAW and DNK and a Monash University Graduate Scholarship awarded to NDA. MCJW is the recipient of an NHMRC Senior Research Fellowship. We thank the Drug Synthesis and Chemistry Branch of National Cancer Institute of the USA for providing the compounds used in the screening and testing. The Victorian partnership for advanced computing (VPAC) is acknowledged for granting us access to the computational facility employed in the study.

References

- (1) Zhang, X.; Nie, D.; Chakrabarty, S. Growth factors in tumor microenvironment. *Front. Biosci.* **2010**, *15*, 151-165.
- (2) Carpenter G.; Cohen, S. Epidermal growth factor. *J. Biol. Chem.* **1990**, *265*, 7709-7812.
- (3) Schlessinger, J. Cell signaling by receptor tyrosine kinases. *Cell* **2000**, *103*, 211-225.
- (4) Margolis, B.; Silvennoinen, O.; Comoglio, F.; Roonprapunt, C.; Skolnik, E.; Ullrich, A.; Schlessinger, J. High-efficiency expression/cloning of epidermal growth factor-receptor-binding proteins with Src homology 2 domains. *Proc. Natl. Acad. Sci. USA.* **1992**, *89*, 8894-8898.
- (5) Han, D. C.; Shen, T. L.; Guan, J. L. The Grb7 family proteins: structure, interactions with other signaling molecules and potential cellular functions. *Oncogene* **2001**, *20*, 6315-6321.
- (6) Stein, D.; Wu, J.; Fuqua, S.A.; Roonprapunt, C.; Yajnik, V.; D'Eustachio, P.; Moskow, J. J.; Buchberg, A. M.; Osborne, C. K.; Margolis, B. The SH2 domain protein GRB-7 is co-amplified, overexpressed and in a tight complex with HER2 in breast cancer. *EMBO J.* **1994**, *13*, 1331-1340.
- (7) Haran, M.; Chebatco, S.; Flaishon, L.; Lantner, F.; Harpaz, N.; Valinsky, L.; Berrebi, A.; Shachar, I. Grb7 expression and cellular migration in chronic lymphocytic leukemia: a comparative study of early and advanced stage disease. *Leukemia* **2004**, *18*, 1948-1950.

- (8) Itoh, S.; Taketomi, A.; Tanaka, S.; Harimoto, N.; Yamashita, Y.; Aishima, S.; Maeda, T.; Shirabe, K.; Shimada, M.; Maehara, Y. Role of growth factor receptor bound protein 7 in hepatocellular carcinoma. *Mol. Cancer Res.* **2007**, *5*, 667-673.
- (9) Tanaka, S.; Pero, S. C.; Taguchi, K.; Shimada, M.; Mori, M.; Krag, D. N.; Arii, S. Specific peptide ligand for Grb7 signal transduction protein and pancreatic cancer metastasis. *J. Natl. Cancer Inst.* **2006**, *98*, 491-498.
- (10) Tanaka, S.; Mori, M.; Akiyoshi, T.; Tanaka, Y.; Mafune, K.; Wands, J. R.; Sugimachi, K. Coexpression of Grb7 with epidermal growth factor receptor or Her2/erbB2 in human advanced esophageal carcinoma. *Cancer Res.* **1997**, *57*, 28-31.
- (11) Dahlberg, P. S.; Jacobson, B. A.; Dahal, G.; Fink, J. M.; Kratzke, R. A.; Maddaus, M. A.; Ferrin, L. J. *Ann. Thorac. Surg.* **2004**, *78*, 1790-1800.
- (12) Kishi, T.; Sasaki, H.; Akiyama, N.; Ishizuka, T.; Sakamoto, H.; Aizawa, S.; Sugimura, T.; Terada, M. Molecular cloning of human GRB-7 co-amplified with CAB1 and c-ERBB-2 in primary gastric cancer. *Biochem. Biophys. Res. Commun.* **1997**, *232*, 5-9.
- (13) Walch, A.; Specht, K.; Braselmann, H.; Stein, H.; Siewert, J. R.; Hopt, U.; Höfler, H.; Werner, M. Coamplification and coexpression of GRB7 and ERBB2 is found in high grade intraepithelial neoplasia and in invasive Barrett's carcinoma. *Int. J. Cancer* **2004**, *112*, 747-753.
- (14) Bai, T.; Luoh, S. W. GRB-7 facilitates HER-2/Neu-mediated signal transduction and tumor formation. *Carcinogenesis* **2008**, *29*, 473-479.
- (15) Pero, S. C.; Shukla, G. S.; Cookson, M. M.; Flemer, S.; Krag, D. N. Combination treatment with Grb7 peptide and Doxorubicin or Trastuzumab (Herceptin) results in cooperative cell growth inhibition in breast cancer cells. *Br. J. Cancer.* **2007**, *96*, 1520-1525.
- (16) Pero, S. C.; Daly, R. J.; Krag, D. N. Grb7-based molecular therapeutics in cancer. *Expert. Rev. Mol. Med.* **2003**, *5*, 1-11.
- (17) Pawson, T.; Gish, G. D.; Nash, P. SH2 and SH3 domains in signal transduction. *Adv. Cancer Res.* **1994**, *64*, 87-110.
- (18) Porter, C. J.; Matthews, J. M.; Mackay, J. P.; Pursglove, S. E.; Schmidberger, J. W.; Leedman, P. J.; Pero, S. C.; Krag, D. N.; Wilce, M. C.; Wilce, J. A. Grb7 SH2 domain structure and interactions with a cyclic peptide inhibitor of cancer cell migration and proliferation. *BMC Struct. Biol.* **2007**, *7*:58.
- (19) Bleicher, K. H.; Bohm, H. J.; Muller, K.; Alanine, A. I. A guide to drug discovery: Hit and lead generation: beyond high-throughput screening. *Nat. Rev. Drug Discov.* **2003**, *2*, 369-378.
- (20) Oprea, T. I.; Matter, H. Integrating virtual screening in lead discovery. *Curr. Opin. Chem. Biol.* **2004**, *8*, 349-358.
- (21) Burke, T. R. Development of Grb2 SH2 Domain Signaling Antagonists: A Potential New Class of Antiproliferative Agents. *Int. J. Pept. Res. Ther.* **2006**, *12*, 33-48.

- (22) Fretz, H.; Furet, P.; Garcia-Echeverria, C.; Schoepfer, J.; Rahuel, J. Structure-based Design of Compounds Inhibiting Grb2-SH2 Mediated Protein-protein Interactions in Signal Transduction Pathways. *Curr. Pharm. Des.* **2000**, *6*, 1777-1796.
- (23) Pero, S. C.; Oligino, L.; Daly, R. J.; Soden, A. L.; Liu, C.; Roller, P. P.; Li, P.; Krag, D. N. Identification of novel non-phosphorylated ligands, which bind selectively to the SH2 domain of Grb7. *J. Biol. Chem.* **2002**, *277*, 11918-11926.
- (24) Luzy, J. P.; Chen, H.; Gril, B.; Liu, W. Q.; Vidal, M.; Perdereau, D.; Burnol, A. F.; Garbay, C. Development of Binding Assays for the SH2 Domain of Grb7 and Grb2 Using Fluorescence Polarization. *J. Biomol. Screen.* **2008**, *13*, 112-119.
- (25) Schrodinger LLC, 120 West 45th Street, New York, New York.
- (26) Friesner, R. A.; Murphy, R. B.; Repasky, M. P.; Frye, L. L.; Greenwood, J. R.; Halgren, T. A.; Sanschagrin, P. C.; Mainz, D. T. Extra Precision Glide: Docking and Scoring Incorporating a Model of Hydrophobic Enclosure for Protein-Ligand Complexes. *J. Med. Chem.* **2006**, *49*, 6177-6196.
- (27) Friesner, R.; Banks, J. L.; Murphy, R. B.; Halgren, T. A.; Klicic, J. J.; Mainz, D. T.; Repasky, M. P.; Knoll, E. H.; Shelley, M.; Perry, J. K.; Shaw, D. E.; Francis, P.; Shenkin, P. S. New Approach for Rapid, Accurate Docking and Scoring. 1. Method and Assessment of Docking Accuracy. *J. Med. Chem.* **2004**, *47*, 1739-1749.
- (28) Burke, T. R. Jr.; Yao, Z. J.; Gao, Y.; Wu, J. X.; Zhu, X.; Luo, J. H.; Guo, R.; Yang, D.; N-terminal carboxyl and tetrazole-containing amides as adjuvants to Grb2 SH2 domain ligand binding. *Bioorg. Med. Chem.* **2001**, *9*, 1439-1445.
- (29) Pantoliano, M. W.; Petrella, E. C.; Kwasnoski, J. D.; Lobanov, V. S.; Myslik, J.; Graf, E.; Carver, T.; Asel, E.; Springer, B. A.; Lane, P.; Salemme, F. R. High-density miniaturized thermal shift assays as a general strategy for drug discovery. *J. Biomol. Screen.* **2001**, *6*, 429-440.
- (30) Matulis, D.; Kranz, J. K.; Salemme, F. R.; Todd, M. J. Thermodynamic stability of carbonic anhydrase: measurements of binding affinity and stoichiometry using ThermoFluor. *Biochemistry* **2005**, *44*, 5258-566.
- (31) Freyer, M. W.; Lewis, E. A. Isothermal titration calorimetry: experimental design, data analysis, and probing macromolecule/ligand binding and kinetic interactions. *Methods Cell Biol.* **2008**, *84*, 79-113.
- (32) Eftink, M. R.; Anusiem, A. C.; Biltonen, R. L. Enthalpy-entropy compensation and heat capacity changes for protein-ligand interactions: general thermodynamic models and data for the binding of nucleotides to ribonuclease A. *Biochemistry* **1983**, *22*, 3884-3896.
- (33) Danho, W.; Swistok, J.; Khan, W.; Chu, X. J.; Cheung, A.; Fry, D.; Sun, H.; Kurylko, G.; Rumennik, L.; Cefalu, J.; Cefalu, G.; Nunn, P. Opportunities and challenges of developing peptide drugs in the pharmaceutical industry. *Adv. Exp. Med. Biol.* **2009**, *611*, 467-469.
- (34) Mezey, P. G. Shape in Chemistry: An Introduction to Molecular Shape and Topology; VCH: New York, **1993**.

- (35) Nikolova, N.; Jaworska, J. Approaches to measure chemical similarity-A review. *QSAR Comb. Sci.* **2004**, *22*, 1006-1026.
- (36) Ambaye, N. D.; Lim, R. C. C.; Clayton, D. J.; Gunzburg, M.J., Price, J. T.; Pero, S. C.; Krag, D. N.; Wilce, M. C. J.; Aguilar, M.I.; Perlmutter, P.; Wilce, J. A. Uptake of a cell permeable G7-18NATE construct into cells and binding with the Grb7-SH2 domain. *Biopolymers* **2010**. DOI: 10.1002/bip.21403
- (37) Dixon, S. L.; Smondyrev, A. M.; Rao, S. N. PHASE: a novel approach to pharmacophore modeling and 3D database searching *Chem. Biol. Drug Des.* **2006**, *5*, 370-372.
- (38) Gschwend, D. A.; Good, A. C.; Kuntz, I. D. Molecular docking towards drug discovery. *J. Mol. Recognit.* **1996**, *9*, 175-186.
- (39) Joseph-McCarthy, D.; Baber, J. C.; Feyfant, E.; Thompson, D. C.; Humblet, C. Lead optimization via high-throughput molecular docking. *Curr. Opin. Drug Discov. Devel.* **2007**, *10*, 264-274.
- (40) Perozzo, R.; Folkers, G.; Scapozza, L. Thermodynamics of protein-ligand interactions: history, presence, and future aspects. *J. Recept. Signal Transduct. Res.* **2004**, *24*, 1-52.
- (41) Weininger, D. SMILES, a chemical language and information system. 1. Introduction to methodology and encoding rules, *J. Chem. Inf. Comput. Sci.* **1988**, *28*, 31-36.
- (42) Janes, P. W.; Lackmann, M.; Church, W. B.; Sanderson, G. M.; Sutherland, R. L.; Daly, R. J. Structural determinants of the interaction between the erbB2 receptor and the Src homology 2 domain of Grb7. *J. Biol. Chem.* **1997**, *272*, 8490-8497.
- (43) Porter, C. J.; Wilce, M. C.; Mackay, J.P.; Leedman, P.; Wilce, J. A. Grb7-SH2 domain dimerization is affected by a single point mutation. *Eur. Biophys. J.* **2005**, *34*, 454-460.
- (44) Pace, C. N.; Vajdos, F.; Fee, L.; Grimsley, G.; Gray, T. How to measure and predict the molar absorption coefficient of a protein. *Protein Sci.* **1995**, *4*, 2411-2423.

Chapter 7

Identification of phenylpropanone derivatives as a novel class of growth factor receptor bound 7 receptor antagonists

This chapter reports the virtual and experimental screening strategies pursued to design small molecular antagonists of Grb7 protein. Starting from the lowest energy conformer of a known tripeptide antagonist, computational tools ranging from shape based similarity searches, molecular docking to 2D-similarity searches was applied to discover and optimize potential candidates. Detailed binding characterization by ThermoFluor based thermal denaturation and isothermal titration calorimetry was made to identify a novel class of Grb7 antagonists possessing low molecular affinity.

Identification of phenylpropanone derivatives as a novel class of growth factor receptor bound 7 receptor antagonists

Nigus D. Ambaye, Menachem J. Gunzburg, Reece C.C. Lim, John T. Price, Matthew C.J. Wilce and Jacqueline A. Wilce

Abstract

Growth factor receptor-bound protein-7 (Grb7) is a cytoplasmic adaptor protein whose over expression has been implicated in a multitude of cancers such as breast, blood, bone, liver and ovarian tumors. This work reports the combined application virtual and experimental screening carried out to identify potent small molecular antagonist against the Grb7 oncoprotein. Specifically, a succession ligand shape based virtual screening, molecular docking, 2D-similarity searching, thermal shift assay and isothermal titration calorimetry have been effected to identify a novel class of small molecular antagonists. A total of 8 leads are suggested from the study which posses in vitro binding affinity in the lower micromolar range (6-17 μ M). Finally, in a cell growth assay the lead compound (NSC241906) was found to reduce the growth of a Grb7 expressing breast cancer cell lines. It is expected that these structures will serve as novel leads in the further development of anticancer therapeutics and to further probe the functional, signaling and structural studies of Grb7 protein.

Keywords: Grb7, adapter protein, SH2 domain, phenylpropanones: cancer cells, similarity search, virtual screening, ITC, ThermoFluor, melting point shift assay

Introduction

Growth factor receptor bound protein 7 (Grb7) is a 532 amino acid long protein that was identified as a binding partner for activated epidermal growth factor receptor [1]. It is a cytosolic protein known to couple membrane bound receptors to downstream effectors in growth factor mediated signal transduction. Because of the role of growth factors in gene regulation, Grb7 forms an important component in the complex network of proteins [2-4] that modulate cellular functions and is frequently up regulated in a number of human oncologies. For example, Grb7 over-expression has been implicated in a variety of human cancers such as breast [5], testicular [6], liver [7], esophageal [8,9] and ovarian carcinomas [10]. Moreover, the level of Grb7 over expression is noted to directly relate with severity of Barrett's carcinoma [11] and lymphocytic leukemia [12] indicating the role of Grb7 to transition cancers to advanced forms. Finally, published works exist that demonstrate that Grb7 is therapeutically amenable where synthetic peptides have been used to specifically block Grb7 which resulted in significant reduction of cancer cell properties [13]. A number of experiments conducted over the years on different aspect of Grb7 and its link with cancer cells have established it as an emerging target for anti-tumor drug development [14].

Grb7 is composed of mainly five well recognized domains namely the proline rich N-terminal domain, Ras-associating domain, pleckstrin homology domain (PH), Src sequence homology 2 (SH2) domain [15] and a region between the PH and SH2 domains termed BPS domain [14, 15]. Each domain is known to have different role that sum up and contribute to the over all signaling function of Grb7 [15,16]. Specifically, the SH2 domain is known to possess a cationic binding site that selectively binds phosphorylated tyrosines, thereby initiating the first step in Grb7 mediated signaling. The SH2 domain is known to control similar signaling events in several other proteins [15]. Moreover, the crystal structure of Grb7 SH2 domain giving detailed atomistic information about the three dimensional fold and binding site characteristics is available [17]. The present work relied upon the use of this domain of Grb7 as a receptor for the biochemical binding and computational studies.

Virtual screening of compound databases is a standard practice in lead identification projects [18, 19]. Depending on the chemical information available,

either structure or ligand based virtual screening can be pursued. Ligand based virtual screening is based on the assumption that similarity in structure will translate into similarity in pharmacological effects [20]. Ligand similarity measures based on 2D and 3D structures or ligand shape are commonly employed in ligand based virtual screening efforts. Specifically, due to the relevance of molecular conformation in biomolecular recognition, molecular shape based tactics have been implemented widely in virtual screening [21,22], quantitative structure activity relationship [23], molecular docking [24], and pharmacophore mapping [25] strategies. The present work employed a shape based similarity search of chemical database to successfully identify novel structural antagonists of Grb7.

There have been numerous reports on the design and optimization of agents geared towards inhibition of the broad class of growth factor receptor bound adaptor proteins, via their SH2 domains [26,27]. Interestingly, all the identified antagonists so far belong to the class of peptides. However, issues related to peptidic structures such as membrane permeability and in vivo stability present a formidable bottleneck to development of peptides to clinically useful agents. Most presumably due to these bottlenecks, to date there has not been a single peptide that is progressed into a useful therapeutic agent, though there have been extensive efforts over the last decade [4, 13]. With this in background, the present work was initiated to design a potent, selective and stable small molecular antagonist of the Grb7 oncoprotein. To the authors knowledge there has not been a single small molecular structure reported to inhibit Grb7. This work reports the successful application of a succession of virtual screening methods comprising shape based similarity search, small molecular docking, 2D-similarity search in conjunction with full thermodynamic characterization of lead binding with the use of melting point shift assay and isothermal titration calorimetric study to come up with novel structural class of Grb7 antagonists.

Material and Methods

Generation of the Shape Query

Since the experimental structure of the tripeptide in complex with Grb7 SH2 domain is not available, conformational search strategy was pursued to establish

the bioactive conformation. To this end, MacroModel's [29] conformation search [30] tool in Schrodinger [31] was employed to generate lowest energy conformer of the tripeptide. The optimal potential for liquid simulation force field with a distance dependent dielectric constant was during the conformation search. Partial charges were computed using the force field. Geometry optimization was effected using the optimal option with maximum iteration of 5000 and a gradient convergent criterion was applied with a threshold of 0.05. The systematic torsional sampling option was employed to generate representative conformations of the tripeptide reference query. All other parameters were kept at their default value.

Ligand Shape based similarity searching

The lowest energy conformer obtained from the conformational search was assumed to be close the bioactive conformer and hence was taken as a shape query to scan the NCI database. A mini-database of known antagonists was created in Schrodinger so as to have a minimal cut-off for the similarity metric value and to assess the relevance of the shape query [30]. The program PHASE [32] was used for the shape based similarity search. The atom type to use for volume scoring was put as none so as not to bias the search to particular hit class during screening the national cancer institute (NCI) chemical database. The average similarity index of the known antagonist was then used as a cut-off during the NCI screening.

Molecular docking

Computational prediction of binding affinity and geometry is a powerful tool in lead design [33, 34]. The program Glide was used to perform docking studies on top hits from the shape search. Glide comprises an incremental docking routine designed to suit to large chemical libraries [35, 36]. The protein used was solved as a co-crystal with a polypeptide antagonist in our lab, the details of which will be published elsewhere. It was read into Maestro in Schrodinger [31] and the protein preparation wizard was used to set up the Grb7 SH2 domain protein using one of the chains containing a co-crystallized peptide ligand. Hydrogen atoms were added and water molecules beyond 5 Å from protein atoms were deleted. Hydrogen bond assignment was effected with exhaustive sampling option and the system was subsequently relaxed with the minimization option. A grid of size 12 Å⁰x12 Å⁰x12 Å⁰ was defined

using the bound peptide to define the binding site. All the other parameters were kept at their default.

ThermoFluor based melting point shift assay

Validated hits from the virtual screening efforts were experimentally pre-screened using the ThermoFluor based melting point shift assay [37, 38]. ThmoFluor relies on differences in melting point between bound and unbound forms macromolecules to detect binding. The environmentally sensitive Sypro Orange dye was used to detect unfolding temperature of the complexes. ThermoFluor based thermal shift assay was conducted in a commercially available quantitative RT-PCR instrument (www.qiagen.com). The wavelength of excitation/emission was set to 470/555 and 470/610 nm with the detector gain kept of 5. A heating rate of at 1 °C/min was programmed over a temperature range of 30-80°C. The buffer used was 50mM MES, 100 mM NaCl at pH 6.6. The thermal denaturation was carried out in a reaction volume of 25 µl using a 72-tube holding rotor. The protein was added to each tube to yield a final concentration of 20 µM. The protein concentration was established using UV-VIS absorption spectroscopy at 280 nm and a molar extinction co-efficient of 8480 M⁻¹cm⁻¹. Each compound was prepared at 100 µM and 200 µM and the required volume mixed with the protein solution containing the dye. The apo form and a known peptide inhibitor were concurrently run as internal control and for comparative purposes. Each thermal denaturation experiment was conducted in duplicates and the average melting temperature was taken to calculate the change in melting points. The Rotor-Gene 3000 software was used to set up experiment and analyze the results.

Binding thermodynamics with isothermal titration calorimetry

The binding thermodynamics of the hits was determined by calorimetry using VP-ITC Microcalorimeter (Microcal, Northampton, MA, USA) at 25 °C [39,40] and pH 6.6. The receptor protein was dialyzed against two liters of 50 mM NaOOCCH₃, 100 mM NaCl and 1 mM DTT at 4 °C overnight. The concentration of Grb7 SH2 was determined by recording its absorbance at 280 nm whereas the concentrations. The hit and protein solutions were degassed and thermostated at 20 °C for 5 min using

the ThermoVac of the VP-ITC Microcalorimeter. The reference power of the experiment was set to 25 μ Cal/sec and the cell contents were stirred continuously at 307 rpm throughout the titrations. The reference cell was filled with MQ water. The concentration of the hits in range of 500-900 μ M concentrations was titrated into Grb7 SH2 solutions of 50-85 μ M concentrations in 7-10 μ L injections with a 3-6min delay between each injection. A binding isotherm was generated by plotting the heat change evolved per injection against the molar ratio of the compounds to Grb7 SH2 domain receptor. A blank determination in which the compounds were titrated against the buffer was carried out to account for heats of dilution and mixing which was then subtracted from the binding data. The corrected data was then employed to fit to a single binding site model using a non-linear least squares with the Origin (Microcal Software, Northampton, MA, USA). All of the thermodynamics parameters were kept floating during the fitting procedure.

Lead optimization by two-dimensional similarity search

From the combination of computational and experimental studies conducted, compound NSC241906 came out as promising lead. It was then taken as a lead to further explore the structure in a bid to optimize the observed affinity. To this end, analogues of this compound was sought and since the objective now was to examine structurally analogues of the above lead, two-dimensional structure based similarity search was found appropriate to extract the desired analogues. The 2D-search was pursued on the same NCI database using the SMILES representation of the lead compound. Hits with a Tanimotto similarity of above 90% were retained for subsequent investigation. In particular, the ThermoFluor based pre-screening and thermodynamic characterization with ITC was conducted on the analogues in identical protocol as described above.

Expression and Purification of Grb7 SH2 domain

The SH2 domain of Grb7 was used as a receptor for the thermal shift and ITC binding experiments. The pGex2T plasmid containing the Grb7 SH2 insert encoding residues 415-532 of human Grb7 protein was obtained from collaborators [41] and expressed in *E. coli* expression system as a GST fusion protein in BL21 (DE3) pLysS

host strains [42]. Cell induction was achieved with a 400 μ M Isopropyl β -D-1-thiogalactopyranoside. Cell resuspension was carried out in ice-cold phosphate buffer saline with 2 mM EDTA, 0.5% Triton-X 100 and lysis by sonication. The fusion protein was purified by glutathione affinity chromatography (GE Healthcare) and cleaved with thrombin. Purification on cation exchange chromatography was then effected using a HiTrap HP column (GE) after an overnight dialysis into 20 mM HEPES pH 7.4, 20% Glycerol and 1 mM DTT at 4 °C. This was followed by dialysis into 50 mM MES pH 6.6, 100 mM NaCl and 1mM DTT and final purification by size exclusion chromatography using a Sephadex 75 XK 16/60 column (GE). Grb7-SH2 domain was concentrated and stored at 4 °C. The final concentration was determined with UV-Visible spectroscopy [43].

Cellular assay

To determine the effects of the compounds on cellular growth, cells were resuspended at 5×10^4 cells/mL and 100 μ L of this cell suspension was plated in 96 well plates (BD Biosciences, California, USA). The following day cells were treated with a range of various concentrations of the compounds, each concentration with triplicates wells. Cells were incubated under standard growth conditions with 10% fetal bovine serum over a four-day period (0-4 days). Adherent cell cultures were fixed *in situ* after 4 days by the addition of 25 ml of cold 50% trichloroacetic acid solution (Sigma-Aldrich, Missouri, USA) and incubated for 60 minutes at 4°C. The supernatant was then discarded and the plate was washed five times with running distilled water before being dried overnight. Fixed cells were stained by the addition of 100 ml of sulforhodamine B (SRB) sodium salt solution (0.4% (w/v) in 1% Acetic Acid; Sigma-Aldrich, Missouri, USA) and incubated for 10 minutes at room temperature. Unbound SRB solution was removed by washing five times with 1% Acetic Acid after which the plates were air-dried overnight. The following day, the bound stain was solubilized with 100 ml of 10 mM Tris buffer (pH 10.5) and the absorbance of the eluted dye was read on the spectrophotometric BMG PolarStar Optima plate reader (BMG Labtech, Offenburg, Germany) at 540 nm. SRB is a total protein stain, which directly correlates with cell number and is used routinely to measure cell proliferation rate. The nonlinear regression analysis of the concentration-response plot was done by GraphPad Prism software.

Results

Structural studies of SH2 domain bound to ligands have revealed the common features of their ligand interaction and shown how they vary to achieve selectivity [17]. As a starting point to the filtering of compounds, the shape query was generated using a tripeptide- m-aminobenzyol-pY (α -Me) pYN-NH₂. The tripeptide amide was selected as it is presently the most potent antagonist of all growth factor bound adaptor proteins and also as it is the smallest and simplest of the known antagonists [28]. Since the overall size is considered in the shape based hit identification process, taking this potent yet small tripeptide is considered more appropriate to identify potential small molecular antagonists.

Shape similarity search

Ligand conformation is important in drug-receptor interactions. When experimental structure is available, the bound conformation is regarded as the bioactive conformation that is complementary to the shape of the binding site [44]. However, in many instances experimental conformation is not available. The practice is then to carry out conformational sampling with to establish the bioactive conformation [45]. This derives from the observation that biologically active conformation of a given ligand is also the lowest energy conformers, at least in the majority of the cases [46]. In the present study, since the experimental conformer is not available the lowest energy conformer from the conformational search was taken to be the bioactive conformer and hence as a shape query. As a rapid assessment of the potential utility of the shape query, it was first applied on a mini-database of known antagonist [47]. The result as shown in Table 7.1 shows a correlation co-efficient of 0.58 between the shape similarity indices of the antagonists and their pIC₅₀ values. This is taken to suggest the existence of a quantitative relationship in using the lowest energy conformer as a shape query ($r^2 = 0.58$) and hence it was used to screen the NCI database in the lead identification efforts.

Table 7.1. Shape similarity index of known Grb7 antagonists using the top five conformers of the tripeptide reference as a query

S.No	Known Antagonist	pIC ₅₀ ^a	Shape Similarity co-efficient ^b
1	PEpYVNQ-NH2	5.96	0.54
2	Ac-pYVNQ-NH2	5.47	0.51
3	EpYVNQ-NH2	5.82	0.51
4	pYVNQ-NH2	5.45	0.45
Correlation Co-efficient (r ²) ^c			0.58

^a The pIC₅₀ values were obtained from the reported IC₅₀ value [47] using the equation $pIC_{50} = -\log IC_{50}$; ^bThe shape similarity co-efficient for the known Grb7 antagonists was obtained using the lowest energy conformer of the query tripeptide; ^cThe correlation co-efficient indicates the correlation between the pIC₅₀ value and the shape similarity co-efficient of the antagonists.

Virtual screening of the NCI chemical database

The lowest energy conformer of the tripeptide was then employed to scan the NCI chemical database. Use of the lowest energy conformer as shape query to screen the database (which contains 250, 251 structures at the time of this work) returned a total of 67,000 hits. The top structures from the shape search were further screened using Glide based molecular docking protocol. The top 2,500 from the search were docked using Glide high-throughput virtual docking. This initial crude docking protocol resulted in 1,255 successfully docked hits. All of the 1,255 hits were subsequently re-docked using the more accurate Glide's standard precision (Glide SP) docking procedure. The top 500 from the Glide SP docking were finally docked with extra precision Glide docking routine. The molecular docking protocol was the same throughout the computational experiment. The top 20 hits were retained as promising after binding mode analysis and comparison with that of the in-house solved co-crystal peptide binding geometry. The details of the binding geometry including the site and retention of interaction with key residues of Grb7 binding site was taken into consideration. Reproduction of this experimentally observed binding mode together with analysis of the docking score and visual inspection of the structures was taken as a criterion of confidence on the hits. The top 20 promising hits identified and their docking score is indicated in Table 7.2.

Table 7.2: Hits obtained from virtual screening experiment.

Rank	Hit ID.	Shape Similarity Index	Glide SP docking	
			Glide Score	Emodel
1	NSC677145	0.413	-5.604	-78.153
2	NSC655103	0.484	-5.602	-69.959
3	NSC677154	0.411	-5.234	-72.376
4	NSC298195*	0.410	-5.001	-62.452
5	NSC677141	0.456	-4.967	-61.855
6	NSC721629	0.411	-4.741	-53.406
7	NSC694862	0.410	-4.698	-60.918
8	NSC109967	0.410	-4.678	-45.845
9	NSC292212	0.411	-4.655	-50.453
10	NSC20097	0.419	-4.627	-59.116
11	NSC677148	0.447	-4.583	-64.829
12	NSC683133	0.448	-4.565	-54.374
13	NSC716944	0.411	-4.534	-57.543
14	NSC181979	0.411	-4.457	-39.459
15	NSC156846*	0.439	-4.362	-57.715
16	NSC677149	0.447	-4.320	-62.313
17	NSC241906*	0.428	-4.277	-44.954
18	NSC160945*	0.411	-4.143	-42.885
19	NSC683134	0.498	-4.108	-53.553
20	NSC21571*	0.448	-3.952	-41.429

Note: * indicates tested experimentally.

Prediction of binding mode of hit NSC241906

The binding mode of the hits was predicted and agreement with that of experimentally observed binding mode investigated as criteria to filter the hits from virtual screening. The binding mode of hit NSC241906 is displayed in Fig. 7.1 as an illustration. As the figure shows, the compound forms three hydrogen bonds by its three hydroxyl groups. The carbonyl carbon of Met495 is predicted to make two hydrogen bonds with the OH of the lead. The other OH of the lead is also noticed to form a hydrogen bond with the backbone NH of Tyr480. Both Met495 and Tyr480 are one of the important residues to which a co-crystal structure is known to bind experimentally. The phenyl ethyl moiety is placed in a hydrophobic pocket defined by the side chains of residues Ile518, Leu519, Pro520 and Tyr480 indicating NSC241906 could make strong hydrophobic/van der Waals bonds with this residues. In addition, the phenoxymethyl moiety of the hit is engulfed by hydrophobic residues including Leu481 and Leu483 indicating another potential

hydrophobic/van der Waals bond between the lead and binding site residues of Grb7. Retention of interaction with key residues of the binding site (Tyr480, Ile518, Leu481, Met495) looks to suggest the binding the potential such hits could have as Grb7 antagonists.

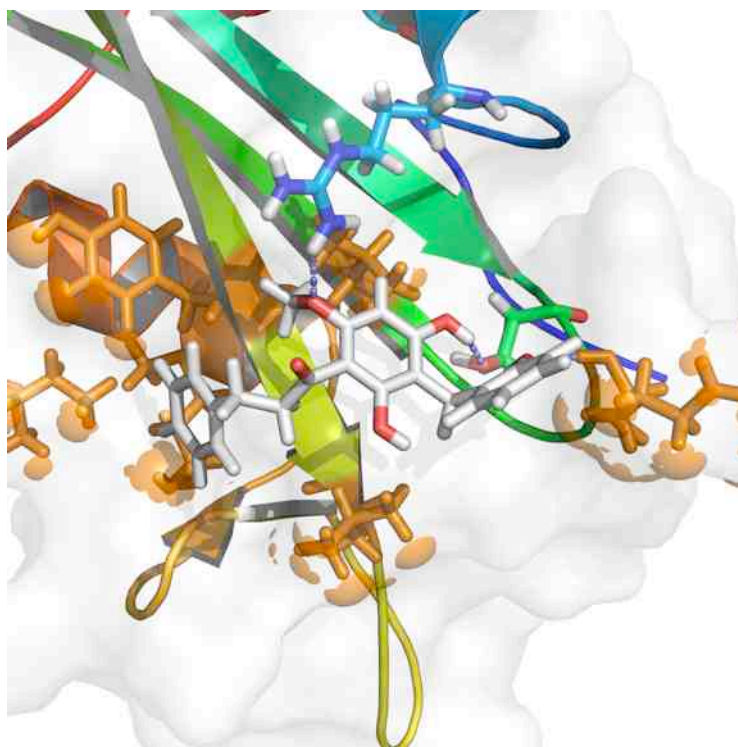


Figure 7.1: Binding mode of hit NSC241906. The hit is displayed in ball and stick format while binding site residues involved in non-polar interaction are shown in orange stick and ball. Hydrogen bonds are shown in blue dots. The Grb7 SH2 domain protein is represented in transparent surface. The secondary structural elements are indicated in the surface.

Experimental pre-screening with melting point shift assay

Experimental hit prescreening was carried out with ThermoFluor based thermal shift assay as it is fast and requires minimal amount of hit and protein [37,38]. Out of the top 20 potential leads, 5 were available at the time of this work and kindly provided by the NCI Developmental and Therapeutic program unit of the USA (Drug synthesis and Chemistry branch, <http://www.cancer.gov/>). The 5 hits were experimentally screened with thermo flour based thermal shift assay. A positive melting point shift of the hit/Grb7 SH2 domain complex when compared to the unbound form of the protein is taken as an indicator of binding phenomenon. From

this preliminary melting experiment, compound NSC241906 produced a positive melting point shift (0.25 at 150 μ M and 0.65 at 300 μ M). Though this is lower than the control polypeptide antagonist (08-5992, 0.65 at 150 μ M and 1.3 at 300 μ M), it is nevertheless significant. Such equivalent values for were previously used by other workers to get micromolar inhibitors [48,49]. Also shown in Table 7.3 is the melting point shift and Tanimotto similarity co-efficient of analogues of NSC241906 obtained from the 2D-similarity searching. As the data show, the values are better than the NSC241906 and most even are comparable to the peptide control or better. Especially NSC75523 (1.6 at 150 μ M, 1.35 at 300 μ M) and NSC75524 (1.4 at 150 μ M, 1.62 at 300 μ M) and NSC89759 (1.1 at 150 μ M, 1.45 at 300 μ M) have clearly produced more stabilization even when compared to the known antagonist. The glide docking scores obtained are found to be comparable. This indicates that the analogues from the 2D-search may be bind in higher affinity as compared to hit NSC241906.

Table 7.3: 2D-similarity and melting point shift data for Phenylbenzamide derivatives

S.No.	Hit	Tanimotto Co-efficient	Glide score		$\Delta T_m(^{\circ}\text{C})$	
			SP	XP	150uM	300uM
1	NSC241906	1.00	-3.57	-3.58	0.25	0.65
2	NSC75523	0.92	-3.58	-2.69	1.60	1.35
3	NSC75524	0.94	-4.24	-4.33	1.4	1.62
4	NSC78015	0.92	-3.44	-2.56	1.25	0.85
5	NSC78638	0.96	-3.88	-3.00	1.85	0.85
6	NSC89759	0.93	-3.72	-3.20	1.1	1.45
7	NSC91849	0.92	-3.64	-3.70	0.6	1.25
8	NSC94613	0.95	-4.07	-3.18	1.75	0.90
A	08-5992	NA	-4.49	-3.59	0.65	1.3
B	Grb7 SH2 apo	Not applicable			$T_m = 51.6$	

Note: NA = not applicable. The change in melting point (ΔT_m) are obtained from duplicate experiments and are obtained after the melting point of Grb7 SH2 apo ($T=51.5^{\circ}\text{C}$) is subtracted from that of the hit bound form

ITC binding study and 2D-similarity searches

Thermodynamic characterization of ligand-receptor interaction by ITC is a useful in lead optimization studies [40]. ITC relates the amount of heat absorbed or released to the amounts of the interacting species and provides parameters such as binding

free energy, enthalpy, entropy and stoichiometry from a single experiment [39]. The thermodynamics of hit NSC241906 from the melting experiment was determined by ITC. As shown in Table 7.4, the experiment is found to confirm that the hit does indeed bind with moderate affinity (ca. 13.7 μ M) and further provides detailed parameters of the binding. The structure is found to bind in with large favorable entropy. This confirms the thermal melting experiment that the compound does indeed bind. Thus, the combinations of virtual and experimental investigation on the hit established it as interesting one worthy of further exploration. With this in mind, 2D-similarity search was then pursued in order to get analogues with better affinity. Use of the lead as a 2D-query returned 61 hits out of which 25 were available from the NCI developmental and Therapeutic program. The 25 compounds were then first assessed using the melting point shift assay as described above. The result, also shown in Table 7.3, indicates that out of the 25 structural analogues tested 7 were able to produce a positive melting point shift. This corresponds to about 28% in hit rate. The structure of the 7 leads identified in addition to the starting structure is displayed in Fig. 7.3.

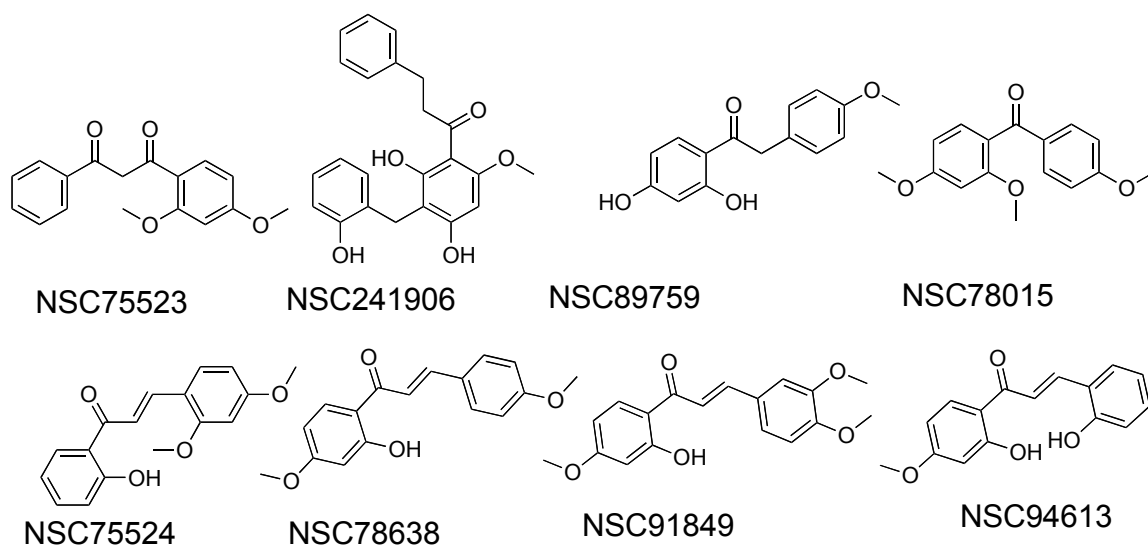


Figure 7.2: Chemical Structures of the PhenoxyPropanone derivatives

Full thermodynamic characterization of three representative compounds from the 2D-similarity search was characterized with ITC. The experimental binding affinities of NSC241906 and its analogues (NSC75523, NSC75524 and NSC78015)

were determined in identical experimental conditions including identical buffer composition and titration schedules. Fig. 7.3. shows the ITC binding isotherm for two of the analogues tested while Table 7.4 shows the values for the thermodynamic binding parameters. Close investigation of the binding data displayed in Fig. 7.3 and Table 7.4 reveals that there is a subtle difference in the mode of associations. Specifically, the prototype lead- NSC241906-is found to bind with absorption of heat while its analogues are observed to interact through evolution of heat energy. This is not immediately clear had one have to consider the dissociation constant alone. In all cases, the stoichiometry of binding is found to be similar at a 1:1 ratio and it is found to be similar to that of peptide antagonist [17]. Moreover, deconvolution of the binding affinity into its parts show additional differences in the relative contribution of each component to the over all free energy of binding. In the case of the parent NSC241906 binding, the entropic part ($T\Delta S$) is about three times higher than the enthalpic (9.3 kcal/mol vs 2.7 kcal/mol) which looks to make its interaction with Grb7 as entropically driven. On the other extreme, lead NSC75523 seems to binding is with large unfavorable entropy (18.5 kcal/mol) which is compensated by a huge enthalpic contribution (24.97 kcal/mol) to the binding. For compounds NSC745524 and NSC78015 seems to bind through favorable enthalpy and entropy even though in both cases the more enthalpic part is pronounced especially with lead NSC75524 where the enthalpic part is found to be six times higher.

Despite differences in the relative contribution of enthalpy/entropy to the over all free energy of binding, the gross binding affinities found remain similar being in a moderate micromolar range (6-17 μM). This look to suggest that there is entropy-enthalpy compensation as the K_d values remain more or less unaffected. This is commonly observed in ligand-receptor binding studies [48]. Overall, the binding affinity of this small molecular leads is slightly better than affinity of the query polypeptide ($K_d = 35 \mu\text{M}$) determined in identical condition [17].

Table 7.4: Binding parameters for PhenoxyPropanone derivatives

Binding Parameter	NSC241906	NSC75523	NSC75524	NSC78015
Stoichiometry	1.08±0.06	1.09±0.05	0.99±0.03	1.1±0.07
$K(10^4\text{M}^{-1})$	7.32±1.68	5.81±1.1	12.1±1.7	15.1±1.3
$\Delta H(\text{kcalmole}^{-1})$	2.68±0.24	-24.97±1.57	-5.95±0.21	-2.89±0.29
$\Delta S(\text{calmole}^{-1}\text{K}^{-1})$	31.2	-61.95	3.26	14.0
$-T\Delta S(\text{kcalmole}^{-1})$	-9.30	-18.47	-0.97	-4.17
$\Delta G(\text{kcalmole}^{-1})$	-6.62±0.24	-6.501±1.57	-6.92±0.21	-7.06±0.29
$K_d(\mu\text{M})$	14.42 ±3.3	17.85±3.4	8.43 ±2.81	6.67 ±0.57

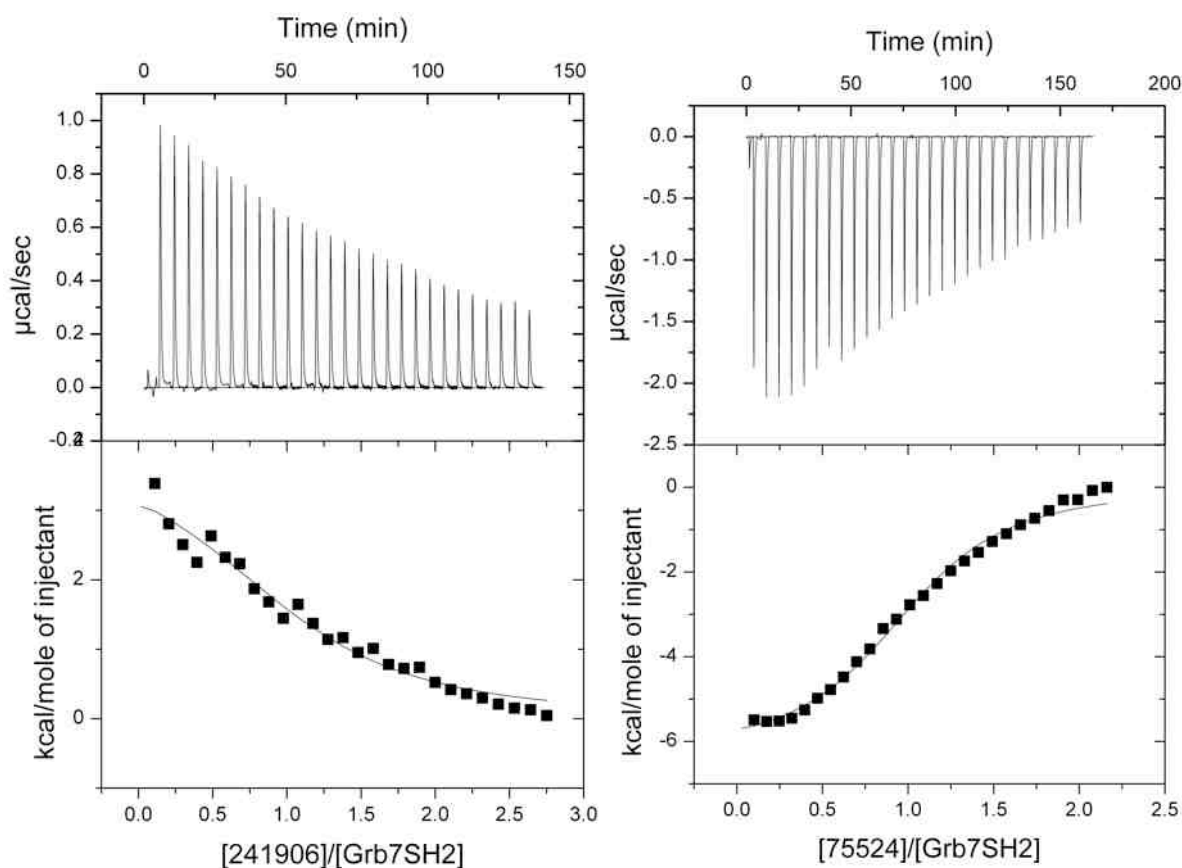


Figure 7.3. ITC thermograms of NSC24906 analogues. The upper panel show raw data obtained from 10µl injections of peptides at 25°C. The lower panels in both figures display plots of integrated total energy exchanged (as kcal/mol of injected peptides) as a function of molar ratio of the peptides to the Grb7 SH2 domain:

Cellular assay

Confirmation of binding by in vivo studies is an important component in ligand design as it gives legitimacy to the overall process. The cytotoxicity study on Grb7 expressing cancer cells as determined as shown in Fig.7.5.

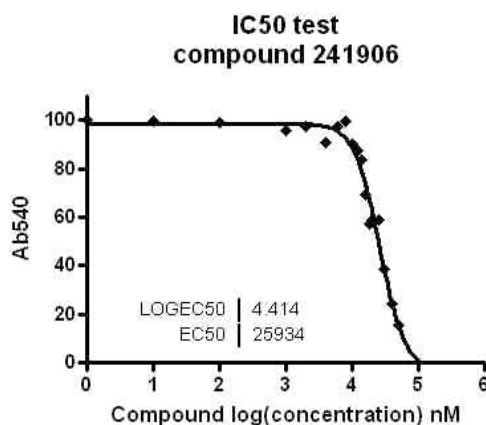


Figure 7.5. Cytotoxicity study on Grb7 expressing cells of the lead compound NSC241906. The lead compound NSC241906 displayed growth inhibitory effects against MDA-MB-468 breast cancer cells. The IC_{50} obtained is 26 μ M, which closely relates the $K_d = 14.42$ μ M obtained by ITC.

Discussion

Grb7 is confirmed to have multi-factorial role in cancer cell biology [13, 15, 17], which render it an attractive target in anti-cancer drug discovery. Up until now, few antagonists have been specifically developed for Grb7 inhibition [17, 49]. Interestingly, all the antagonists identified so far belong to a single class peptides [47,49] that are designed based on the recognition motif around the phosphotyrosine residues on binding partners of Grb7. However, issues inherent to peptide structures such as membrane permeability, bioavailability, stability, poor solubility, synthetic difficulty and immunogenicity means that non-peptide leads are invaluable in the development of Grb7 based anti-cancer therapeutics [50]. Moreover, as Grb7 is an intracellular protein whose downstream effectors remain virtually unknown, the availability of small molecular antagonists will be of aid to further explore the signaling and functional studies involving Grb7 protein.

The lock-and-key concept in biomolecular interactions assumes that ligand and binding site shapes are complementary and that ligands that preset the best complementarity are expected to be potent agonists/antagonists. Exploiting this concept, the shape based virtual screening experiment was able to identify potential lead candidate. However, the shape searches alone was not that productive as most of the best scoring hits from the shape similarity search did not even pass the docking test. The application of a succession of virtual screening tools was effective enough to yield promising hits. As we went from the gross shape based to the more specific 2D-similarity search, an increase in hit rate is noted. This is consistent to the similarity principle that states that structurally similar molecules are expected to be similar in their physicochemical and biological properties [20,21]. The virtual screening experiments attest to the usefulness of the application of a succession of virtual screening tools in conjunction to experimental screening approaches.

The melting point shift assay is based on the fact that chemical bond formation results in stabilization of products and that the strength of the bond formed reflects the overall stability of the product. In ligand-receptor associations, potent ligands are expected to form more strong bonds or more number of atom-to-atom binding interactions than weaker ones. ThermoFluor applies heat energy to the ligand-receptor complex and detects differences in the heat energy required to bring about dissociations. In this manner the observed changes in melting temperature is taken to be directly proportional to the potencies ligand binding. The melting point shift data for the leads identified are close to each other and this is analogously reflected in the binding affinity value obtained from the ITC data. This is to be expected since both the melting and binding experiments measure the strength of the ligand-receptor complex formed. Indeed this parallelism has allowed workers to estimate the binding affinity of biomolecular associations [37, 38] from the thermal shift data alone. Moreover, both the thermal shift and affinity values are also comparable to that of known peptide inhibitor, even though those of the small leads are better in their dissociation constant values (cf. $K_d = 35 \mu\text{M}$)[17]. This looks to be attributed to the better entropy component of binding as compared to that of the polypeptide (data to be not shown). Considering their non-peptidic structure and the comparable affinity values obtained as compared to the polypeptide antagonist of

Grb7, the identified structures are presumed to overcome the problems of peptide based antagonist.

In sum, starting with a potent tripeptide the present work reported the successful application of a succession of computational ligand design tools comprising conformational searching, shape based similarity screening, molecular docking and 2D-similarity methods to identify a novel class of small molecular antagonists of Grb7. Experimental binding study with melting-point shift assay and isothermal titration calorimetry has enabled full thermodynamics characterization of the interaction and to shed some light into the mechanistic aspect of the binding interaction. That the phenylpropanone based antagonists bind with moderate affinity was confirmed by cellular assay illustrating the potential of the antagonists in living systems. It is expected that the identified scaffolds will be useful additional agents to further explore and accelerate the functional, signaling and structural studies of adaptor proteins.

Acknowledgement

This work was funded by an Australian Research Council Project Grant awarded to JAW and DNK and a Monash University Graduate Scholarship awarded to NDA. We thank the Drug Synthesis and Chemistry Branch of National Cancer Institute of the USA for providing the compounds used in the screening and testing. The Victorian partnership for advanced computing (VPAC) is acknowledged for granting us access to the computational facility employed in the study.

References

- [1] B. Margolis, O. Silvennoinen, F. Comoglio, C. Roonprapunt, E. Skolnik, A. Ullrich, J. Schlessinger, High-efficiency expression/cloning of epidermal growth factor-receptor-binding proteins with Src homology 2 domains, *Proc. Natl. Acad. Sci. USA.* 89 (1992) 8894-8898.
- [2] D.C. Han, J.L. Guan, Association of focal adhesion kinase with Grb7 and its role in cell migration, *J. Biol. Chem.* 274 (1999) 24425-24430.
- [3] D.C. Han, T.L. Shen, J.L. Guan, Role of Grb7 targeting to focal contacts and its phosphorylation by focal adhesion kinase in regulation of cell migration, *J. Biol. Chem.* 275 (2000) 28911-28917.
- [4] T.L. Shen, J.L. Guan, Differential regulation of cell migration and cell cycle progression by FAK complexes with Src, PI3K, Grb7 and Grb2 in focal contacts. *FEBS Lett.* 499 (2001) 176-181.
- [5] D. Stein, J. Wu, S.A. Fuqua, C. Roonprapunt, V. Yajnik, P. D'Eustachio, J.J. Moskow, A.M. Buchberg, C.K. Osborne, B. Margolis, The SH2 domain protein GRB-7 is co-amplified, overexpressed and in a tight complex with HER2 in breast cancer, *Embo. J.* 13 (1994) 1331-1340.
- [6] N.C. Goddard, A. McIntyre, B. Summersgill, D. Gilbert, S. Kitazawa, J. Shipley, KIT and RAS signaling pathways in testicular germ cell tumors: new data and a review of the literature, *Int. J. Androl.* 30 (2007) 337-348.
- [7] S. Itoh, A. Taketomi, S. Tanaka, N. Harimoto, Y. Yamashita, S. Aishima, T. Maeda, K. Shirabe, M. Shimada, Y. Maehara, Role of growth factor receptor bound protein 7 in hepatocellular carcinoma, *Mol. Cancer Res.* 5 (2007) 667-673.
- [8] S. Tanaka, M. Mori, T. Akiyoshi, Y. Tanaka, K. Mafune, J.R. Wands, K. Sugimachi, Coexpression of Grb7 with epidermal growth factor receptor or Her2/erbB2 in human advanced esophageal carcinoma, *Cancer Res.* 57 (1997) 28-31.
- [9] P.S. Dahlberg, B.A. Jacobson, G. Dahal, J.M. Fink, R.A. Kratzke, M.A. Maddaus, L.J. Ferrin, ERBB2 amplifications in esophageal adenocarcinoma, *Ann. Thorac. Surg.* 78 (2004) 1790-1800.
- [10] Y. Wang, D.W. Chan, V.W. Liu, P. Chiu, H.Y. Ngan, Differential functions of growth factor receptor-bound protein 7 (GRB7) and its variant GRB7v in ovarian carcinogenesis, *Clin. Cancer Res.* 16 (2010) 2529-2539.
- [11] A. Walch, K. Specht, H. Braselmann, H. Stein, J.R. Siewert, U. Hopt, H. Höfler, M. Werner, Coamplification and coexpression of Grb7 and ERBB2 is found in high grade intraepithelial neoplasia and in invasive Barrett's carcinoma, *Int. J. Cancer*, 112 (2004) 747-753.
- [12] M. Haran, S. Chebatco, L. Flaishon, F. Lantner, N. Harpaz, L. Valinsky, A. Berrebi, I. Shachar, Grb7 expression and cellular migration in chronic lymphocytic leukemia: a comparative study of early and advanced stage disease, *Leukemia* 18 (2004) 1948-1950.
- [13] S.C. Pero, G.S. Shukla, M.M. Cookson, S. Flemer Jr, D.N. Krag, Combination treatment with Grb7 peptide and Doxorubicin or Trastuzumab (Herceptin)

- results in cooperative cell growth inhibition in breast cancer cells, *Br. J. Cancer* 96 (2007) 1520-1525.
- [14] S.C. Pero, R.J. Daly, D.N. Krag, Grb7-based molecular therapeutics in cancer *Expert Rev. Mol. Med.* 5 (2003) 1-11.
- [15] T. Pawson, G.D. Gish, P. Nash, SH2 and SH3 domains in signal transduction, *Adv. Cancer Res.* 64 (1994) 87-110.
- [16] D.C. Han, T.L. Shen, J. L. Guan, The Grb7 family proteins: structure, interactions with other signaling molecules and potential cellular functions. *Oncogene* 20 (2001) 6315-6321.
- [17] C.J. Porter, J.M. Matthews, J.P. Mackay, S.E. Pursglove, J.W. Schmidberger, P.J. Leedman, S.C. Pero, D.N. Krag, M.C. Wilce, J.A. Wilce, Grb7 SH2 domain structure and interactions with a cyclic peptide inhibitor of cancer cell migration and proliferation, *BMC Struct Biol.* (2007) 7:58.
- [18] K.H. Bleicher, H.J. Bohm, K. Muller, A.I. Alanine, A guide to drug discovery: Hit and lead generation: beyond high-throughput screening. *Nat. Rev. Drug Discov.* 2 (2003) 369-378.
- [19] T.I. Oprea, H. Matter, Integrating virtual screening in lead discovery, *Curr. Opin. Chem. Biol.* 8 (2004) 349-358.
- [20] Y.C. Martin, J.L. Kofron, L.M. Traphagen, Do structurally similar molecules have similar biological activity, *J. Med. Chem.* 45 (2002) 4350-4358.
- [21] N. Nikolova, J. Jaworska, Approaches to measure chemical similarity-A review. *QSAR Comb. Sci.* 22 (2004) 1006-1026.
- [22] S. Putta, C. Lemmen, P. Beroza, J. Greene, A novel shape-feature based approach to virtual library screening, *J. Chem. Inf. Comput. Sci.* 42 (2002) 1230-1240.
- [23] R.D. Cramer III, D.E. Patterson, J. D. Bunce, Comparative Molecular Field Analysis (CoMFA). 1. Effect of Shape on Binding of Steroids to Carrier Proteins, *J. Am. Chem. Soc.* 110 (1988), 5959-5967.
- [24] B.B. Goldman, W.Y. Wipke, QSD quadratic shape descriptors. 2. Molecular docking using quadratic shape descriptors (QSDock), *Proteins*, 38,2000,79-94.
- [25] H. Verli, M.G. Albuquerque, R. Bicca de Alencastro, E.J. Barreiro, Local intersection volume: a new 3D descriptor applied to develop a 3D-QSAR pharmacophore model for benzodiazepine receptor ligands, *Eur. J. Med. Chem.* 37 (2002) 219-229.
- [26] T.R. Burke, Development of Grb2 SH2 Domain Signaling Antagonists: A Potential New Class of Antiproliferative Agents, *Int. J. Pept. Res. Ther.* 12 (2006) 33-48.
- [27] H. Fretz, P. Furet, C. Garcia-Echeverria, J. Schoepfer, J. Rahuel, Structure-based design of compounds inhibiting Grb2-SH2 mediated protein-protein interactions in signal transduction pathways, *Curr. Pharm. Des.* 6 (2000) 1777-1796.
- [28] W.-Q. Liu, M. Vidal, N. Gresh, B.P. Roques, C. Garbay, Small Peptides Containing Phosphotyrosine and Adjacent α -Me-Phosphotyrosine or Its

- Mimetics as Highly Potent Inhibitors of Grb2 SH2 Domain, *J. Med. Chem.* 47(2004) 1223-1233.
- [29] F. Mohamadi, N.G.J. Richard, W.C. Guida, R. Liskamp, M. Lipton, C. Caufield, G. Chang, T. Hendrickson, W.C. Still, MacroModel-an Integrated Software System for Modeling Organic and Bioorganic Molecules Using Molecular Mechanics, *J. Comput. Chem.* 11 (1990) 440-467.
- [30] M. Christen, W.F. van Gunsteren, On searching in, sampling of, and dynamically moving through conformational space of biomolecular systems: A review, *J. Comput. Chem.* 29 (2008) 157-66.
- [31] Schrodinger LLC, 120 West 45th Street, New York, New York.
- [32] S.L. Dixon, A.M. Smondyrev, S.N. Rao, PHASE: A Novel Approach to Pharmacophore Modeling and 3D Database Searching, *Chem. Biol. Drug Des.*, 67 (2006) 370-372.
- [33] N. Huang, C. Kalyanaraman, K. Bernacki, M.P. Jacobson, Molecular mechanics methods for predicting protein-ligand binding, *Phys. Chem. Chem. Phys.* 8 (2006) 5166-5177.
- [34] A.T. Laurie, R.M. Jackson, Methods for the prediction of protein-ligand binding sites for structure-based drug design and virtual ligand screening, *Curr. Protein Pept. Sci.* 7 (2006) 395-406.
- [35] R.A. Friesner, R.B. Murphy, M.P. Repasky, L.L. Frye, J.R. Greenwood, T.A. Halgren, P.C. Sanschagrin, D.T. Mainz, Extra Precision Glide: Docking and Scoring Incorporating a Model of Hydrophobic Enclosure for Protein-Ligand Complexes, *J. Med. Chem.* 49 (2006) 6177-6196.
- [36] R.A. Friesner, J.L. Banks, R.B. Murphy, T.A. Halgren, J.J. Klicic, D.T. Mainz, M.P. Repasky, E.H. Knoll, M. Shelley, J.K. Perry, D.E. Shaw, P. Francis, P.S. Shenkin, Glide: A New Approach for Rapid, Accurate Docking and Scoring. 1. Method and Assessment of Docking Accuracy, *J. Med. Chem.* 47 (2004) 1739-1749.
- [37] M.W. Pantoliano, E.C. Petrella, J.D. Kwasnoski, V.S. Lobanov, J. Myslik, E. Graf, T. Carver, E. Asel, B.A. Springer, P. Lane, F.R. Salemme, High-density miniaturized thermal shift assays as a general strategy for drug discovery, *J. Biomol. Screen.* 6 (2001) 429-440.
- [38] D. Matulis, J.K. Kranz, F.R. Salemme, M.J. Todd, Thermodynamic stability of carbonic anhydrase: measurements of binding affinity and stoichiometry using ThermoFluor, *Biochemistry* 44 (2005) 5258-5266.
- [39] M.W. Freyer, E.A. Lewis, Isothermal titration calorimetry: experimental design, data analysis, and probing macromolecule/ligand binding and kinetic interactions. *Methods Cell Biol.* 84 (2008) 79-113.
- [40] R. Perozzo, G. Folkers, L. Scapozza, Thermodynamics of protein-ligand interactions: history, presence, and future aspects, *J. Recept. Signal Transduct. Res.* 24 (2004) 1-52.
- [41] P.W. Janes, M. Lackmann, W.B. Church, G.M. Sanderson, R.L. Sutherland, R.J. Daly, Structural determinants of the interaction between the erbB2 receptor

- and the Src homology 2 domain of Grb7, *J. Biol. Chem.* 272 (1997) 8490-8497.
- [42] C.J. Porter, M.C. Wilce, J.P. Mackay, P. Leedman, J.A. Wilce, Grb7-SH2 domain dimerisation is affected by a single point mutation, *Eur. Biophys. J.* 34 (2005) 454-460.
- [43] C.N. Pace, F. Vajdos, L. Fee, G. Grimsley, T. Gray, How to measure and predict the molar absorption coefficient of a protein, *Protein Sci.* 4 (1995) 2411-2423.
- [44] R.P. Bahadur, M. Zacharias, The interface of protein-protein complexes: analysis of contacts and prediction of interactions, *Cell Mol. Life Sci.* 65 (2008) 1059-1072.
- [45] M. Botta, F. Corelli, F. Manetti, A. Tafi, Molecular modeling as a powerful technique for understanding small-large molecules interactions, *Farmaco*, 57 (2002) 153-165.
- [46] J. Bostrom, Reproducing the conformations of protein-bound ligands: a critical evaluation of several popular conformational searching tools, *J. Comput.-Aided Mol. Des.* 15 (2001) 1137-1152.
- [47] J.P. Luzy, H. Chen, B. Gril, W.Q. Liu, M. Vidal, D. Perdereau, A.F. Burnol, C. Garbay. Development of Binding Assays for the SH2 Domain of Grb7 and Grb2 Using Fluorescence Polarization, *J. Biomol. Screen.* 13 (2008) 112-119.
- [48] M.R. Eftink, A.C. Anusiem, R.L. Biltonen, Enthalpy-entropy compensation and heat capacity changes for protein-ligand interactions: general thermodynamic models and data for the binding of nucleotides to ribonuclease A. *Biochemistry* 22 (1983) 3884-3896.
- [49] S.C. Pero, L. Oligino, R.J. Daly, A.L. Soden, C. Liu, P.P. Roller, P. Li, D.N. Krag, Identification of novel non-phosphorylated ligands, which bind selectively to the SH2 domain of Grb7, *J. Biol. Chem.* 277 (2002) 11918-11926.
- [50] W. Danho, J. Swistok, W. Khan, X.J. Chu, A. Cheung, D. Fry, H. Sun, G. Kurylko, L. Rumennik, J. Cefalu, G. Cefalu, P. Nunn P, Opportunities and challenges of developing peptide drugs in the pharmaceutical industry, *Adv. Exp. Med. Biol.* 611 (2009) 467-469.

Declaration for Thesis Chapter [8-9]

Declaration by candidate

In the case of Chapter [8] and [9], the nature and extent of my contribution to the work was as follows:

Nature of contribution	Contribution (%)	Signature
Protein expression/purification, set up crystallization trials, data collection and structure determination, manuscript preparation	80%	

The following co-authors contributed to the work. Co-authors who are students at Monash University must also indicate the extent of their contribution in percentage terms:

Name	Nature of contribution	Signature
Daouda Troare ¹	Assisted in data collection and structure solution	
Menachem J Gunzburg ¹	Participated in protein expression/purification	
Nicole R Pendini ¹	Contributed in data collection	
Mark del Borgo ¹	Assisted in peptide synthesis	
Matthew CJ Wilce ¹	Contributed in data collection, structure solution, data interpretation	
Patrick Permuter ²	Contributed to peptide synthesis	
Mibel I Anguilar ¹	Contributed to peptide synthesis and Data interpretation	
Jacqueline A Wilce ¹	Planned and supervised the overall experiments and oversaw the reporting of the results	

¹Department of Biochemistry and Molecular Biology, Monash University, VIC 3800, Australia; ² Department of Chemistry, Monash University, VIC 3800, Australia;

Declaration by co-authors

I hereby certify that:

- (1) the above declaration correctly reflects the nature and extent of the candidate's contribution to this work, and the nature of the contribution of each of the co-authors.
- (2) they meet the criteria for authorship in that they have participated in the conception, execution, or interpretation, of at least that part of the publication in their field of expertise;
- (3) they take public responsibility for their part of the publication, except for the responsible author who accepts overall responsibility for the publication;
- (4) there are no other authors of the publication according to these criteria;
- (5) potential conflicts of interest have been disclosed to (a) granting bodies, (b) the editor or publisher of journals or other publications, and (c) the head of the responsible academic unit; and
- (6) the original data are stored at the above location(s) and will be held for at least five years from the date indicated below:

Chapter 8

Crystallization and Preliminary characterization of the Grb7-SH2 domain apo and in complex with a bicyclic polypeptide antagonist

This chapter describes the crystallization of the Grb7 SH2 domain in its apo form and in complex with a rigid bicyclic G7-18NATE derived polypeptide. Diffraction quality crystals were obtained after rounds of micro seeding experiment. The apo form of the protein was solved to 1.6 Å in the $P6_3$ space group while the co-crystal structure was solved to a resolution of 1.7 Å in the $P2_1$ space group. The experimental aspects of crystallization and data collection are presented in a format suitable for a crystallization note.

Crystallization and Preliminary characterization of the Grb7 SH2 domain apo and in complex with a bicyclic polypeptide antagonist

Synopsis

Human growth factor receptor bound protein-7 (Grb7) is a non-catalytic protein known to affect processes such as cell growth, migration, angiogenesis, inflammation and proliferation and is implicated with the development of some human tumors. As an attempt to further probe the foundation for the development of Grb7 antagonists, we report the crystallization and preliminary data collection of apo and bound forms of Grb7 SH2 domain. After rounds of crystal optimization by micro seeding, crystals of the apo form were obtained that diffracted to 1.6 Å while that of the co-crystal was collected to 1.7 Å resolutions. The two crystals were obtained in different conditions and space groups (apo = $P6_3$; complex = $P2_1$). These structures are expected to facilitate the design and development of Grb7 based anticancer therapeutic agents.

Keywords: Grb7; crystallization; seeding; SH2 domain

Introduction

Grb7 is an adapter protein that links membrane bound and cytoplasmic receptors to downstream signalling effectors.^{1,2} Studies conducted over the years have shown that Grb7 is a central protein in divergent pathways affecting processes such as cell growth, migration, angiogenesis, inflammation and proliferation. Targeting Grb7 is especially promising in cancers on a number of grounds. First, Grb7 is overexpressed in a number of cancer cell lines. In particular, it is found to be co-overexpressed and co-amplified with ErbB2 is widely investigated.³ The over expression of Grb7 has been frequently connected with the development of aggressive, recalcitrant and advanced tumours.⁴ Moreover, as Grb7 is a downstream mediator of a number of oncogenic pathways, targeting Grb7 might provide an attractive alternative for the inhibition of multiple oncogenic pathways. Finally, Grb7 is demonstrated to be a druggable protein that can be blocked by synthetic agents.⁵ Put together, these investigations make Grb7 an attractive target for the development of therapeutics that may have a potential against cancers and inflammations.

Grb7 is composed of 532 residues that are arranged in well-conserved protein domains such as a Ras-associating (RA) domain, a pleckstrin homology (PH) domain and Src homology 2 (SH2) domains. In addition, Grb7 has a proline rich N-terminal domain and another domain termed BPS domain (for between the PH and SH2 domains).^{1,6} Each domain plays a complementary role in the overall signalling function of Grb7. The SH2 domain is especially interesting to target for it is the domain responsible for binding to the upstream partners of Grb7. The SH2 domain commences the first and hence the fate determining step in the entire process of Grb7 dependent signalling.^{1,7} Moreover, it possesses a well-defined and characterized binding pocket amenable to a variety of ligand design efforts. Furthermore, the SH2 domain of Grb7 is the most extensively studied module where its interaction with a diverse array of signalling and non-signalling biomolecules is researched and its requirement to bind to the myriad of Grb7 partners is conserved.^{1,6,7} These factors endow the SH2 domain as an attractive module in the development of Grb7 based therapeutic agents. Indeed, this has been demonstrated by the recent discovery of peptide antagonists that were specifically designed to act on the SH2 domain.⁵

Currently there exist three experimental structures corresponding to two domains of Grb7 protein: a crystal structure of the apo forms of SH2 domain (pdb code = 2QMS), a solution structure of the RA domain (pdb code = IWGR) and another solution structure of the holo form of the Grb7 SH2 domain (PDB ID = IMW4).^{8,9} The detail of the RA domain structure is yet to be published. The holo structure of G7-18NATE in complex with Grb7 SH2 domain is solved by our group. The x-ray structure of the apo Grb7 SH2 domain was reported earlier by our group to a 2.1 Å resolution. It concurs with the solution structures in its overall fold having a pair of α -helices flanking two pairs of β -sheets. This has contributed to the better understanding of the binding phenomenon underlying target specificity. However, the reported structure was found to assemble in a tetrameric arrangement and it was not clear whether this represented a functional organization or a crystallographic artifact. Furthermore, in the holo structure it was found that only one peptide antagonist was bound per Grb7 SH2 dimer. Thus in order to clarify the issue of dimer formation and antagonist stoichiometry, we embarked on the further crystallization efforts. In addition, we design a rigid analogue of G7-18NATE peptide based on our biophysical and structural studies. By introducing a second ring, it was intended to introduce a conformational restraint and hence improve the binding affinity of the peptide. The present work reports the crystallization and preliminary characterization of high-resolution data of the Grb7 SH2 domain both in apo and bound form.

Materials and methods

Expression and Purification of Grb7 SH2 domain

The pGex2T plasmid containing the Grb7 SH2 domain insert encoding residues 415-532 of human Grb7 protein was obtained from collaborators¹⁰ and expressed in *E. coli* expression system as a GST fusion protein in the BL21 (DE3) pLysS host strain.¹¹ Cell induction was achieved with a 400 μ M Isopropyl β -D-1-thiogalactopyranoside. Cell resuspension and lysis was carried out in ice-cold phosphate buffer saline with 2 mM EDTA, 0.5% Triton-X 100 and by sonication. The fusion protein was purified by glutathione affinity chromatography (GE Healthcare) and cleaved with thrombin. Purification on cation exchange chromatography was

then effected using a HiTrap HP column (GE) after an overnight dialysis into 20 mM HEPES pH 7.4, 20 % Glycerol and 1 mM DTT at 4 °C. This was followed by dialysis into 50 mM MES pH 6.6, 100 mM NaCl and 1 mM DTT and final purification by size exclusion chromatography using a Sephadex 75 XK 16/60 column (GE). Grb7-SH2 domain was concentrated and stored at 4 °C. The final purity and the progress of the purification steps were monitored by SDS-PAGE electrophoresis. The final concentration was determined with UV-Visible spectroscopy using extinction coefficient of 8480 cm⁻¹M⁻¹.¹²

Crystallization

The purified protein sample was concentrated using Eppendorf concentrator of MWCO of 3500 cutoff at 4 °C to 7 mg/ml corresponding to about 511 μM in molarity. The hanging drop vapor diffusion method was used to set up the crystallization trials in 24 well tissue culture plates. For the apo form of Grb7 SH2, 1 μl was mixed with 1 μl of the reservoir solution to make a final drop of size of 2 μl. For the co-crystallization trials, a 1.5:1 molar ratio of the bicyclic peptide with Grb7 SH2 domain was prepared first. The complex solutions was mixed with the reservoir in a 1:1 ratio to form a 2 μl drop and sealed with the vaseline afterwards. All the protein and protein/peptide complex solutions were filtered by prior to making the drops. A variety of commercially available screens from Hamptons, Sigma-Aldrich, and Jena Biosciences were trialed. All the crystallization set-ups were carried out at room temperature and kept and monitored at a temperature controlled room of 20 °C.

Crystal Optimization

Once initial crystals were obtained and confirmed to be protein by diffraction measurements, crystal optimization was effected by micro seeding experiments.¹³ Specifically, the crystallization condition that produced the first crystal was prepared by hand and filled into 4 wells under similar conditions as the initial trial. The apo and complex solutions and drops were made as described above. A micro seeding experiment was conducted using a cat whisker to streak seed the microcrystal into the newly setup drop over the 4 wells. Firstly, the whisker was

splashed over a 10 µl reservoir solution to reduce the number seeds and was subsequently streaked over the 4 wells sequentially.

Data collection

Diffraction data were collected at the Australian Synchrotron on the Macromolecular Crystallography (MX2) beam line. Crystals were soaked in a cryoprotectant composed of 20 % v/v glycerol/mother liquor prior to data collection. The crystals were then flash frozen in liquid nitrogen. The oscillation angle for each frame was 0.5-1 while the exposure time was 2-3 seconds. The XDS package¹⁴ was employed to reduce and scale the reflections.

Bicyclic peptide synthesis

The bicyclic peptide used for co-crystallization study was prepared by solid phase synthesis as a peptide amide using the Fmoc based tactic on a rink amide resin (1.0 mmole/g). The synthesis was carried out manually at room temperature. The 9-fluorenyl methoxy carbonyl protecting group on the resin and the amino acids was removed with 20% v/v piperidine/DMF in 45 min. The Kaiser test¹⁵ was employed to check the success of Fmoc removal. The coupling and activating agents used were *O*-benzotriazol-1-yl-*N,N,N',N'*-tetramethyluronium hexafluorophosphate (HBTU) and di-isopropyl ethylamine (DIPEA). Residue coupling reactions were carried out for 45 min and, in cases where less than efficient coupling was noted as indicated by the Kaiser's colour reaction, the coupling time was increased up to 1 hr and a more effective coupling agent 2-(7-Aza-1H-benzotriazole-1-yl)-1,1,3,3-tetramethyluronium hexafluoro phosphate (HATU) was employed. Double couplings were employed for residues Phe, Tyr and Asn and the coupling time was doubled.

Ring closing metathesis (RCM) was employed to form the first ring as follows:¹⁶ 20 mol % second-generation Grub-Hoveyda catalysts in DCM was applied to the resin-bound crude peptide. The metathesis reaction was effected on the fully protected resin bound crude peptide for 48 hours. After successful RCM, the N-terminal Fmoc group was removed with 20% piperidine/DMF and Chloroacetylation on the freed N-terminal amino moiety was carried out using chloroacetic acid anhydride (171

mg, 2 ml DMF, 100 μ l DIPEA, 45 min). The resin was then dried for 1 hr and the peptide cleavage effected using a cocktail consisting of 94.5% Trifluoroacetic acid (TFA) /2.5% Triisopropylsilane (TIPS)/2.5% H_2O / 0.5% ethanedithiothreitol (EDT) for 3 hours. TFA evaporation and resin drying was effected with a stream of nitrogen gas. This was followed by precipitation of the peptide in ice-cold diethyl ether. Finally the crude peptides were dissolved and extracted with successive small volumes of 50%ACN/ H_2O and were lyophilized overnight. Thioether formation was achieved by dissolving the crude, deprotected, lyophilized peptide at 2 mg/ml in 50 mM NH_4HCO_3 in 50% ACN/ H_2O of pH 8.0 for 11/2 hrs. The cyclized peptides were freeze-dried overnight and purified using preparative RP HPLC. Final peptide homogeneity and identity as well as the success of capping, RCM and thioether formation reactions were monitored by analytical reverse phase HPLC and electrospray ionization mass spectroscopy.

Results and discussion

Crystallization

The first step in crystal structure determination is the identification of appropriate crystallization conditions. In the initial step Index, SaltreX, PEG/ION and SIGMA screens, each containing 96 conditions, were tried. Even though needles and spherulites were obtained in other conditions from the random trial, the best initial screen was observed in Hamptons condition; crystals of the apo form appeared in 14 days in condition 33 of Hampton's Index screen (1.1 M Sodium malonate, 0.1 M HEPES, pH 7.0, 0.5% v/v Jeffamine®ED-2001) while the co-crystal form appeared in 10 days in 0.1 M BIS-TRIS pH 5.5, 25% w/v PEG 3,350.

The initial apo crystals from the random trials diffracted well to 1.8 Å resolution while the co-crystal ones were poorly diffracting. So optimization was pursued to get better diffracting crystals. To this effect a micro-seeding strategy was effected using a cat whisker. The initial apo crystals from the micro seeding were so many that they never grew to a diffracting size. A second round of micro seeding was initiated using the tiny crystals from the first round. Again even though the crystals grew to a bigger size, they were not of sufficient size. Finally a third round using seeds from the second seeding was conducted to successfully grow single crystals

that diffracted to 1.6 Å. Fig. 8.1 and 8.2 show the apo crystals obtained and the optimization strategies pursued. On the other hand, a high quality crystal for the complex form was obtained in the first micro seeding experiment.

The crystallization conditions were slightly different compared to each other and the previous condition in which the Grb7 SH2 domain was crystallized (100 mM sodium citrate pH 6.1, 22.5% PEG 4000, 0.2 M ammonium sulphate and 5% glycerol). However, all contained negatively charged oxygen species that are potential binders at the SH2 domain cationic phosphate recognition pocket. Fig. 8.3 shows the crystals obtained after the optimization.



Figure 8.1: The initial crystals of the apo Grb7 SH2 domain obtained from random screening. The crystal was found to diffract to 1.8Å

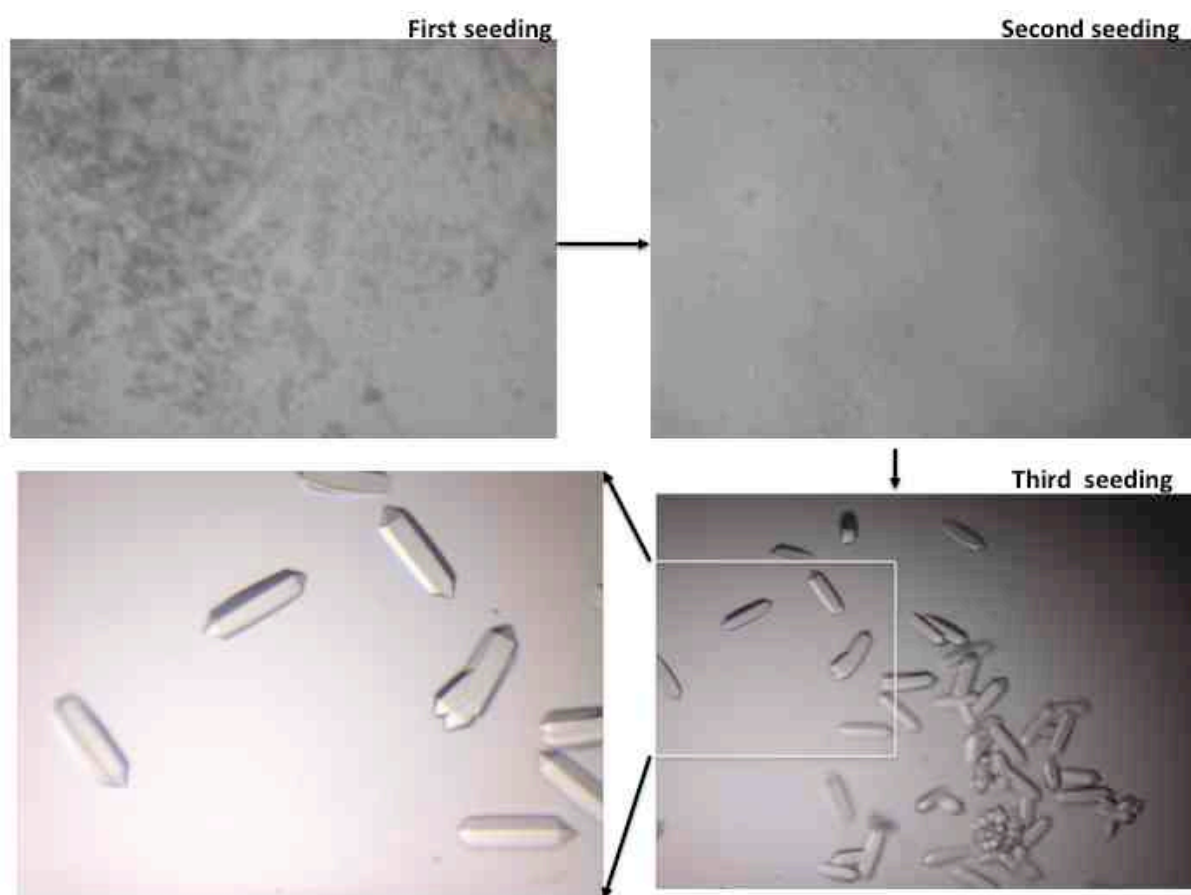


Figure 8.2. The process of crystal optimization by micro seeding



Figure 8.3. Monoclinic crystals of the Grb7 SH2-bicyclic G7-18NATE peptide complex. Diffraction quality crystals were obtained after micro seeding

Table 8.1. Data Collection parameters

Parameters	apo	holo
Resolution	1.6 Å	1.7 Å
Temperature	100 K	100 K
Crystal to detector distance(mm)	150	224.5
Wavelength (Å)	0.954	0.954
Number of images	180	720
Oscillation range (deg.)	1.0	0.5
Number of reflections used	62,921	36,82
Number of unique reflections	38,123	25,448
Completeness (%)	100	99.87
Crystal	trigonal	monoclinic
Space group	P6 ₃	P2 ₁
Crystal geometry	a= b= 83.96, c= 75.92 $\alpha = \beta = 90.0$ $\gamma = 120.0$	a=37.10, b=63.87, c = 52.07 $\alpha = \gamma = 90.0$ $\beta = 92.41$

A total of 180 images were collected at oscillation angle of 1.0 degrees for the apo Grb7 SH2 domin form while 720 images at 0.5 oscillation angles were collected at 100 K maintained by stream of nitrogen gas. See Table 8.1 for details. The apo form was found to crystallize in trigonal crystal form while the peptide/grb7 SH2 domain complex form was formed as a monoclinic crystal with a space group of P2₁. Cell content analysis shows that both crystals contain two chains of protein molecules per asymmetric unit. For the Grb7 SH2/bicyclic peptide complex, the Matthews co-efficient obtained is 2.25 corresponding to 45.47% in solvent content with a probability of 0.98. Similarly for the Grb7 SH2 apo crystal a Matthews co-efficient of 2.81 with a solvent fraction of 56.31% and probability of 0.77 was observed. This is in contrast to the previous report of a tetrameric arrangement.

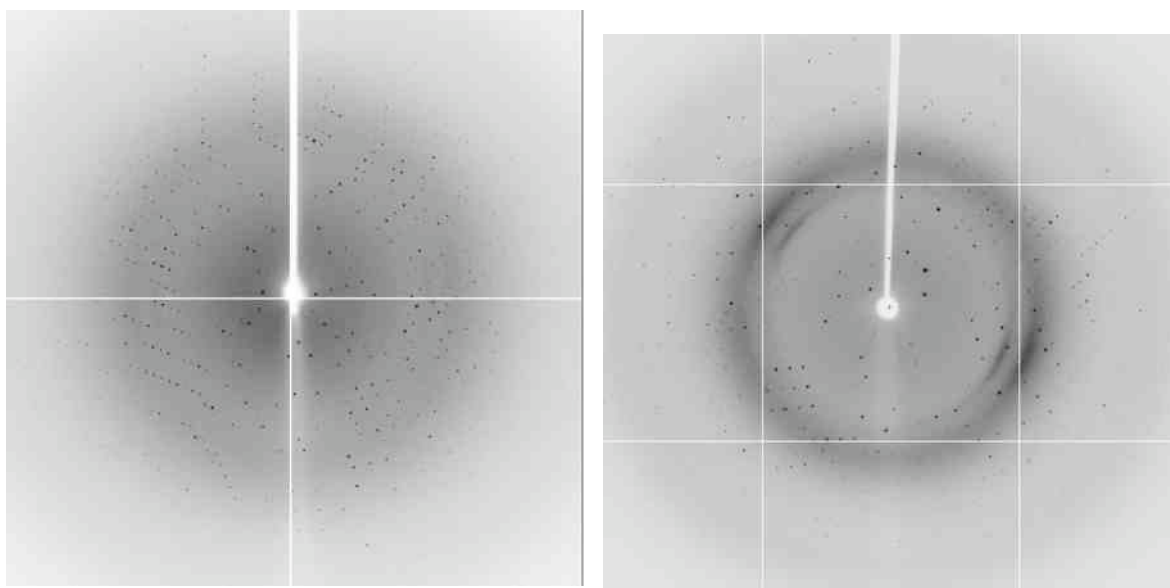


Figure 8.4. Diffraction images of Grb7 Sh2 domain crystals. *Left*: Diffraction images of the trigonal crystals of Grb7 SH2 domain apo; *Right*: diffraction images of bicyclic G7-18NATE/Grb7 SH2 domain co-crystal.

Phases for these data sets will be sought using a molecular replacement approach. We anticipate that these high-resolution structures will provide greater detail than previously available for the analysis of the Grb7 SH2 domain and its ligand interactions.

References

1. Han, D. C.; Shen, T. L.; Guan, J. L. The Grb7 family proteins: structure, interactions with other signaling molecules and potential cellular functions. *Oncogene* **2001**, *20*, 6315-6321.
2. Margolis, B.; Silvennoinen, O.; Comoglio, F.; Roonprapunt, C.; Skolnik, E.; Ullrich, A.; Schlessinger, J. High-efficiency expression/cloning of epidermal growth factor-receptor-binding proteins with Src homology 2 domains. *Proc. Natl. Acad. Sci. USA*, **1992**, *89*, 8894-8898.
3. Shen, T.L, Guan, J.L. Grb7 in intracellular signaling and its role in cell regulation. *Front Biosci.* **2004**, *9*, 192-200.
4. Ramsey B, Bai T, Hanlon Newell A, Troxell M, Park B, Olson S, Keenan E, Luoh SW. GRB7 protein over-expression and clinical outcome in breast cancer. *Breast Cancer Res. Treat.* 2010, DOI: 10.1007/s10549-010-1010-0.
5. Pero, S.C.; Oligino, L.; Daly, R.J.; Soden, A.L.; Liu, C.; Roller, P.P.; Li, P.; Krag, D.N. Identification of novel non-phosphorylated ligands, which bind selectively to the SH2 domain of Grb7. *J. Biol. Chem.* **2002**, *277*, 11918-11926.

6. Pero, S. C.; Daly, R. J.; Krag, D. N. Grb7-based molecular therapeutics in cancer *Expert Rev. Mol. Med.* **2003**, *5*, 1-11.
7. Daly, R. J. The Grb7 family of signalling proteins. *Cell Signal.* 1998, *10*, 613-618.
8. Porter, C. J.; Matthews, J. M.; Mackay, J. P.; Pursglove, S. E.; Schmidberger, J. W.; Leedman, P. J.; Pero, S. C.; Krag, D. N.; Wilce, M. C.; Wilce, J. A. Grb7 SH2 domain structure and interactions with a cyclic peptide inhibitor of cancer cell migration and proliferation. *BMC Struct. Biol.* **2007**, *7*:58
9. Ivancic, M.; Daly, R. J.; Lyons, B. A. Solution structure of the human Grb7SH2 domain/erbB2 peptide complex and structural basis for Grb7 binding to ErbB2. *J. Biomol. NMR.* **2003**, *27*, 205-219.
10. Janes, P. W.; Lackmann, M.; Church, W. B.; Sanderson, G. M.; Sutherland, R. L.; Daly, R. J. Structural determinants of the interaction between the erbB2 receptor and the Src homology 2 domain of Grb7. *J. Biol. Chem.* **1997**, *272*, 8490-8497.
11. Porter, C. J.; Wilce, M. C.; Mackay, J. P.; Leedman, P.; Wilce, J. A. Grb7 SH2 domain dimerisation is affected by a single point mutation. *Eur. Biophys. J.* **2005**, *34*, 454-460.
12. Pace, C. N.; Vajdos, F.; Fee, L.; Grimsley, G.; Gray, T. How to measure and predict the molar absorption coefficient of a protein. *Protein Sci.* **1995**, *4*, 2411-2423.
13. Sweeney, A.M.; D'Arcy, A. Seeding. In *Protein crystallization*, 2nd ed, Bergfors T, Ed., IUL Biotechnology Series, 2009, pp. 95-113
14. White, P.D.; Chan, W.C. Basic Principles, in *Fmoc Solid Phase Peptide Synthesis: A Practical Approach*, Chan, W.C. and White, P.D., Eds., Oxford University Press, Oxford, 2000, pp.9-37.
15. Kaiser, E.; Colescott, R. L.; Bossinger, C. D.; Cook, P.I. Color test for detection of free terminal amino groups in the solid-phase synthesis of peptides. *Anal. Biochem.* **1970**, *34*, 595-598.
16. Jacobsen, O.; Klaveness, J.; Rongved, P. Structural and pharmacological effects of ring-closing metathesis in peptides. *Molecules* **2010**, *15*, 6638-6677.

Chapter 9

Crystal structure of Grb7 SH2 domain apo and in complex with bicyclic polypeptide antagonist: A structural basis for binding selectivity

This chapter describes the crystal structure determination of Grb7 SH2 domain apo and its complex with rigid bicyclic G7-18NATE polypeptide. Crystal optimization by micro seeding was effected to grow diffraction quality crystals. The apo form of the protein was solved to 1.6 Å in P6₃ space group while the co-crystal structure has a resolution of 1.7 Å in a P2₁ symmetry. Both structures are found to display the typical overall fold of SH2 domain proteins. The structural analysis made is presented in detail.

Abstract

Human growth factor receptor bound protein-7 (Grb7) is a non-catalytic protein known to mediate multiple signal transduction pathways. Grb7 is shown to be a central protein affecting process such as cell growth, migration, angiogenesis, inflammation and proliferation and associated with the development a variety of human tumors and inflammatory disorders. In an attempt to further probe the foundation for the development of Grb7 antagonists, we solved the crystal structure of the apo Grb7 SH2 domain to 1.6 Å resolutions. The co-crystal structure of Grb7 SH2 domain in complex with a bicyclic polypeptide was also determined to 1.7 Å resolution. The two structures are solved as dimers. The atomistic details of the ligand-protein interaction, the dimerization interfaces as well as the overall fold is described. Comparative structural investigation with that of related SH2 domains and the mechanistic insight into the ways binding specificity is achieved is presented. We also report the synthesis and binding characterization of a bicyclic peptide antagonist. The *in vitro* binding affinity of this rigid peptide is found to be 2.6 μM by isothermal titration calorimetry. Finally, the binding strength of malonic acid picked from the crystallization condition is also estimated by ThermoFluor based melting point shift assay. It is expected that these structures and the detailed description reported will help in the further understanding of Grb7 mediated signal transduction mechanisms in general and in the development of Grb7 based anticancer therapeutics in particular.

Keywords: Grb7; SH2 domain; Adaptor; crystallography; ITC; malonic acid

Introduction

Growth factors regulate many aspects of cellular life.¹ The binding of growth factors induces dimerization and auto phosphorylation of growth factor receptors, giant trans-membrane proteins with an intracellular kinase domain.^{2,3} The receptor phosphorylation is essential for the formation of signaling complexes with intracellular proteins for information transfer to downstream effectors. One of the cytosolic proteins recruited by the phosphorylated growth factor receptor is Growth factor receptor bound protein 7 (Grb7). Grb7 was identified through screening of a mouse cDNA expression library with the tyrosine phosphorylated C-terminus of the epidermal growth factor receptor.^{4,5} It has since been shown that Grb7 acts as an adapter for numerous tyrosine kinases, including cytosolic focal adhesion kinase that plays a role in cell migration.⁵

Grb7 has come into the research spotlight since its over-expression was found to be correlated with a variety of tumors ranging from breast,⁶ blood,⁷ hepatic,⁸ pancreatic,⁹ esophageal,¹⁰ gastric carcinomas,¹¹ ovarian,¹² testicular,¹³ and rheumatoid arthritis.¹⁴ Targeting Grb7 is especially promising in cancers on a number of grounds. Not only is Grb7 over-expressed in a number of cancer cell lines,¹⁵ the over expression has been frequently connected with development of aggressive, recalcitrant, invasive, high grade, high size and advanced tumors.¹⁵⁻¹⁸ Moreover, as Grb7 is a downstream mediator of a number of oncogenic pathways, targeting Grb7 might provide an attractive alternative to turn off multiple oncogenic pathways. Finally, Grb7 is demonstrated to be a druggable protein that can be blocked by synthetic agents.^{19,20} Put together, these investigations make Grb7 an attractive target for the development of therapeutics that may have a potential in cancers and inflammation.

The Grb7 protein is organized into a number of well conserved modules including a Ras-associating (RA), a pleckstrin homology (PH), Src homology 2 (SH2), a proline rich and a BPS (for Between the PH and SH2 domains) domain.^{5,15} Each domain is characterized to possess a distinct but complementary role that contribute to the overall adaptor function of Grb7. Of these, the SH2 domain is the most widely researched where its interaction with a diverse array of signaling and non-signaling biomolecules is documented.^{5,15,21} More importantly, the requirement of the SH2

domain to bind to the myriad of Grb7 partners is found to be conservative,²¹⁻²³ with a minimal YXN recognition motif on peptide inhibitors delineated.^{5,21-23} In addition, the SH2 domain is responsible for recognizing and binding to the upstream partners of Grb7 thereby commencing the first and hence the fate determining step in the entire process of Grb7 dependent signaling.^{20,24} These factors endow the SH2 domain as an attractive module for structural and inhibitor development studies.

Currently there exist three experimental structures corresponding to two domains of the Grb7 protein: a crystal structure of the apo forms of SH2 domain (pdb code = 2QMS), a solution structure for the RA domain (pdb code = IWGR) and another solution structure for a holo form of Grb7 SH2 domain (pdb code = IMW4).^{25,26} Also the crystallization and of G7-18NATE/Grb7 SH2 complex solved in our group is just published with the structural analysis being under investigation.²⁶ The detail of the RA domain structure is yet to be published. The x-ray structure of the apo form of Grb7 SH2 domain was reported earlier by our group to a 2.1 Å resolution. It concurs with the solution structures in its overall fold having a pair of α -helices flanked by two pairs of β -sheets. This has contributed to a better understanding of the details of the binding site underlying target specificity. The reported structure was found to assemble in a tetrameric arrangement and it was not clear whether this is a functional organization or a crystallographic artifact. Moreover, additional interface was found in the crystal as opposed to the expected dimerization interface shown to occur in solution.²⁵ This is an important question as dimerization is critical for the functioning of Grb7 protein. To get a clear picture understanding of the mechanistic basis of dimer formation and to map the peptide interaction site, the present work reports a high-resolution structure of the Grb7 SH2 domain both in apo and peptide bound form. Detailed structural analysis of the binding site characteristics and dimerization interface of structures is reported. Moreover, a comparative analysis with the previous structure and related SH2 domains is made.

Materials and methods

Expression and Purification of Grb7 SH2 domain

The expression, purification and crystallization and crystal optimization is described previously.²⁶ Briefly the S2 domain was produced in an *E.coli* expression system, concentrated to 7 mg/ml. The hanging drop vapor diffusion was used to set

up crystal trial using Hampton, Sigma Aldrich and Gena biosciences kits. Initial crystals were then optimized by micro seeding.

Data collection and processing

Diffraction data were collected at the Australian Synchrotron on Macromolecular Crystallography (MX2) beam line as described in. The XDS package²⁷ was employed to reduce and scale the reflections. The previously reported structure of the Grb7 SH2 domain (PDB ID: 2QMS) was used as a template for molecular replacement phasing with the MOLREP²⁸ program in Collaborative Computational Project Number 4 (CCP4).²⁹ The template structure²⁵ was available as a tetrameric complex and hence was pre-treated by removing its water molecules and the other three chains. The MOLREP experiment was effected by applying the multicopy search option. The REFMAC5³⁰ package was then used for refinement purposes after the phasing in CCP4. Initially rigid body refinement was applied with no prior phase information. This was followed by cycles of restrained refinement and model building by COOT.³¹

Bicyclic peptide synthesis

The bicyclic peptide used for co-crystallization and binding studies is synthesized as a peptide amide as described²⁶ on a rink amide resin using the Fmoc chemistry. Ring closing metathesis reaction was effected to form the olefin ring while the peptide was still on the resin and fully protected. The thioether formation reaction was conducted to form the second ring in aqueous solution. Peptide purity and the progress of RCM and thioether formation reactions were monitored by RP-HPLC and ESI-MS. The chemical structure of bicyclic G7-18NATE is shown in Fig. 9.1.

Thermodynamic binding studies of the bicyclic peptide

The binding thermodynamics of the bicyclic G7-18NATE peptide was determined by calorimetry on a VP-ITC Microcalorimeter (Microcal, Northampton, MA, USA) at 25 °C.³² The Grb7 SH2 domain was dialyzed against 2 litres of 100 mM sodium phosphate, pH 6.0 and 1 mM DTT at 4 °C overnight. The peptide was dissolved in the filtered dialysis buffer to make a 1.15 mM solution. The concentration of the Grb7

SH2 was determined by absorbance measurement at 280 nm. The peptide and protein solutions were degassed and thermostated at 20 °C for 5 min using the ThermoVac of the VP-ITC Microcalorimeter. The reference power of the experiment was set to 20 μ Cal/sec and the cell contents were stirred continuously at 307 rpm throughout the titrations. The reference cell was filled with MQ water. The peptide was titrated into Grb7 SH2 solutions of 70 μ M concentrations in 10 μ L injections. A binding isotherm was generated by plotting the heat change evolved per injection against the molar ratio of peptides to the Grb7 SH2 domain receptor. The heat generated by the last titration was used to estimate the heats of dilution and mixing which was then subtracted from the binding data. The corrected data was then employed to fit to a single binding site model using a non-linear least squares with the Origin (Microcal Software, Northampton, MA, USA). All of the ITC fitting parameters were kept floating during the fitting procedure.

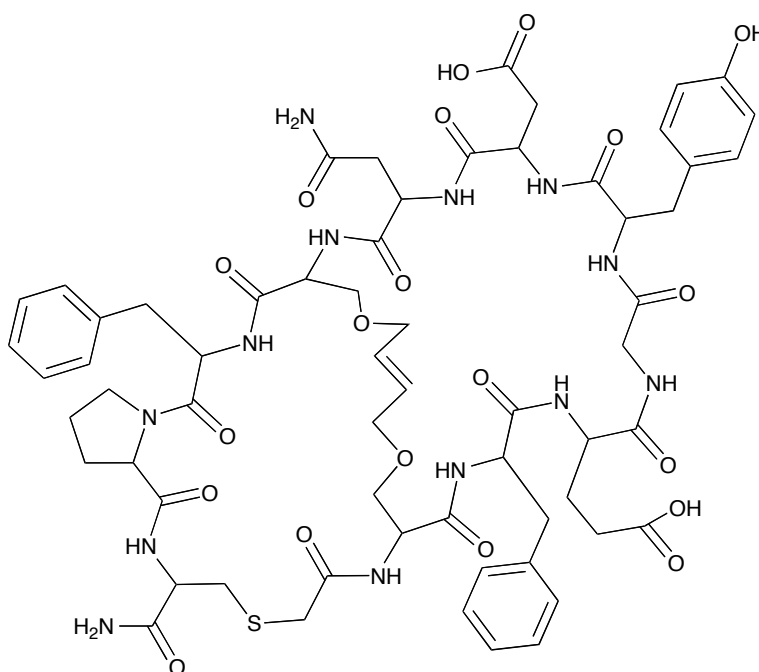


Figure 9.1. Chemical Structure of bicyclic G7-18NATE

Stability test of Grb7 SH2 domain with malonic acid

The stability of the Grb7 SH2/malonic acid complex was assessed by the ThermoFluor based melting point shift assay^{33,34} using sypro orange dye to detect the melting transitions. The melting point shift experiment was conducted in

Quiagen's quantitative RT-PCR instrument (www.qiagen.com). The wavelength of excitation/emission was set to 470/555 and 470/610 nm. A heating rate of at 1 °C per minute was programmed over a 30-80 °C temperature range with a holding time of 60 sec. The buffer used was 50 mM MES, 100 mM NaCl, pH 6.6, 1 mM dithiothriethol. The Grb7 SH2 domain concentration employed was 20 µM. 500 µM malonic acid solution was then added to the protein solution. After thorough mixing, 25 µl of the protein/malonic acid complex solution was transferred to the PCR tubes for the melting experiment. A known peptide inhibitor²⁵ was also tested as a positive control. The denaturation experiment was conducted in duplicate. The Rotor-Gene 3000 software was used to set up the experiment and analyze the results.

Results and discussion

1. The Overall Structure of the apo form of the Grb7 SH2 domain

Diffraction quality crystals were obtained after rounds of micro seeding experiments. The apo crystals were found to diffract to a resolution of beyond 1.6 Å. The statistical parameters associated with the structure solution process are presented in Table 9.1. As shown in the table, the final structure comprised 1841 non-hydrogen proteins atoms, 329 water molecules and a 7-atom malonic acid picked from the crystallization condition. The structure was refined to a final free-R factor of 21.47 % and R-factor of 18.04 %. The protein was found to crystallize in a trigonal crystal system possessing a P6₃ space group. This is in contrast to the previous structure of the Grb7 SH2 apo which was solved in a space group of P22₁.²⁵ The asymmetric unit of the Grb7 SH2 domain structure is shown to comprise a total of two Grb7 SH2 domains arranged in the form of a dimer. This also contrasts the previous report of a tetrameric arrangement.²⁵ Overall, the entire system was refined to an rmsd in bond length of 0.026 Å and an rmsd in bond angle of 2.19. The two protein chains are observed sandwiching a single malonic acid molecule. The dimeric assembly noticed looks to be in line with the fact that dimerization is previously found to be important for the functioning of Grb7 protein.^{25,35} Nevertheless, the dimerization arrangement is different from the previous report as well as from the co-crystal form (discussed below). In the apo structure, the

dimerization interface and the binding site overlap and dimer formation is assisted by the malonic acid picked from the crystallization condition. However, the significance of such an interface is not immediately clear and calls for further investigation. Within the crystal lattice are also other minor interfaces between SH2 domains including the expected dimer interface between $\alpha\beta$ helices established to occur in solution.²⁵

Table 9.1. Data collection and refinement parameters

A	Data Collection	apo	holo
	Resolution	1.6 Å	1.7 Å
	Temperature	100 K	100 K
	Crystal to detector distance(mm)	150	224.5
	Wavelength(Å)	0.954	0.954
	Number of images	180	720
	Oscillation range(deg.)	1.0	0.5
	Number of reflections used	62,921	36,82
	Number of unique reflections	38,123	25,448
	Completeness (%)	100	99.87
B	Crystal	Trigonal	Monoclinic
	Space group	P6 ₃	P2 ₁
	Crystal geometry	a= b= 83.96, c= 75.92 $\alpha = \beta = 90.0$ $\gamma = 120.0$	a=37.10, b=63.87, c = 52.07 $\alpha = \gamma = 90.0$ $\beta = 92.41$
	No. Protein molecules/asymmetric unit	2	2
C	Refinement Statistics		
	Resolution(Å)	19.5 Å-1.6 Å	40.32 Å-1.7 Å
	Mean temperature factor(Å ²)	21.78	31.86
	R ^a _{free}	21.47%	24.77%
	Correlation co-efficient Fo-Fc	0.96	0.96
	Correlation co-efficient Fo-Fc free	0.94	0.94
	Overall R ^b _{factor}	18.04%	18.73%
D	Final Model		
	Number of protein atoms	1841	1626
	Number of ligand atoms	7	200
	Number of water molecules	329	106
	R.M.S.D bond Length	0.026	0.019
	R.M.S.D bond Angle	2.19	2.069

Figure 9.2. displays the overall arrangement the apo structure. The overall fold of the structure is in agreement with the previously reported low-resolution apo structure (pdb id = 2QMS) and exhibits the typical fold characteristic of SH2 domain proteins in general.⁶ It is made of a pair α -helices, two pairs of β -sheet structures which are connected by a number of loop structures. The N-terminal helix, labeled as α A is found to be 11 residues long while the C-terminal one is labeled as α B is found to be 10 residues long. The designation of secondary structural elements follows the system proposed by Eck et al.³⁶ A total of four β -strands labeled β B, β C, β D and β E are present in between the α -helices. The β D strand is noted to form an anti-parallel sheet with both β C and β E strands. Present also is another small helix, termed helix H, comprised of four residues in chain A alone. Besides a total of five loops are shown to connect the helices and β -strands (see Fig. 9.2, for nomenclature).

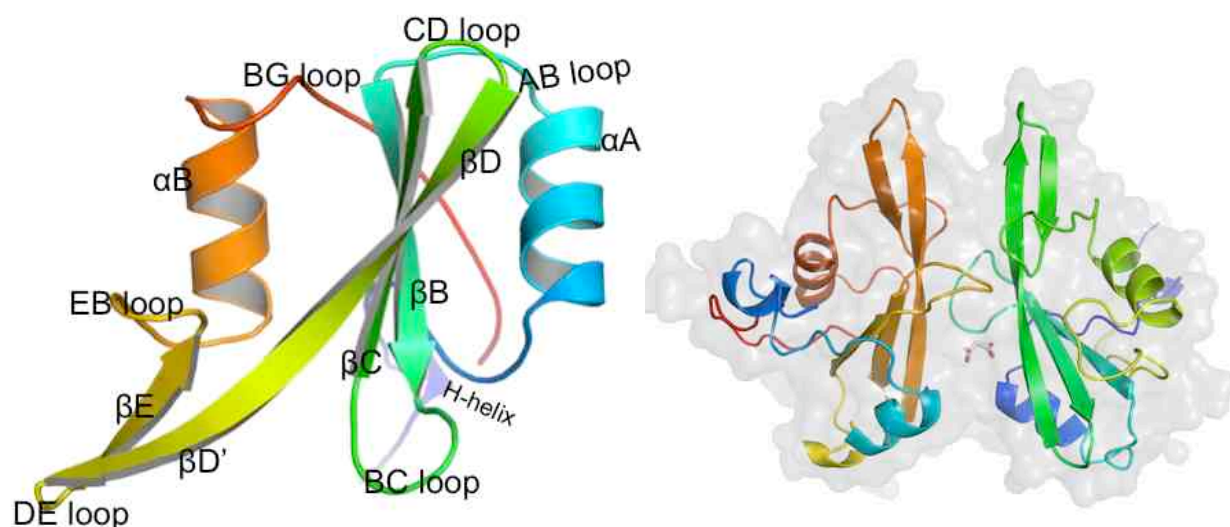


Figure 9.2. *Left*: Cartoon representation of the secondary structural elements of Grb7SH2 domain: *Right*: The dimeric arrangement of Grb7 SH2 domain apo showing the two chains and malonic acid. The pictures were generated using PYMOL.³⁷

The two protein chains are noticed to form the dimer interface via their peptide-binding site. Interestingly, the dimer interface is observed to comprise two different regions: hydrophobic and electrostatic regions. See Fig. 9.3. The hydrophobic part is

comprised of pairs L481 and L483 from both chains. The electrostatic half is largely comprised of positively charged residues such as pairs of H479 and R438 on both chains but also K476 on chain B and Q439 on chain A. Importantly, this region is observed to pick and contain malonic acid from the screen. As shown below malonic acid is noticed to form a number of direct and indirect hydrogen bonding interaction with residues on the two chains and hence appears to be important to keep the two chains in this unusual dimeric arrangement. Interface analysis using the PISA (Protein Interface, Surface and Assemblies) server³⁸ reveals that the interfaces formed between the monomers are not extensive.³⁹ The total solvent accessible surface area of interface formed by the two chains is 630.8 Å² is comprised of 31 residues and 125 atoms. Nonetheless, the complexation significance score for the interface obtained is 0.791 indicating that the interface might have an essential role to play.

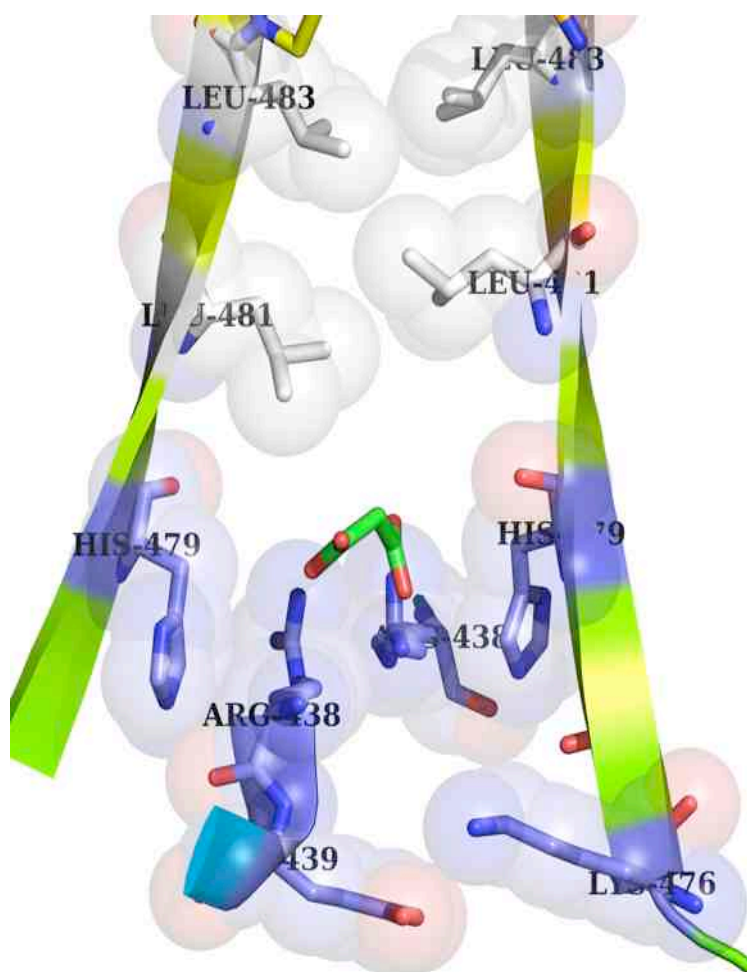


Figure 9.3: The interface formed between the two chains in the apo structure. Malonic acid is shown in green and red stick format. The upper half of the interface is formed by the non-polar residues (L481 and L483) while the lower part comprises basic polar residues (R438, K476, H479) on both chains.

Bonding interactions with malonic acid

The malonic acid binding site on chain A is formed by residues on β C strand, β A strand, α A helix, AB loop, DB loop and by the long C-terminal loop. A total of 15 residues comprising 52 atoms form the malonic acid binding interface. The total solvent-accessible surface area of the site is found to be 128.8 Å² which makes 74.5 % of the total accessible area of malonic acid. The ligand is noticed to be largely found on one of the chain A of Grb7 SH2 domain, which indicates the interactions are not equivalent. Considering the buried surface area of the residues upon binding, the most important residues of the binding site in increasing order are Leu481 (12.80 Å²), Arg438 (31.98 Å²), Arg458 (3.5 Å²), Ser460 (5.41 Å²), Gln461 (7.57 Å²), Arg462 (24.87 Å²), Val468 (4.53 Å²).

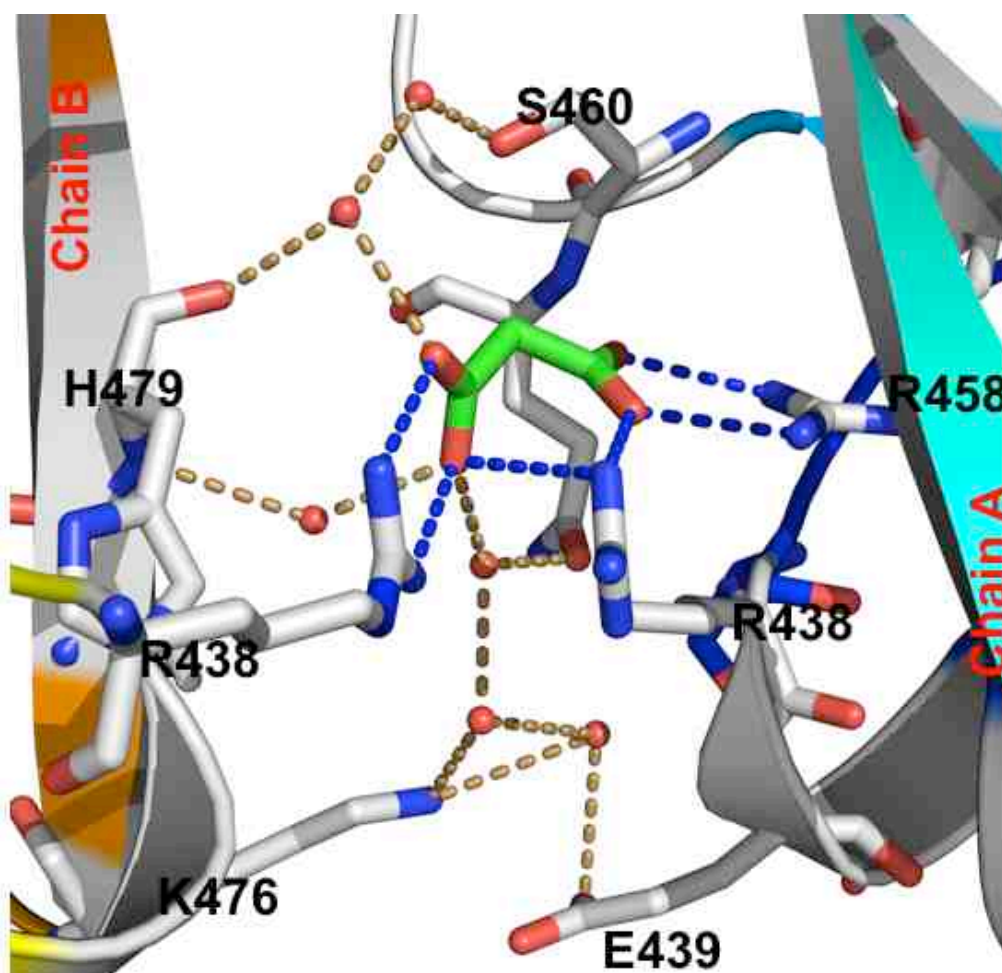


Figure 9.4. The overall binding interaction of malonic acid within the two chains and water molecules. Water bridged hydrogen bonding interactions are shown in orange while direct hydrogen bonding interactions are displayed in blue dots. Malonic acid is shown in red (oxygen) and green (carbon) in stick.

Malonic acid is seen to make a number of direct and water mediated hydrogen bonding interactions with both chain A and chain B of Grb7 SH2 domain. Specifically, the COOH group of malonic acid forms a pair of direct hydrogen interaction with the guanidine group of Arg458 of chain A. It is also noted to form another hydrogen bond with Arg 438 of Chain A. Indirect hydrogen formation to chain A including a network of hydrogen bond formation via water 1950, water 1867 and water 1868 to CO of Glu439. Additional indirect hydrogen bonding interactions exist with Ser460 bridged with water molecules 1856 and 1895. Fig. 9.4 shows this pictorially. The electron density map showing the region around the malonic acid is depicted in Fig.9.5.

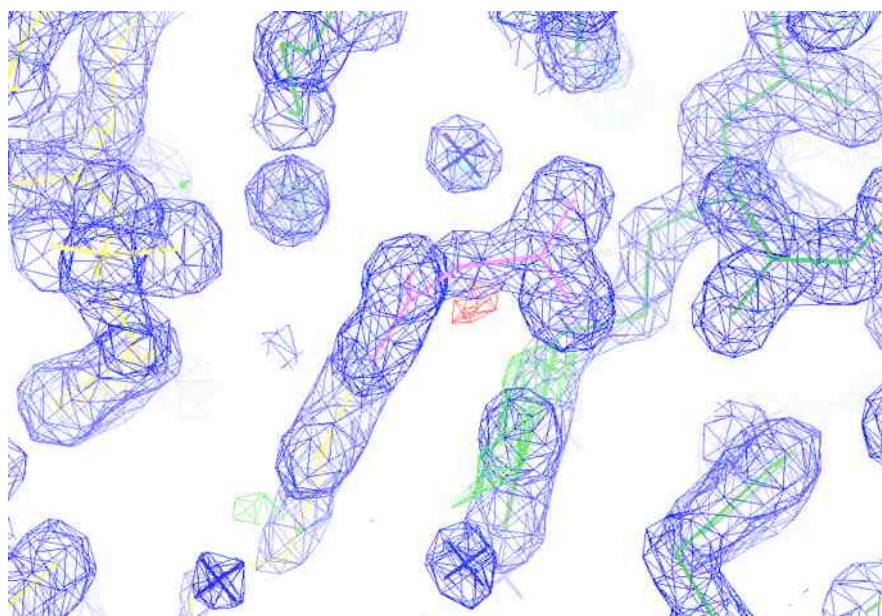


Figure 9.5: The electron density map of the apo Grb7 SH2 surrounding the malonic acid (shown in violet lines) and parts of the chain A (shown in yellow) and chain B (shown in red) with water molecules (shown in crosses). The map clearly shows the localization of malonic acid in the apo structure.

Most of the interactions with chain B are via bridging water molecules. Hydrogen bonding interactions with Chain B include direct interactions with Arg438. Moreover, indirect hydrogen bonding interactions with His479 occur via bridging water 1859. Another water-bridged hydrogen bonding interaction is observed with Lys476 via bridging waters at 1924, 1870, and 1871. Additional hydrogen bonds exist with the backbone NH of His479 via bridging waters 1924 and 1842. On Chain B, the most important residues are; R438 (BSA =32.33Å²) and H479 (BSA

=14.93Å²). This clearly establishes the most important binding site residues of Grb7 SH2 domain, see Fig. 9.6 for comparisons.

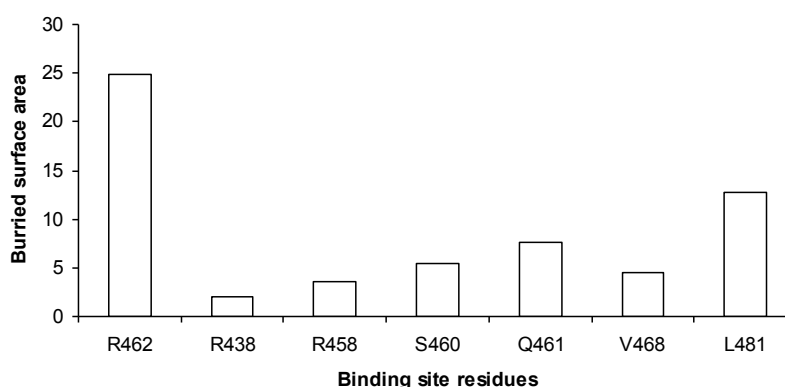


Figure 9.6: Residue contribution to interaction with malonic acid highlighting the most important residues of the Grb7 SH2 domain of chain A binding site. The histogram indicates residues R462, L481 and Q461 as the three most important binding partners of malonic acid in the Grb7 SH2 binding site.

The strength of malonic acid interactions with

Malonic acid seems to form a number of hydrogen bonding interactions with the apo structure, and it is well placed in the phosphotyrosine recognition pocket of Grb7 SH2 domain. Interestingly, malonic acid is also found as a structural feature of several Grb2 antagonists as part of phosphotyrosine mimetics. Even more, it has become clear that when the activities of those Grb2 antagonists are compared, it is found that malonic acid containing antagonists possess one of the highest binding affinity.^{40,41} Given its proven role in enhancing the binding affinity of Grb2 antagonists and the observation that it formed a number of close to ideal hydrogen bonding interactions with the present Grb7 SH2 domain structure, a quantitative estimation of its binding affinity was sought. To that effect, a ThermoFluor based melting point shift assay was employed. The system detects changes in melting points between apo and holo forms of proteins. A positive melting point shift of the hit/Grb7 SH2 domain complex is taken as an indicator of binding phenomenon. From this experiment it is found that malonic acid binds with incredibly high affinity to the Grb7 SH2 domain as indicated by the high melting point shift for the association event, i.e., close to 10 °C as shown in Table 9.2. This is especially when

compared to that of a known polypeptide antagonist of Grb7 SH2 domain-G7-18NATE ($\Delta T_m = 1.3$ °C).

Table 9.2: Thermal stability data

Compound	Concentration (μ M)	T_m (°C)	ΔT_m (°C)
Sodium Malonate/Grb7	100	62.1	9.53
	200	61.57	9.0
	500	62.33	9.76
Grb7 SH2 domain	20	52.57	-----

2. The bicyclic G7-18NATE/Grb7 SH2 domain complex structure

The Overall Structure

The crystal structure of bicyclic G7-18NATE/Grb7 SH2 domain complex was solved to 1.7 Å resolution. The statistical parameters associated with the structure solution process are shown in Table 11.1, along with that of the apo structure. As shown in the table, the final structure was comprised of 1626 non-hydrogen proteins atoms, 106 water molecules and 200 atoms from the peptide and phosphate picked from the peptide solution during the crystallization. The structure was solved to a final free-R factor of 24.77% and R-factor of 18.73%. The protein was found to crystallize in a monoclinic crystal system possessing a $P2_1$ space group. This is in contrast to the apo structure that was found in a trigonal crystal system with $P6_3$ space group. It also differs from the previous structure of the Grb7 SH2 domain, which was solved in a space group of $P22_1$.²⁵ Overall, the entire system was refined to rmsd in bond length of 0.019 Å and to 2.069 in bond angle.

The asymmetric unit of the Grb7 SH2/Bicyclic G7-18NATE co-crystal structure comprises a total of two Grb7 SH2 domains and two peptides. The structures are arranged as dimers with each monomer comprising a peptide on each chain of the Grb7 SH2 domain. Interestingly, this is in contrast to the crystal structure of Grb7 SH2/G7-18NATE structure in which only one peptide was bound to each Grb7 SH2 dimer due to crystal packing restraints. Fig. 9.7 displays the overall arrangement observed pictorially. That the protein assembles in dimeric form is also what is observed for the apo form of Grb7 SH2 domain (1) suggesting that the overall

arrangement of the apo and holo forms are similar. In common with the structure of the apo form and to that of other SH2 domains,⁶ the co-crystal structure exhibited the typical fold with each monomer comprising a pair of α -helices flanking either side of anti-parallel β -sheets. In common to the apo structure the two chains, are made of two α -helices (α A and α B) and five β -strands, labeled β B, β C, β D, β D' and β E. (see Fig.9.2 for designations) and a number of loop structures. A centre of inversion relates the two chains.

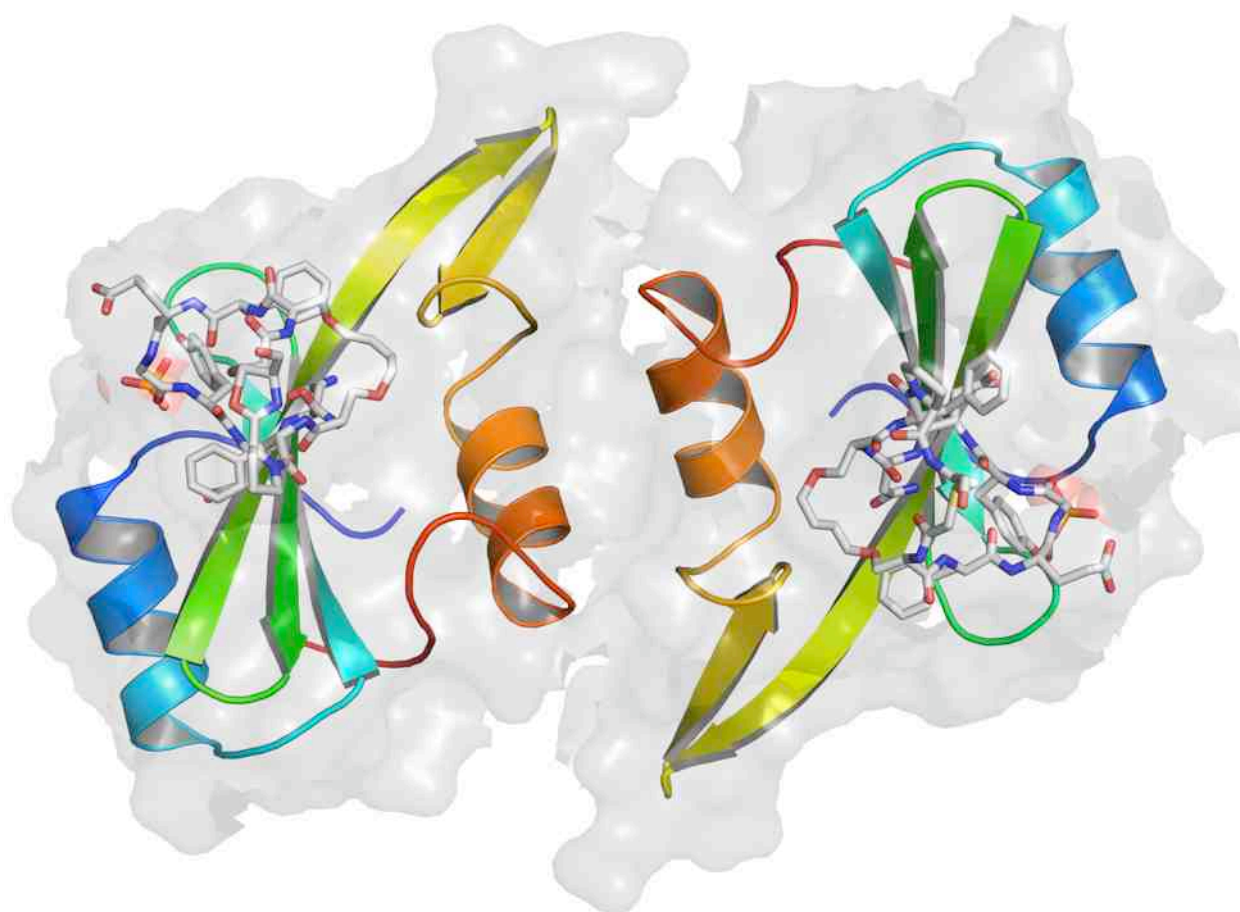


Figure 9.7: The overall fold of the bicyclic G7-18NATE/Grb7 SH2 domain co-crystal structure. Cartoon representation of the secondary structural elements of Grb7SH2 domain is shown with in the surface representation. The two peptides on each chain are indicated by stick representation. Phosphate ions picked from the peptide solution are indicated in by red spheres and stick form of PO_4^{2-} ion. The PO_4^{2-} ions are placed in the recognition site of the Grb7 SH2 domain where the phosphate group would normally reside. The picture was generated using PYMOL

The dimerization interface

The interface between the two chains is made by the two C-terminal alpha helices ($\alpha\beta$) of the two chains, see Fig.9.8, in a side ways arrangement as opposed to via its peptide-binding site in the apo structure. The interface is held together predominantly by hydrophobic interaction whereby four phenylalanines (comprising two Phe511 from the alpha helices and two Phe502 from the loops) and Ile514 on both ends of the αA helix form the core of the hydrophobic interaction. Of these Phe511 in both chains is found to be the central interacting residue all the other three phenylalanine and isoleucine residues. Moreover, the two Phe511 residues are seen to make two hydrogen bonds with Asn515 via their backbone carbonyl carbon.

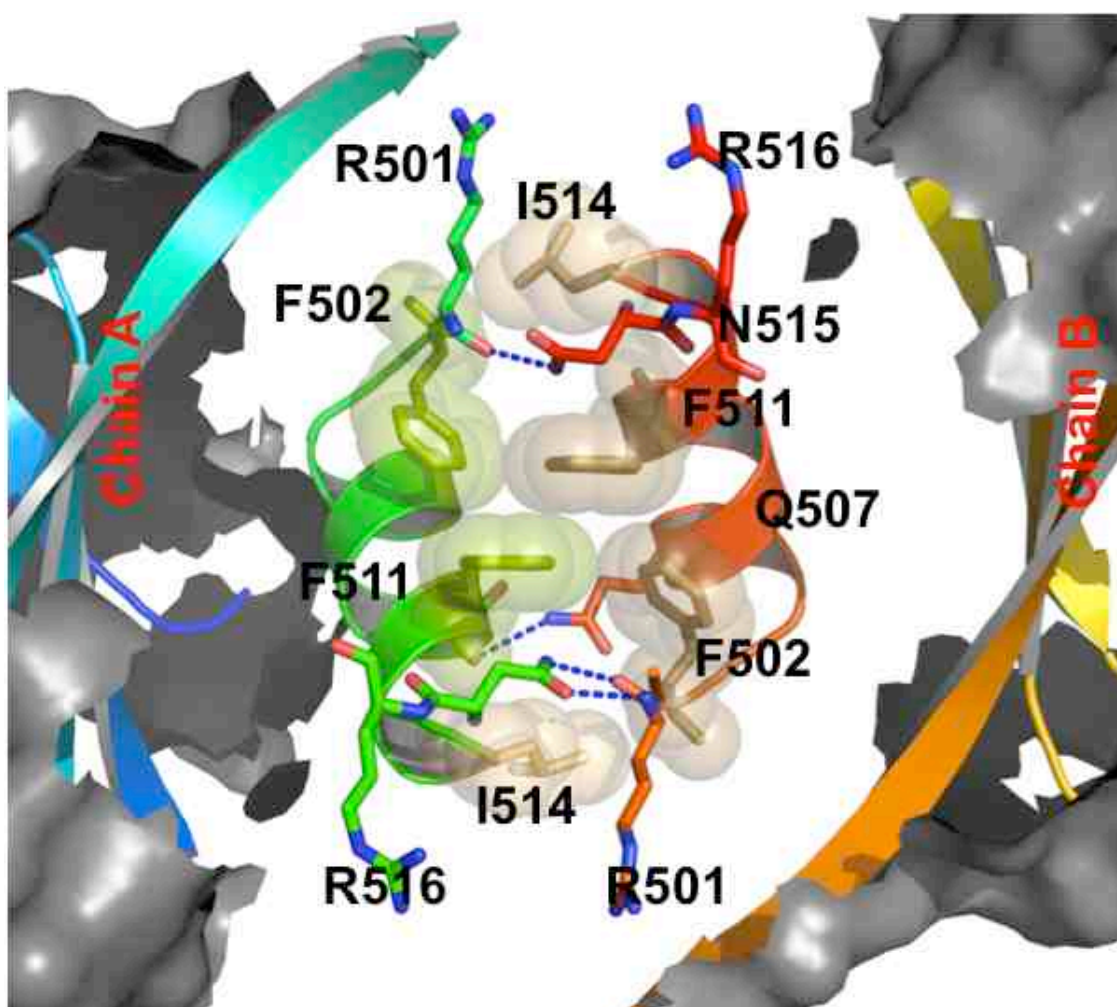


Figure 9.8: The dimerization interface formed by the two chains of the Grb7 SH2 domain. The four Phe residues on both chains (F511 on the helix and F502 on the loop) are shown to form a predominantly hydrophobic dimer interface. Also shown are the four hydrogen bonds

This suggests that the two residues a key role in the dimerization of Grb7 SH2 domain. Indeed, this has been found the case previously^{25,42} where Grb7 SH2 domain lacking these residues was found to be devoid of their dimerization property-i.e., exist in monomeric forms. Additionally a pair of hydrogen bonds exist between the backbone carbonyl of Arg501 on both chains and the side chain of Asn515. Lastly, potential electrostatic interaction pair exists between Arg501/Arg516 on both ends of the dimer. Judging by residue buried surface area for dimer formation, the five most important residues for dimerization are Leu514 (BSA: Chain A = 91.51, Chain B = 112.51), Phe511 (BSA, Chain A = 64.82, Chain B = 66.13), Gln507 (Chain A = 66.21, Chain B = 64.54), Arg501 (Chain A = 51.11, Chain B = 50.57) and Asn515 (Chain A = 49.83, Chain B = 49.28). The last two residues are also noticed to participate the directional hydrogen bonding interaction. Fig.9.9 shows the histograms of interface residues according to their buried surface area during dimer formation. As the histogram shows, the two chains are seen to make the dimer with identical residues and the residues are shown to make a more or less identical contribution, i.e., they are symmetrical dimers.

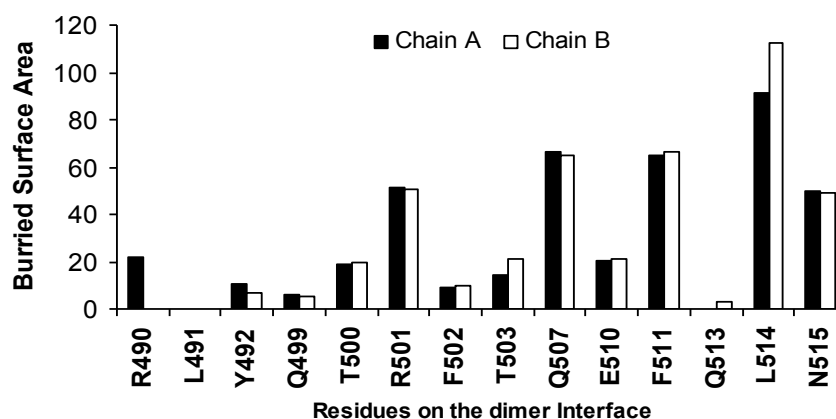


Figure 9.9: Interface residues of chain A and chain B by their buried surface area in dimer formation. The dimer is seen to be formed by identical residues on the two chains and the identical residues are seen to make a more or less identical contribution as assessed by their buried surface area.

The binding interaction of the peptide with Grb7 SH2 domain

As shown in Fig.9.10, the bicyclic peptide is seen to make a number of hydrogen bonding and potential hydrophobic interactions. The interacting residues on the protein are located on α A, β D, β D', AB loops. Specifically Arg438 on α A helix is seen to make two hydrogens bonds with its guanidine group with the backbone carbonyl of Gly4 of the bicyclic G7-18NATE peptide. D6 of the peptide is also seen to make three hydrogen bonds: via its side chain COOH with the backbones amide of His479 and one via its backbone NH with the backbone CO of Tyr480. N7 of the peptide is also noticed to make three hydrogen bonds via its side chain carboxamide group with backbone CO of Met495 and CO of Ile482. E3 of the peptide is also noticed to form two hydrogen-bonding interactions with the Arg462 both via its side chain and backbone carbonyl group. F2 of the peptide is seen engulfed by a hydrophobic region defined by residues Leu483 and Leu481 indicating potential hydrophobic interactions.

The two chains of the Grb7 SH2 domain are noticed to interact almost identically to their respective peptides. In particular, the PISA analysis of binding site residues in terms of their buried surface area upon interaction with the peptides shows identical amino acids on both chains are interacting in identical fashion, this is because it is a symmetrical dimer. As per the residues BSA (in Å²), the five most important binding site residues in interacting with the peptides are Arg462 (BSA, Chain A = 74.76, Chain B = 69.27), Leu481 (Chain A = 58.09, Chain B = 60.18), Asp497 (Chain A = 40.29, chain B = 38.01), Arg438 (Chan A = 40.38, Chain B = 39.80), Ile518 (Chain A = 32.62, Chain B = 34.80). Fig.11.11 depicts the most important binding site residues in interacting with the bicyclic peptide.

Grb7 SH2 domain was discovered first exploiting its ability to recognize phosphotyrosine residues on its binding partners. Indeed, SH2 proteins in general are known as phosphotyrosine binding modules. The peptide was dissolved in phosphate buffer for the co-crystallization study. Not surprisingly, the structure was seen to pick and contain a phosphate ion. The phosphate ion is well placed on the phosphate-binding pocket of the Grb7 SH2 domain. It forms a number of hydrogen bonds with Arg438, Arg458, Arg462 and Asn461 of the phosphotyrosine binding pocket.

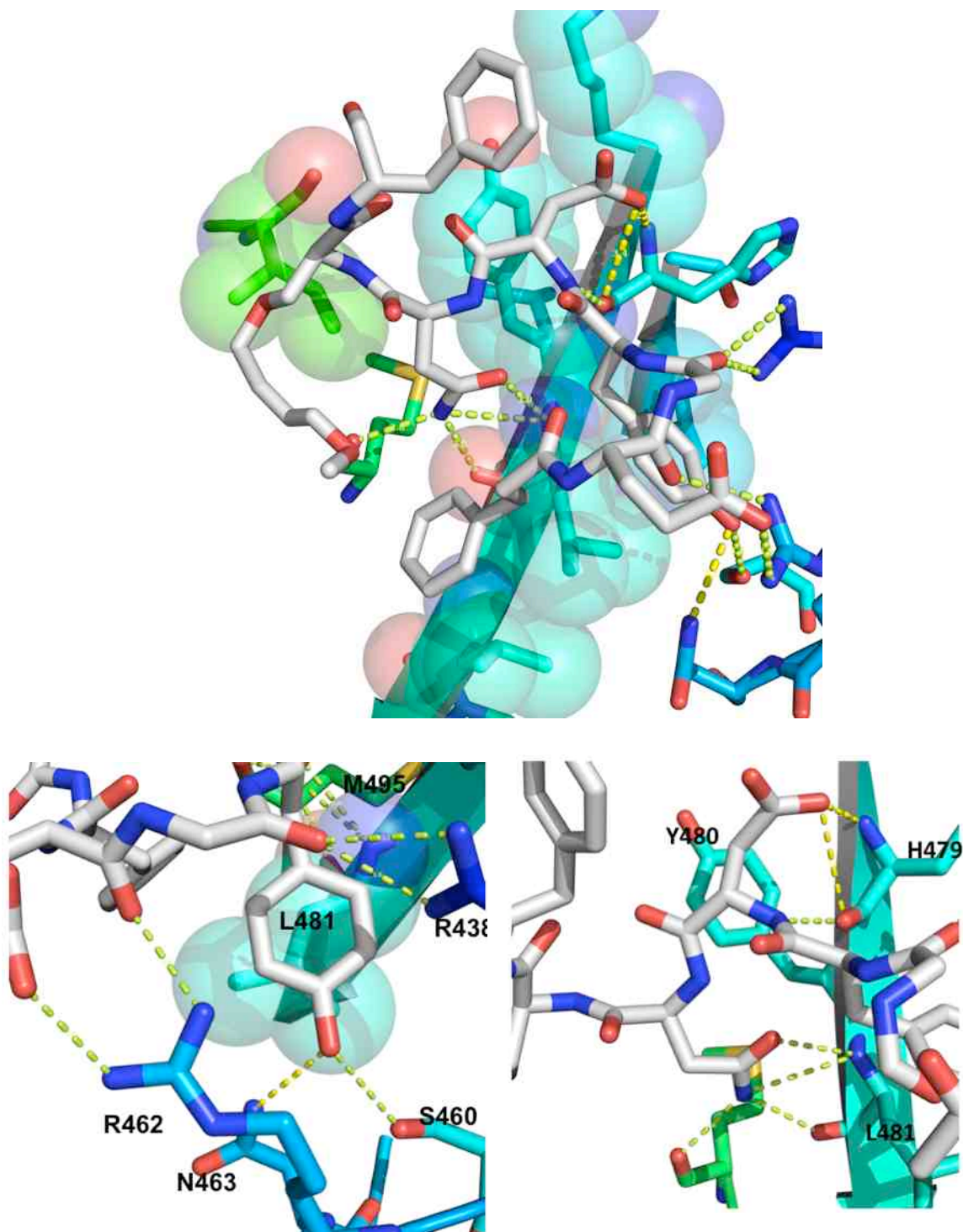


Figure 9.10. Bonding interaction of the peptide with Grb7 SH2 binding site atoms. Hydrogen bonding interactions are shown in dots. Protein residues that may form hydrophobic residues are shown in translucent spheres. The top picture depicts the overall interactions while the bottom ones are zoomed over specific regions and protein residues are labelled.

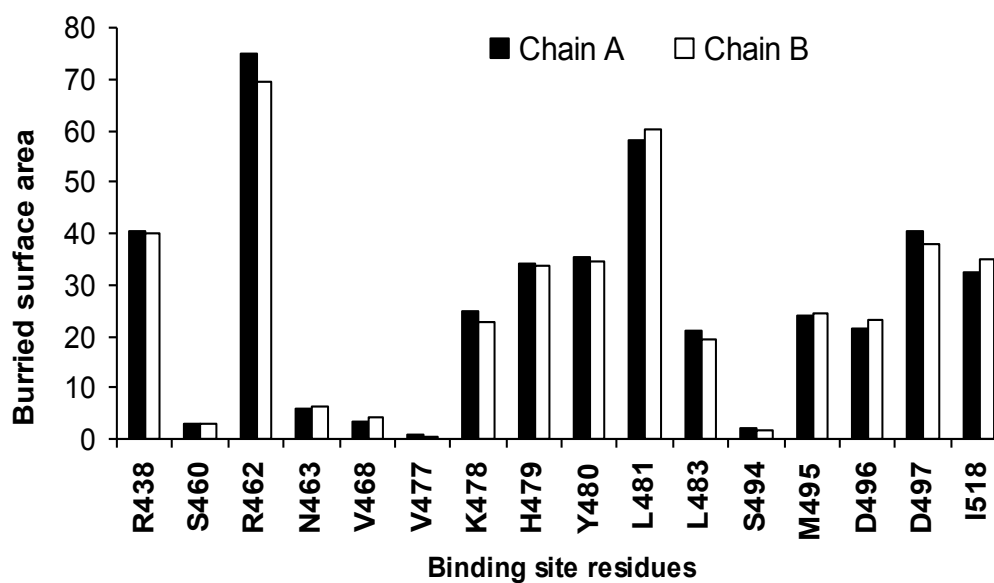


Figure 9.11: Relative importance of binding site residues in interacting with the bicyclic peptide. The plot shows that the two chains are interacting in more or less identical manner to the peptide.

Interestingly, it is observed to form a hydrogen bond with the OH of Y5 of the peptide and thereby acting as a bridge between the peptide and the residues on the phosphotyrosine-binding pocket. Fig. 9.12 shows these position and interaction of the phosphate with the Grb7 SH2 domain-binding site.

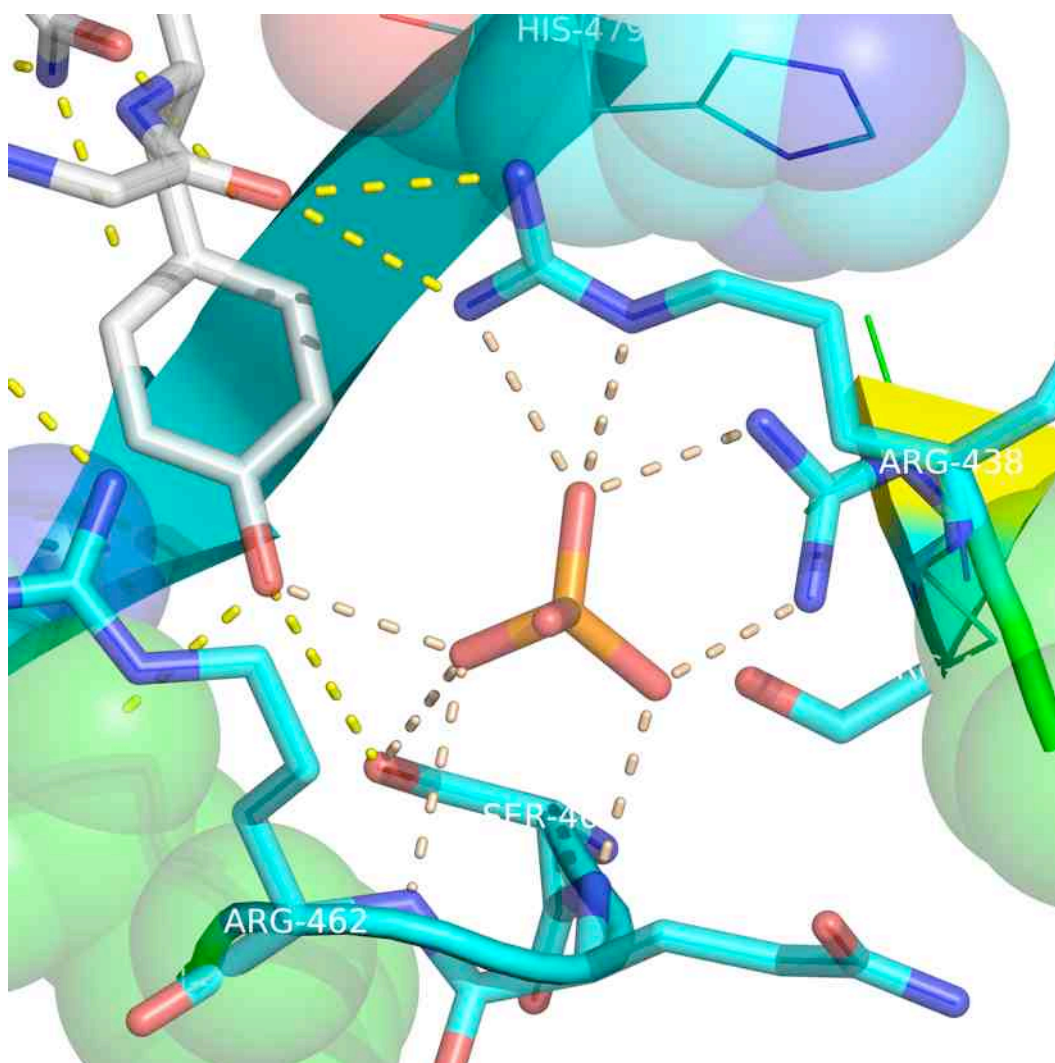


Fig. 9.12. The interactions of the phosphate ion with Grb7 SH2 domain and the peptide. The ion is shown to form a number hydrogen bonding interaction with basic residues of the binding site as well as with the Y5 of the bicyclic peptide. The phosphate ion, thus, served to form a bridge to enable the peptide form more bonds with the cationic pocket of the binding site. Bonding interaction made by the phosphate ion is indicated in dotted magenta color.

3. Structural Comparisons

In order to gain insight into the structural differences that may contribute to functional and specificity of differences among the related Grb proteins, a sequence and structural comparison by alignment was made. Since the apo form has a better resolution and more complete in the sequence, it was chosen as a template for comparative purposes. The structures of the apo protein of the related SH2 domains were then chosen and the sequences extracted from their structure file. The summary of the comparison is displayed in the Table 9.4 and shown pictorially in

Fig.9 .13. As the data indicate the sequence similarity vary considerable from 14.08 % in case of Grb2 SH2 domain, to 53.85 for Grb14 SH2 domain and 56.9 % for Grb10 SH2 domain. Interestingly, the sequences the current apo structure lacks 7 N-terminal residues as compared to the previously solved Grb7 SH2 domain structure (pdb id = 2QMS) which makes its sequence similarity only to be 83.6 %. From the sequence alignment, a total of 19 residues are shown to be conserved among the SH2 domain of the Grb proteins which translates to about 20% in sequence conservation.



Figure 9.13. Sequence alignment of the SH2 domain of Grb proteins. The alignment shows about 20% sequence conservation. The bottom is a phylogenetic tree derived from the sequence alignment. The overall alignment shows Grb2 is distantly related to the other three SH2 domains with Grb10 and Grb14 as closely related to each other.

Table 9.4: Structural comparrison among different SH2 domain of Grb protein

Structure	Sequence similarity	RMSD	pdb id	References
Grb7 SH2 apo	---	----	-----	----
Grb7 SH2 complex		0.382	----	----
Grb7 SH2 apo	83.6	1.1644	2QMS	25
Grb10 SH2 apo	56.9	0.9377	1NRV	58
Grb14 SH2 apo	53.85	1.0879	2AUG	59
Grb2 SH2 apo	14.08	1.6228	1JYU	60



Figure 9.14; The over structural alignments of the SH2 domains of Grb7 SH2 domain apo shown in green(loop)-yellow(B-sheet)-red(helix)) with the co-crystal structure(left) and previous structure of Grb7 SH2 domain(right). The Grb7 SH2 apo is used as template on which the other structures are overlaid.

Structural alignment of the Grb7 SH2 domain apo with the co-crystal structure and with the previously reported Grb7 SH2 apo structure reveals the structures are more or less similar, see Fig. 9.14 and Table 9.4. The structural alignment of the apo protein with the co-crystal structure is found to have a low RMSD of 0.382. The alignment looks similar except for the absence of the N-terminal helix in the co-crystal form and slight disagreement in the BE and BC loops. Comparison of the apo and previous structure of Grb7 SH2 domain apo (pdb id = 2QMS) once again shows similar arrangement except in the loop connecting the secondary structural elements. It is found that the loops are more disordered and look longer in the previous structure (pdb id = 2QMS) while they now look more ordered and tighter. This might have to do with the resolution of the two structures otherwise the overall fold is similar. Another point of difference is in the H-helix where there is a complete disagreement as to their orientation as these helices orient in opposite direction from the common loop that gives rise to them by 180 degrees. The overall RMSD obtained is 0.92.

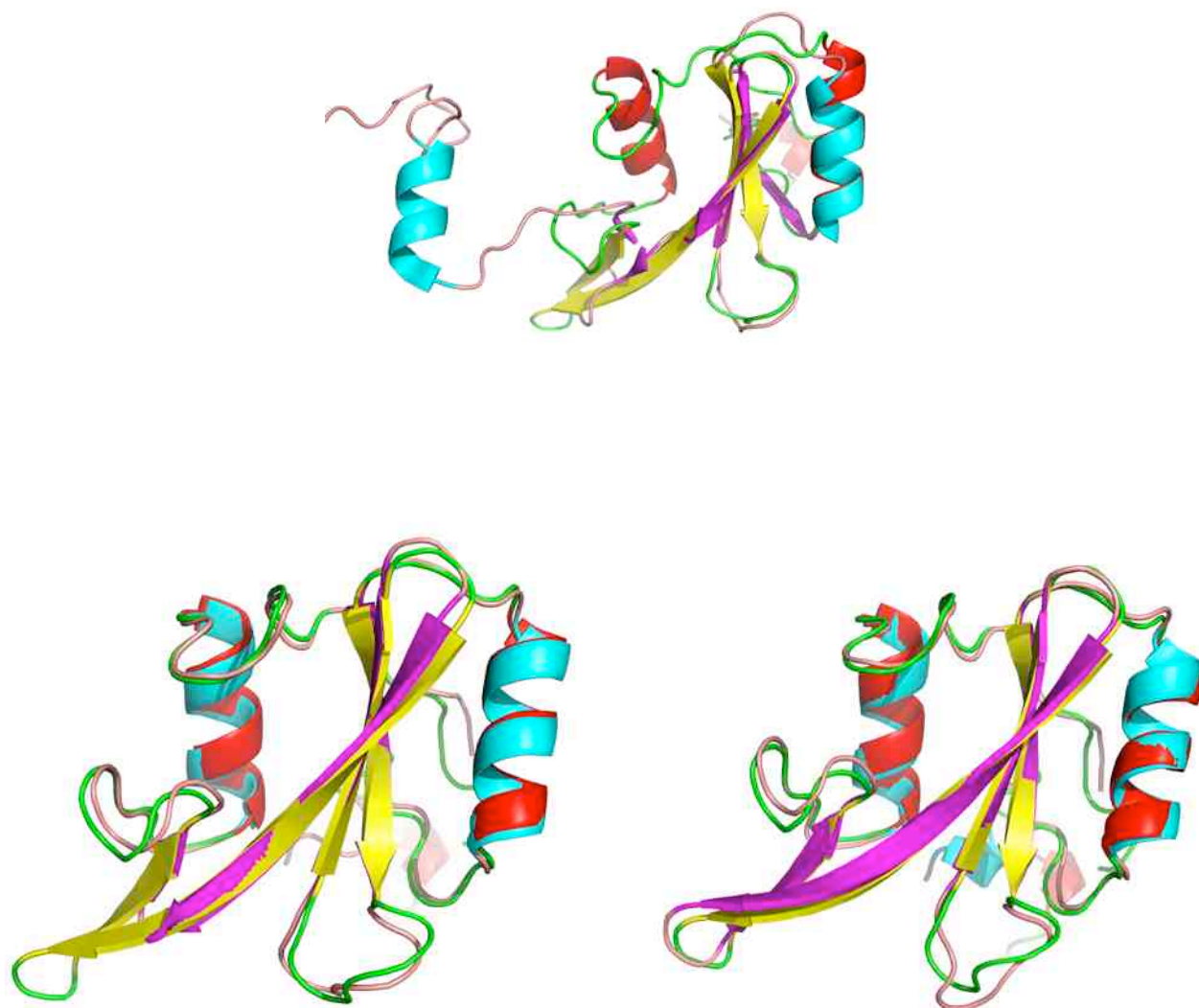


Figure 9.15. Structural alignment of the SH2 domains of Grb2 (top), Grb10 (bottom, left) and Grb14 (bottom, right) with Grb7 SH2 domain apo structure as a reference. Grb7 SH2 domain is shown in yellow, green and red in all the alignments

In case of alignment with the Grb2 SH2 domain, shown in Fig. 9.15, big structural differences appeared. First the α B helices never align together as it is noticed to orient in different directions. Second, β C' and β D strands are absent in case of Grb2 apo structure. However, there is additional β -strand in case of Grb2 SH2 domain that comes prior to the α A helix. Moreover, the H-helix is absent from the Grb2 SH2 domain structure. In addition, slight differences in the way the α A helices and α B strands align exist with slight differences in the length of the corresponding

structural elements. The loop structures look more or less similar as compared to the comparison with the Grb7 SH2 domain structure. The overall RMSD was 1.528, which reflects the poor sequence similarity.

The structural alignment of Grb7 SH2 with Grb10 SH2 reveals striking similarity. See Fig. 9.15. The two structures were aligned to an overall RMSD of 0.662. The major source of differences appears on the length of the β C and β D strands. In case of Grb10, it is found that such structural elements are shorter both by three residues. In addition, the H-helix of Grb7 SH2 domain is absent in the Grb10 SH2 domain structure. The loops and other structural elements are shown to possess remarkable alignment similarity. Finally, the Grb14 SH2 domain displays remarkable alignment similarity with Grb7 SH2 domain. It is shown the alignment to have an over all alignment score in RMSD of 0.814. The secondary structural elements are well aligned. The only exception is the H-helix which is found to divulge at 180 degree from the common loop that gives rise to them. Otherwise, of all the Grb10 SH2 domains, Grb14 is found to align the best with Grb7 SH2 domain.

In vitro binding thermodynamics studies with ITC

The determination of thermodynamic binding parameters for ligand-receptor interactions can provide an insight into the molecular mechanism of complex formation.³² In that regard, binding measurements by titration calorimetry is invaluable as it affords a detailed quantitative description of the interaction.⁴² For example, the ITC enthalpic readout gives a direct measure of the binding contribution from the formation or breakage of non-covalent bonds while the entropic data provides a quantitative value for changes in order of the system associated with the conformational and/or solvation phenomenon during ligand-receptor complex formation. The precise determination of both these parameters along with the number of binding sites (N), free energy of binding (ΔG) and dissociation constant (K_d) contributes to a clearer understanding of the overall attributes of the ligand-receptor associations under investigation.^{32,42}

Previous studies on G7-18NATE binding in acetate buffer systems and the present study on phosphate buffer have all made it clear that the entropic component of binding is unfavourable for the complex formation. This observation has

encouraged us to make use of the concept of peptide cyclization as a strategy to introduce a conformational restraint on the G7-18NATE structure. To this effect, the bicyclic G7-18NATE derivative has been synthesized and tested accordingly. The thermogram in Fig. 9.16 shows that the peptide binding is similar to the lead G7-18NATE peptide, i.e., exothermic binding.⁴² Moreover it is also seen to bind in the 1:1 manner, as shown in Table 9.5. However, the thermodynamics binding data for the bicyclic G7-18NATE peptide is slightly different with the dissociation constant slightly improved ($K_d = 1.94 \mu\text{M}$, compared to $K_d = 4.8 \mu\text{M}$). More importantly, the unfavourable part of entropy was turned into favourable one as a by product of the cyclization effort. Nevertheless, still the enthalpic part remain the predominant factor to binding ($\Delta H = 6.5 \text{ kcal/mole}$) as compared to $T\Delta S = -1.2 \text{ kcal/mole}$), i.e. close to five-fold contribution over the entropic part of interaction to Grb7 SH2 domain. Whereas the measured affinity is only a slight improvement, the enthalpy/entropy readout could provide different starting points as far as optimizing the affinity is concerned. This information together with the structural analysis could potentially aid the further optimization of the affinity of these peptide antagonists.

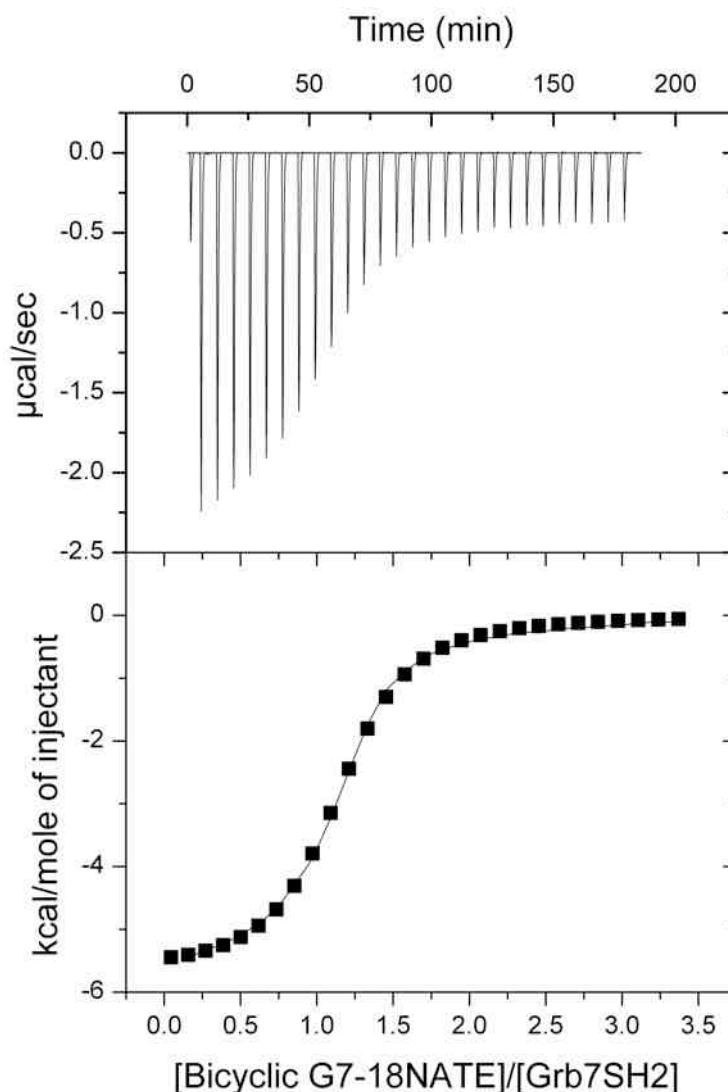


Figure 9.16. ITC thermograms obtained for the binding of Bicyclic G7-18NATE against Grb7 SH2 domain. The upper panel show raw data obtained from 10 μ l injections of peptide at 25 $^{\circ}$ C. The lower panels in both figures display plots of integrated total energy exchanged (as kcal/mol of injected peptide) as a function of molar ratio of the peptide to the Grb7 SH2 domain.

Table 9.5: Thermodynamic binding parameters of Bicyclic G7-18NATE analogues

Binding Parameter	N	K(10^5)	ΔH (Kcal/mol)	$-T\Delta S$ (Kcal/mol)	ΔG (Kcal/mol)	K_d (μ M)
Value	1.08 \pm 0.01	5.16 \pm 0.29	-6.53 \pm 0.05	-1.26 \pm 0.11	-7.79 \pm 0.16	1.94

Conclusion

Grb7 is an emerging novel drug target especial in cancer. Structural studies are invaluable inputs to drug discovery and development. In line with this, high-resolution structures of Grb7 SH2 apo and Grb7 SH2 domain in complex with a bicyclic peptide were reported. The details of the peptide atom receptor atom interaction chemistry as well as the overall three-dimensional structure of the Grb7 SH2 domain proteins is described. Sequence and structural comparisons with other SH2 domains were presented in a bid to indicate structural differences that might be exploited in the design of selective antagonists. While Grb2 SH2 domains differ structurally, it is found that Grb7, Grb10 and Grb14 are very related in their structure. Binding studies of the cyclic peptide was conducted by ITC and a moderate affinity was found. Together the structural and biophysical studies are expected to lay a fertile ground for the development of novel Grb7 antagonists.

References

- (1) Zhang, X.; Nie, D.; Chakrabarty, S. Growth factors in tumor microenvironment. *Front. Biosci.* **2010**, *15*, 151-165.
- (2) Carpenter G.; Cohen, S. Epidermal growth factor, *J. Biol. Chem.* **1990**, *265*, 7709-7812.
- (3) Schlessinger, J. Cell signaling by receptor tyrosine kinases. *Cell* **2000**, *103*, 211-225.
- (4) Margolis, B.; Silvennoinen, O.; Comoglio, F.; Roonprapunt, C.; Skolnik, E.; Ullrich, A.; Schlessinger, J. High-efficiency expression/cloning of epidermal growth factor-receptor-binding proteins with Src homology 2 domains. *Proc. Natl. Acad. Sci. U.S.A.* **1992**, *89*, 8894-8898.
- (5) Han, D. C.; Shen, T. L.; Guan, J. L. The Grb7 family proteins: structure, interactions with other signaling molecules and potential cellular functions. *Oncogene* **2001**, *20*, 6315-6321.
- (6) Stein, D.; Wu, J.; Fuqua, S.A.; Roonprapunt, C.; Yajnik, V.; D'Eustachio, P.; Moskow, J. J.; Buchberg, A. M.; Osborne, C. K.; Margolis, B. The SH2 domain protein GRB-7 is co-amplified, overexpressed and in a tight complex with HER2 in breast cancer. *EMBO J.* **1994**, *13*, 1331-1340.
- (7) Haran, M.; Chebatco, S.; Flaishon, L.; Lantner, F.; Harpaz, N.; Valinsky, L.; Berrebi, A.; Shachar, I. Grb7 expression and cellular migration in chronic lymphocytic leukemia: a comparative study of early and advanced stage disease. *Leukemia* **2004**, *18*, 1948-1950.

- (8) Itoh, S.; Taketomi, A.; Tanaka, S.; Harimoto, N.; Yamashita, Y.; Aishima, S.; Maeda, T.; Shirabe, K.; Shimada, M.; Maehara, Y. Role of growth factor receptor bound protein 7 in hepatocellular carcinoma. *Mol. Cancer Res.* **2007**, *5*, 667-673.
- (9) Tanaka, S.; Pero, S. C.; Taguchi, K.; Shimada, M.; Mori, M.; Krag, D. N.; Aarii, S. Specific peptide ligand for Grb7 signal transduction protein and pancreatic cancer metastasis. *J. Natl. Cancer Inst.* **2006**, *98*, 491-498.
- (10) Tanaka, S.; Mori, M.; Akiyoshi, T.; Tanaka, Y.; Mafune, K.; Wands, J. R.; Sugimachi, K. Coexpression of Grb7 with epidermal growth factor receptor or Her2/erbB2 in human advanced esophageal carcinoma. *Cancer Res.* **1997**, *57*, 28-31.
- (11) Kishi, T.; Sasaki, H.; Akiyama, N.; Ishizuka, T.; Sakamoto, H.; Aizawa, S.; Sugimura, T.; Terada, M. Molecular Cloning of Human *GRB-7* Co-amplified with *CAB1* and *c-ERBB-2* in Primary Gastric Cancer. *Biochem. Biophys. Res. Commun.* **1997**, *232*, 5-9.
- (12) Wang, Y.; Chan, D. W.; Liu, V. W.; Chiu, P.; Ngan, H. Y. Differential functions of growth factor receptor-bound protein 7 (GRB7) and its variant GRB7v in ovarian carcinogenesis. *Clin. Cancer Res.* **2010**, *16*, 2529-2539.
- (13) McIntyre, A.; Summersgill, B.; Spendlove, H. E.; Huddart, R.; Houlston, R.; Shipley, J. Activating mutations and/or expression levels of tyrosine kinase receptors GRB7, RAS, and BRAF in testicular germ cell tumors. *Neoplasia* **2005**, *7*, 1047-1052.
- (14) Kim, C. W.; Cho, E. H.; Lee, Y. J.; Kim, Y. H.; Hah, Y. S.; Kim, D. R. Disease-specific proteins from rheumatoid arthritis patients. *J. Korean Med Sci.* **2006**, *21*, 478-484.
- (15) Shen, T. L.; Guan, J. L. Grb7 in intracellular signaling and its role in cell regulation. *Front Biosci.* **2004**, *9*, 192-200.
- (16) Tanaka, S.; Mori, M.; Akiyoshi, T.; Tanaka, Y.; Mafune, K.; Wands, J. R.; Sugimachi, K. A novel variant of human Grb7 is associated with invasive esophageal carcinoma. *J. Clin. Invest.* **1998**, *102*, 821-827.
- (17) Stein, D.; Wu, J.; Fuqua, S. A.; Roonprapunt, C.; Yajnik, V.; D'Eustachio, P.; Moskow, J. J.; Buchberg, A. M.; Osborne, C. K.; Margolis, B. The SH2 domain protein GRB-7 is co-amplified, overexpressed and in a tight complex with HER2 in breast cancer. *EMBO J.* **1994**, *13*, 1331-1340.
- (18) Ramsey, B.; Bai, T.; Newell, H. A.; Troxell, M.; Park, B.; Olson, S.; Keenan, E.; Luoh, S.W. GRB7 protein over-expression and clinical outcome in breast cancer. *Breast Cancer Res Treat.* **2010**, DOI: 10.1007/s10549-010-1010-0.
- (19) Pero, S. C.; Shukla, G. S.; Cookson, M. M.; Flemer, S.; Krag, D. N. Combination treatment with Grb7 peptide and Doxorubicin or Trastuzumab (Herceptin) results in cooperative cell growth inhibition in breast cancer cells. *Br. J. Cancer* **2007**, *96*, 1520-1525.

- (20) Pero, S. C.; Oligino, L.; Daly, R. J.; Soden, A. L.; Liu, C.; Roller, P. P.; Li, P.; Krag, D. N. Identification of novel non-phosphorylated ligands, which bind selectively to the SH2 domain of Grb7. *J. Biol. Chem.* **2002**, *277*, 11918-11926.
- (21) Pero, S. C.; Daly, R. J.; Krag, D. N. Grb7-based molecular therapeutics in cancer *Expert. Rev. Mol. Med.* **2003**, *5*, 1-11.
- (22) Daly, R. J. The Grb7 family of signaling proteins. *Cell Signal.* **1998**, *10*, 613-618.
- (23) Margolis B. The Grb family of SH2 domain proteins. *Prog. Bioph.Mol.Biol.* **1994**, *62*, 223-244.
- (24) Pawson, T.; Gish, G. D.; Nash, P. SH2 and SH3 domains in signal transduction. *Adv. Cancer Res.* **1994**, *64*, 87-110.
- (25) Porter, C. J.; Matthews, J. M.; Mackay, J. P.; Pursglove, S. E.; Schmidberger, J. W.; Leedman, P. J.; Pero, S. C.; Krag, D. N.; Wilce, M. C.; Wilce, J. A. Grb7 SH2 domain structure and interactions with a cyclic peptide inhibitor of cancer cell migration and proliferation. *BMC Struct. Biol.* **2007**, *7*:58.
- (26) Yap, M. Y.; Wilce, M. C. J.; Clayton, D. J.; Perlmutter, P.; Aguilar, M.-I.; Wilce, J. A. Preparation and crystallization of the Grb7 SH2 domain in complex with the G7-18NATE non-phosphorylated cyclic inhibitor. *Acta Cryst.* **2010**, *F66*, 1640-1643.
- (27) Kabsch, W. Automatic processing of rotation diffraction data from crystals of initially unknown symmetry and cell constants. *Appl. Cryst.* **1993**, *26*, 795-800.
- (28) Vagin, A.; Teplyakov, A. MOLREP: an Automated Program for Molecular Replacement. *J. Appl. Cryst.* **1997**, *30*, 1022-1025.
- (29) The CCP4 Suite: Programs for Protein Crystallography. *Acta Cryst.* **1994**, *D50*, 760-763
- (30) Murshudov, G. N.; Vagin, A. A.; Dodson, E. J. Refinement of macromolecular structures by the maximum-likelihood method. *Acta Crystallogr. D Biol. Crystallogr.* **1997**, *53*, 240-255.
- (31) Emsley, P.; Cowtan, K. Coot: model-building tools for molecular graphics. *Acta Crystallogr. D Biol. Crystallogr.* **2004**, *60*, 2126-2132.
- (32) Freyer, M. W.; Lewis, E. A. Isothermal titration calorimetry: experimental design, data analysis, and probing macromolecule/ligand binding and kinetic interactions. *Methods Cell Biol.* **2008**, *84*, 79-113.
- (33) Pantoliano, M. W.; Petrella, E. C.; Kwasnoski, J. D.; Lobanov, V. S.; Myslik, J.; Graf, E.; Carver, T.; Asel, E.; Springer, B. A.; Lane, P.; Salemme, F. R. High-density miniaturized thermal shift assays as a general strategy for drug discovery. *J. Biomol. Screen.* **2001**, *6*, 429-440.
- (34) Matulis, D.; Kranz, J. K.; Salemme, F. R.; Todd, M. J. Thermodynamic stability of carbonic anhydrase: measurements of binding affinity and stoichiometry using ThermoFluor. *Biochemistry* **2005**, *44*, 5258-566.

- (35) Porter, C. J.; Wilce, M. C.; Mackay, J. P.; Leedman, P.; Wilce, J. A. Grb7-SH2 domain dimerization is affected by a single point mutation. *Eur. Biophys J.* **2005**, *34*, 454-460.
- (36) Eck, M. J.; Shoelson, S. E.; Harrison, S. C. Recognition of a high-affinity phosphotyrosyl peptide by the Src homology-2 domain of p56lck. *Nature* **1993**, *362*, 87-91.
- (37) DeLano, W.L. The PyMOL Molecular Graphics System. DeLano Scientific, San Carlos, CA, USA, **2002**. <http://www.pymol.org>
- (38) Jones, S.; Thornton, J. M. Protein-protein interactions: a review of protein dimer structures. *Prog. Biophys. Mol. Biol.* **1995**, *63*, 31-65.
- (39) Jones, S.; Thornton, J. M. Principles of protein-protein interactions derived from structural studies. *Proc. Natl Acad. Sci. USA*, **1996**, *93*, 13-20.
- (40) Burke, T. R. Development of Grb2 SH2 Domain Signaling Antagonists: A Potential New Class of Antiproliferative Agents. *Int. J. Pept. Res. Ther.* **2006**, *12*, 33-48.
- (41) Fretz, H.; Furet, P.; Garcia-Echeverria, C.; Schoepfer, J.; Rahuel, J. Structure-based Design of Compounds Inhibiting Grb2-SH2 Mediated Protein-protein Interactions in Signal Transduction Pathways. *Curr. Pharm. Des.* **2000**, *6*, 1777-1796
- (42) Ambaye, N. D.; Lim, R. C. C.; Clayton, D. J.; Gunzburg, M. J.; Price, J. T.; Pero, S. C.; Krag, D. N.; Wilce, M. C. J.; Aguilar, M. I.; Perlmutter, P.; Wilce, J.A. Uptake of a cell permeable G7-18NATE construct into cells and binding with the Grb7-SH2 domain. *Biopolymers* **2010**. DOI: 10.1002/bip.21403.

Chapter 10

General Summary and Discussion

In this chapter the summary of the project is presented.

General Summary and Discussion

Cancer remains a growing menace. According to WHO, cancer causes some 8 million deaths or about 13% of all the deaths worldwide per year. The mortalities and morbidities associated with cancer can only be expected to rise exponentially as, among other things, an attendant to the socio-environmental changes. Whereas there are over 100 antitumor drugs available clinically, the growing inefficacy and toxicity means new chemotypes with novel mechanism of action are always sought. Experimental agents acting on novel therapeutic targets provide the necessary foundations whereupon drug discovery and development campaigns are conceived, initiated and successfully executed. In line with this, this thesis was designed to provide experimental antagonists and contribute to the groundwork necessary for future development of Grb7 based anti-tumour therapeutics.

With advances in genomic and proteomic sciences a variety of biological process are being interrogated at a greater level of detail to understand the molecular basis of human maladies and the potential to present a novel therapeutic mechanism of action. Among these, the process of signal transduction is in a research spotlight as a potential source of antitumor targets. This arises from the fundamental role signalling plays in cellular life and the frequent observation of errors in signal transduction in a number of diseases such as cancers. Grossly, the components of signal transduction pathways can be categorized as the extracellular, membrane bound and intracellular parts, with each part comprising a diverse spectrum of biomolecules. Though biological membranes might present the first challenge, intracellular components of signalling pathways can sometimes provide better selectivity and hence all the benefit associated with it. As a result, intracellular components of signal transduction are increasingly being investigated as a drug targets in cancers.

Among the intracellular anticancer targets being sought are the growth factor binding proteins. Grb proteins are cytosolic adaptor molecules that are devoid of any catalytic activity. These proteins are specifically known for their ability to recognize activated and phosphorylated membrane bound growth factor receptors. Currently there exist some 14 Grb proteins where most are frequently implicated in cancers. Grb7 belongs to sub family of Grb proteins known to possess remarkable

sequence, structural and functional similarity, though not always. The entire project was dependent on the use of the non-enzymatic cytosolic Grb7 protein as receptor.

Grb7 is found to be an important antitumor target. It has been shown to be over expressed in a number of human cancers such as breast, liver, pancreatic, testicular, blood, ovary, stomach, oesophagus and in others. Even interesting is the fact that Grb7 over expression is associated with the development of aggressive, refractory, invasive, high grade, high tumour, drug-resistant and advanced cancer phenotypes. Furthermore, the fact that Grb7 is druggable target is demonstrated with the use of peptide antagonists. These and other related works means that Grb7 is a valid therapeutic target and hence might be worthy of inhibitor development effort.

The first part of this project was a comprehensive literature review on the fundamentals of Grb7 and its relevance in different diseases states. In the first section of the review, the gene structure, sequence and domain composition of Grb7 was presented in detail. It was found that Grb7 is located on the long arm of Chromosome 17 with a cytogenetic map of 17q12-21. This localization is very critical to the overall behaviour of Grb7 as it is found on the frequently amplified region, termed the ErbB2 amplicon. Furthermore, Grb7 is noted to form functional signalling complex with the membrane bound growth factor receptors. The domain structure of Grb7 is noted to comprise conserved modules such as the proline rich domain, Ras-associating domain(RA), pleckstrin homology domain(PH), and the Src homology 2 domain. The RA, PH and another termed the BPS domains are clumped as the GM domain (from *Grb* and *Migratory* 10). Each domain is known to fold and function independently to carry out the overall signalling function of Grb7. Overall the GM domain is known to possess some 50% sequence similarity to the *Migratory-10* protein of the nematode *C. elegans* and hence is known to be responsible for the migratory property of Grb7 expressing cancer cells.

The SH2 domain is the most widely researched domain and is shown to commence the first step in the involvement of Grb7 in a variety of signal transduction pathways. The structure of Grb7 SH2 domain is solved and is noted to fold in a canonical fold comprising a pair of a pair of α -helices and pairs of β -sheet structures. The SH2 domain binding site is characterized well and is noted to possess a well defined cationic pocket which selectively recognizes phosphotyrosine

residues on the upstream binding partners of Grb7, the selectivity of which is determined by on the sequences surrounding the pTyr residue.

The second section of the review extensively summarizes the role of Grb7 in different disease states and processes. In particular the therapeutic role of Grb7 in different human cancers, inflammatory disorders, and process such as transcription, ion channel regulation, immune system activation and possible role in analgesia is presented. In breast cancer, for example, the expression of Grb7 has been implicated in the development of refractory breast cancer cell lines that resist to treatment with oestrogens antagonists and it was suggested that the level of Grb7 expression could be used to devise the course of therapy. Indeed, Grb7 is part of a commercially available kit used to assess the status and prediction of prognosis for patients with breast cancer. Interestingly, Grb7 alone was found to be capable of being a factor in the genesis of breast cancer cell lines, though co-expression and physical association with ErbB2 represent the most carcinogenic combination. In gastric carcinoma, up to 32 % over expression of Grb7 was noted and this over expression was shown to contribute to the development of more aggressive and invasive gastric carcinomas. In pancreatic tumour, more than 62 % overexpression of Grb7 was noted in patients with lymph node metastasis where it is shown to directly correlate with the metastatic and migratory potential of the cancer cells.

Similar stories exist in oesophageal carcinoma where up to 45 % Grb7 expression was noted and known to contribute to lymph node metastasis. In hepatic cancer Grb7 overexpression was noted to relate with the development of invasive and metastatic potential of hepatocellular carcinoma. Moreover, such behaviour was shown to be reduced when Grb7 was knocked out with siRNA technology. In addition, up to 40-fold expression of Grb7 was noted in ovarian cancer and the expression was found to significantly enhance ovarian cancer cell proliferation, migration and invasion potential. In testicular cancer, up to 63 % over expression is noted and Grb7 alone is found to contribute to testicular cancer formation. Finally, a direct relationship between Grb7 overexpression and the stages of chronic lymphocytic leukaemia (CLL) was observed. In stage IV of the disease up to 88% overexpression was noted as compared to the 18 % in stage I of CLL, which indicates that Grb7 level might be a useful for diagnostic purpose and to devise the course of therapeutic intervention.

Grb7 is also noted to be involved in a number of inflammatory disorders such as Rheumatoid arthritis and atopic dermatitis (AD). In RA, Grb7 was found to associate with antibodies isolated from the synovial fluid of RA patients along with fibronectin and other proteins. It is shown that by coupling NF-kappa-inducing kinase with erbB/EGFR family receptors, Grb7 is found to regulate inflammation. The role of Grb7 in this inflammatory disorder was investigated by considering the level of eosinophilia in AD patients. Experiments to delineate the precise role of Grb7 in AD have showed that increased phosphorylation of Grb7 and FAK was detected in low viability eosinophils. These results suggest that Grb7 phosphorylation may be one factor related with the anti-apoptosis mechanism of eosinophilia.

Among the other roles of Grb7 that are deciphered quite recently are its influence in inflammation, transcription, regulation, its possible impact on K-channel regulation and analgesia. In particular, Grb7 expression in lymphocytes and G6bf of the immunoglobulin superfamily was noted and found to have an immunostimulatory role. Grb7 was shown to be over expressed in a number of K-channels including hERG, Kir1.1, Kv1.5, Kir2.2, Kir2.3, Kv4.3 and ROMK. Grb7 overexpression was noted to decrease the amplitude of most of the K-ion channels and hence affect cardiac excitability. Acting via Netrins and HuR proteins, Grb7 over expression is noted to have a repressive effect on transcription. Finally, the potential role of Grb7 in analgesia is proposed as it was shown to function as a constitutive repressor for kappa opioid receptor, a classical narcotic drug receptor. The last section of the review dealt with development of Grb7 antagonist. It showed how the basic background work was used to design a potent polypeptide antagonist and how the membrane barrier problem is overcome with the use of permeabilising agents. Also described is the development of short phosphorylated peptides based on the YXN recognition motif of Grb7 SH2 domain.

The sample preparation part of the thesis presented the synthetic chemistry, Grb7 SH2 domain expression and purification as well as the crystallization, diffraction data collection and processing strategies pursued. The first section presented the overall protocol and the mechanistic basis of the entire peptide synthesis. A total of 11 peptides were synthesized throughout the project. The solid phase synthesis tactic followed was the Fmoc based peptide synthesis on a resin amide resin. The

rink resin and the amino acids were available in Fmoc protected forms. The Fmoc elimination was achieved with 20% piperidine in DMF. Each residue was pre-activated before coupling reaction for 3 minutes. The HBTU in the presence of DIPEA was applied as coupling agents. In all cases the first residues was loaded to the resin manually at room temperature. The successes of manual deprotection/coupling reaction steps and in cases of the manually synthesised peptides, the full-scale synthesis, were made by Kaiser's ninhydrin based test. In cases of less than efficient coupling a strategies such as use of more powerful coupling agents such as HATU or use of a di-isopropyl carbodimide as a catalyst was carried out, double coupling and increasing the reaction time was effected.

Ring forming reactions were conducted at RT manually. The thioether ring formation was achieved by exploiting the properties of thiols to become oxidized above pH 8 and thereby to act as a nucleophile. Chloroacetylation by chloroacetic anhydride provided the electrophilic centre for displacement by the generated sulphur nucleophile and thus form the thioether ring. In cases of the bicyclic G7-18NATE peptide, the second ring was introduced via the use of ring closing metathesis reaction. In fact, this second ring was introduced first on the fully protected crude peptide while the thioether ring was conducted after cleavage of the peptides. Biotin was coupled for SPR and cellular uptake experiments with Streptavidin antibodies. It was coupled in a reaction analogous to a peptide coupling reaction.

The peptide purification and characterization was achieved by RP-HPLC and mass spectrometry. For those peptides that contained the penetratin residues, positive ion mode of was employed in the ESI-MS analysis while for the rest non-permeable peptides negative ion mode was found appropriate typically as such peptide contain a relative excess of acidic residues where in the former case a contiguous stretch of basic residues are found. The overall synthetic yields vary considerably from poor 2 % to about 20 %. Specifically, penetratin and penetratin containing residues were found difficult to obtain in good yield. Nevertheless, the yields we obtain were enough for some round of in vitro and in vivo binding experiments.

The Grb7 SH2 domain purification scheme relied on the over expression of the C-terminal 415-435 residues of Grb7 in BL21(DE3)pLysS cell lines. These cell lines are

protease deficient cells. A series of chromatographic purification techniques embracing affinity, ion exchange and size exclusion chromatographic purification were adopted. Buffer exchange between different chromatographic runs was achieved via dialysis for 18 hrs using dialysis membrane of MCW3000. SDS-PAGE as well as chromatographic analysis was employed to follow the success of each purification stage. A final yield of varying from 3-9 mg per litre of culture media was achieved. Though the overall procedure could have been optimized further, there was no attempt to improve as the focus of the study was to generate sufficient protein for inhibitor binding studies.

Chapter three describes the design and characterization of a short cell permeablising construct as a G7-18NATE fusion peptide. Grb7 is an intracellular protein. Since G7-18NATE is a polypeptide, plasma membrane represents a bottleneck for its use in cellular systems. Even though this has been achieved with the use of a 17-member cell permeablising residues previously, we hypothesized that this residue could be made as short as 8 residues in length and that could well be sufficient to assist the membrane translocation of G7-18NATE. For this purpose, G7-18NATE-penetratin-Biotin polypeptide was synthesized. The possible interference on binding of G7-18NATE by the attached shorter penetratin sequence was then investigated by ITC. The data showed that there was no negative interference of G7-18NATE binding as nearly the same in vitro equilibrium dissociation constants for G7-18NATE with and without the penetratin tail were found. Furthermore, the cellular localization of G7-18NATE with this short penetratin tail has been confirmed. Compared to the original 17-residues penetratin, the economy of and ease of synthesis and, perhaps, stability as well is expected to be in favour of the short penetratin sequence. All in all, we were able to get short cell permeablising peptide that works as good as the original 17-residues polypeptide.

Chapter four describes the synthesis and thermodynamic characterization of second-generation G7-18NATE antagonists. The overall purpose of the study was to perform a structural exploration around the parent G7-18NATE polypeptide with the aim of improving the affinity. For that purpose our collaborators conducted a PHAGE display technique to identify the four analogue peptides that were provided to us for synthesis and affinity studies. As can be seen the structures are

conservative in the sense that no major changes were introduced such as alteration of the ring size and drastic changes in amino acid type. The synthesis was carried out as described above. The ITC binding studies were then effected to determine binding thermodynamics with a freshly purified Grb7 SH2 domain. As the results show the affinity determined was in the same range as that of the G7-18NATE, perhaps reflecting the conservative nature of the substitutions. Nevertheless, the fact that such compounds are as equipotent as G7-18NATE confirms the common features required for binding.

Chapter 4 also reports separate experiments. From the previous chapters dealing with biophysical, dynamical and structural studies it is clear that the lead peptide needs to be optimized further so as to be useful cellular or in vivo studies. It is also clear, especially from our simulation (not part of this Thesis) and structural analysis, that residues Trp1 and Thr8 of G7-18NATE are not required at all for binding to the Grb7 SH2 domain. The “unimportant” residues were then replaced by allyl Glycine and the resulting Allyl G7-18NATE was synthesized and tested to have equivalent potency to G7-18NATE. The ITC data on this modified peptide-Allyl G7-18NATE appears to justify the simulation and structural analysis made on the relative importance of G7-18NATE residues for binding to Grb7 SH2 domain.

Mutational studies are commonly employed to assess amino acid replacements to protein functions. One important assumption is that such mutants leave the entire protein in a virtually unaffected state such that the mutant behaves as if it is the wild type at all amino acid positions. In Grb7 SH2 domain, a Phe511 mutation has been previously conducted to assess dimerization status and its impact on the function of Grb7 protein. The impact of Grb7 SH2 mutation on the binding of G7-18NATE has been described in chapter 4. Mutant Grb7 was expressed and purified. ITC binding experiments were conducted in an identical manner to the wild type. The result shows that the peptide binds with similar affinity both to the mutant and wild type Grb7 SH2 domains, indicating the mutant is as equally functional as the wild type Grb7. This is important outcome as a single residue change is often big enough to disrupt biological function. Other works described in the chapter include the impact of experimental conditions on ITC experiment. It is shown that in case of Grb7 SH2/G7-18NATE interaction, the nature of the buffer plays a big role in affinity. The impact of the short penetratin tail on binding of the (D->E)G7-18NATE-

Penetratin-Biotin is also reported and it is shown that the short penetratin sequence appears to work on a different peptide as well, demonstrating its potential use in a different settings.

Experiments conducted thus far concentrated on binding characterization of peptides. Peptides, however, are actually plagued by a number of properties including stability, immunogenicity, synthetic difficulty, etc. Though the permeability issue was resolved by the design of a short permeabilizing sequence, it still comes at the additional cost of synthetic chemistry. This is especially true considering the inherent difficulty of synthesizing the highly basic permeabilizing sequences. Again, despite efforts including the analogue design and rigidization, significant improvements on affinity was not achieved. To address this, Chapters 5-7 take on a different path to tackle the same issue-to design potent and selective antagonist. This was achieved by a resorting to screening for small molecular antagonists of Grb7. Given the limit in number and diversity of the so far reported inhibitors, a structure based virtual screening experiment was found appropriate to commence the lead identification campaign.

Chapters 5 and 7 deal with the use of a potent tripeptide antagonist as a shape query to scan the NCI database. As the crystal information was not available, the bioactive conformation was established using conformational analysis. Also a mini-database was created to serve as an interrogation set. The relevance of the top five conformers as shape queries were analysed with the use of the mini database prepared. The fifth conformer was found to have the most explanatory power out of the top five investigated. Nevertheless, since the top conformer represented the lowest energy and hence the most populated conformer of the tripeptide, it was also considered for the shape search. Following the establishment of the query, the conformer shape queries were submitted to scan the NCI chemical database. The shape search was complimented by docking analysis that together with extensive binding mode analysis, 15 to 20 hits were prioritized. Available compounds were then requested and tested first by ThermoFluor based thermal denaturation experiment. In both cases one structure was found to provide stability. Its binding was then fully characterized by ITC. A moderate affinity was obtained in both cases. Now, the plan was to optimize the affinity. To this effect, 2D-similarity searching two small molecular structures as a conformer was conducted. The

available compounds were requested and tested by ThermoFluor and binding thermodynamics of representative structure done by ITC. The lead structures were subjected to in vivo cell growth inhibitory experiment using Grb7 expressing breast cancer cells. Not only were the leads found to possess activity in real life system, a very good in vivo- in vitro correlation was obtained. Overall, the observed affinity was improved as compared to the prototype G7-18NATE polypeptide. The fact that the two compounds were found to have an affinity close to the in vitro values is consistent with the intracellular action of the compounds and suggests that the compounds might not have the permeability problem.

Chapter 6 is analogously done to the previous two chapters. The major difference being the starting molecule for the shape search. This chapter exploited the availability of an in-house solved co-crystal structure of the G7-18NATE/Grb7SH2 complex. The bioactive conformation/shape of the peptide was directly extracted from the crystal structure and, after adding the hydrogen atoms, the all atom structure was then employed to screen the database. As in the above case, the shape query was applied first the mini-database to test its general validity. After confirming its relevance, it was directly applied to screen the NCI database in an analogous fashion as in the above chapters. 15 compounds were first obtained from the analysis based on the shape similarity indices and glide docking scores. The available hits were requested and tested. Again, one out of the five tested by ThermoFluor based assay was found to be a positive hit. Its affinity was then fully characterized by ITC and found to possess moderate affinity. It was then subjected to cell growth inhibition study and proved to do so with moderate affinity. From these combined assays, the structure was declared as a lead and was then subjected to structural exploration. The same 2D-similarity was conducted on the lead compound. All the available compounds were tested first by ThermoFluor and representative structures were then tested by ITC. All in all, the study showed that moderate affinity leads were obtained with strong in vitro–in vivo correlation.

The last two chapters describe the crystallization and structure determination conducted to obtain more relevant information for ligand optimization. High-resolution structures of both the apo and bound form of the Grb7 SH2 domain were obtained. The apo form was solved to a resolution of 1.6 Å while the bound form was solved at a resolution of 1.7 Å. In both cases the typical fold of the Grb7 SH2

domain was preserved as comprising a pair of peripheral alpha helices and two pairs of B-sheet structural elements. A rigid bicyclic analogue of G7-18NATE was designed, synthesized tested and co-crystallized with Grb7 SH2 domain. The second ring was introduced by replacing the relatively unimportant residues-(W and T) by O-allylserine and closing the cycle by ring closing metathesis reaction. The synthetic yield, not surprisingly was poor, due to the difficulty of forming the dicycle. Nevertheless, the ITC data for the bicyclic peptide was not as expected, i.e., affinity did not improve much. But the entropy part was made to play a positive favourable role as expected from the cyclization effort. The details of interactions, binding site topography analysis and structural comparisons of the apo and bound form of the structures as well as with related SH2 domain structures was made.

In conclusion, the project reports the successful undertaking of an antagonist design effort against Grb7, an emerging antitumor target. A number of peptides were designed and found to have moderate binding affinity. A permeable form of the peptides were designed and investigated. Impact of dimerization status and experimental variation on the out come of ITC experiments was investigated. Three classes of novel potent, permeable and selective Grb7 antagonists were discovered and high-resolution structures of the apo and bound form of Grb7 SH2 domain were solved.

This sets the groundwork for future endeavours to develop inhibitors of Grb7 SH2 domain. Whilst we have established that the peptidic nature of the inhibitor may not be necessarily an obstacle to its intracellular delivery, we still have not enhanced its affinity to beyond micromolar K_d . Thus future studies will be desired to extend the optimization and further characterization endeavour.